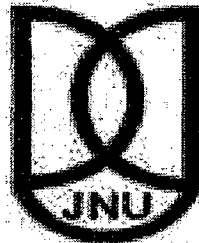


**An Integrated Approach through Remote Sensing,
GIS and Geophysical tools to Assess Water
Resources in a part of National Capital Region**

THESIS SUBMITTED TO JAWAHRLAL NEHRU UNIVERSITY
FOR THE AWARD OF DEGREE OF
DOCTOR OF PHILOSOPHY

SAYTANARAYAN SHASHTRI

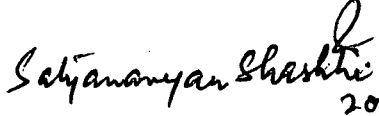


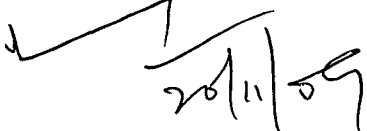
**REMOTE SENSING APPLICATIONS LABORATORY
SCHOOL OF ENVIRONMENTAL SCIENCES
JAWAHARLAL NEHRU UNIVERSITY
NEW DELHI-110067
2009**

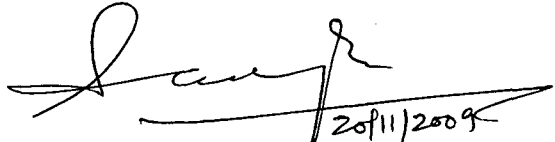
जवाहरलाल नेहरू विश्वविद्यालय
Jawaharlal Nehru University
SCHOOL OF ENVIRONMENTAL SCIENCES
New Delhi- 110 067, INDIA

CERTIFICATE

certify that the research work embodied in this thesis entitled “**An
d Approach through Remote Sensing, GIS and Geophysical
ssess Water Resources in a part of National Capital Region**” is
to Jawaharlal Nehru University for the award of the Degree of
Philosophy. The work is original and has not been submitted in
full for any other degree or diploma to any university / institution


20/11/2009
Satyanarayan Shashtri
(Candidate)


20/11/09
of.K.G.Saxena
(Dean)
Prof. K. G. SAXENA
Dean
School of Environmental Sciences
Jawaharlal Nehru University
New Delhi - 110067


20/11/2009
Professor S.Mukherjee
(Supervisor)

ACKNOWLEDGEMENT

There is no word which can really express my gratefulness to my supervisor **Prof.Saumitra Mukherjee** who has been a constant source of moral, material and cerebral support. He opened a window to the highest academic level for me.

I express my deep sense of gratitude to Prof. K.G.Saxena, Dean, School of Environmental Sciences, JNU for providing me facilities necessary for execution of the work.

I owe my sincere thanks to Chander Kumar Singh, Amit Singh, Manoj Pant, Arvind, Dr. Azeem, Vijay Singh, Vijay Veer, Prabir Mukherjee, Reena, Ramavtar, R.P.Singh, Bindu and Vikas,

My thanks to Mr. Daya Ram Yadavji my lab assistant for his support in the field work. I wish to thank my office staff Shri.S.D.S.Rawat for his kind help during my PhD work.

Date 30, October, 2009

Satyanarayan Shashtri

CONTENTS

Chapter I

INTRODUCTION

1.1. Metaphysical Detour	1
1.2. Why Water is a Serious Concern Today? - A Historical Discourse	2
1.3. Causes for the Rise in the Consumption of Water	3
1.4. Causes for the Decline in Availability of Fresh Water	3
1.5. Global Scenario	3
1.6. Water Scenario in India	4
1.7. Exploitation of Groundwater is the Hobson's choice for NCR	5
1.8. Techniques to Locate Groundwater Reservoirs	6
1.9. Role of Remote Sensing and GIS in Groundwater Studies	7
1.10 Objective of the Study	7

Chapter -II

LITERATURE REVIEW

2.1. Application of Remote Sensing and GIS in Hydrogeology and Hydrology	9
2.2. Application of Remote Sensing in Groundwater Exploration	11
2.2.1. Water Resource Mapping Through Remote Sensing	13
2.2.2. Outcropping Rock Type	14
2.3. Hydromorphogeological Conditions and Groundwater Resources	14
2.4. Lineament Analysis/ Inference	15
2.4.1. Lineament Classification	17
2.5. Geophysical Techniques and its Relevance in Hydrogeology	18
2.6. Hydrogeological Consideration	20
2.7. Digital Elevation Model	20
2.8. GIS in Hydrology	22
2.8.1. Interpolation in GIS	23
2.9. Role of Remote Sensing and GIS in Landuse/Land cover Mapping	23

2.10. Statistical Analysis	24
2.10.1. Principal Component Analysis	26

Chapter-III

STUDY AREA

3.1 General	28
3.2 Physiography	29
3.3 Geology	31
3.3.1 Lineament	33
3.3.2 Alwar group	33
3.4 Basement Topography	34
3.5 Stratigraphy of Delhi	35
3.6. Hydrogeology (Subsurface configuration and aquifer disposition)	
3.6.1. (a) New Delhi	35
3.6.2. (b) North West District	36
3.6.3. (c) South District	37
3.6.4. (d) South-West District	37
3.6.5. (e) West District	38
3.7. Geomorphology	38
3.7.1. Low Residual/Structural Hills	38
3.7.2. Pediment	39
3.7.3. Buried pediment	40
3.7.4. Drain	40
3.8. Temperature	40
3.9. Humidity	41
3.10. Anomalous Behaviour of Weather	41
3.11. Rainfall Pattern	41

Chapter-IV

MATERIAL AND METHODS

4.1. IRS - Indian Remote Sensing Satellite	42
4.1.1. Characteristics of IRS Satellite and their Sensors	42

4.1.2. Panchromatic	44
4.1.3. Linear Imaging and Self Scanning Sensor (LISS-III)	45
4.1.4. Wide Field Sensor (WiFS)	45
4.2 Shuttle Radar Topographic Mission (SRTM)	46
4.2.1 Wavebands commonly used in Radar Remote Sensing	46
4.2.2. Polarization Combinations for Radar	46
4.3 The Pre-Processing of Satellite Images	47
4.4. Survey of India Toposheet	48
4.5. Software used	48
4.6. Principles of Instruments used	50
4.6.1. Electrical Resistivity Method	50
4.6.2. Magnetic Anomaly Studies	52
4.6.3. X- Ray Diffractometer	52
4.6.4. ICP-AES Analysis- Multielement analysis by BRGM Procedure	54
4.7. Soil Particle Size Analysis	56
Chapter V	
RESULT AND DISSCUSSION	
5.1 Land use And Land cover	57
5.2 Litholog of Study Area	61
5.3 Land use and Land cover of RR Hospital	68
5.4 Soil Texture Analysis of RR Hospital	71
5.5 Resistivity Survey carried Out Various Sites in RR Hospital	75
5.5.1 Parade Ground	75
5.5.2 Personnel Lines	77
5.6 Image Processing of Satellite Image for JNU area	81
5.7 Comparison of LULC of Year 2000 and 2005	84
5.8 TIN & Digital Elevation Model of JNU	88
5.9 Geo-Magnetic Survey	91
5.10 Geo-Electrical Survey in JNU	92
5.10.1 Lay Out Of Geoelectrical Survey	93
5.10.2 Site 1 (JNU 1)	94

5.10.3 Site 2 (JNU 2)	95
5.10.4 Site 3 (JNU 3)	96
5.10.5 Site 4 (JNU 4)	97
5.10.6 Site 5 (JNU 5)	98
5.10.7 Site 6 (JNU 6)	99
5.10.8 Site 7 (JNU 7)	100
5.10.9 Site 8 (JNU 8)	102
5.10.10 Site 9 (JNU 9)	102
5.10.11 Site 10 (JNU 10)	103
5.10.12 Paschimabad (Discarded Site)	105
5.11 Yield Description	108
5.12 Striplogs of Drilling Sites in JNU	110
5.12.1 Description of Site1 (JNU 1)	112
5.12.2 Description of Site 2 (JNU 2)	112
5.12.3 Description of Site 3 (JNU 3)	116
5.12.4 Description of Site 4 (JNU 4)	116
5.12.5 Description of Site 5 (JNU 5)	117
5.12.6 Description of Site 6 (JNU 6)	117
5.12.7 Description of Site 7 (JNU 7)	121
5.13 GRIDDING METHODS	127
5.13.1 Inverse-Distance	127
5.14 Spatial Distribution of Water Quality Parameters	131
5.14.1 pH	132
5.14.2 Total dissolved solids	132
5.14.3 Electrical Conductivity	132
5.14.4 Bicarbonate	134
5.14.5 Chloride	134
5.14.6 Fluoride	135
5.14.7 Nitrate	136
5.14.8 Sulphate	138
5.14.9 Silica	139

5.14.11 Calcium	141
5.14.12 Potassium	141
5.14.13 Magnesium	142
5.14.14 Sodium Absorption Ratio	143
5.15 STATISTICAL ANALYSIS	145
5.15.1 Principal component analysis	145
5.15.2 Correlation Analysis	146
Chapter VI	
SUMMARY AND CONCLUSION	156-161
REFERENCES	
APPENDIX I	<u>PHOTOMICROGRAPHS</u>
APPENDIX II	<u>XRD DATA ANALYSIS</u>
APPENDIX III	<u>ICPAES ANALYSIS</u>

LIST OF TABLES

Table1.1 Distribution of Water stored on Earth (Source: From Franklin W: Schwartz 2003)	Pg. No. 3
Table1.2 Distribution of World's unfrozen freshwater supply (Source: From Franklin W: Schwartz 2003)	4
Table 2.1 Sensor Specific Eco-hydromorphogeology of Aravalli Ridge Area. (Source: Sensors, Mukherjee, S. 2008)	16
Table3.1.1 Geological succession around National Capital Territory (CGWB Report 2005)	32
Table 3.1.2 Geological succession around National Capital Territory	32
Table 3.2 Stratigraphy of Delhi	34
Table3.3 Seasons in study area	40
Table 4.1.1 Characteristics of IRS Satellite and their Sensors	42
Table 4.1.2 Pan Sensor Characteristics	43
Table 4.1.3 LISS-III Sensor Characteristics	43
Table 4.1.4 WiFS Sensor Characteristics	43
Table 4.1.5 Specifications of Different Sensors	44
Table 4.2.1 Wavebands commonly used in radar remote sensing	46
Table 4.2.2 Polarization combinations for radar	46
Table 4.4 Survey of India toposheet	48
Table.5.1 The area occupied by various LULC classes and its percent contribution	60
Table 5.2 The litholgy of Drilling Sites within the study area as per CGWB	64
Table 5.3 Sample no.1 In front of shopping complex and temple	72
Table 5.4 Sample no.2 in front of officer mess	72
Table 5.5 Sample no.3 in front of mortuary, Personnel Lines	73
Table 5.6 Sample no.4 in front of Cafeteria	74

Table 5.7 Magnetic Data of Parade Ground at Center in RR Hospital	75
Table 5.8 Magnetic Data in front of JRC and MRI at RR Hospital	77
Table 5.9 Magnetic Data at near personnel lines	77
Table 5.10 Magnetic Data at P-18 ground residence	78
Table 5.11 Magnetic Data behind P-18 and civil officers quarters	79
Table 5.12 Magnetic Data in front of RR hospital Adjacent to parade ground	80
Table 5.13 Magnetic data of Plot of behind RR hospital	80
Table 5.14 Change in various classes of land use and land cover in sq.km in JNU area from year 2000 & 2005	84
Table 5.15 NDVI values at various drilling sites in year 2000, 2004, 2005	87
Table 5.16 Resistivity of different zones as per litholog	94
Table 5.17 Magnetic data of Site 4 (PSR JNU)	97
Table 5.18 Magnetic Data at Site 6	99
Table 5.19 Magnetic Data at Site 7	100
Table 5.20 Details of different Drilling sites	107
Table 5.21 Tabulation of discharge in Lt/hr from circular orifice	108
Table 5.22 The lithology of primary drilling sites Site 1 (JNU1) and Site 2 (JNU2) within JNU	111
Table 5.23 The litholgy of primary drilling sites Site 3 (JNU3) and Site 4 (JNU4) within JNU	115
Table 5.24 The litholgy of primary drilling sites Site 5 (JNU5) and Site 6 (JNU6) within JNU	119
Table 5.25 The litholgy of primary drilling sites Site 5 (JNU5) and Site 6 (JNU6) within JNU	121
Table 5.26 Water levels observed at 7 primary drilling locations in JNU	126
Table 5.27 Individual Cumulative Water yields of 7 bore wells	126
Table 5.28 A few part of study area in north and south west falls in very high salinity category	144
Table 5.29 Correlation matrix of water quality parameters	148
Table 5.30 Correlation matrix of water quality parameters together with spectral reflectance of various bands of satellite image and NDVI values	149

Table 5.31 Extraction Method: Principal Component Analysis	151
Table 5.32 Extraction Method: Principal Component Analysis. Rotation Method: Varimax with Kaiser Normalization	153
Table 5.33 Various ICP-AES parameter and NDVI, spectral reflectance at different sites in JNU	155

LIST OF FIGURES

	Pg. No.
Fig.3.1. Location of Study Area	29
Fig 3.2 Geo-referenced Image of Study Area	30
Fig 3.3 Structural Map of the Study Area	31
Fig.3.4 The Fence diagram of the Study Area	36
Fig.3.5.Geomorphology of the Study Area	39
Fig.4.1. Resourcesat-1, mounted on top of the PSLV-C5's fourth stage and LISS - III Camera (Source: ISRO)	45
Fig.4.2 Methodology Adopted for Image Processing and GIS Analysis	49
Fig.4.3 DDRIII resistivity meter (IGIS Hyderabad)	50
Fig.4.4 Electrical Circuit for resistivity determination and electrical field for a homogenous subsurface stratum	51
Fig.4.5 Schlumberger arrangement	52
Fig.4.6 Proton precession magnetometer (igishyderabad)	53
Fig.4.7 X-Pert PRO X-Ray Diffraction System	53
Fig. 4.8 Methodology adopted for ICP-AES analysis	54
Fig 4.9 Sampling Sites of the Water Quality data	55
Fig.5.1. LU/LC of the Study Area	58
Fig.5.2. Percentage Contribution of Various LULC classes	58
Fig.5.3. Digital Elevation Model (DEM) of the Study Area	60
Fig.5.4. Drilling Sites within the study area as per CGWB (Central Ground Water Board) datasets of year 2000-2005 and their location plan	62
Fig.5.5. Elevation Contours (in metres) within the Study Area	63
Fig.5.6. Three Dimensional Contours (in metres) of the Study Area	63
Fig.5.7. Three Dimensional Fence Diagram of the Study Area (View 1)	65
Fig.5.8. Three Dimensional Fence Diagram of the Study Area (View 2)	65
Fig.5.9. Lithologs Plotted for the Study Area	66
Fig.5.10. Aquifer Model generated for the Study Area	66
Fig.5.11. Aquifer Thickness (Isopach) of the Study Area (in metres)	67
Fig.5.12. Image classification of RR hospital to infer change in	

land use and land cover (2001 & 2003)	68
Fig.5.13.Change in various classes of land use and land cover in RR Hospital area from year 2000 & 2003	69
Fig.5.14 Resistivity Survey carried out various sites in R. R. Hospital	70
Fig.5.15. Triangle of soil textures for describing various combinations of sand silt and clay (soil survey staff)	71
Fig.5.16. Soil textural class In front of Shopping Complex and Temple	71
Fig.5.17. In front of officer's mess	72
Fig.5.18. Soil textural class in front of mortuary, Personnel Lines	73
Fig.5.19. Soil textural class in front of Cafeteria	74
Fig.5.20. Vertical Electrical Sounding Plot of Parade Ground	75
Fig.5.21. Vertical Electrical Sounding Plot of point in front of JRC and MRI	76
Fig.5.22. Vertical Electrical Sounding Plot at near Personnel lines	77
Fig.5.23. Vertical Electrical Sounding Plot at P-18 ground residence	78
Fig.5.24. Vertical Electrical Sounding Plot behind P-18 and civil officers quarters	79
Fig.5.25. Vertical Electrical Sounding Plot in front of RR hospital Adjacent to parade ground	79
Fig.5.26. Vertical Electrical Sounding Plot of behind RR hospital	80
Fig.5.27. Image analysis to infer change detection in JNU between year 2000 & 2004, 2000 & 2005	81
Fig.5.28. Image classification of RR hospital to infer change in land use and land cover (2000 & 2005)	82
Fig.5.29.Change in various classes of land use and land cover in RR Hospital area from year 2000 & 2005	83
Fig.5.30. NDVI output for the respective images of years 2000, 2004, 2005	85
Fig 5.31 NDVI values at different sites in jnu in year 2000, 2004 and 2005	86
Fig 5.32 Geological setup of JNU	88
Fig 5.33 Digital Elevation Model of JNU	89
Fig 5.34 Triangular Irregular Network of JNU	89
Fig 5.35 Magnetic survey points in JNU campus	91

Fig 5.36 VES survey points of JNU	92
Fig 5.37 Vertical Electrical Sounding Plot in JNU at site 1	94
Fig 5.38 Vertical Electrical Sounding Plot in JNU at site 2	95
Fig 5.39 Vertical Electrical Sounding Plot in JNU at site3	96
Fig 5.40 Vertical Electrical Sounding Plot in JNU at site 4	97
Fig 5.41 Vertical Electrical Sounding Plot in JNU at site 5	98
Fig 5.42 Vertical Electrical Sounding Plot in JNU at site 6	99
Fig 5.43 Vertical Electrical Sounding Plot in JNU at site7	100
Fig 5.44 Vertical Electrical Sounding Plot in JNU at site 8	101
Fig 5.45 Vertical Electrical Sounding Plot in JNU at site 9	102
Fig 5.46 Vertical Electrical Sounding Plot in JNU at site 10	103
Fig 5.47 Vertical Electrical Sounding Plot in JNU at site 11	104
Fig 5.48 Vertical Electrical Sounding Plot in JNU at site 12	104
Fig 5.49 Vertical Electrical Sounding Plot in JNU at site 13	105
Fig 5.50 Vertical Electrical Sounding Plot in JNU at site Pashimabad	105
Fig 5.51 Vertical Electrical Sounding Plot in JNU at site 14	106
Fig 5.52 Location Plan for 7 sites selected for primary drilling	107
Fig 5.53 Three dimensional elevation contours of the sites within study area	109
Fig 5.54 Elevation contours of the sites within study area	109
Fig 5.55 Striplogs of drilling sites, Site 1 (JNU1) and Site 2 (JNU2) (depth in metres)	110
Fig 5.56 Striplogs of drilling sites, Site 3 (JNU3) and Site 4 (JNU4) (depth in metres)	114
Fig 5.57 Striplogs of drilling sites, Site 5 (JNU5) and Site 6 (JNU6) (depth in metres)	118
Fig 5.58 Striplogs of drilling Site 7 (JNU7) (depth in metres)	120
Fig 5.59 Three Dimensional Lithologs generated for Drilling Sites (View 1)	122
Fig 5.60 Three Dimensional Lithologs generated for Drilling Sites (View 2)	122
Fig 5.61 Lithology Solid Model (generated using data from drilling sites)	123
Fig 5.62 A sliced panel from Lithology Solid Model across all 7 drilling sites	124
Fig 5.63 Three Dimensional Fence Diagram	125

Fig 5.64 The Weighting Exponent was chosen as 2.0 and Sector Angle as 450(8 Sectors) with 3 points per sector	128
Fig 5.65 Aquifer Model generated for 7 primary Drilling Sites (View 1)	129
Fig 5.66 Aquifer Model generated for 7 primary Drilling Sites (View 2)	129
Fig 5.67 Aquifer Thickness (Isopach) for JNU - (in metres)	130
Fig.5.68 Spatial distribution of pH in the study area	131
Fig.5.69 Spatial distribution of TDS in the study area	131
Fig 5.70 Spatial distribution of TDS in the Study Area	132
Fig.5.71 Spatial distribution of Bicarbonate in the Study Area	133
Fig 5.72 Spatial distribution of Chloride in the Study Area	135
Fig 5.73 Spatial distribution of Flouride in the Study Area	136
Fig 5.74 Spatial distribution of Nitrate in the Study Area	137
Fig 5.75 Spatial distribution of Nitrate in the Study Area	138
Fig 5.76 Spatial distribution of Silica in the Study Area	139
Fig 5.77 Spatial distribution of Sodium in the Study Area	140
Fig 5.78 Spatial distribution of Calcium in the Study Area	141
Fig 5.79 Spatial distribution of Potassium in the Study Area	142
Fig 5.80 Spatial distribution of Magnesium in the Study Area	143
Fig 5.81 Spatial distribution of SAR in the Study Area	144
Fig 5.82 Scree Plot	152
Fig 5.83 PCA Analysis: Factor loading (Component Loading for various PCA factors)	154

Introduction

INTRODUCTION

Chapter-I

1.1. METAPHYSICAL DETOUR

Since antiquity man believed that there are five primal elements of the universe-Earth, Water, Air, Fire and Ether. In Bhagvad Gita Krishna Says:

भूमिरापोऽनलो वायुः खं मनो बुद्धिरेव च।

अहंकार इतीयं मे भिन्ना प्रकृतिरष्टधा॥

Earth, Water, Air, Fire, Ether, Mind intelligence and false ego –all together these eight constitute my separated material energies (Chapter 7 Text IV).

In chapter 10 Lord Krishna reiterates

सरसामस्मि सागरः॥

Among the bodies of water I am the ocean.

There is no wonder that all the religions of the world have taken pains to emphasize the importance of water for all kinds of life on earth. The concern was simple; to keep the water bodies pure and potable.

Hinduism: Rivers have been and continue to be an integral part of Hindu religious practice. More than fifty Vedic hymns praise the Saraswati, a river (now dry) associated with the goddess of learning and culture. To Hindus all rivers are sacred, but the seven are sacred of the sacreds namely Ganges, Yamuna, Godavari, Saraswati, Narmada, Sindhu and Kaveri. Taking bath in sacred rivers, it is believed, purifies the sinners. Hence there is strong religious injunction not to defile and dirty the rivers and any other water bodies.

Christianity: Almost all Christian churches or sects have an initiation ritual involving the use of water in Baptism. Baptism is a symbol of liberation from the yoke of sin that separates believers from God. The use of water is important for its own symbolic value in

three ways: it cleans and washes away dirt, fills everything it enters as God fills those who are immersed in Him and one need water to survive physically as one need God to survive spiritually.

Islam: Water is of profound importance in Islam. It is considered a blessing from God that gives and sustains life and purifies human kind and the earth. God's throne is described as resting on the water and paradise is described as "Gardens beneath which river flows". It seems that for the holy Quran the most precious creation on Earth is water whose availability creates the condition of possibility of positivity of life and thereby birth and burgeoning of human civilization.

Judaism: In Judaism ritual washing is intended to restore or maintain a state of ritual purity. During the Pre-exilic times ablutions were indispensable for initiation rite and to administer the rituals. It survived in exilic and Post exilic eras as well.

Zoroastrianism: The cardinal canon of Zoroastrianism is the conflict between GOOD and EVIL, in other words the PURE and the IMPURE. Hence everything must remain in PURE. Water being a substance which purifies other things, it holds a sovereign status in Zoroastrianism. To maintain the sovereignty and sacredness of water there is stringent injunction against urinating, spitting or washing dirty linens in rivers and for that matter in any other water body.

Sikhism: Amrit is the top institution of the Sikh faith. It is "Abae-Hayat" the water bestowing eternal life – eternity and immortality.

1.2. WHY WATER IS A SERIOUS CONCERN TODAY? - A Historical Discourse:

It is said that civilization is order, justice and beauty. It is not only the civilisational demand of beauty which has led to the rise in the demand of water consumption but also the mundane quotidian needs of water have also gone up. Historically speaking the water consumption has by and large exponentially grown because of the need of modern agriculture, industry and household consumption. With the advent of industrialization two secular trends have been observed first the rise in the consumption of water leading to downfall availability of groundwater and second with the discharge of industrial effluents the water bodies are getting polluted and toxified (anthropogenic and geochemical induced). In other words the onward march of the civilization necessitates more and more consumption of water.

1.3 CAUSES FOR THE RISE IN THE CONSUMPTION OF WATER:

- 1- Irrigation – Rise in the population necessitates exploitation of land to the utmost by going for more than one crop cycle.
- 2- High Yielding Variety seeds require more water than the traditional seeds.
- 3- Non electronic industries also require more and more water.
- 4- With the spread of the modern sanitation the water consumption has gone up.
- 5- Expansion of transport sector has led to the rise in water consumption.

It is ironical that there is exponential growth in the consumption of water on the one hand; on the other hand there is tremendous decline in the availability of fresh water.

1.4. CAUSES FOR THE DECLINE IN AVAILABILITY OF FRESH WATER:

- 1- With the increasing pace of industrialization the water bodies/ on surface and below surface both/ are getting contaminated leading to the decline in the availability of fresh water.
- 2- With the neck break pace of urbanization the traditional tanks available for surface water and recharging of groundwater have been reclaimed for building purposes. The result is there is no surface structure available to hold rain water to recharge the underground wells despite having good amount of rainfall.
- 3- Seismotectonic activity is also partially responsible for the change in aquifer disposition, which is further responsible for quantitative and qualitative changes in fresh groundwater (Mukherjee, 2003& 2001).
- 4- Improper landuse practices have drastically reduced the groundwater recharge (Mukherjee, 1997).

1.5. GLOBAL SCENARIO:

By and large the whole of the New World, Sub Saharan Africa and the whole of Europe are water rich continents of the world in terms of both/ glacial and rain fed waters. The major regions which face the problem of potable water deficiency are North Africa, West Asia and South Asia. The Earth has an estimated 330 million cubic miles (mcm) of water, with most of it occurring as non-potable seawater (Table1.1).

Pools of water	Stored Volume(cubic miles)
Oceans	322,600,000
Glacial Ice	6,000,000
Groundwater	2,000,000
Atmosphere	3,000

Table1.1 Distribution of Water stored on Earth (Source: From Franklin W: Schwartz 2003)

Interestingly, groundwater makes up only a tiny fraction, just 0.06%, of the total water available on the Earth. However this relatively small volume is critically important because it represents 98% of the fresh water readily available for civilizational needs (Zaprozec and Miller, 2000).

Source	Volume(million cubic miles)
Groundwater	2.0
Lakes	0.031
Soil Moisture	0.012
Streams	0.002
Swamps	<0.002

Table1.2 Distribution of World's unfrozen freshwater supply (Source: From Franklin W: Schwartz 2003)

1.6. WATER SCENARIO IN INDIA:

The water scenario of India is not very bright it has got only two perennial rivers in North India Ganges and Brahmaputra. In south all the rivers are rain fed but for Godavari and Kaveri. In other words the water availability through rivers is as skewedly distributed as that of rainfall in the country. 70% of the rainfall in the country takes place within a fortnight. The current population of India is approximately 1.10 billion and it is projected that by the year 2025 the population of India will be about 1.4 billion (FAO, 2005).

The National Capital Region (N.C.R) falls in the Western zone of the country. It gets an average rainfall of 632mm/year. Moreover National Capital Territory (NCT) is situated on the banks of Yamuna which is tributary of Ganges. Yamuna's water has been channelized to other areas. Therefore by the time Yamuna reaches Delhi it does not remains a river but turns into a drain. The water problem in National Capital Territory is

not an exception. There is a universal and secular trend in this country and elsewhere that with the unprecedented growth of urbanisation, the traditional surface structures like tanks, hauz been filled for constructing buildings. The result is that there is neither surface water nor recharge wells.

With the rising population of NCR and the declining availability of water due to industrial pollution filling up of the surface tanks and ponds the water scenario of NCR is mortally alarming. The result is, in summers many zones of NCR fail to quench their thirst. It is the societal need of NCR which compelled me to take up a topic “**An Integrated Approach through Remote Sensing, GIS and Geophysical tools to Assess Water Resources in part of National Capital Region**” whose result should not remain a dead letter but a blue print for action to alleviate the common suffering of water deficiency of the denizens of NCR.

Continuous failure of monsoon, increasing demand and over exploitation leads to depletion of groundwater level in many part of the country. Groundwater is not only an important component of the hydrological cycle but also the important source of drinking water. Comparative estimation indicates that probably at least two hundred times the volume of annual run off from the world’s river is stored as groundwater beneath the land surface(Maning, 1987).Therefore detailed investigation regarding the occurrence and renewal of groundwater has become utmost necessity. Safe use, tactical exploration and management of groundwater resources require good knowledge and proper understanding of the groundwater regime and its control

1.7. EXPLOITATION OF GROUNDWATER IS THE HOBSON’S CHOICE FOR NCR:

Groundwater is the water found in spaces between soil particles and rocks, and within cracks of the bedrock (Mukherjee et.al., 2007). Because of its availability and general good quality, groundwater is widely used for the household needs and other purposes. Groundwater is more desirable than surface water for the following reasons-

1. It is commonly free of pathogenic organisms and need no elaborate purification for domestic and industrial uses.

2. Temperature is nearly constant which a great advantage is if the water is used for heat exchange.
3. Turbidity and colour are generally negligible.
4. Chemical composition is generally constant.
5. Groundwater storage is always greater than surface water storage, so that groundwater supplies are not seriously affected by short duration droughts.
6. Biological contamination in groundwater is seldom noticed.

Groundwater is always taken for granted, but recent circumstances indicate that it is seriously vulnerable to pollution and depletion. In many locations, pollution poses the great threat. Contaminants, which threaten people's health, have been found in several important groundwater reservoirs (Mukherjee, 1998). Some of the contaminants like persistent organic pollutants (POPs) may be so expensive to remove that they make the water virtually non-potable for years (Mukherjee et al, 2004). Because of this threat, it is important to understand the processes that make groundwater available for use and how human activities sometimes threaten this resource.

1.8. TECHNIQUES TO LOCATE GROUNDWATER RESERVOIRS:

Groundwater becomes depleted in an area where more water is being drawn out of an aquifer and consumptively used than in entering or recharging the aquifer. A situation may involve someone pumping a large amount of water from a small aquifer and causing a neighbour's well to go dry (lowering the water table below the well screen). Rapidly expanding urban area often imposes an extra burden on the groundwater supplies in the form of both depletion and pollution.

In the present work, more thrust has been given on the detection of suitable location in the area which has poor groundwater potential and area which can serve as good point to recharge to the groundwater, also undertaken in this exercise an endeavour is made to generate a model to find the trend of flow of the surface water during rainy months so that this water can be diverted toward the areas selected for recharging the groundwater. All this has been achieved using geophysical technique viz. resistivity survey, magnetic survey, soil analysis, litholog analysis draw down test of existing pumps and using

RESULT AND DISSCUSSION

	pH	EC	TH	HCO ₃	Cl	SO ₄	NO ₃	F	PO ₄	Ca	Mg	Na	K	SiO ₂
pH	1.000													
EC	-0.386	1.000												
TH	-0.452	0.795	1.000											
HCO ₃	-0.297	0.376	0.106	1.000										
Cl	-0.341	0.970	0.827	0.224	1.000									
SO ₄	-0.381	0.820	0.678	0.499	0.810	1.000								
NO ₃	-0.170	0.152	0.000	0.311	0.047	0.220	1.000							
F	0.170	-0.093	-0.222	0.074	-0.119	0.073	0.255	1.000						
PO ₄	-0.191	-0.038	0.003	0.159	-0.065	0.047	-0.149	-0.035	1.000					
Ca	-0.448	0.682	0.959	0.004	0.719	0.519	-0.099	-0.290	0.016	1.000				
Mg	-0.360	0.750	0.918	0.020	0.739	0.537	0.015	-0.142	-0.042	0.861	1.000			
Na	-0.234	0.912	0.604	0.329	0.867	0.671	0.092	0.025	-0.063	0.525	0.636	1.000		
K	-0.280	0.449	0.323	0.627	0.345	0.549	0.188	-0.072	-0.013	0.232	0.232	0.220	1.000	
SiO ₂	0.127	-0.332	-0.402	0.115	-0.337	-0.269	0.220	-0.369	0.039	-0.377	-0.503	-0.368	0.108	1.000

Table 5.29 Correlation matrix of water quality parameters

The main objective of the thesis is to assess the water resources of a part of National Capital Region through integrated approach of Remote sensing, GIS and Geophysical tools. Following points were considered to achieve this objective:-

- (1) To carry out the resistivity survey in the study area
- (2) To carry out the magnetic survey of the study area
- (3) Collection of water samples from various sites rivers, ponds and groundwater
- (4) Chemical Analysis of water to measure various chemical parameters (Anions and Cations) and if any organic pollutant present
- (5) Soil samples collection and its chemical and textural analysis
- (6) Mode of vegetation present
- (7) Develop an integrated GIS model incorporating all above data for assessment of water resources in a part of National Capital Region.

Literature Review

LITERATURE REVIEW

CHAPTER -II

Review of literature on theories, methods and case studies by various researchers is an indispensable exercise to initiate any research. In this case the literature reviews are related to techniques and their applications in water resources assessment and management.

2.1. APPLICATION OF REMOTE SENSING AND GIS IN HYDROGEOLOGY AND HYDROLOGY:

Remote sensing, which is defined as the science of deriving information about an object from measurements made at a distance from the object and without the sensor actually coming into contact with it (Buiten,1993; Michel,1986; Sabins,1997). Remote sensing technique by virtue of synoptic coverage, repetitive data acquisition capability, spatial information, real time data collection and computer compatibility offers an effective first hand tool in mapping and monitoring of natural resources within a reasonable short time frame (Buiten,1993; Druny,1986; Sabins,1997; Wirdum,1993). Satellite remote sensing is the use of sensors, normally operating at wavelength from visible (0.4m) to the microwave (0.25m), on board satellite to collect information about the earth's atmosphere, oceans, lands and ice surfaces. The main function of remote sensing is to provide spatial information about the surface and near surface feature of the Earth in form of aerial photograph and satellite imageries for analysis, interpretations and mapping (Mukherjee, 2004). There are many hydrologically relevant parameters that can be determined by using remote sensing data (Hochschild et al., 2000). It can supply input and validation data for hydrological models and concentrate on water balance and water demand. One of the key points in the remote sensing applications is use of different image sources for improving the result. The main limitations of the remote sensing technique in hydrogeological applications is due to small subsurface penetrations of the electromagnetic radiations available in present satellite sensors, while groundwater is present at ten of meters below ground surface(Mukherjee,2008). Therefore, use of remote sensing technique is considered as an indirect tool with reference to groundwater investigations. Geographic Information System (GIS) is the

tool that serves as the platform for integrated analysis and interpretations and modelling (Mukherjee, 1998).

Synoptic view facilitates the study of objects and their relationships. Spectral signatures permit identification of various features, while the temporal aspect allows change detection in environment. The real advantage is the real time measurement that facilitates constant and effective monitoring. The main advantage of the remote sensing is that the data is in the digital form and can be analyzed easily with the help of computers. The wavelengths widely used in the remote sensing are visible and near infrared in the wavelength of 0.4 - 3 μ m. Colour Composite images from Landsat Thematic Mapper and Indian Remote Sensing Satellite (IRS) meticulously used to deal groundwater potential over extensive geographical area of Varah river basin, India (Murthy2000). Use of microwave remote sensing has added advantage in areas which has scanty vegetation (Mukerjee et. al., 2003).

The application areas for remote sensing data are both wide and varied (Slogget and MaGeachy, 1986). Radiometric data potentially represent a very useful source of information in pedological research and in the study of water quality (Leone et al., 1995) though remote sensing cannot be used for ground water studies. But the remote sensing data allows us to make indirect references regarding subsurface through surficial expression of the aquifer. The subsurface hydrological conditions are inferred based on identification and correlation of surface phenomenon involving geological features and structures, geomorphology, surface hydrology, soils and soil moisture anomalies, vegetation types and distribution, land use and many others as indicators. The benefits that occur in the use of remotely sensed data are usually greatest when they are applied for large-scale preliminary investigation of ground water reserves. Remote sensing data have two distinct advantages. Remote sensing platforms provide data with high resolution in space and data can be obtained for areas that has no record of measurements (e.g. remote areas) therefore remote sensing data, particularly satellite data can be most helpful for design and operation purposes if they are used in combination with ground truth. Selection of suitable sensor and analysis of the combination of the multisensor data has proved its potential to infer suitable location for groundwater exploration (Mukherjee, 2008). The disadvantage of satellite data are unfavourable combination of resolution in time and space (Cracknell and Nirala, 1997). Air borne geophysical exploration is highly used in ground water prospects (Patterson and Bosschart,

1987). Remote sensed data proven to be much useful in targeting lineaments in igneous and metamorphic rock for groundwater exploration (Sander 2007).

2.2. APPLICATION OF REMOTE SENSING IN GROUNDWATER EXPLORATION:

The science of remote sensing depends upon the wavelength of electromagnetic radiation. These radiations are either emitted or reflected from the surface or from a relatively shallow layer of the earth. Because of their underground dispositions, the groundwater aquifers cannot be detected directly through satellite images. An expert hydrogeologist can however infer subsurface hydro geological conditions based on various key indicators (Roy, 1991). Presence of groundwater largely depends upon the availability of porosity in the rocks, on degree of weathering and intensity/nature of fractures and lineaments (Mukherjee, 2006). The phreatophitic vegetation cluster as directly separated from other vegetation groups and areas of these vegetation zones were indicated as groundwater discharge zones. Digitally analysed results matched well with groundwater levels were superimposed on the raster image (Mukherjee, 2004).

The various surface features normally captured through remote sensing data, which serve as guides for groundwater investigation, could be grouped into two categories; first order or direct indicators, i.e., features directly related to groundwater occurrence and movement and second order or indirect indicators, i.e., surface features indirectly linked with ground water regime (Ellyett and Pratt, 1975; Gupta, 1991; Singhal and Gupta, 2001).

(a) First Order or Direct Indicators

- Features associated with recharge zones: rivers, canals, lakes, ponds etc.
- Features associated with discharge zones, springs and other sites of effluent seepage.
- Soil moisture anomaly
- Anomalous vegetation

(b) Second Order or Indirect Indicators

- Topographic features or general surface gradients
- Types of rocks –hard rock and soft rock
- Geological features such as major faults, thrusts, shear zones, folds etc.
- Depth of weathering and regolith
- Landforms
- Lineaments, joints and fold axial traces

- Drainage characteristics
- Fracture system in hard rock areas
- Types of soil and humus content
- Natural vegetation
- Special geological features like karsts sink holes, alluvial fans, buried paleo channels, dikes and reefs, unconformities, salt encrustation etc. that may have a unique bearing on ground water occurrence and movement.
- Extra hydraulic continuity of formations like surface water divides vis-a vis recharge and discharge zones from synoptic overview.

Selection of spectral bands of remote sensing data is crucial since different objects reflect their characteristic features at different wavelengths. Seasonal impacts are well manifested on vegetation, land use, fluvial morphology and soil tones of pre-monsoon and post monsoon periods. Temporal resolution matters for analysis of rainfall, drought and flood frequency, as well as for soil moisture and crop growth study. Landforms geological structures and lineaments are studied more clearly through images of pre-monsoon period due to thin vegetation cover. Surface water bodies such as stream, channels, lakes, etc. are clearly distinguishable in both optical and microwave data due to their typical shape, tone and pattern. Soil moisture anomaly is better studied through NIR, TIR, and microwave frequencies. On a panchromatic photograph, regions with high soil moisture show darker tones. Very high reflectance in visible and NIR bands and low drainage density implies deep water table. Springs mark ground water discharge sites and are detectable on panchromatic aerial photographs, multispectral images and TIR data for higher surface moisture, anomalous vegetation, and temperature anomaly associated with them visible, NIR, SWIR and TIR data are used for the qualitative study of soil moisture, while passive and active remote sensing data are used for quantitative evaluation of soil moisture variations (Singhal and Gupta, 2001; Singh et al., 2005). Vegetation and its state is also an indicator of groundwater occurrence. Vegetation density, state and its growth can be studied through red and NIR bands, as reflectance in these wavelength ranges is governed by leaf pigments. Vegetation stress can be studied using SWIR band since the reflectance in this range is governed by leaf water content. Presence of phreatophytic vegetation indicates a shallow water table, whereas xerophytic plants imply a dry arid climate. Some specific plants are indicative of groundwater table as well as chemical or mineralogical nature of groundwater. Therefore,

identification of plant species through high resolution aerial photographs and satellite imageries are highly useful for groundwater investigation. Rock types are identified and interpreted based on associated structures and landforms. Geological structures such as bedding, foliation, folds, joints, faults, shear zones etc play an important role in lateral and vertical movements of ground water and therefore their mapping is very important. Mapping of special hydrogeological features are extremely helpful for ground water investigation.

Radar energy penetrates upto several meters below the ground surface. Since radar is diffusively scattered by rough surfaces, the mountains appear bright, the smooth sand plains throw darker tones, and the irregular trajectories of buried channels unveil their position in radar imageries. Therefore radar data is useful in delineation of ground water potential zones and targeting well drilling sites (Drury, 1998; Wang et al., 2000; 2002). Out of all geological structures, study of lineaments is most important for groundwater investigation as they are surface manifestations of subsurface weak zones, thus influence infiltration (Mukherjee, 1999).

2.2.1. WATER RESOURCE MAPPING THROUGH REMOTE SENSING:

Remote sensing technology has opened new vistas for the study of various components of hydrologic cycle and thus for forecasting, evaluation, assessment and management of highly dynamic water resources. Overall, remote sensing can augment the existing methods to a great extent in hydrologic data collection (Engman and Gurney, 1991). Remote sensing plays useful role in delineation of country's available water resources when the need of water is increasing with respect to the increasing demographic pressure. The use of remotely sensed data for water resource monitoring and management is basically for the following

- (a) River morphological analysis
- (b) Flood –Plain Mapping and Monitoring
- (c) Surface Water Inventories
- (d) Groundwater Mapping
- (e) Detection of Abandoned /Paleochannels
- (f) Water logging and Salt affected Mapping

In groundwater studies aerial and satellite data in conjunction with ground surveys have been applied to (i) select likely areas for groundwater exploration, (ii) progressively narrow down the areas in pinpointing the well drilling sites, (iii) find the indicators of the presence of groundwater recharge and discharge (v) indicate the quality of groundwater and (vi) monitor and acquire

certain remote sensing based parameters of use in hydrologic equations for assessment of groundwater resource potential. However most contribution of remote sensing are oriented towards improving upon the ground surveys and probability of success in well drilling in the exploration of regional and local groundwater supplies (Agarwal, 1998). Remotely sensed data used for groundwater exploration mostly includes photography or imagery obtained in the visible or NIR region with the possible exception being the TIR data (Myer and Welch, 1975). Superficial features identified on aerial photographs that aid in evaluating groundwater conditions (Balakrishnan, 1986).

Detection keys for rocky and other aquifers

2.2.2. OUTCROPPING ROCK TYPE:

- Landforms: Topographic relief
- Outcrop pattern: Banded patterns for sedimentary rocks (outlined by vegetation in humid regions) plateau or homocline for basalt flows, or curving patterns for folded beds.
- Shape of drainage basin
- Drainage patterns, density and texture
- Fracture types and symmetry(as inferred by lineaments)
- Relative abundance, shape and distribution of lakes
- Tones and Texture: Difficult to describe, best determined by study of known examples
- Types of native land cover

2.3. HYDROMORPHO GEOLOGICAL CONDITIONS AND GROUNDWATER RESOURCES:

Hydrmorphogeology terminology was first used by Prof. A.K.Roy of Indian Institute of Remote Sensing, Dehradun, India in the PhD thesis of S. Mukherjee from Banaras Hindu University, Varanasi (Mukherjee, 1989). Geomorphic processes are the result of complex interaction between agents of geology, climate, hydrology, topography, soils and organisms, while few of these properties can be measured directly, the remotely sensed data can provide useful surrogate information (McKean et al, 1991; McDermid, 1994). Quantitative morphometric parameters of the drainage basin also play a major role in evaluating the hydrologic parameters which in turn help us to understand the ground water situation (Krishnamurthy and Srinivas, 1995). Valley fills, paleochannels, river terraces, buried pediment zones, lineaments, fault/thrust zones, shear zones etc identified by remote sensing techniques are considered suitable for ground water

exploration (Chi and Lee, 1994; Mukherjee, 1996; Roy, 1991). The use of thematic overlays as an aid to the interpretation of remotely sensed data has great potential in water resource management (Sharma and Anjanayu, 1993). Conventional prospecting tools viz., hydrogeological and geophysical instruments generally do not yield the relevant details and occasionally exhibit lack of resolution. Integration of satellite data and vertical electrical sounding (VES) data as well as magnetic intensity data, indirectly giving the potential fracture zones using other collateral data generated from the imagery as well as collected from various institutions is used to assess the ground water potentiality of various geomorphic units (Chandu, 1997). In the region where bedrock is exposed, multispectral remote sensing have been found useful for recognizing altered rock because their reflectance spectra differ from those of country rocks (Rowan et al., 1975). Various hydrogeomorphological features such as abandoned channels, buried channels, lineament, water bodies, vegetation and flood plain, were mapped using Landsat imagery in coalescence resistivity survey to explore groundwater in Saurashtra peninsula, India (Shahi and Sood, 1985). IRS LISS III data along with collateral data set has been utilized to extract information on the geomorphic features of a hard rock terrain in Vidisha district of Madhya Pradesh for ground water exploration and artificial recharge (Saraf and Choudhary, 1997). Further GIS is developed to use select suitable site groundwater. Geomorphic studies helps in deciphering the shallow and deep aquifer in the exploration of groundwater (Chatterjee and Singh 1980).

2.4. LINEAMENT ANALYSIS/ INFERENCE:

Lineaments are linear alignments for structural lithological, topographical, vegetational, drainage anomalies etc., either as straight lines or as curvilinear features. There are usually fractures, joints or faults in the bedrock (Gary et al., 1972). Remotely sensed data can provide for the explanation of ground water, mineral and hydrocarbon, location of dam sites and study of earthquake and lineament pattern of the area (Rowan, 1975). Lineaments are linear alignments of regional or zonal morphological features. Its surface expressions in many areas are found as fracture or fault zones ranging from a few kilometers to hundreds of kilometers (Goetz and Rowan, 1981; Drury, 1986; Prost, 1994; Sabins, 1997). Lineaments are referred as natural geological features. However, identification and separation of natural lineaments from artificial linear features on aerial photographs and satellite imageries need understanding of the physiographic and geology of the region.

Geomorphic Unit	Landform	Hydrogeology	Suitable flora	Sensor
Residual/ structural hills	Rocky ridges tors and mounds.	Massive compact jointed quartzites. Poor ground water	Prosopis juliflora (Kabulikikar) Azadirachta indica (Neem) Miragyna parviflora	Lineaments intersection and species identification is possible with IRS-1D LISS-III merged with PAN data.
Pediment	Undulating, eroded and dissected, shallow buried pediment with rock exposures. Thickly vegetated with scrub.	Weathered coarse Gritty or arcose quartzite with cover of clayey and silty soil along stream course. Moderate to good ground water prospects along fracture and shear zones.	Acacia senegal (Kumta) Wringhitia tinctoria (Dudhi) Balanites aegyptiaca (Hingot) Streculia urens (Kullu) Boswellia serrata (Salai)	Groundwater potential Pediment and NDVI based species identification possible in AWIFS, IRS-LISS-III and PAN data.
Buried Pediment	Plain to gently sloping ground with occasional rock outcrops.	Silty clayey and at places gravelly soil derived from weathering of arcose and gritty quartzite. Good ground water prospects	Ficus benghalensis (Bargad) Cassia fistula Albizia lebeck (Siras) Ficus religiosa (Peepal) Ficus infectoria (Pilkhan) Terminalia arjuna (Arjun)	Buried Pediment delineation with Pediment is possible by using IRS-PAN and LISS-III merged data but the landform units are difficult to infer by using AWIFS data.

TABLE 2.1 Sensor Specific Eco-hydromorphogeology of Aravalli Ridge Area.

(Source: Sensors, Mukherjee, S. 2008)

Mapping of geological lineaments using satellite images for hydrogeological and hydrological investigation has following two steps.

Step I: The correct identification of lineaments representing crustal fracturing of thick – unconsolidated materials overlying buried structures.

Step II. The correct interpretation and assessment of these linear features with regard to their influence on the ground water movement and accumulation

The various factors affecting lineament analysis involved are as follows;

At stage I:

- a. The scale of the imagery used.
- b. The density of the non-geological features present.
- c. The orientation of the important geological features.
- d. The surface expression of the important geological features.

At stage II:

- a. The subsurface morphology of the lineaments.
- b. The hydrological functions of the lineaments.
- c. The amount of ancillary information available.

2.4.1. LINEAMENT CLASSIFICATION:

Differentiation of geological lineaments is important for groundwater, from investigation point of view since they could act as promoters (faults, joints, shear zones etc.) or barriers to subsurface flow. High resolution satellite data and aerial photographs might be helpful in this regard. Further, characterization of faults (normal, reverse and strike slip), fractures (tensile, compressional and shear), and joints (dilatational and compressional) in remote sensing data without any supportive evidence from field study or past mapping is almost impossible. However, certain supportive evidence could be collected from the satellite images itself, for example if some fracture trends are associated with the principal streams or vegetation lines, this is an indication of the present day stress field and surface manifestation of groundwater movement (Onorati et al., 1985; Seasoran, 1985; Waters et al., 1990).

Categorization of lineaments into multiple classes in terms of their hydrogeological significance is more effective than to deal with a single lineament class. However, it demands various supportive data which are difficult to obtain. Integration of tectonic history, outcrop mapping, vegetation pattern, drainage, along with data of subsurface fracture depth enables a better understanding and interpretation of the hydrological functions of the lineaments and their subsequent classification (Sander, 1996). The most productive fractures might be suppressed

under thick alluvium or weathered materials and these are less conspicuous than the prominent lineaments (Greenbaum, 1987).

While some researchers have advocated for classification of lineaments on the basis of their inferred hydrological and geological function (Waters et al, 1990), others have favoured classification based on their certainty (Wheeler, 1983). In the same way, some researchers (Moore and Hollyday, 1975) have opined that longer lineaments with stronger surface expressions are more significant hydro geologically. Other investigators (Banks et al., 1992; 1993) have reported that larger fracture zones are unfavourable as associated with clay mineralization, whereas small and intermediate fracture zones having more transmissivity. The general assumption in lineament mapping is their depth propagation and surface manifestation of vertical fracture zones, an early hypothesis was developed based on field observations (Blanchet, 1957; Lattman, 1985). However, this hypothesis was neither consistent nor firmly established. Except the steeply dipping thrusts most faults and other linear fractures might devoid of subsurface fracture zones (Drury, 1993). In hard rock terrain, lineaments interpreted from satellite imagery represent faults, joints and dikes of several ages. Such fissured rocks are more and more susceptible to deep weathering and therefore ideal location for bore well drilling (Greenbaum ,1992). In the region where bedrock is exposed, multispectral remote sensing have been found useful for recognizing altered rock because there reflectance spectra differ from those of country rocks (Rowan et al, 1975).

2.5. GEOPHYSICAL TECHNIQUES AND ITS RELEVANCE IN HYDROGEOLOGY:

Geophysical exploration is the scientific measurement of physical properties of the earth crust for investigation of mineral deposits or geological structures (Griffith, D.H. & R.F. King, 1965).

A ground geophysical survey is often carried out to locate the ground water aquifer accurately. The most commonly used geophysical techniques for groundwater exploration is electrical resistivity. The electrical resistivity method is one of the most useful techniques in groundwater hydrology exploration because the resistivity of a rock is very sensitive to its water content. In turn, the resistivity of water is very sensitive to its ionic content. In general, it is able to map different stratigraphic units in a geologic section as long as the units have a resistivity contrast. Often this is connected to rock porosity and fraction of water saturation of the pore spaces.

The aim of electrical resistivity is the identification of high conductivity anomalies, normally thought to be due to deep weathering. Such anomalies are often further investigated by sounding

in order to provide a more quantitative information on the geo-electrical profile through the weathered zone as an aid in sitting borehole. Electrical and electromagnetic geophysical methods have been widely used in groundwater investigations because of good correlation between electrical properties (electrical resistivity etc), geology and fluid content (Flathe, 1955; Zohdy, 1969; Fitterman and Stewart, 1986; McNeill, 1990).

In hard rock areas, groundwater is found in the cracks and fractures of the local rock. Groundwater yield depends on the size of fractures and their interconnectivity. Use of Schlumberger sounding is well known for determining the resistivity variation with depth. However, it is very difficult to perform resistivity soundings everywhere without prior information. The VLF method has been applied successfully to map the resistivity contrast at boundaries of fractured zones having a high degree of connectivity (Parasnis, 1973). Further, the VLF method yields a higher depth of penetration in hard rock areas because of their high resistivity (McNeill et al., 1991). Therefore, a combined study of VLF and DC resistivity has potential to be successful (Benson et al., 1997, Bernard and Valla, 1991). VLF data are also useful in determining the appropriate strike direction to perform resistivity soundings (i.e. parallel to strike), again improving the likelihood of success.

Ground water investigation are based on only one physical property of water i.e. its electrical conductivity. Almost all geological materials are inherently conductive and virtually all subsurface conductivity is related to the presence of water. Exceptions are metallic minerals and graphite formations but these present anomalies, can be easily identified. Clay content enhances the conductivity of a formation but dry clay is inherently resistive (Patterson, N.R. & Bosschart R.A., 1987).

Geophysical techniques are easily being recognised to study the contaminants in shallow aquifers and to infer subsurface hydrologic connections in geologically complex areas (Cartwright and Mccomas, 1968; Warner, 1969; Merkel, 1972; Stollar and Roux, 1975; Kelly, 1976; Macaz et al., 1987; Ebraheem et al., 1990) but alternative techniques exist, including groundwater penetration radar and various other electromagnetic methods.

Vertical Electrical sounding using offset Wenner array proven to be successful technique to demarcate potential source of groundwater in Karstic limestone in Perlis, Peninsula of Malaysia (Arafin & Lee, 1985). Jayakumar (1997) made an attempt to unearth the depth persistence of lineament by integrated IRS 1A satellite imagery and resistivity data. Electrical resistivity is

indispensable in detection of fracture pattern in hard rock terrain as they are good source for groundwater exploration (Raju and Reddy, 1998). Gradient profiling integrated geological sounding (GS) helped in quantitative estimation of groundwater in hard rock of Mirzapur district, India (Yadav and Singh, 2007). Vertical electrical sounding was used to find contact zone which are potential site for the groundwater exploration in lower Voltanian sedimentary basin of northern region of Ghana (Bening and Bayor, 2007). Groundwater occurs in secondary porosity generally developed due to weathering, fracturing, jointing, faulting etc. within hard rock formations. Gradient profiling integrated geological sounding (GS) helped in quantitative estimation of groundwater in hard rock of Mirzapur district, India (Yadav and Singh, 2007).

2.6. HYDROGEOLOGICAL CONSIDERATION:

Lineaments inferred from remote sensing data do not provide the three-dimensional nature of the geological structure influencing ground-water flow. Structural geological data and knowledge usually acquired through field mapping and outcrop features or borehole logs, help to understand the three dimensional nature, expected geometry and extent of the surface and subsurface linear geological features, and thus improve the interpretation of the lineament zones and their hydrogeological nature (Brown, 1994). Integrated information model deals with the study of formations of a hard rock terrain and interpretation of geological structures in relation to ground water occurrence (Larson, 1972). The model deals with demarcation of different stress regimes through integrated study of deformations, dyke patterns and identification of open and closed fracture systems. From hydrogeological point of view, four main types of fractures are considered for hard rock terrains such as tensile joints, tensile fractures, shear fractures, and non-tectonic fractures (Rao, 1983). Hydrogeochemical parameters are of much importance for assessment of groundwater quality (Raju, 2007).

2.7. DIGITAL ELEVATION MODEL:

Due to their importance for the hydrological system dynamics, the integration of Digital Elevation Models (DEM) is prerequisite for improved regional hydrological model applications (Flugel, 1996). There has been a noticeable trend to obtain such information from remote sensing data using digital photogrammetry over the last few years (Brockelbanks & Tam, 1991; Connorssasowski et al., 1992; Al-Rousan et al., 1997; Helmschrot, 2000). Finally the DEM could be used successfully to extract hydrologically relevant information such as altitude, slope, aspect, curvature, and drainage network, etc. which are important to improve distributed

hydrological model applications (Flugel, 1996). Digital Elevation Model data from SRTM (Shuttle Radar Topographic Mission) is useful for extracting drainage, river gradient, elevation and slope maps. To create stream network and sub basin flow direction, filling of sink, flow accumulation, stream network, stream ordering and watershed algorithms were used (Strahler, 1952; Jenson and Domingue, 1998; Tarboton et al., 1991). The most common use of DEM data is the generation of slope values. Slope is an important factor in understanding the groundwater movement and also in suggesting artificial recharges sites (Saraf and Choudhury, 1997, 1998; Saraf, 1999; Saraf et al., 1999). Slope values are also used as input to models. Slope comprises two components namely gradient, the maximum rate of change of altitude, and aspect, the compass direction of this maximum rate of change (Burrough, 1986). A pseudo relief image of the terrain can be created from a DEM, which gives a more effective way of representing slope. It provides a better perception of the landforms. The concept of DEM can also be used to represent groundwater table. DEMs are very useful for automated terrain analysis (Mark, 1984; Mark et al., 1984; Jenson and Domingue, 1988; Riazanoff et al., 1988; Moore et al., 1991; Weibel and Heller, 1991; Donker, 1992; Dymond and Harmsworth, 1994; Dymond et al., 1995). The flow direction dataset is used to create a flow accumulation dataset where each cell is assigned a value equal to the number of cells that flow to it. It is defined flow accumulation as an operator which, given the drainage direction matrix and a weight matrix, determines a resulting matrix such that each element represents the sum of the weights of all elements in the matrix which drain to that element'. If the weight matrix is set to one, the flow accumulation matrix will contain the contributing drainage area of every cell. For example, the value of the flow accumulation matrix at the catchment outlet will represent the catchment area. Cells having a flow accumulation value of one, which means no inflow, will correspond to ridges or hilltops. All cells with a value higher than a certain threshold will form a connected drainage network provided that the DEM has no pits or depressions without outlet (Meijerink et al., 1994). Determination of the threshold value is subjective, and the simulated drainage network depends further only on the DEM and not on hydrological information. As the threshold value decreases the density of the drainage increases (Jenson and Domingue, 1988). Automated channel segment ordering can be done from drainage network matrix and flow direction data (Donker, 1992). The interpolation of the elevation contours and spot heights generate a digital elevation model (DEM). The interpolation scheme and finer details of interpolation differ depending upon the

TH-16267


 551.095456
 SA 249
 152

objective. Water table has been found to be a subdued replica of the land surface topography (Heath, 1983) or controlled by topography (Haitjema and Mitchell-Bruker, 2005). Therefore, besides representing the land surface, a DEM may also reflect the groundwater surface or the configuration of the aquifer basement. The DEM generated through contour and spot height interpolation is a raster or grid which is most widely used data structures. Grid based DEM has several disadvantages such as misrepresentation of abrupt changes in elevation; effects of grid size on the results and the computational efficiency and unrealistic representation of the computed upslope flow paths used for hydrologic analyses (Vieux, 2001).

2.8. GIS IN HYDROLOGY:

Geographic Information System (GIS) help to integrate information using large volume of spatial data derived from different sources, and efficiently store, retrieve, manipulate, analyze, model and display these data according to user's defined specification. In system, the word 'geographic' emphasizes the location of the area. GIS possess the unique ability to answer about five generic questions. These include – (i) Location: what exists at a particular location, (ii) Condition: a location where certain conditions are satisfied, (iii) Trend: both of the first two questions and seeks to find out the difference within an area over time, (iv) Pattern; what spatial pattern exists at a particular location, (v) modelling: "what happens when" a particular situation appears.

Traditionally geographic data are represented by maps. However, conventional maps have limitations to meet modern needs of spatial data arrangement .GIS has unique capability to analyze and model a huge amount of geo referenced data. Besides, cartographic software represents the output only in map form while GIS can generate tabular outputs (Demers, 1999). GIS deals with both spatial data and associated non-spatial attribute data. The spatial data represents features occupying geographic space and having definite geographic coordinates. Geographic features may be represented by points, lines, arcs and polygons. The non spatial or attribute data provide descriptive and qualitative information like soil type, name of streams, chemical quality of water, compositions of rocks etc. It is the spatial analysis capable of computer-based GIS that distinguishes from related graphics oriented computer packages. GIS has emerged as a quick and efficient decision making technology.

Geographic information system (GIS) is a computer assisted powerful tool for collection, storing, transforming and displaying various graphic and non graphic data in a desired way (Aronoff,

1986; Worrel, 1990). The potential for applying geomorphological knowledge depends not only on the problem but also on the willingness of the environmentalist to appreciate the value of this knowledge (Cooke and Doornkamp, 1974). For better delineation of lithological and structural features, remotely sensed data must be used along with the existing field geological map (Goetz and Rowan, 1981; Krishnamurthy et al., 1996) developed Geographical Information System to demarcate groundwater potential zones of Marudaiyar basin using different thematic maps such as lithology, landforms, lineaments and surface water bodies. Geographic Information System can be efficiently used to demarcate groundwater potential zones using remote sensing data in coalescence with electrical sounding for hydrogeological explorations (Shahid et al., 2007). Remote sensing and GIS have been successfully utilised to assess groundwater potential zones in hard rock terrain of Chittor area, Rayalaseema region of Andhra Pradesh, India (Rao and Jagran, 2003).

2.8.1. INTERPOLATION IN GIS:

The objective of interpolation is to estimate values at unsampled sites using known values of existing observation at neighbouring locations. Interpolation involves points and lines within values. The preference and selection of interpolation methods over others depends on the level of accuracy, number of points or lines, their distance and distribution, compatibility and applicability of the interpolation function to represent the spatial distribution of the concerned parameter (Meijerink, et al., 1994). Different interpolation techniques have their strong and weak points which are based on the applications. Hydrological, hydrometeorological and hydrogeological point data provide information and idea of discrete points only. Regional overview about any such parameters cannot be obtained until unless these data points are interpolated. Geological borelogs are important for GIS interpolation for multifaceted evaluation of geologic condition of Kalmar landfill, Olmsted County's (Rust, 1998).

2.9. ROLE OF REMOTE SENSING AND GIS IN LANDUSE/LAND COVER MAPPING:

Land is the most important natural resource on which most developmental activities are based. The application of remotely sensed data for land use mapping is one of the most acceptable techniques since 1940. Landuse is defined as the expression of human management of land ecosystem in order to meet some of his needs (Vink, 1975). Whereas land cover describes the vegetation and artificial construction covering the land surface (Burley, 1961). Land use includes cultural (building, fields), vegetation (herbs, shrubs, trees) and other (water, soil and lithology)

features on the earth's surface (Gills et al., 1991). Multispectral satellite data with synoptic view and repetitive coverage has brought a sea change in evaluation of land use/ land cover dynamics (Luong, 1993; Rathore and Wright, 1992). Change detection both long term and short term change in the land cover can be found out using post classification comparison techniques (Kushwaha, 1985). Land use/land cover change is critically linked to the intersection of natural and human influences on environmental change (Turner, 1995).

2.10. STATISTICAL ANALYSIS:

Multivariate analysis techniques are very useful in the analysis of data corresponding to a large number of variables. Analysis via these techniques produces easily interpretable results. Multivariate data consists of observations on several variables for a number of samples (also called sample vectors, or individuals). Data of this type arise in all branches of science, ranging from physiology to biology, and methods of analyzing multivariate data constitute an increasingly important area of statistics.

A wide variety of multivariate analysis techniques is available. The choice of the most appropriate technique depends on the nature of the data, problem, and objectives. The underlying theme of many multivariate analysis techniques is simplification. In other words, it is desired to summarize a large body of data by means of relatively few parameters. One fundamental distinction between the techniques is that some analysis is primarily concerned with relationships between variables, while others are primarily concerned with relationships between samples. Techniques of the former type are called variable-directed, while the latter are called individual-directed (sample-directed) multivariate analysis. In the analysis of dependence between variables, if the variables do not arise on an equal footing, multivariate regression analysis is recommended. It should be noted that the term 'equal footing' does not imply that some variables are more important than others, though they may be. Rather it indicates that there are dependent and explanatory variables. In multiple regressions, the variation in one dependent variable is explained by means of the variation in several explanatory variables. In multivariate regression, more than two dependent variables are in question. If the variables arise on an equal footing, as for example when different dimensions of different members of a particular species are measured and the primary interest is in the variables, then analysis of interdependence of variables is the subject of interest. When there are only two variables, correlation analysis provides the desired information to some extent. With more than two variables, principal

components analysis may be appropriate. This technique aims to transform the observed variables to a new set of variables which are uncorrelated and arranged in decreasing order of importance. The principal aim is to simplify the problem and to and new variables (principal components) which make the data easier to understand. In this multivariate analysis study, principal component analysis was employed to investigate the factors which caused variations in the observed quality data at the Agackoy water quality monitoring station in the Sakarya river-basin. This study also demonstrates the usefulness of the technique in the analysis of water quality data. A literature review on principal components analysis, a technique that was formerly used in the field of hydrology, has shown its appropriateness for water quality data, as confirmed by some recent case studies in the literature (Mahloch, 1974; Schetagne, 1985; Karpuzcu & Senes, 1987). Principal components analysis requires the interpreter to be experienced in the field of inquiry. For instance, a mathematician or statistician, applying psychological data to principal components analysis, cannot interpret the components reliably. This point, interpretation, constitutes the most problematic aspect of principal components analysis.

The statistical analysis of the basic geochemical data of the groundwater using R-mode factor analysis is a widely accepted technique for characterizing and interpreting a few empirical hydrochemical factors controlling the chemical budget of water. Reeder and others (1972) identified the likely weathering processes controlling the chemical composition of surface waters of the Mackenzie River drainage basin in Canada. Ashley and Lloyd (1978) used the factor analysis to evaluate the hydrogeochemical process in the Santiago basin of Chile and the Derbyshire Dome of England. Lawrance and Upchurch (1983) also used the technique to delineate the zones of natural recharge to groundwater in the Floridan aquifer. Ruiz and others (1990) mentioned that the basic purpose of such an analysis is to study the hydro-geochemistry of aquifers by simplifying the numerous and complex groundwater data into a set of factors, few in number which can explain a large amount of the variance of the analytical data and also indicates the source of origin of various ions present in the water. Briz-kishore and Murali (1992) have delineated the areas prone to salinity hazard in Chitravati watershed of India. Similarly Munaf et al (2005) used the multivariate factor analytical technique to assess the water quality and source of contamination in an irrigation project at Al-Fadhli, Saudi Arabia. Many studies combining the effects of multiple water quality variables evaluating the water quality and the extent and nature of contamination have been undertaken (Shuxia et al., 2003). Chemical

composition in groundwater is determined by a number of factors, such as precipitation, infiltration, groundwater flow patterns and characteristics of soil type of the aquifer. Factor score studies reflect the station-wise variation of the geochemical factors controlling the water chemistry. Scores showing negative values denote areas essentially unaffected by the said factors; most affected areas are denoted by extreme positive score and a near zero score may be considered as areas affected to an average degree to unaffected (Dalton and Upchurch, 1978; Gupta and Subramanian, 1994).

2.10.1. PRINCIPAL COMPONENT ANALYSIS:

Principal components analysis (PCA) helps to classify correlated variables into groups more easily interpreted as these underlying processes. The number of factors for a particular dataset is based on the amount of non-random variation that explains the underlying processes. The more factors extracted, the greater is the cumulative amount of variation in the original data. Principal components analysis (PCA) has previously been used to generate accurate maps of monitoring wells grouped by their water-quality characteristics (Suk and Lee 1999; Ceron et al., 2000; Güler et al., 2002; Suk and Lee, 1999) used multivariate analysis and geographic information systems (GIS) to correlate contaminant data with groundwater quality parameters for the purpose of identifying contaminated aquifer zones. They used this method to reduce several measured aquifer water-quality variables into a smaller series of underlying factors. Cluster analysis is another multivariate statistical data reduction technique that can be used to group monitoring wells by aquifer water-quality behaviour (Suk and Lee, 1999). This method links variables hierarchically in the configuration of a tree with different branches. Branches that have linkages closer to each other indicate a stronger relationship among variables or clusters of variables. Suk and Lee (1999) ran factor scores generated by the PCA through a cluster analysis to group monitoring wells based on underlying water-rock interactions and recharge characteristics. These grouped wells were then mapped as aquifer zones using GIS software; zones identified by the researchers compared favourably with zones delineated with traditional hydrogeologic techniques. Suk and Lee's (1999) multivariate analysis of geochemical data operated on the concept that each aquifer zone has its own unique groundwater quality signature, based upon the chemical makeup of the sediments that comprise it (Fetter, 1994; Kehew, 2001). Groups of water in aquifer zones delineated in this manner are known as hydro-chemical facies (Fetter, 1994). Groundwater dissolves minerals and other geochemical constituents from the geologic media

that it inhabits. The dissolved mineral and chemical composition is unique to the water in each aquifer, forming a groundwater quality signature that can serve to identify the parent aquifer. In north western Spain, Vidal et al. (2000) performed a principal components analysis (PCA) to reduce 14 water quality variables to two factors correlated with saline and organometallic contamination. Vidal et al. plotted the two sets of factor scores from the PCA against each other, graphically labelling each observation according to spatial location (either a well or spring sampling point). Sampling points fell into different clusters on the graph, illustrating those that shared common groundwater quality signatures. The location of the sampling points on the graph ranked their respective aquifers according to vulnerability to saline and/or organometallic contamination. Abu-Jaber et al. (1997) used a similar multivariate statistical exploration of geochemical data to identify predominant chemical interactions in known aquifer zones and to determine zone sensitivity to pollution from domestic sewer leakage. Meng and Maynard (2001) processed geochemical data using cluster and factor analysis; these groundwater classifications were then used as a basis for developing a conceptual geochemical model of their study area. Ochsenkühn et al. (1997) performed a cluster analysis on groundwater geochemical data to identify major trend axes representing dominant groundwater flow pathways. Other studies have used similar principles to correlate groundwater pesticide contamination with different crop rotations and for the inference of groundwater flow direction (Grande et al. 1996; Zanini et al., 2000).

Study Area

STUDY AREA

Chapter-III

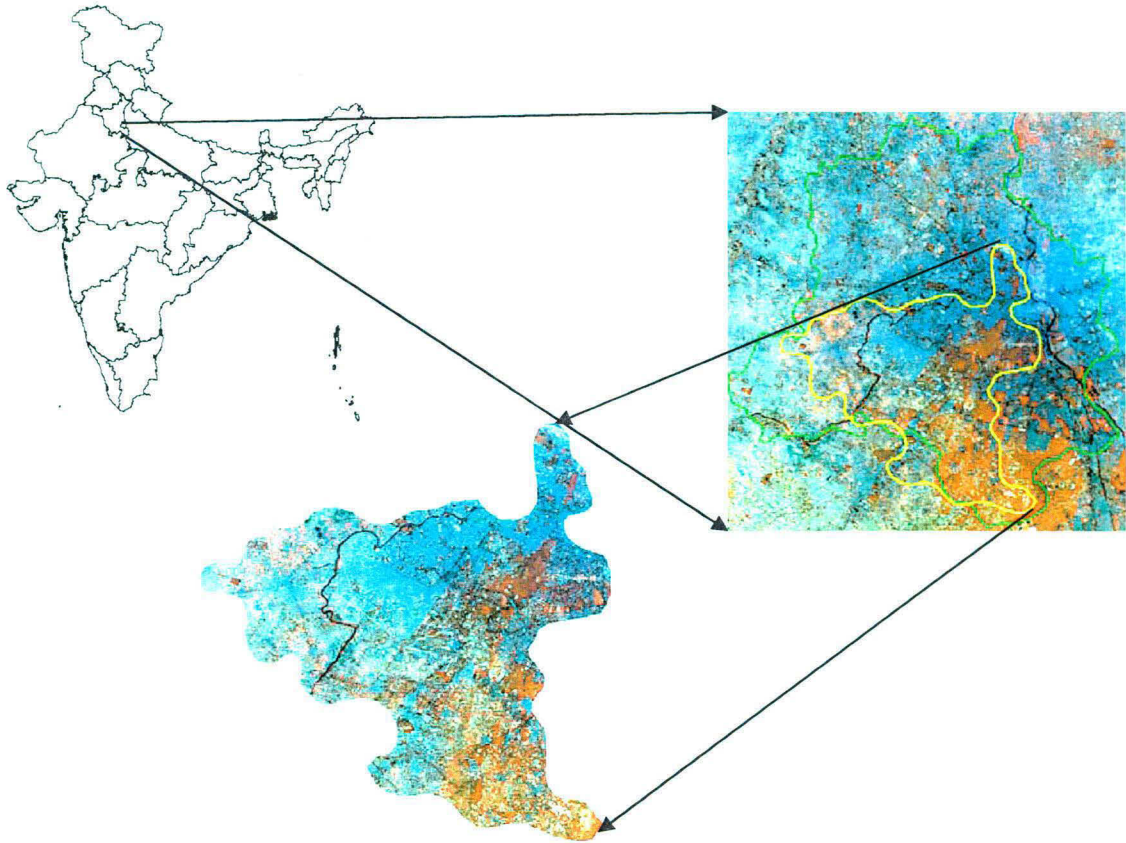


Fig.3.1. Location of Study Area

3.1 GENERAL

The National Capital Region (NCR) lies between $27^{\circ} 03'N$ to $29^{\circ} 29'N$ latitude to $76^{\circ}77'E$ to $78^{\circ}29'E$ longitude. The region includes the National Capital Territory (NCT) of Delhi and parts of the States of Haryana, Rajasthan and Uttar Pradesh. The study area includes the part of Haryana and Delhi. In Haryana it covers the parts of Gurgaon and in Delhi it includes parts South West Delhi, West Delhi, North-West Delhi, New Delhi, Central Delhi and South Delhi.

The study area lies between $26^{\circ} 25'0''N$ to $28^{\circ}44'0''N$ latitude to $76^{\circ}54'0''E$ to $77^{\circ}16'0''E$ longitude. It covers an area of 547.73sq.km approximately.

3.2 PHYSIOGRAPHY:

The study area has 3 distinct physiographic units, these are as follows:

1. Delhi(Quartzitic) Ridge.
2. Older alluvium on both sides of the Delhi Ridge.
3. Alluvium Deposits of Chattarpur enclosed basin.

The quartzite ridge enters the area from the South-Eastern part and passes through the eastern part extending up to the eastern bank of river Yamuna and Wazirabad. The rocky ridge has a length of about 35km and shows trends in a NNE-SSW direction. Isolated exposures of the quartzite are also found in Western part of the area. The elevation of the crest of the ridge varies from 213m to 314m above mean sea level with an average elevation of 40m from the surrounding plain.

The alluvial plain in the area almost flat and is interrupted by cluster of sand dunes and quartzite ridges. The sand dunes which are more prominent in the western part of the area are of varying dimensions and have N-E to S-W trend. The crests of these dunes generally lie between 3 to 10 meters above surrounding plains. The dunes in the area are more or less fixed with vegetation on them. The dunes are mostly longitudinal in nature.

The nearly closed alluvial basin of Chattarpur ($28^{\circ} 25'30''N$ to $28^{\circ} 32'30''N$ and $77^{\circ} 07'30''E$ to $77^{\circ}13'00''E$) in south Delhi occupies an area of about 78km^2 . This is a closed inland basin, the boundary of which is marked by the quartzite ridge. The general slope of land is towards the centre of the basin from the surrounding ridges. The maximum land altitude in the basin is about 259m mean sea level whereas the land at the ridges is about 274m above mean sea level. A number of micro-watersheds originate from the quartzite ridge. The drainage on the east of ridge enters River Yamuna, whereas on the west, it enters natural depression located in Najafgarah Tehsil of S-W district. The Najafgarah drain is about 39km long, flows N-E and joins Yamuna River of Wazirabad in North Delhi.

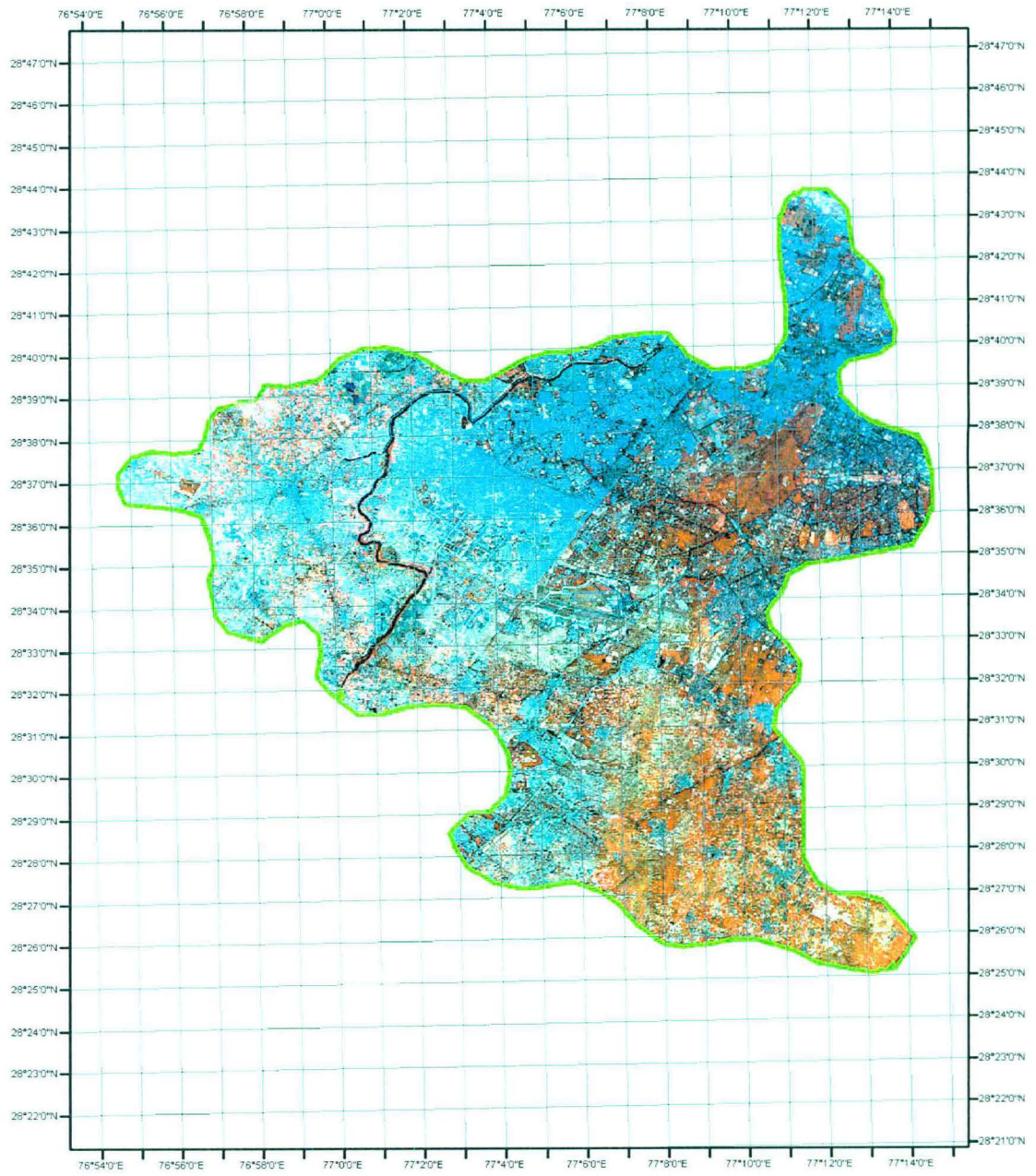


Fig 3.2 Geo-referenced Image of Study Area

3.3 GEOLOGY

Geologically the area is occupied by the alluvium/buried pediment plain at an elevation ranging from 213m to 314m above mean sea level. NCT Delhi is occupied by the Quartzite inter-bedded with Mica-Schist belonging to Delhi Super Group. The rock type exposed in the area belongs to Delhi Super-group of Lower Proterozoic age consist of the Alwar Group, Phyllite and Slate of the Ajabgarh Group. The Quartzite is massive, thickly bedded, hard, compact, highly jointed and intercalated with thin beds of Phyllite and Slates. The strike of the beds is NNE-SSW and dip westerly at moderate angles. These rocks are mostly covered by quaternary sediments and are exposed in isolated residual and structural hills and pediments. The hills are exposed in South and S-W of Delhi in Delhi, Gurgaon (major part of the study area), Rewari and Alwar.

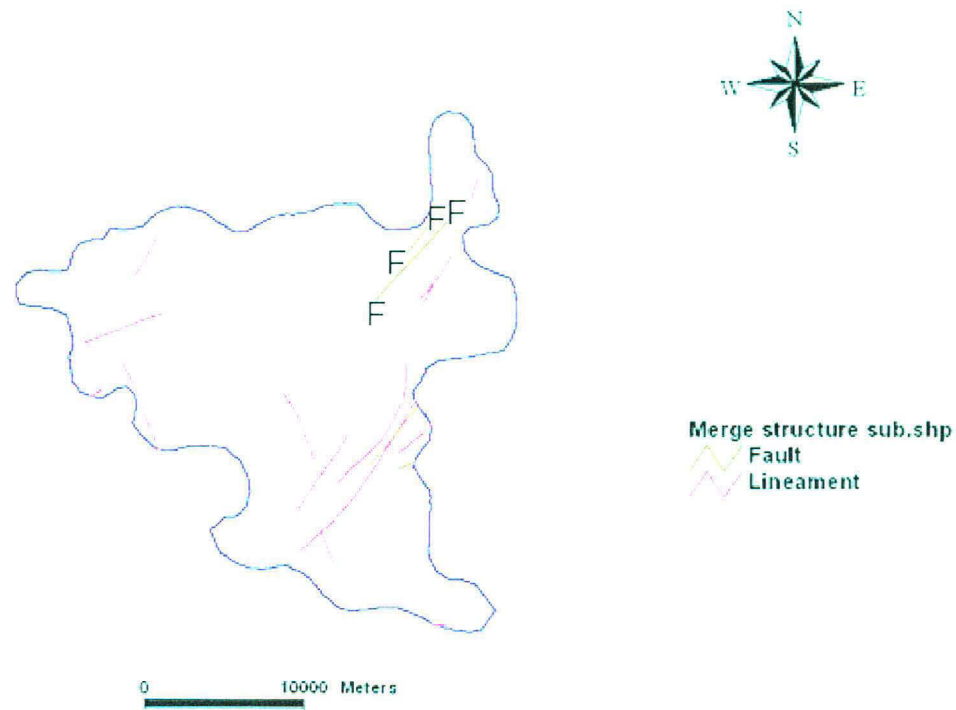


Fig 3.3 Structural Map of the Study Area showing faults and lineaments.

Post Tertiary	Recent and sub-recent Alluvium	Blown sand and Nodular limestone (Kankars)
-----	--Unconformity--	-----
Delhi System (Proterozoic)	Intrusive pegmatite, and quartz veins, granite, amphibolites	Hornstone Breccias Kushalgarh Limestone
		Alwar Series Quartzite, arkoses Grits, Schist, mica and contemporaneous volcanic- Railo Series and quartzite
-----	--Unconformity--	-----
Aravali System (Archaean)	Intrusive quartz veins, granite amphibolites.	Mica Schist, Quartzite Schistose conglomerates.

Table 3.1.1 Geological succession around National Capital Territory (Heron 1917, CGWB Report 2005)

Recent and sub-Recent	Younger Alluvium	Yamuna River Sand and deposits in stream bed
	Older Alluvium	Yellow and reddish soil comprising Silt/clay with local Kankar beds Sand lenses and small Ferruginous concretions
Post Delhi Intrusive	----- ---	Quartz Veins , Pegmatite
Delhi Group	Alwar Series	Quartzite, crystallized bluish, greyish and pinkish in colour, Arkoses grits, thin inter beds of micaceous schist's Quartzite containing pyrite specks, stringers and Occasionally graphitic stringers.

Table 3.1.2 Geological succession in Delhi (Heron 1917, CGWB Report 2005)

3.3.1 LINEAMENT:

N.C.T Delhi is occupied by quartzite inter-bedded with mica schist belonging to Delhi super group. The quartzite is grey to brownish grey, massive to thinly bedded and structurally form a coaxially refolded regional anticline plunging towards southwest. The major planar structure strikes NE-SW with steep southeasterly dips. Quartzite occurs in the central and southern part of the area while the quaternary sediments comprising older and newer alluvium cover the rest of the area. The older alluvium comprises silt, clay mixed with kankar in varying proportions. The newer alluvium mainly consists of un-oxidized sands, silt and clay occurring in the Yamuna flood plain. The thickness of alluvium on eastern and western side of the ridge is variable but in west of the ridge it is generally thicker (>300m). The area is dissected by number of faults, fractures and shears; the trend of these varies from NNE-SSW to ENE-WSW. The important faults in west of the ridge area are Rajendra Nagar fault, MES Depot- East Patelnagar fault, Anand Parbat-West Patelnagar fault and Inderpuri fault. The notable faults east of the ridge are Kishangarh fault, a WNW-ESE trending fault between Qutab Minar and Mehrauli and Lado Sarai fault. The geological succession in the area around NCT, as worked out by Heron (1917), is given in table 3.1.

The area under study has two types of formation viz. Quartzites belonging to Alwar group and alluvium of Quaternary age.

3.3.2 ALWAR GROUP:

The Alwar group belongs to the Delhi super group pre-cambrian age. These are composed mainly of quartzites with inter- bedded mica schists. There are three prominent rock types as noted in one of the boreholes in the study area.

(a) Siliceous quartzite

These are hard compact, massive and jointed and are not susceptible to high grade of weathering and erosion and hence they stand out as ridges/tors.

(b) Ferruginous quartzite

These are less compact, moderately hard and highly fractured along the bedding planes. As these easily weather and on disintegration produces coarse sand. This rock type normally occupies the piedmont portions of the land surface.

(c) Sericite – mica schist

These bands of sericite mica schist is observed in borehole and also in the rock exposures, their thickness varies from few centimeters to 10meter. The schists are sometimes accompanied with the quartz veins that are fractured and this type of schist is remnant of original clay layers, which had undergone thermodynamic metamorphism. Schists are loose, not compact and get easily weathered. They generally occupy lower valley levels. With the drop in slope, these valleys become broadly separated.

3.4 BASEMENT TOPOGRAPHY

The basement topography of study area (part of NCR) is highly uneven depicting the presence of sub-surface ridges and valleys because of folding of the geological formations during the pre-cambrian and subsequent periods. In the S-W, western and northern parts of the area, the thickness of sediments is more than 300m except at Dhansa where the bedrock has been encountered at 297 m below land surface. The nature of bedrock topography in different parts of NCT, Delhi is rendered uneven due to existence of sub-surface ridges. Thickness of alluvium overlying the quartzites increases away from the outcrops. The thickness of alluvium is 300m or more in most parts of S-W, West and N-W districts. In Chattarpur basin of Mehrauli block, the alluvial thickness varies from a few meters near periphery to 115m around Satbari bund.

Period	Formation	Description
Quaternary	Newer alluvium	Unconsolidated interbedded line of sand, silt, gravel and clay confined to flood plains Yamuna river
	Older alluvium	Unconsolidated interbedded, interfingering deposit sand clay and kankar, moderately sorted thickness variables, at places more then 300m
Precambrian	Alwar quartzite	Well stratified thick bedded brown to buff color, hard to compact, intruded locally by pegmatite and quartz vein inter bedded with mica sheets

Table 3.2. Stratigraphy of Delhi

3.5. STRATIGRAPHY OF DELHI. Already given in Geology and table 3.2

3.6. HYDROGEOLOGY (SUBSURFACE CONFIGURATION AND AQUIFER DISPOSITION)

3.6.1. (a) NEW DELHI:

New Delhi district of NCT Delhi is located centrally in the state with varied surface altitude due to Delhi ridge. Nearly 10sq.km area falls within ridge area with altitude ranging from 213m to 314m (above m.s.l). The surface is sloping gradually towards east up to the Yamuna river course where altitude is 210m (above m.s.l). The total area of New Delhi district is 35sq.km. The sub-surface configuration of New Delhi is different at various places, the western part which is adjoining to Delhi ridge is characterized by marginal alluvium where 0 to 30m thick layer of alluvium overlain on weathered and fractured quartzite rocks (Delhi Ridge). The alluvium consists of clay, silt and fine to medium sand. A substantial amount of Kankar is also admixed with the clayey-silt below 20m depth bgl. This is the main aquifer material found in these areas. The top soil zone predominantly consists of silty-clay material followed by thin partings of clayey-silt, sandy-silt and clay layers alternatively. Sandy-silt strata are favorable aquifer zone and provide substantial discharge. The western part of New Delhi district covering areas of Rashtrapati Bhavan, Chanakyapuri, Shantipath, South and North Avenue and Connaught Place tubewells are tapping both prevailing formation i.e. alluvium as well as hard rock whereas in the eastern part tube wells tapping of alluvium are giving yield of 200 to 500 (l.p.m) .The extreme eastern part of New Delhi district is bounded by river Yamuna and represents a elongated plain of Yamuna. Groundwater potential in this formation is relatively high i.e. ranging from 500 to 1600 (l.p.m). Groundwater in the area occurs both under water table as well as under semi-confined conditions in alluvium. The depth to water level in the district ranges from 5 to 25m below ground level and the wide variation occurs due to wide range of topographic relief. The Yamuna flood plain area depth to water level ranges from 5 to 8mbgl whereas in the Delhi ridge areas it varies from 10 to 25mbgl. The tube wells usually tap kankar zone admixed with clayey-silt and sandy-silt aquifer zone. These aquifer zones (3 to 7) were generally encountered alternatively below the depth of 20mbgl and onward up to the basement rock.

3.6.2. (b) NORTH WEST DISTRICT

The North West district of NCT Delhi covers 440sq.km area and is characterized by unconsolidated quaternary alluvium deposits. Thick pile of alluvium over the basement rock possesses various natures of sediment strata in an alternate fashion of geological setting. Nearly fine to medium and silt grade of sediment are frequent up to the depth of 50 m along with buff coloured clayey bed admixed with coarse kankars. On the other hand after the depth of 50m, silty-clay and clay (light yellow) beds with Kankars increases with depth. The semi-plastic and plastic clay beds are also common at deeper depth i.e. 80 to 250mbgl. The granular zones (fine sand and silty-sand) at deeper depth are not as frequent as in the shallower depth. Depth to water level is shallow i.e. 2 to 8mbgl in major parts of the district but in the northern border in Narela area depth to water level is 6 to 12mbgl.

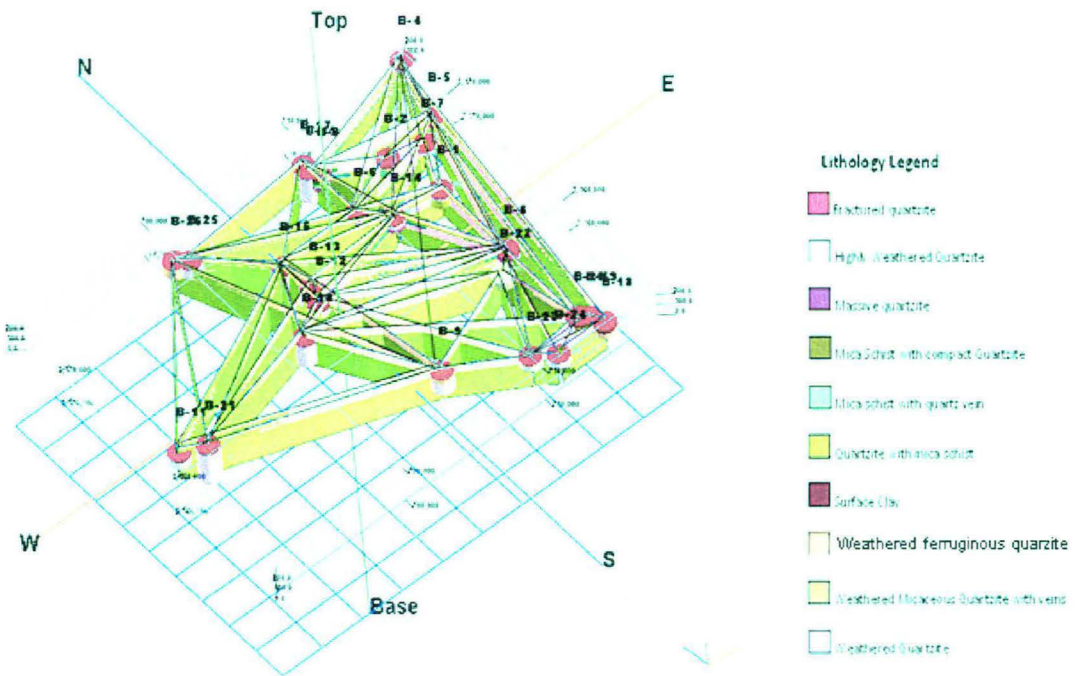


Fig. 3.4 The Fence diagram of the Study Area

3.6.3. (c) SOUTH DISTRICT

The South district of NCT Delhi covers 250sq.km of area in which 45.2sq.km area shows mountainous undulating terrain exposed with Delhi quartzite. The district is also characterized by a saucer shaped vast alluvium field in the central part of the district popularly known as Chattarpur Basin. Virtually this is valley fill deposit and the alluvium thickness varies from 0 to 140mbgl (Satbari village), below which quartzitic basement rock prevails. Some of the villages like Chattarpur, Gadaipur, Mandi, Ghitorni, Ayanagar, Fatehpur Beri and Satbari fall within this vast alluvium tract. The overburden is composed of unconsolidated clay, silt, sand and varying proportions of kankars. In the deep basin area, depth zone of 38m to 55m is characterized as prominent gravel zone admixed with silt and fine sand followed by clayey-silt and fine sand with occasional kankar nodules. Near to the depth zone of basement somewhat medium sand and angular gravel (ferruginous and gritty type quartzites) are also encountered. At some places viz. Aya Nagar & Fatehpur Beri, near to the basement rock, lenses of sticky yellowish clay are also encountered. The area across southern Delhi ridge namely Hauz khas, Saket, Khanpur, Pushpavihar, Lalkunwa and Saritavihar are characterized with marginal alluvium deposits where depth of overburden ranges from 60m to 94m. Below this quartzitic basement rock occurs. The borehole drilled in quartzitic body (Jaunapur, Asola mandi Tugalakabad) reveals that moderately fractured zones are prevalent in the depth of 30m to 90m and the fractures gradually decrease as depth increases. The weathered zone is found at every place above hard rock but thickness of weathered zone varies from place to place. The depth to water level varies widely in this district and is ranging from 8m to 65m. In the eastern tract of the district in Yamuna flood plain, depth to water level varies from 8mbgl to 22mbgl but in rest of the area it ranges from 30mbgl to 65mbgl. The depth of fresh/saline water interface varies from 75m to 100m. The thickness of the fresh water zone varies from 30m to 85m. Quality and quantity of groundwater in alluvium also depends on seismo-tectonic activity and relative deposition of clay and sand/silt on either side of the shifting river basin (Mukherjee 1996).

3.6.4. (d) SOUTH-WEST DISTRICT

The S-W district of NCT Delhi covers 420sq.km area and is characterized by unconsolidated quaternary alluvium deposits. Only 18sq.km area is covered by denudation hills especially in the eastern part of the district. Groundwater exploration has been carried upto 302m depth. The bed rock has been encountered at many places i.e. in Dhansa (297m) Pindwalakala (300m), Toghanpur (298m) and Jhuljhli (251m). Thick pile of alluvium overlies the basement rock and consists of alternate layer of silt, clay, sand and kankar. Nearly fine to medium and silt grade sediments occur frequently up to the depth of 50m along with buff colored clayey bed admixed with coarse kankars. On the other hand after the depth of 50m, silty clay and clay (light yellow) beds with kankars increases with depth. The semi-plastic and plastic clay beds are also common at deeper depth i.e. 80mbgl to 250mbgl. Depth to water level in major part of the district ranges from 5mbgl to 23mbgl but in the eastern part of the district in Delhi ridge area depth to water level ranges from 22mbgl to 50mbgl. The line of fresh-saline water interface also varies greatly in entire area. In the eastern part, characterized by hard rock, the fresh saline water interface rests at deeper depth i.e. around 80mbgl to 90mbgl.

3.6.5. (e) WEST DISTRICT

West district is occupied by unconsolidated quaternary alluvium underlain by Pre-Cambrian meta-sediments of Delhi system. Quaternary alluvium comprises of sand, clay, silt, gravels/pebbles and kankars. The aquifer system include fine sand to coarse grained sand mixed with kankars with little amount of clay and silt. Clay is sticky and plastic in nature, light grayish in color mixed with a little sand and kankars, fine to medium grained. The depth of water level varies in the district from 2m to 15m. The depth of fresh saline interface varies from 25m to 50m at different places. The depth of fresh water zone varies from 10m to 45m.

3.7. GEOMORPHOLOGY:

Geomorphology is the study of landforms and landscapes. Certain agents function to bring out gradation, which results in changes in landforms. The mapping and analysis of geomorphic landforms involves the identification of the geomorphic units, which are classified and subsequently evaluated for specific type of land utilization. The study area comprises of following features:

3.7.1. LOW RESIDUAL/STRUCTURAL HILLS: These are parts of Delhi ridge forming N-S to NS- SW trending structural ridges, tors, and mounds and composed of folded and jointed quartzites. Joints allow only limited groundwater infiltration. This unit constitutes the surface runoff and therefore, has very poor prospects of groundwater. They are mostly barren, with scanty vegetation along joints and slopes.

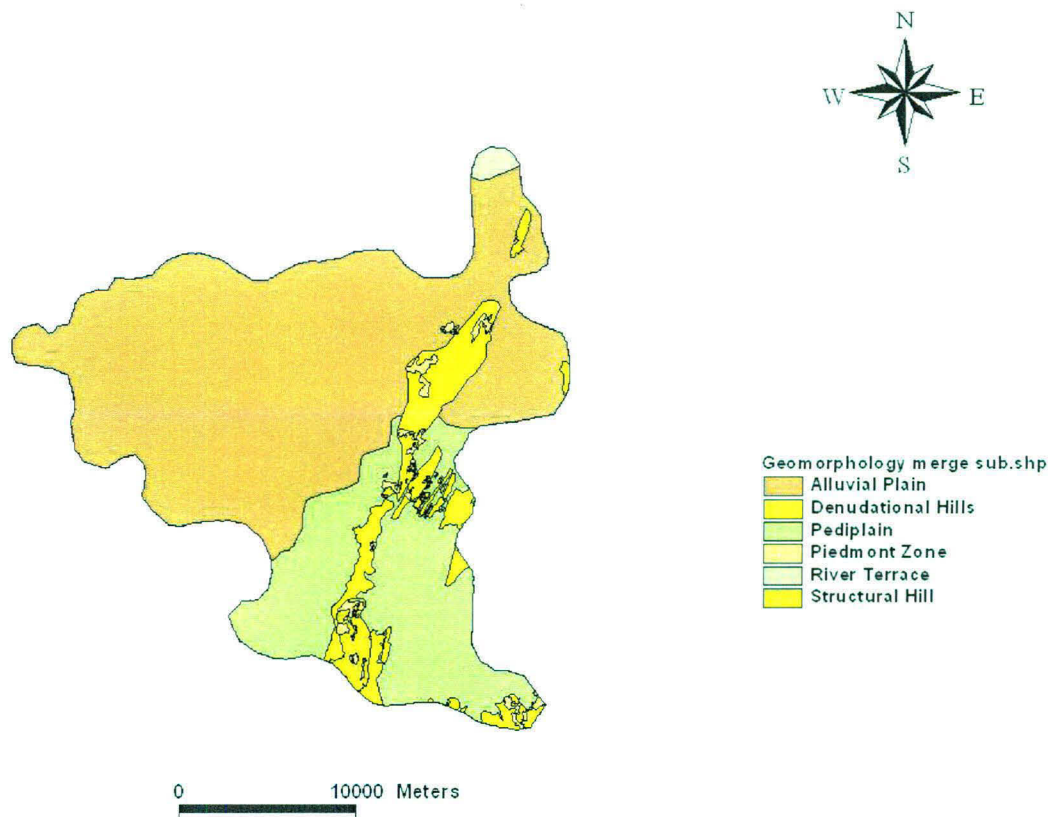


Fig. 3.5. Geomorphology of the Study Area

3.7.2. PEDIMENT:

The undulating, eroded and dissected shallow, buried planer surface along the fringe and slopes of ridges and tors form this unit. The main drainage systems have developed in this unit. The soil is generally clayey and fine silty, and partly gritty and gravelly. Drainage dissection is quite intense at many places as Gurgoan, Mahipalpur, Chattarpur often developing gullies. Weathering is more intense in coarse gritty or arkosic quartzite. Groundwater potential is generally low due to poor infiltration and high runoff resulting from varying slopes and clay mantle. But the presence of fractures, joints and shears in the

rock renders this unit locally potential for groundwater occurrence. In the southern part of JNU campus, a long abandoned quarry trench which forms a prominent feature in the area i.e along a weathered and sheared pegmatite vein is a high water potential zone. At present a tube well and an open well are located at the northern tip of this trench yielding fairly good amount of water. Most of the productive tube wells in the campus are located in pediment zone.

3.7.3. BURIED PEDIMENT:

This unit forms the almost flat terrain in the northeastern part of the study area. It has a shallow to moderately thick soil cover, which is mainly silty and clayey and at Rangpuri Pahari, Mehruali, Badarpur it is gritty and gravelly. The surface slopes gently towards northeast and merges with deeply buried pediment beyond the Jawaharlal Nehru University campus and with the Yamuna alluvial plain further east. This unit forms a moderate to good groundwater potential especially along fracture and drainage.

3.7.4. DRAIN: The study area is divided by Najafgarh drain which flows from the SW to NE direction and finally falls in the Yamuna River near Wazirabad barrage.

3.8. TEMPERATURE:

The cold season starts towards the latter half of November when both day and night temperature drop rapidly with the advance of the season. January is the coldest month with the mean daily maximum temperature at 21.3°C and the mean daily minimum at 7.3°C. In the winter months cold waves which affect the district in the wake of western disturbances passing across north India, minimum temperatures sometimes go down to the freezing point of water. From about the middle of March, temperature begins to rise fairly rapidly. May and June are the hottest months. While day temperature is higher in May the nights are warmer in June. From April the hot wind known locally as 'loo' blows. In May and June maximum temperature sometimes reaches 46 or 47°C. With the advance of the

Season	Starting	Termination
Cold/ Winter	End of November	Middle of March
Summer	Middle/End of March	End of June
Rainy Season	Early July	September

Table 3.3 Seasons in study area

monsoon into the area towards the end of June or the beginning of July day temperatures drop appreciably while the night temperatures remain high.

3.9. HUMIDITY:

The air over Delhi is dry during most of the year. Humidity is high in the monsoon months. April and May are the driest months with relative humidity of about 30% in the morning and less than 20% in the afternoons.

3.10. WEATHER:

April to June is the period with the highest incidence of thunderstorms and dust storms. Some thunderstorms give rise to violent squalls. While some of the thunderstorms are dry others are accompanied with heavy rain and less frequently with hail. Thunderstorms also occur in the winter months in association with western disturbances. Dense fog is observed in the winter months.

3.11. RAINFALL PATTERN:

The normal annual rainfall in the district is 611.8mm. The rainfall in the district increases from the SW to the NW. About 81% of the annual rainfall is received during the monsoon months July, August and September. The rest of the annual rainfall is received as winter rain and as thunderstorm rain in the pre and post monsoon months. The variation of rainfall from year to year is large.

Material & Methods

MATERIALS AND METHODS

Chapter-IV

4.1. IRS - INDIAN REMOTE SENSING SATELLITE

The Indian Remote Sensing satellite system is India's first domestic dedicated earth resources satellite program and an element of the National Natural Resource Management System. IRS is an Indian program to develop an indigenous capability to image earth, particularly India. Its mission is ground water exploration, land use, forest & flood mapping, inventory of surface water. The first satellite in the IRS series (IRS-1A) was launched by a Soviet Vostok booster. As of December 1997, seven IRS family satellites have been launched; IRS-1A, -IB, -1E, -P2, -1C, -P3, -1D, IRS-P2, IRS-P3, IRS-P4 (Oceansat-1), IRS -P5 (Cartosat), IRS- P6 (Resourcesat) and other remote sensing and communication satellites also. In the present research the satellite imagery used is of IRS-1D and IRS-P6 (Resourcesat-1) along with the SRTM data of Radarsat.

4.1.1. CHARACTERISTICS OF IRS SATELLITE AND THEIR SENSORS

IRS-1D: Launched in September 1997, IRS-1D was launched from Sriharikota using the PSLV. However the PSLV placed in an elliptical orbit, instead of a circular orbit. The snag was partly fixed. It is being used to map and monitor calamities. IRS-1D has LISS III, PAN, WiFS sensors on board.

Orbit	Near Polar, Sun synchronous
Altitude	737 km (perigee) 821 km (apogee)
Inclination	98.53 deg
Local Time	10.30 A.M to 10.47 A.M
Repetivity	25 days
Orbits/cycle	358
Period	100.56 minutes
Sensors	PAN, LISS-III, WIFS

Table 4.1.1 Characteristics of IRS Satellite and their Sensors

Resolution	5.2 to 5.8 m
Swath	63 to 70 km
Revisit	5 days by tilting the camera
Spectral Bands	0.50 – 0.75 Microns
Quantization	6 bits
Steerability	+/- 26 degrees

Table 4.1.2 Pan Sensor Characteristics

Resolution	21.2 to 23.5 m (Visible and near IR region) 63.6 to 70.5 m (Shortwave IR region)
Swath	127 to141 Km (Visible and near IR region) 133 to148 Km (Shortwave IR region)
Repetivity	25 days
Spectral Bands	0.52 - 0.59 microns (B2) 0.62 - 0.68 microns (B3) 0.77 - 0.86 microns (B4) 1.55 - 1.70 microns (B5)
Quantization	7 bits

Table 4.1.3 LISS-III Sensor Characteristics

Resolution	169 to 188 meter
Swath	728 to 812 Km
Revisit	3 days (by combining paths)
Spectral Bands	0.62 - 0.68 microns (Visible) 0.77 - 0.86 microns (near infra-red)
Quantization	7 bits

Table 4.1.4 WiFS Sensor Characteristics

Sensor	Resolution(m) & No. of Bands	Coverage Km x Km	Data Products		
			Type	Media	Scale of Photo products
PAN	5.8 (one)	63x70.8	Full Scenes with SAT	Digital, B&W	1:125, 000
		70x69.1	Sub-scenes with SAT	Digital, B&W	1:50, 000
		23x23	Sub-scenes stereo pairs	Digital	-
		23x23	Geocoded (7 1/2'x7 1/2')	Digital, B&W	1:25, 000
		14x14	Geocoded (5' x 5')	Digital, B&W	1:12, 500
LISS-III	23.5 2(V),1 (NIR)) 70 1(SWIR)	127x145.5	Full Scenes with SAT	Digital, FCC	1:250, 000
		141x142.1	Quadrants	Digital, FCC	1:125, 000
		70x70 28x28	Geocoded (15'x15') (map & floating)	Digital, FCC	1:50, 000
WIFS	188 two (V, NIR)	720x778 812x760	Full Scenes with SAT	Digital, FCC (Bands 3,3,4)	1.2 Million

Table 4.1.5 Specifications of Different Sensors

4.1.2. PANCHROMATIC:

The IRS-1D's high-resolution digital panchromatic data is the best imagery commercially available today. The Pan sensor on IRS-1C is the first commercial satellite imagery to break the 10 meter barrier and offer regular repeat coverage. Compared to aerial photography, IRS-1D PAN data save users time and money. Its generous scene size (70 x 70 km) eliminates the time-consuming need to mosaic dozens of individual aerial photos. And because it is digital data, IRS-1D Pan Images are immediately ready for loading into your image processing or GIS system. The high resolution makes it an excellent tool for creating and maintaining up-to-date thematic maps of even the most

remote area of our planet. In addition, with off-nadir viewing, repeat coverage is available as often as every five days, enabling users to monitor rapidly evolving environmental situations, and stereoscopic coverage can be acquired (with off-track viewing up to $\pm 26^\circ$). Unlike most aerial photography, IRS-1D PAN data is already digital, it can easily combine it with other data. Merged with multi-spectral data, pan data adds spatial detail to thematic maps. In a GIS, Pan Data is an excellent base on which to display other data layers. With stereo capability, digital terrain models can be created for 3-D analysis.

4.1.3. LINEAR IMAGING AND SELF SCANNING SENSOR (LISS-III):

A multi-spectral sensor with a spatial resolution of 23.5m, operating in the visible, near infra-red bands and 70.5m resolution in the short wave infra-red band, with a swath of 141Km.

4.1.4. WIDE FIELD SENSOR (WiFS):

It has a spatial resolution of 188m, two spectral bands in the visible and near infra-red regions, with a swath of 810 Km.

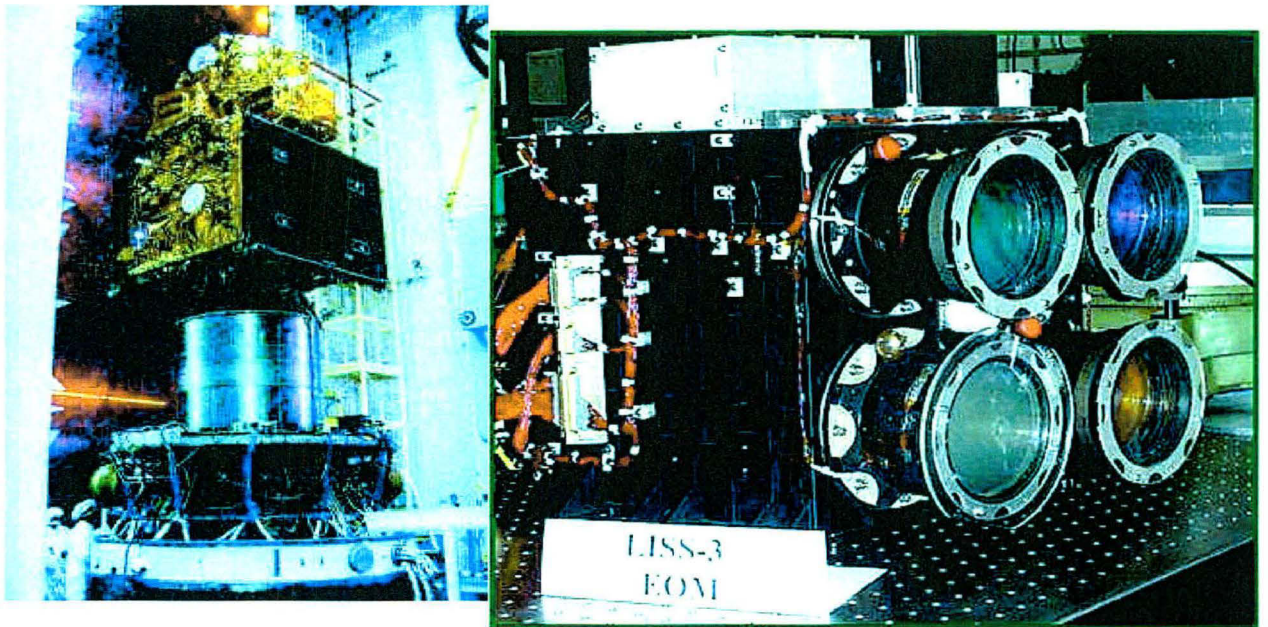


Fig 4.1; Resourcesat-1, mounted on top of the PSLV-C5's fourth stage and LISS - III Camera (Source: ISRO)

4.2 SHUTTLE RADAR TOPOGRAPHIC MISSION (SRTM):

Prior to the Shuttle Radar Topographic Mission, the only elevation datasets covering the Earth's entire surface such as GTOPO 30 (U.S.Geological Survey, 1999.) and GLOBE (Hastings and Dunbar, 1998.) had a comparatively coarse spatial resolution of 1km², which is often not sufficient for hydrologic modelling at smaller scales. Radar remote sensing radiation employs electromagnetic energy in the microwave part of the spectrum and radar wavelengths are measured in mm or cm. Because radar wavelengths are so long they are not affected by the relatively small cloud particles therefore it can penetrate clouds. This is of great benefit in the cloudy mid-altitude and tropical areas.

4.2.1 WAVEBANDS COMMONLY USED IN RADAR REMOTE SENSING

Band Designation	Wavelength Range (mm)	Frequency (GHz)
Ka	8-11	28-37.5
K	11-17	18-28
X	24-38	8-12.5
C	38-75	4-8
L	150-300	1-2

In addition to its wavelength characteristics, radar energy can also be polarized. Polarization indicates the plane in which the electromagnetic energy travels. Radar systems employ horizontal (H) and vertical (V) polarization as follows: -

4.2.2. POLARIZATION COMBINATIONS FOR RADAR

Transmitted Energy	Received Energy	Polarization Combination
Horizontal (HH)	Horizontal	Like polarization
Vertical (VV)	Vertical	Like polarization
Horizontal (HV)	Vertical	Cross polarization
Vertical (VH)	Horizontal	Cross polarization

Having a fixed antenna baseline and acquiring data at two frequencies (C-band and X-band), SRTM was the first space-borne single-pass interferometric SAR (Farr and Kobrick, 2001; Rabus et al., 2003). The Shuttle Radar Topography Mission was an international, collaborative project involving the National Aeronautics and Space Administration (NASA), the German Aerospace Agency (DLR) and the Italian Space Agency (ASI). The responsibility of DLR and ASI was the design of an X-band instrument (X-SAR) and the processing of the resulting data. While the C-band (5.6 cm) instrument mapped the topography of the Earth with nearly global gap-less coverage, the coverage for the X-band (3.1 cm) has gaps due to the reduced swath width. However, since it was not necessary to use the Scan SAR mode (Monti Guarnieri and Prati, 1996) for the X-band instrument, the quality of the interferograms and therefore of the DEMs is expected to be better than of those obtained from the C-band (Rabus et al., 2003).

4.3 THE PRE-PROCESSING OF SATELLITE IMAGES:

(1) The LISS- III image was obtained from NRSA for the year 2005.

- Satellite image from IRS-1D, LISS-III sensor, on a scale of 1:50,000(geo-coded) representing synoptic view of earth's surface at 25mX25m ground resolution in three spectral bands have been procured. The details of the IRS data used to accomplish the study are given below.
- Data product –Standard FCC (False colour composite), bands 1, 2 and 3 in the range of (0.52-0.59 microns) B2, (0.62-0.68microns) B3 and (0.77-0.86microns) B4 respectively.
- Projection: The image was projected to Lambert Conformal Conic Projection, Spheroid and datum Everest.

(2) The SRTM data were processed to transform it into product usable in GIS:-

- Conversion of raw data: the image was converted from the DTED Level-2 format to ESRI grid format (resolution 79.6mX79.6meter).
- Mosaicking: the individual tiles were mosaicked and then was clipped using shape file of study area.
- Projection: The final output of step b was projected into Lambert Conformal Conic projection, spheroid and datum Everest.

The Resourcesat-1 (PAN and LISS III merged) satellite image was projected in the same manner as stated above in 4.3. This ultimately helps in increasing the spatial resolution which helped to determine the lineaments in the area easily.

4.4. SURVEY OF INDIA TOPOSHEET:

S.No	Toposheet No.	Scale
1	53H/1	1:50,000
2	53H/2	1:50,000
3	53H/3	1:50,000
4	53H/5	1:50,000
5	53H/6	1:50,000
6	53H/7	1:50,000
7	53D/13	1:50,000
8	53D/14	1:50,000
9	53H	1:250,000
10	53D	1:250,000

4.5. SOFTWARE USED:

- (i) Arc/Info GIS Workstation version 9.1
- (ii) Arc View GIS 3.1
- (iii) Auto CAD Map 2000
- (iv) ERDAS Imagine Image Processing Software Version 8.4
- (v) Rockworks 6.9.8
- (vi) Geoimage
- (vii) SPSS 14 for Windows

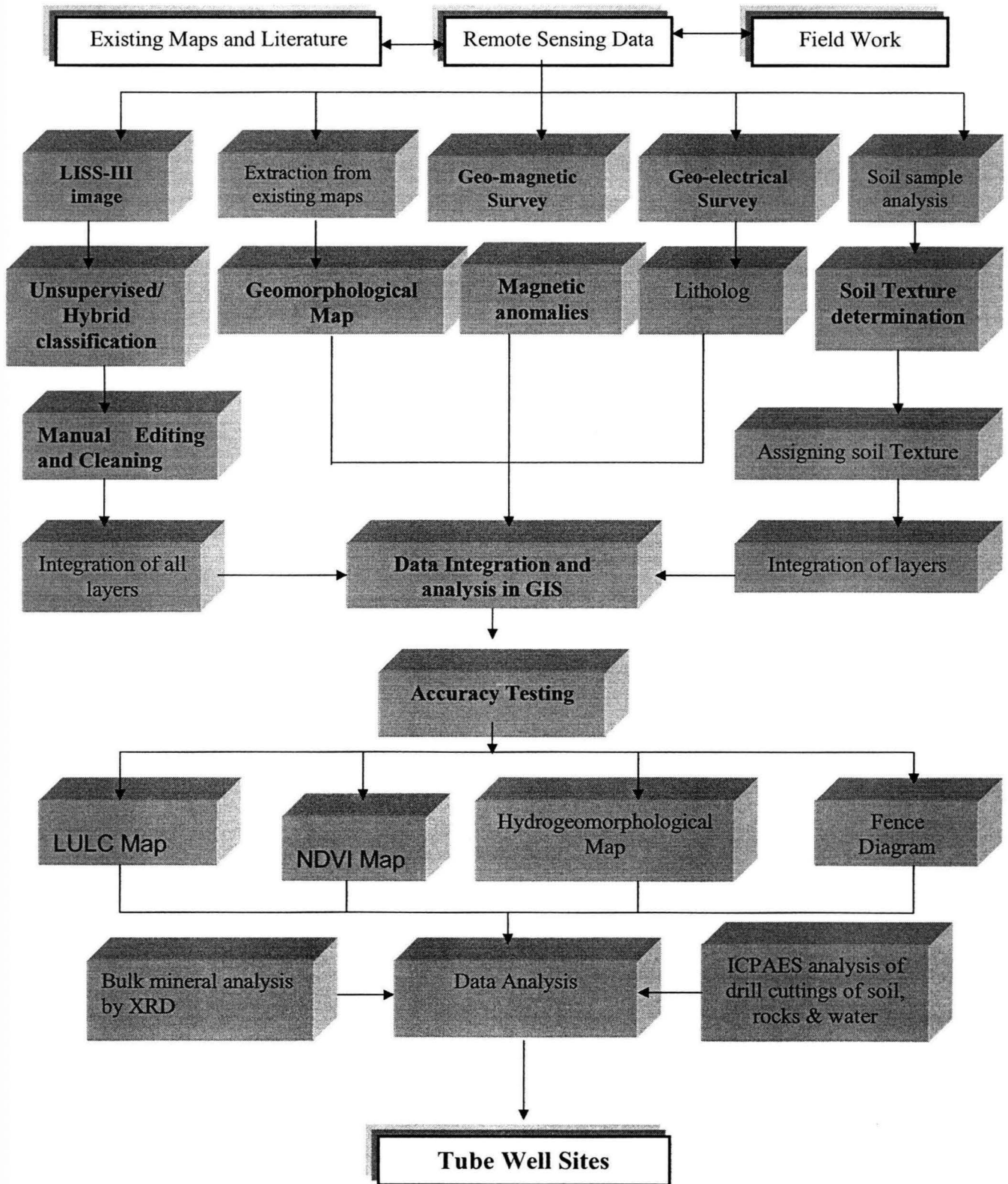


Fig.4.2 Methodology Adopted for Tube Well site selection

4.6. PRINCIPLES OF INSTRUMENTS USED:

1. ELECTRICAL RESISTIVITY METHOD

The electric resistivity of a rock formation limits the amount of current passing through the formation when an electric potential is applied. It may be defined as the resistance in ohms between opposite faces of a unit cube of the material. If a material of resistance R has a cross-sectional area A and a length L, then its resistivity can be expressed as

$$\rho = RA/L$$

units of resistivity (ρ) are ohm-m (Ωm).

Resistivity of rock formations vary over a wide range, depending on the material, density, porosity, pore size and shape, water content and quality, and temperature. There are no fixed limits for resistivities of various rocks. In relatively porous formations, the resistivity is controlled more by water content and quality within the formations than by the rock materials itself. For aquifers composed of unconsolidated materials, the resistivity decreases with the degree of saturation and the salinity of groundwater. Clay mineral conduct electric current through their matrix, therefore clayey formation tend to display lower resistivities than do permeable alluvial aquifers.



Fig.4.3 DDRIII resistivity meter (IGIS Hyderabad)

Actual resistivity is determined from apparent resistivity, which is computed from measurements of current and potential differences between pairs of electrodes placed in

the ground surface. The procedure involves measuring a potential difference between two electrodes (potential electrode) resulting from an applied current through two other electrodes (current electrode) outside but in line with the potential electrode. If the resistivity is everywhere uniform in the subsurface zone beneath the electrodes, an orthogonal network of circular arcs will be formed by the current and equipotential lines, as shown in (fig 4.2). The measured potential difference is a weighted value over a subsurface region controlled by the shape of the network. Thus the measured current and potential differences yield an apparent resistivity over an unspecified depth. If the spacing between the electrodes is increased, a deeper penetration of the electric field occurs and a different apparent resistivity is obtained. In general, actual subsurface resistivity vary with depth; therefore, apparent resistivity will change as electrode spacing are increased, but not in a like manner. Because changes of resistivity at great depths have only a slight effect on the apparent resistivity compared to those at shallow depths, the method is seldom effective for determining actual resistivity below a few hundred meters. Electrodes consist of metal stakes driven into the ground. In practice various standard electrode spacing arrangements have been adopted; most common are the Wenner and Schlumberger arrangements.

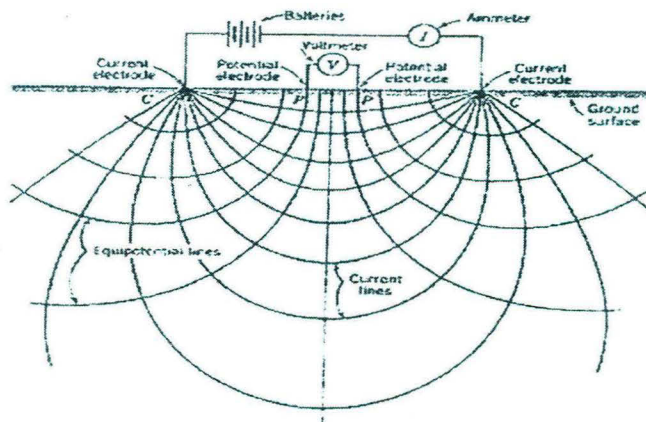
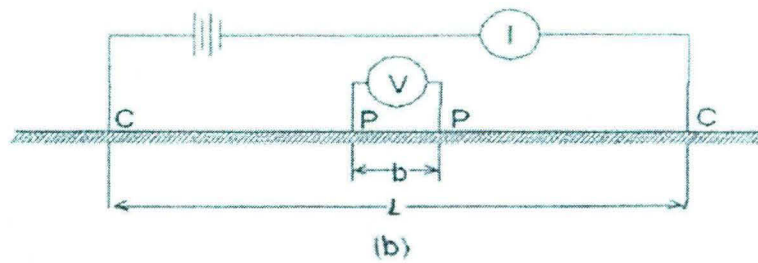


Fig No. 4.4 Electrical Circuit for resistivity determination and electrical field for a homogenous subsurface stratum

The Schlumberger arrangement used for this study is shown in Fig 4.3 has the potential electrodes close together. The apparent resistivity is given by



$$\rho_a = \frac{\pi(L/2)^2 - (b/2)^2 V}{b \cdot I}$$

Fig. 4.5 Schlumberger arrangement

Where 'L' and 'b' are current and potential electrode spacing, respectively. Theoretically $L \gg b$, but for practical application good results can be obtained if $L \geq 5b$.

2. MAGNETIC ANOMALY STUDIES

Magnetic survey was carried out in and around, the RR Hospital complex, using the instrument called Proton Precession Magnetometer modal PM - 600 manufactured by Integrated Geo Instruments and Services (p) ltd.

Proton precession Magnetometer utilizes the spinning of protons or nuclei of the hydrogen atoms in a sample of hydrocarbon fluid to measure the total magnetic field intensity. Water, kerosene, alcohol etc. are taken as samples. The protons in these fluids behave as small spinning magnetic dipoles. These magnetic dipoles are temporarily aligned (polarized) by application of strong uniform magnetic field by sending a current through a coil wound on the bottle containing the hydrocarbon fluid / water. When the current is removed i.e., when the applied field is removed, the spin of protons causes frequency of which is proportional to the ambient field intensity. The total magnetic intensity as measured by a proton precession magnetometer is a scalar measurement i.e., it gives simply magnitude of the total earth's magnetic field independent of its direction. The magnetic intensities over the Indian subcontinent are given in FIG 4.5. The study area complex comes in a region with normal magnetic intensity around 47000 gamma.

3. X- RAY DIFFRACTOMETER:

X-ray diffraction analysis was performed on drill cuttings (both rock and soil samples) using XRD model no. PW 3040/60 X' Pert PRO Console (Phillips, The Netherlands) to

confirm mineralogical nature/bulk composition, which in turn helped in ascertaining presence of pollutant minerals, if any.

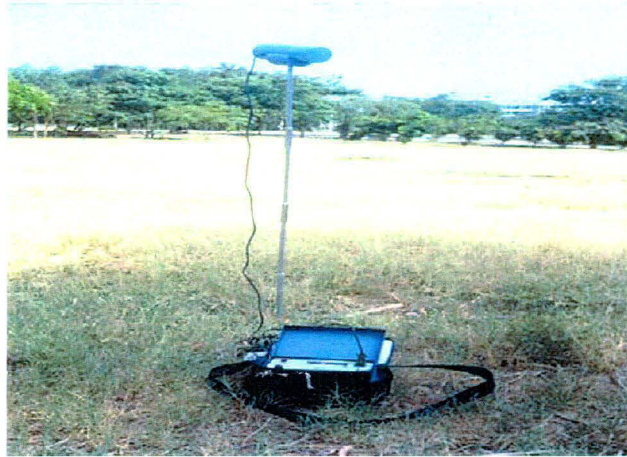


Fig. 4.6 Proton precession magnetometer (IGIS Hyderabad)



Fig. 4.7 X// Pert PRO X-Ray Diffraction System

Interpretation of modern x-ray diffractograms requires several steps

1. Completely drying the samples
2. The rocks (drill cuts) samples are crushed – 200 mesh in agate, pestle and mortar for analysis.
3. Slides are prepared from the meshed samples and put in the X-ray diffractometer to get the x-ray diffractometer in the rd, dat and udf format.
4. The results were then analyzed on X-Pert High Score software.

4. ICP-AES ANALYSIS: MULTIELEMENT ANALYSIS (BRGM PROCEDURE)

The geological materials such as rocks, soils and stream sediment samples were crushed –200 mesh in agate, Pestle and mortar for analysis. The geological samples can be digested with mixed acid (HF, HCl, HNO₃ and HClO₄).

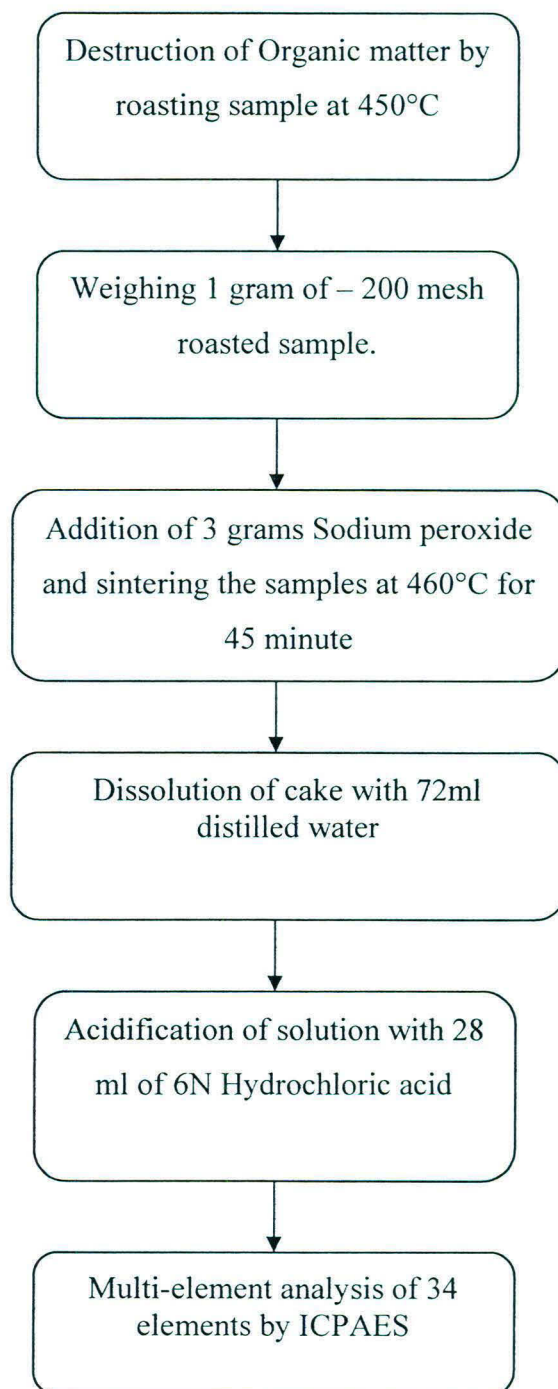


Fig. 4.8 Methodology adopted for ICP-AES analysis

Alkaline and acid fluxes are also very effective for the decomposition of refractory minerals. Basic Fluxes efficiently decompose complex silicate and minimize volatilization of minerals. Among these Fluxes, Sodium Hydroxide, Carbonate, Peroxide and their mixtures have been used. Sodium Peroxide is very effective for decomposing materials containing Sn, W, Cr and Mo. The flow sheet scheme for sample treatment, decomposition and dissolution for multi element analysis of rocks, soils and stream sediments by ICP-AES is shown in the figure 4.8

BRGM program for the determination of major, minor and trace elements, special wavelengths and limits of detection in solid materials, for geotechnical exploration samples, based on 1 g sample in 100 ml.

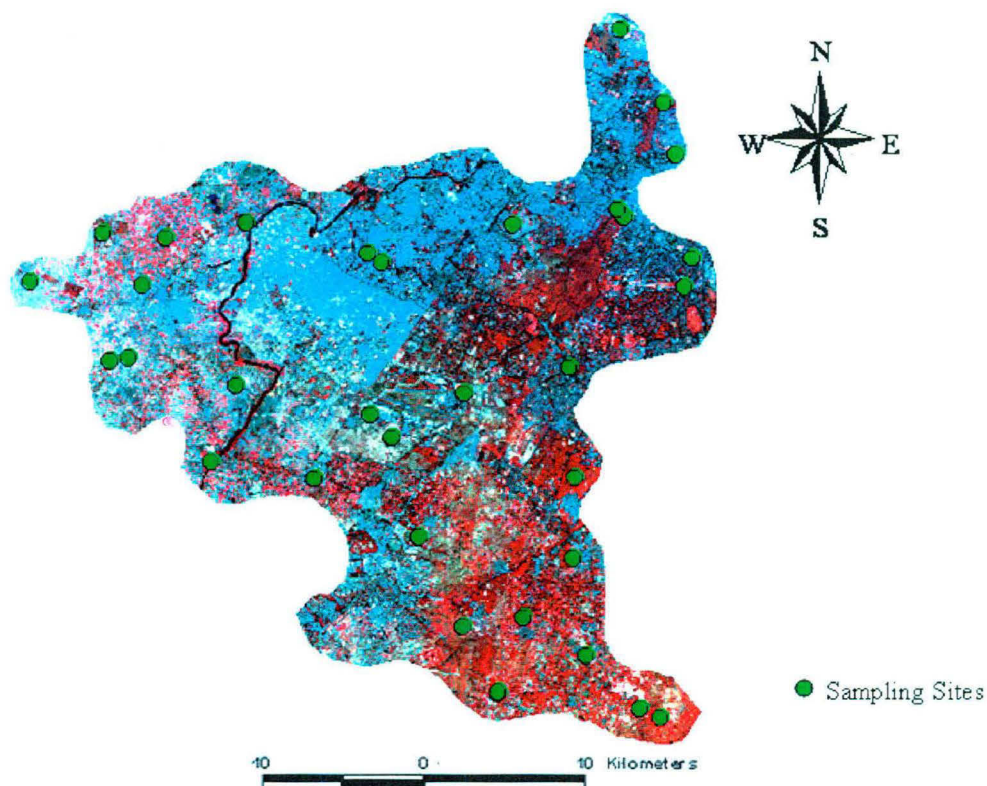


Fig 4.9 Sampling Sites of the Water Quality data

5. SOIL PARTICLE SIZE ANALYSIS

The particle size analysis of soil estimates the percentage sand, silt and clay contents of the soil and is often reported as percentage by weight of oven dry and organic matter free

soil. The analysis is usually performed on air-dry soil. Based on the proportion of different particle sizes, a soil texture category may be assigned to the sample. The first stage in a particle size analysis is the dispersion of the soil into individual particles - sand ($>1000\mu\text{m}$ - $<600\mu\text{m}$), silt ($>600\mu\text{m}$ - $<37\mu\text{m}$) and clay ($>37\mu\text{m}$). The hydrometer method of silt and clay measurement relies on the effects of particle size on differential settling velocities within a water column. Theoretically the particles are assumed to be spherical and have a specific gravity of 2.65. If all other factors are constant, the settling velocity is proportional to the square of the radius of the particle in accordance with stoke's law

Reagents

1. Calgon (sodium hexametaphosphate), 10% - dissolved 100 gm calgon in 1L DDW (double distilled water).
2. Amyl alcohol

Procedure

To 50 gm air dried (passed to 2mm sieves), added 100 ml water and 50 ml calgon solution and left for six hours. The above treated soil suspension was stirred with high-speed soil stir for 2 minutes and then sieved through 0.053mm sieve. Transferred the solution ($<0.053\text{mm}$) into 1000ml measuring cylinder and made to volume. Dried the fraction greater than 0.053mm fraction in a pre-weighted crucible and weighed again to get sand percentage. To the solution in 1000 ml cylinders, added 2-3 drops of amyl alcohol to check frothing. Soil in the cylinder was agitated and left to stabilize for two to three hours. A 20ml pipette was marked at levels of 5 cm and 20cm from the top for the determination of the silt and clay fraction. Agitated the soil with perforated disc and started the stopwatch as soon as it was taken out of the suspension. The 20ml pipette was inserted to 20cm depth from the surface of the solution after 10 second. Started sucking after 20 second unto the 20 ml mark in the pipette and transferred it to a pre-weighted petri-disc. Dried it at 105°C in an oven to obtain the silt plus clay fraction. Re-stirred the suspension in the measuring cylinder and allowed to stand. After 1 hour 7 minute and 12 second (from the chart for correction for temperature of the liquid), dipped the pipette up

to 5 cm mark from the surface of the soil and sucked up to 20 ml mark and transferred to a pre-weighted petri-dish and left to dry completely. It is the clay fraction.

The weight of silt and clay fraction is given by

$$(\text{Silt and clay fraction} - \text{clay fraction}) * 50 = \text{weight of silt}$$

$$\text{Clay fraction} * 50 = \text{weight of clay.}$$

From the weight of the sand, silt and clay fractions of each sample, the percentage of each of the fractions was calculated and texture assigned to each of the sample by reference to the soil textural triangle. The results are given in Chapter V (page 71-74).

Result and Discussion

RESULT AND DISSCUSSION

Chapter V

5.1 LAND USE AND LAND COVER

Multitemporal and multispectral data coverage capability of satellite provides efficient tool for planning for water resource management. The use of remote sensing technology involves large amount of spatial data management and the GIS technology provides an alternative for efficient and effective management of large and complex databases. To demonstrate the efficiency of the GIS for groundwater studies, information on the parameters controlling groundwater such as a lithology, structure, and recharge condition were analyzed using GIS. The clue to ground water search is the premise that sub-surface geologic elements forming aquifers have surface expressions, which can be discerned by remote sensing techniques. These surface expressions are drainage, landforms of depositional nature, moist pockets seen as anomalous vegetation patches, lineaments etc.

There are several urban applications where satellite based remotely sensed data are being applied, namely, urban sprawl/ urban growth trends, mapping and monitoring land use/ land cover, urban change detection and updation, urban utility and infrastructure planning, urban land use zoning, urban environment and impact assessment, urban hydrology, urban management and modeling (Raghavswamy, 1994). Remote sensing techniques offer benefits in the field of land use/ land cover mapping and their change analysis. Detection of changes in the land use/ land cover involves use of at least two period data sets (Jenson, 1986). The changes in land use/ land cover due to natural and human activities can be observed using current and archived remotely sensed data (Luong, 1993). Land use/ land cover change is critically linked to natural and human influences on environment. Keeping the above in view, the present work has been undertaken to prepare the multi-date land use/ land cover maps of study area and area of interest from multi-sensor satellite data and to monitor the changes in various land use/ land cover classes using digital remote sensing techniques. For monitoring the changes in the pattern of land utilization, preparation of multi-date land use/ land cover maps are necessary. Limited field visits have been undertaken for collecting the training samples. The various land use/ land cover classes selected include built-up, agriculture, sand, water, scrub and open/ barren land. The multispectral classification was carried out using supervised classification techniques with maximum likelihood classifier. The overall accuracy of the classification is finally obtained through the computation of confusion matrix to assess the reliability of the prepared maps. The various land use and land cover classes delineated include built-up, agriculture, sand, water, scrub and open/ barren land. The spatial coverage of each class may be visualized on both maps.

LULC of Study Area

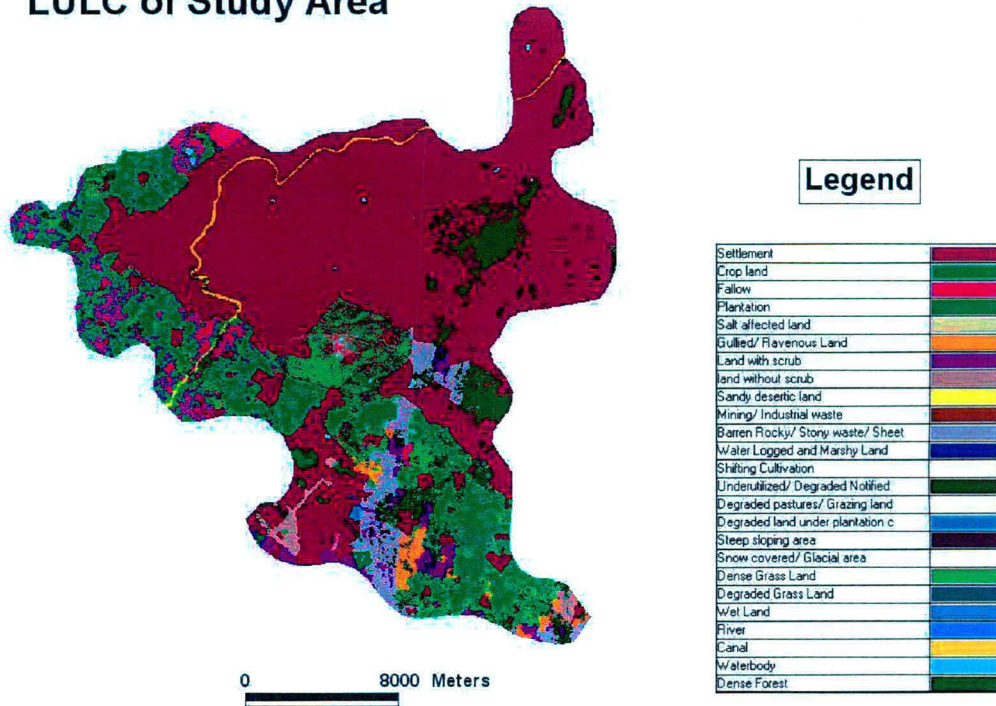


Fig.5.1. LU/LC of the Study Area

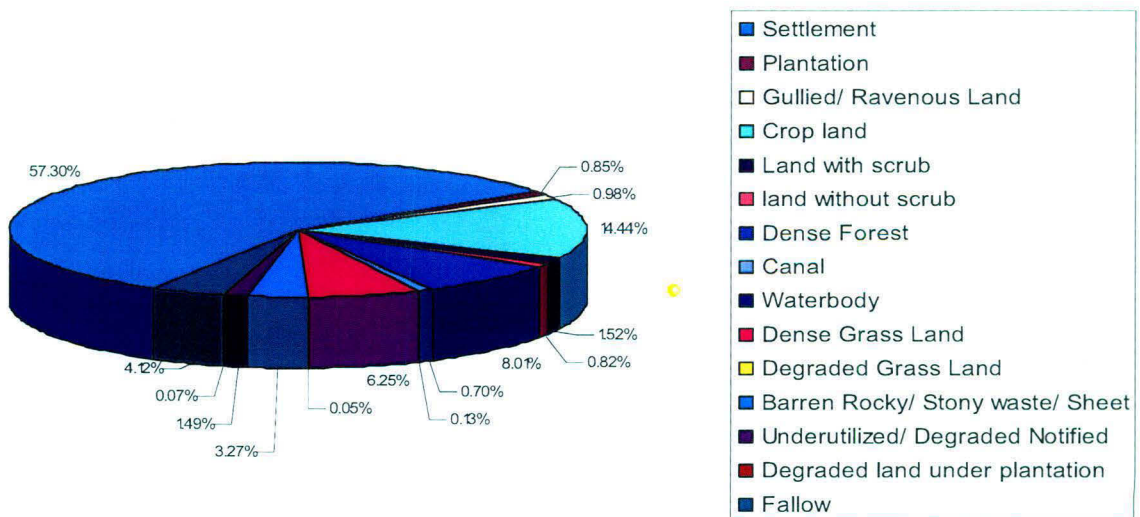


Fig.5.2. Percentage Contribution of Various LULC classes

RESULT AND DISSCUSSION

The characteristic of groundwater is reflected on the soil and vegetation of the surface above it in unconfined aquifers. Hence, the characteristics of the groundwater at a particular area can be determined to a particular extent, by its surface manifestation in terms of the landuse/ landcover pattern. This is the basis on which the classification of the image was performed by using unsupervised classification. In this particular type of classification spectral classes are grouped first, based solely on the numerical information in the data, and are then matched by the analyst to information classes. Unsupervised classifiers do not utilize training sets as the basis for classification. Rather it involve algorithms called clustering algorithms, that examine the unknown pixels in an image and aggregate them into a number of classes based on the natural groupings or clusters present in the image values. The analyst specifies the desired number of classes. Thus unlike supervised classification, it does not start with a pre-determined set of classes, however it is neither done completely without human intervention.

The classes so created and the proportion of total area of the image covered by them, provide an insight into the composition of total area vis-à-vis the different features being represented by these classes. On account of analysis of these classified images, we are able to infer to a certain extent, the changes that occurred in the spatial composition with reference to the different physiographic features. In the current study the multispectral image was classified in fifteen classes, except some other class relevant to the study, which was prominently observed, were also taken into account. The images were classified into following fifteen classes.

1. Settlement
2. Plantation
3. Gullied/ Ravenous Land
4. Crop land
5. Land with scrub
6. land without scrub
7. Dense Forest
8. Canal
9. Water body
10. Dense Grass Land
11. Degraded Grass Land
12. Barren Rocky/ Stony waste/ Sheet
13. Underutilized/ Degraded Notified

14. Degraded land under plantation

15. Fallowland

Class	Total Area in sq.km	% of total area
Settlement	252.29	57.30
Plantation	3.72	0.85
Gullied/ Ravenous Land	4.30	0.98
Crop land	63.58	14.44
Land with scrub	6.71	1.52
land without scrub	3.63	0.82
Dense Forest	35.27	8.01
Canal	3.09	0.70
Waterbody	0.59	0.13
Dense Grass Land	27.50	6.25
Degraded Grass Land	0.20	0.05
Barren Rocky/ Stony waste/ Sheet	14.41	3.27
Underutilized/ Degraded Notified	6.57	1.49
Degraded land under plantation	0.29	0.07
Fallow	18.15	4.12

Table.5.1 The area occupied by various LULC classes and its percent contribution

The settlements occupied 57.30% (252.29sq.km.) of the total study area of 547.73sq.km the plantation, cropland, dense forest occupied a total area of 23.29% (102.57sq.km.) of the total area.



Fig.5.3. Digital Elevation Model (DEM) of the Study Area

5.2 Data utilized for generating Elevation contours, Isopach, Fence diagram, Litholog in Rockworks

- Secondary data of lithologs from CGWB (Central Ground Water Board) datasets of year 2000-2005 was utilized for studying the water quality, water level (aquifer depths) and lithology within the selected study area.
- Lithology data was modelled using the software Rockworks (version 2006, revision 6.9.8) for the whole study area to interpret the general lithological composition within study area. It's an integrated software package for geological data management, analysis, and visualization. When working with surface or sub-surface data, it offers a complete suite of easy-to-use tools for modeling, image creation, and report generation.
- This was supplemented with water level data to determine general trend of aquifer depths within study area.
- This served as a background for analyzing and interpreting data from primary drilling sites within the study area.
- Resistivity and magnetic surveys were carried out at various locations in 2 areas within the whole study areas -RR hospital and JNU campus - based on ground points selected from processed satellite imagery.
- The primary data was modelled for a particular site, within the study area, selected for groundwater exploration. This made possible correlating the hypothesis and reasoning behind site selection (based on satellite image interpretation and ground survey) with the actual field observations regarding groundwater level and subsurface geology.

Well No.	Place
B-1	Chanakyapuri
B-2	Rajendra Nagar
B-3	Baljeet Nagar
B-4	Qudasia Garden
B-5	Lady Harding hospital
B-6	Naraina-II
B-7	Willingdon Hospital
B-8	I.I.T., Hauz Khas (A)
B-9	Rajokri
B-10	Toghanpur
B-11	Pindwala kalan (dw)
B-12	Sadhnagar-ii (dw)
B-13	Sadhnagar-i (dw)
B-14	Nicolson Range
B-15	Kirtinagar
B-16	Pankha Road
B-17	Moti Nagar
B-18	Satbari – II (DW)
B-19	Satbari – III (DW)
B-20	Chatterpur (DW)
B-21	Dhansa
B-22	J.N.U. , Sanjay Van
B-23	Ghitorni
B-24	Gadaipur-5
B-25	Ranhola-I (DW)
B-26	Ranhola-II (DW)

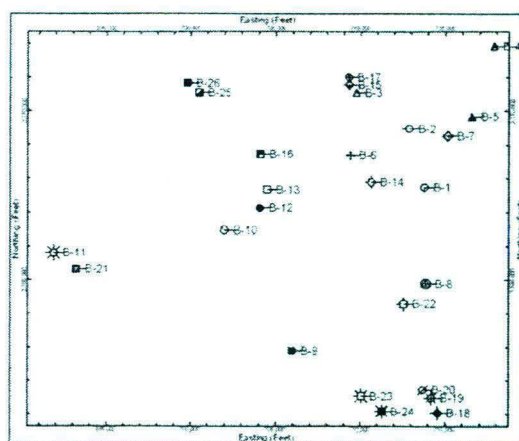


Fig.5.4. Drilling Sites within the study area as per CGWB (Central Ground Water Board) datasets of year 2000-2005 and their location plan

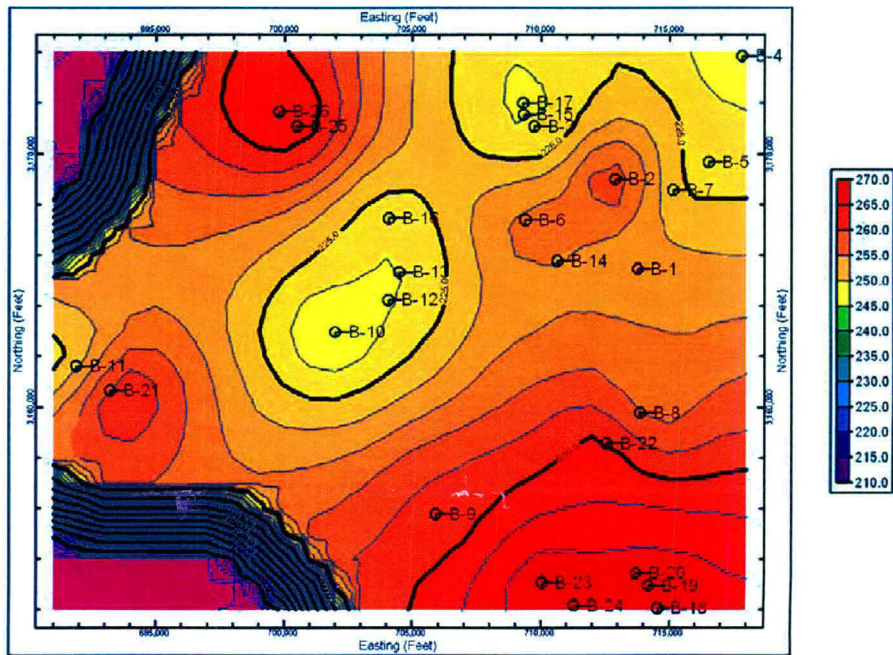


Fig.5.5. Elevation Contours (in metres) within the Study Area

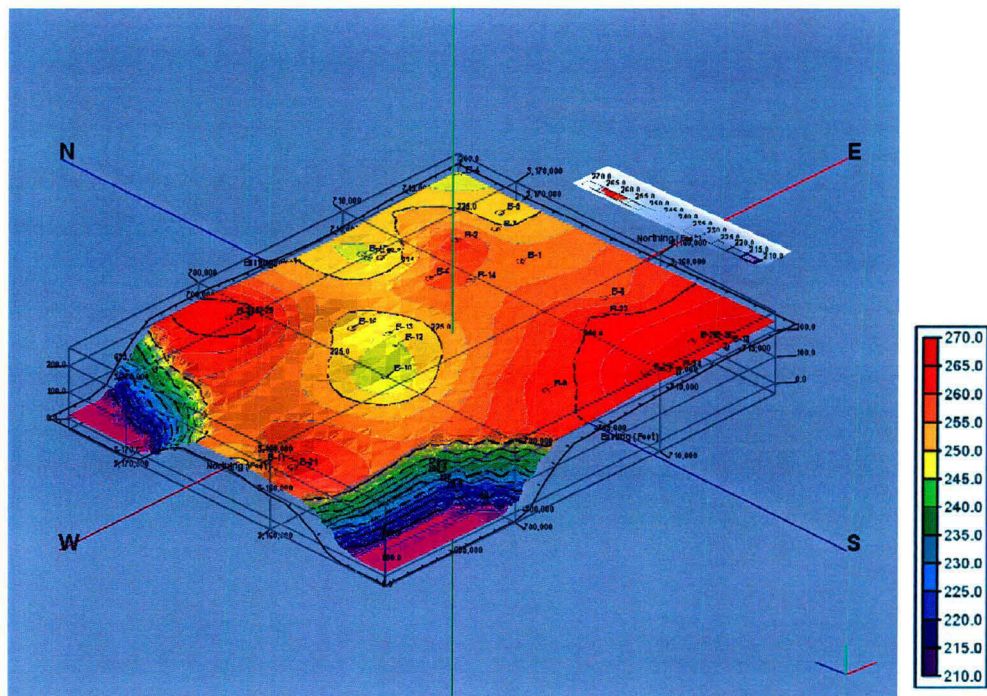


Fig.5.6. Three Dimensional Contours (in metres) of the Study Area

Elevation contours of the study area indicate that elevation naturally decreases towards south-west and north-west regions of the study area. Towards northern and south-eastern parts of study area elevation can reach as high as 265-270 metres (a.s.l.). Rest of the study area has average elevation of 245-255m.

RESULT AND DISSCUSSION

Bore No.	Lithology	Bore No.	Lithology
B-1	Surface Clay	B-13	Surface Clay
	Weathered Quartzite		Highly Weathered Quartzite
	Quartzite with Mica schist		
		B-14	Surface Clay
			Weathered Quartzite
B-2	Surface Clay		Massive Quartzite
	Weathered Ferruginous Quartzite		
	Mica Schist with Quartz vein	B-15	Surface Clay
	Mica Schist with compact Quartzite		Weathered Quartzite
B-3	Surface Clay	B-16	Surface Clay
	Crushed Schist with Quartz Vein		Weathered Quartzite
	Mica Schist with Quartz vein		
	Massive Quartzite	B-17	Surface Clay
	Fractured Quartzite		Weathered Quartzite
B-4	Surface Clay	B-18	Surface Clay
	Weathered Quartzite		Weathered Ferruginous Quartzite
B-5	Surface Clay	B-19	Surface Clay
	Weathered Micaceous Quartzite with veins		Weathered Ferruginous Quartzite
	Massive Quartzite		Massive Quartzite
B-6	Surface Clay	B-20	Surface Clay
	Weathered Quartzite		Weathered Ferruginous Quartzite
B-7	Surface Clay	B-21	Surface Clay
	Weathered Quartzite		Weathered Quartzite
B-8	Surface Clay	B-22	Highly Weathered Quartzite
	Massive Quartzite		Weathered Micaceous Quartzite with veins
	Weathered Quartzite		
		B-23	Surface Clay
B-9	Surface Clay		Weathered Quartzite with pegamatite veins
	Weathered Ferruginous Quartzite		
	Weathered Quartzite	B-24	Surface Clay
			Highly Weathered Quartzite
B-10	Surface Clay		Massive Quartzite
	Weathered Quartzite		
		B-25	Surface Clay
B-11	Surface Clay		Weathered Quartzite
	Highly Weathered Quartzite		
		B-26	Surface Clay
B-12	Surface Clay Highly Weathered Quartzite		Weathered Ferruginous Quartzite

Table 5.2. The lithology of Drilling Sites within the study area as per CGWB

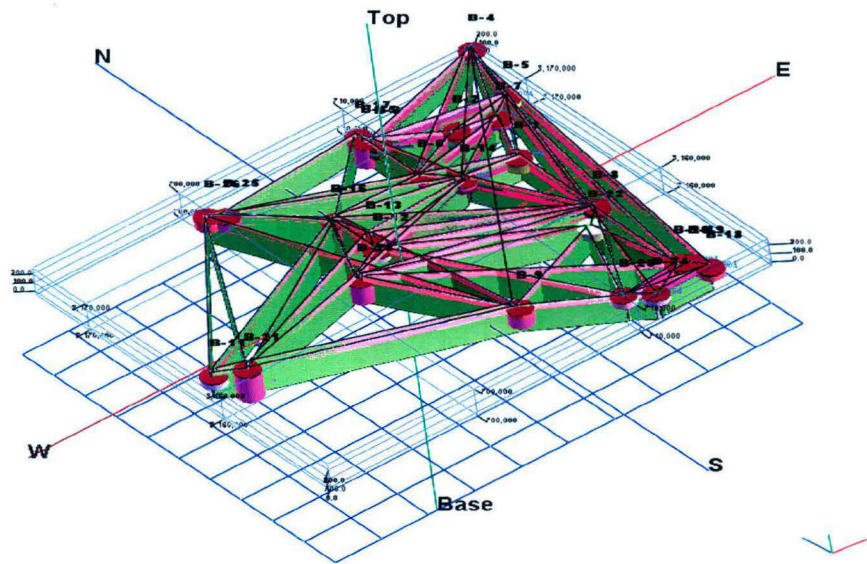


Fig.5.7. Three Dimensional Fence Diagram of the Study Area (View 1)

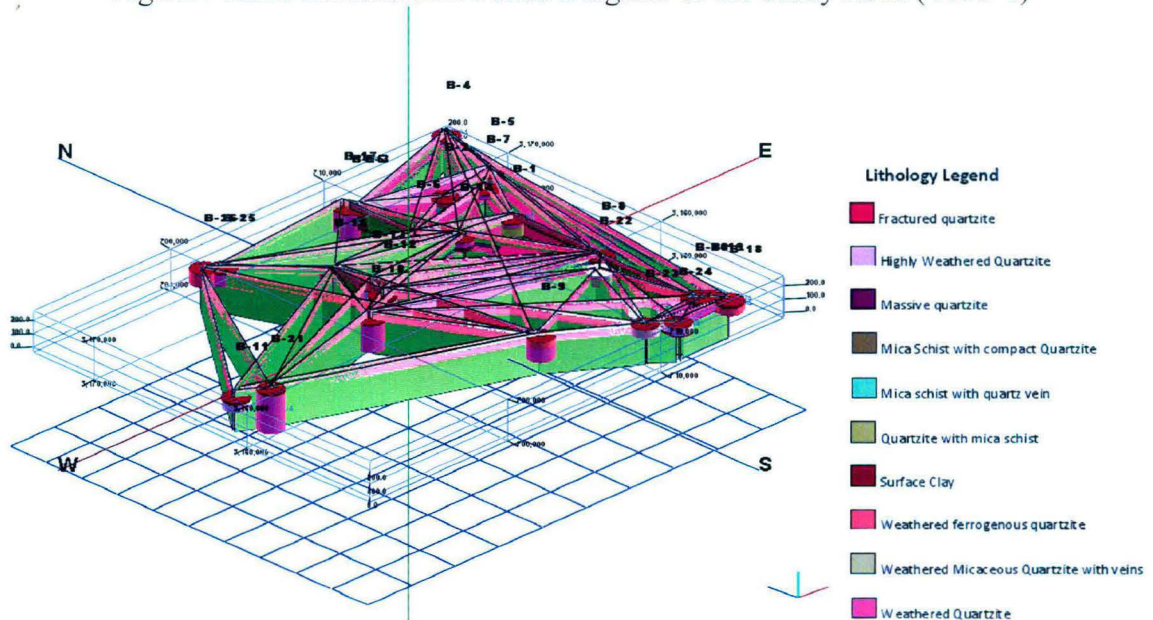


Fig.5.8. Three Dimensional Fence Diagram of the Study Area (View 2)

3-Dimensional Fence Diagram generated for the whole study area using secondary data from CGWB datasets of year 2000-2005 clearly shows that top layers in the north-eastern, eastern and south-eastern parts of study area are predominantly composed of Weathered/Fractured Quartzite (primarily ferruginous in nature). On the other hand the lower layers throughout the study area are mostly composed of Mica Schist and Compact Quartzite. Weathering/Fractures in Ferruginous Quartzite over

RESULT AND DISSCUSSION

Water level data was used to generate aquifer model for the study area to visualize and interpolate the water depth and aquifer thickness within the study area. This is helpful in selecting the sites for primary drilling (after resistivity and magnetic surveys). As evident from the aquifer model and the Aquifer Thickness (Isopach) generated for the study area, groundwater is quite surplus in the North-Western and Western parts of the study area whereas Southern, Eastern and South-Eastern parts of the study area are comparatively quite deficient in groundwater.

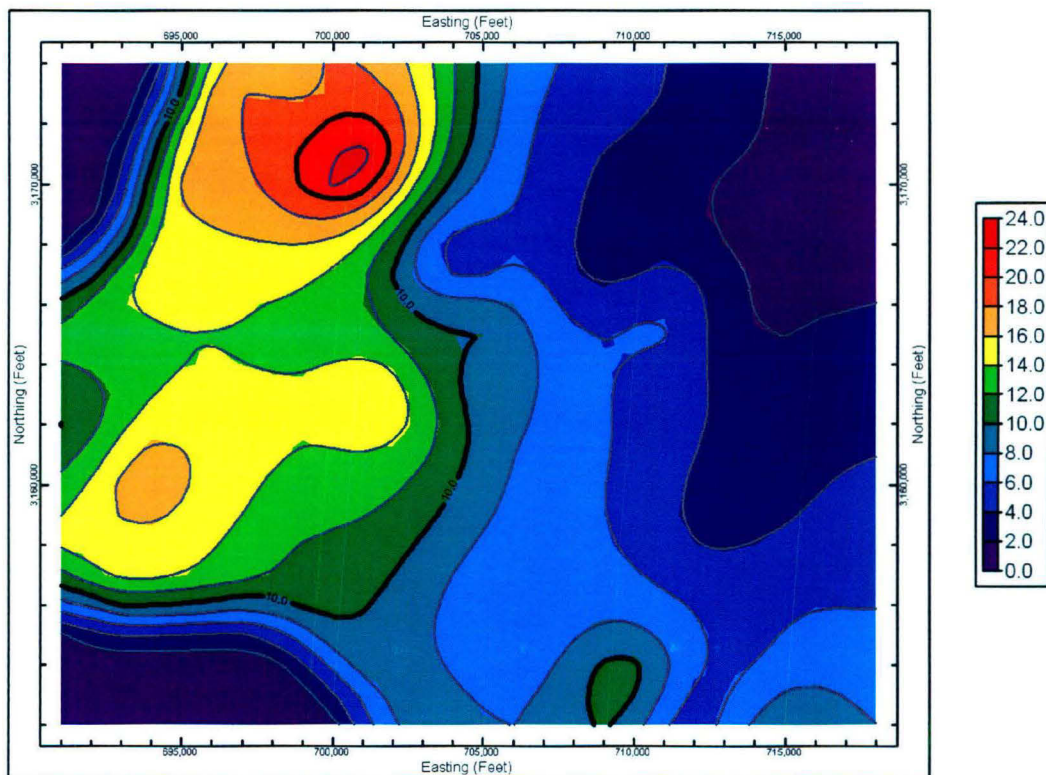


Fig.5.11. Aquifer Thickness (Isopach) of the Study Area (in metres)

5.3 LAND USE AND LAND COVER OF RR HOSPITAL

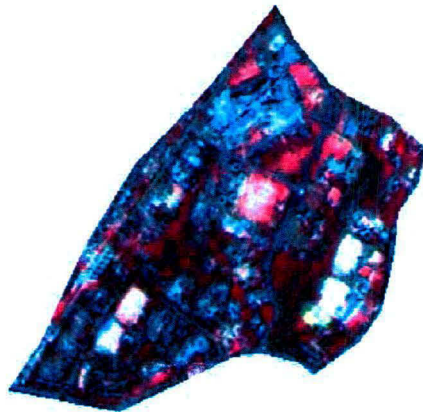


Image 2001

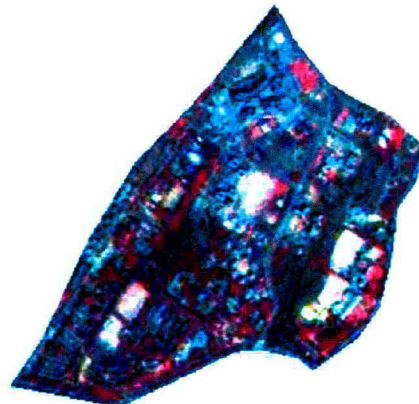
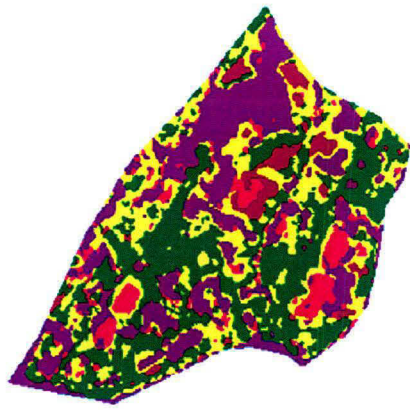
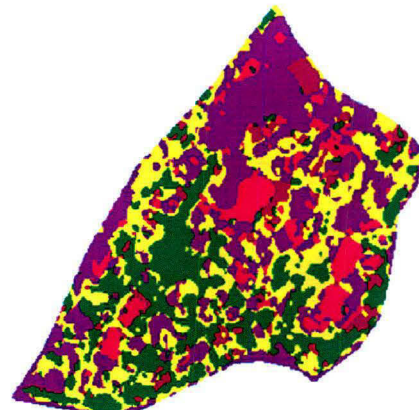


Image 2003



Unsupervised classification of image of 2001



Unsupervised classification of image of 2003

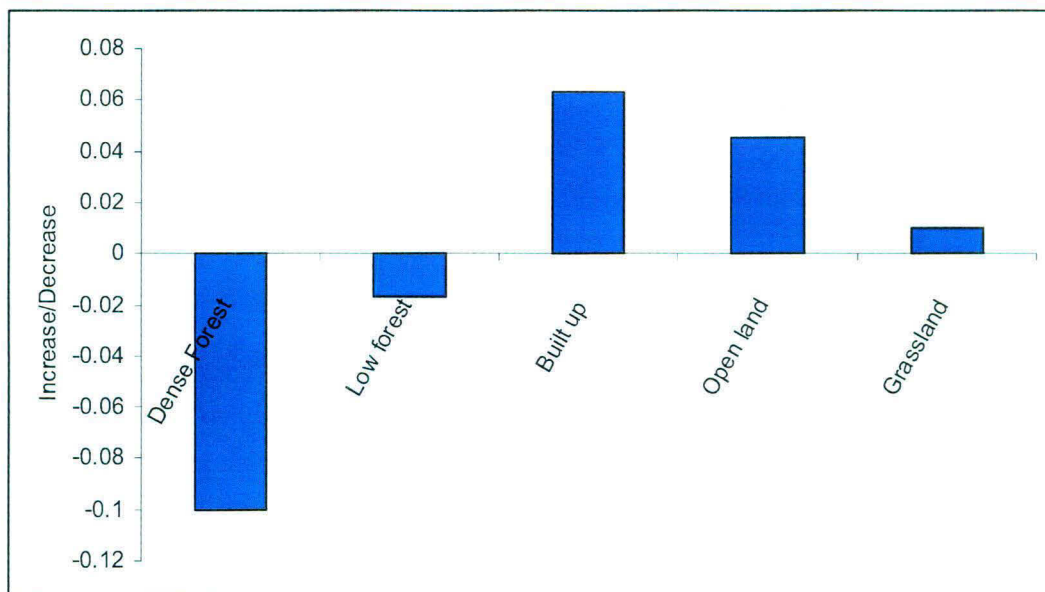
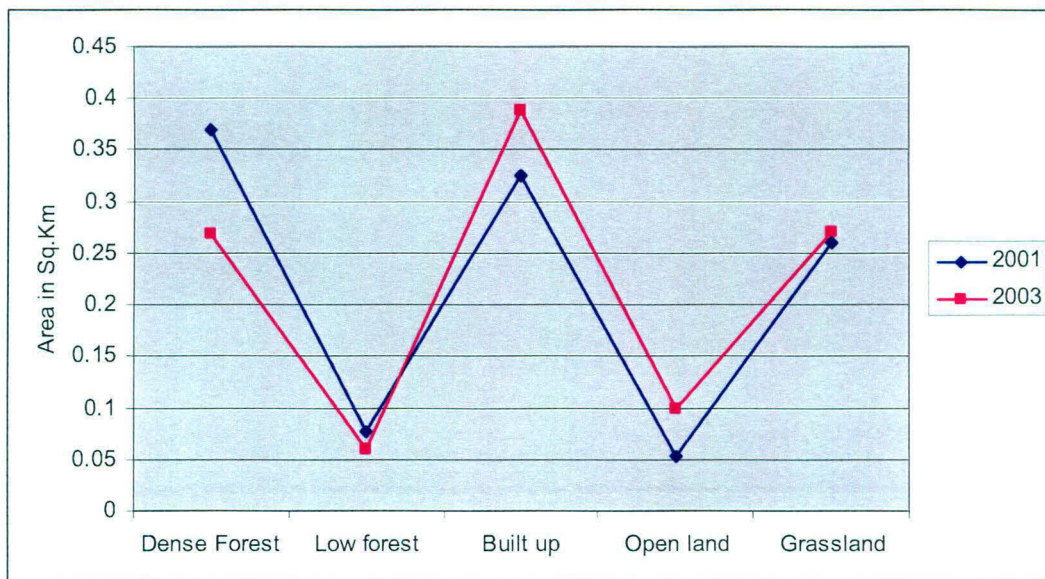
Row	Histogram	Class	Color	Opacity
0	0	Unclassified		0
1	14754	Dense forest		1
2	13016	Builtup		1
3	3090	Open land		1
4	10396	Grassland		1
5	0	Class 5		1
6	2151	Low forest		1

Attributes of classified of image of 2001

Row	Histogram	Class	Color	Opacity
0	0	Unclassified		
1	10753	Dense Forest		
2	2406	Low forest		
3	15525	Built up		
4	3973	Open land		
5	10784	Grassland		

Attributes of classified of image of 2003

Fig.5.12. Image classification of RR hospital to infer change in land use and land cover (2001 & 2003)



Class	LISS III Image 2003	Resourcesat Image 2001	Increase/Decrease in sq.km.	% Increase/ Decrease in respective classes
Dense Forest	0.269	0.369	-0.100	-9.217
Low forest	0.060	0.077	-0.017	-1.576
Built up	0.388	0.325	0.063	5.780
Open land	0.099	0.054	0.046	4.197
Grassland	0.270	0.260	0.010	0.894

Fig.5.13.Change in various classes of land use and land cover in RR Hospital area from year 2000 & 2003

A multispectral resourcesat satellite image of RR Hospital for the year 2001 was classified into five classes using unsupervised classification technique. Similarly LISS III image of year 2003 was also classified using unsupervised (hybrid) classification technique. The results obtained are given in table no 5.3

A subset image of area of interest (RR Hospital and its surrounding area) was taken into consideration for LULC analysis for the following classes-

1. Built up
2. Grassland
3. Low forest
4. Open/fallow land
5. Dense forest

It is observed from the classification that the dense forest area decreased from 0.369sq.km in year 2001 to 0.269sq.km in year 2003, showing overall decrease in the area of dense forest to 9.21%. A decrease of 1.57% was also observed in area occupied by low/sparse forest. The decrease in area occupied by dense forest and low/sparse forest can be very well observed by a 5.78% increase in built-up area and increase in open land due to the developmental activities occurring in the hospital premises.

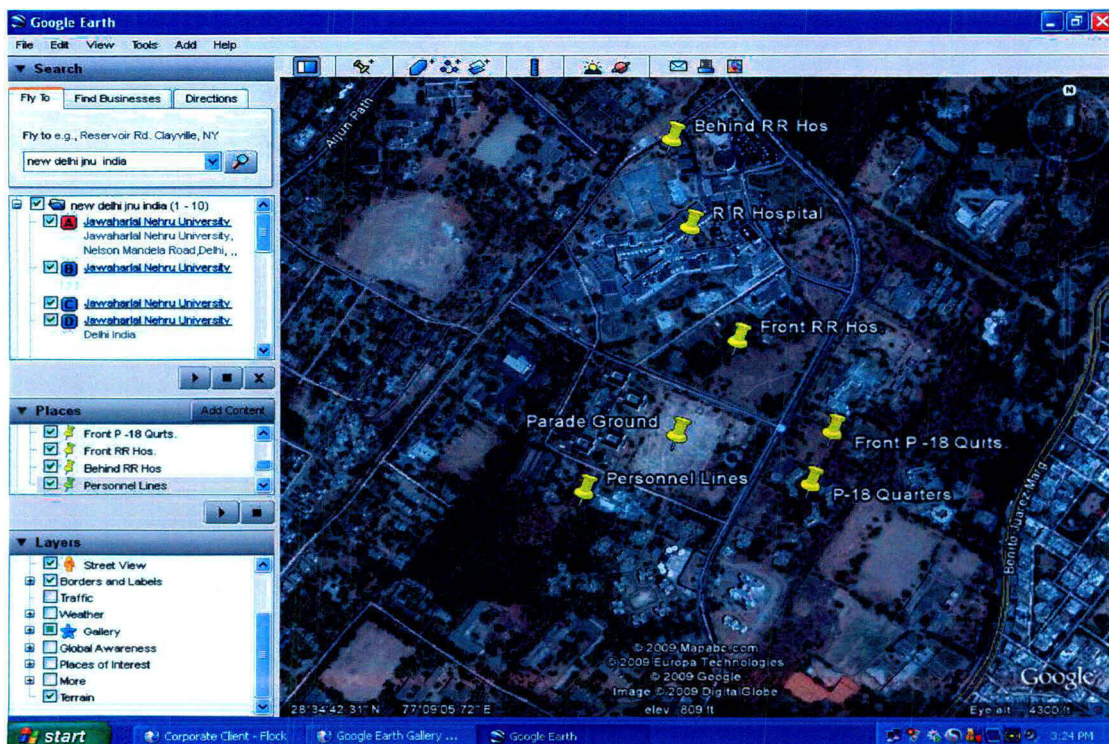


Fig.5.14. Resistivity Survey carried out various sites in R. R. Hospital

5.4 SOIL TEXTURE ANALYSIS OF RR HOSPITAL

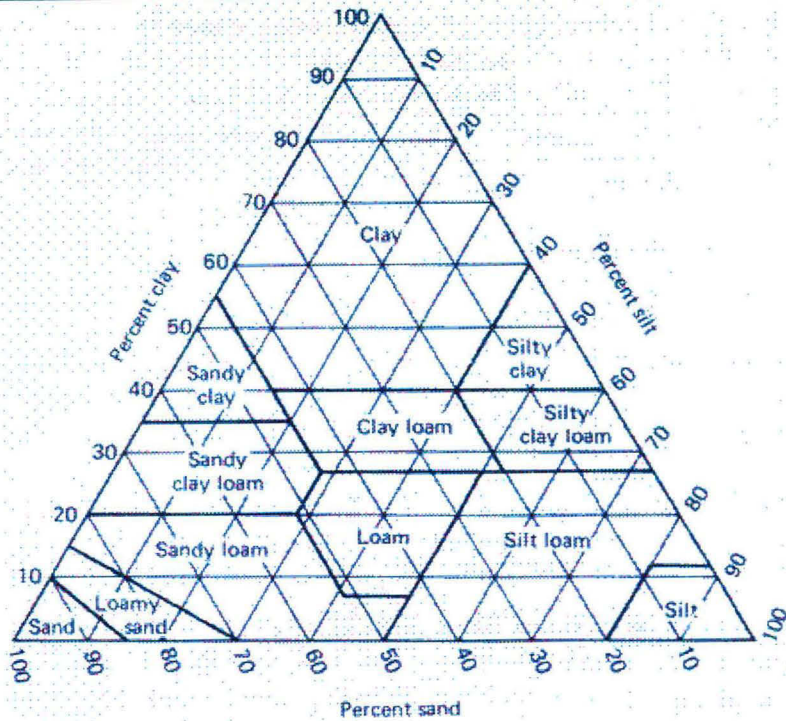


Fig.5.15. Triangle of soil textures for describing various combinations of sand silt and clay (soil survey staff)

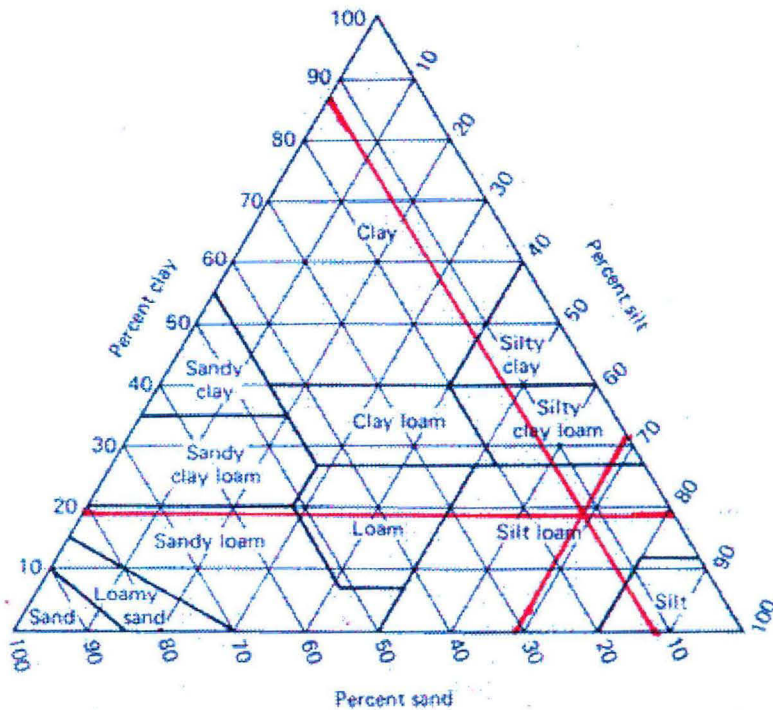


Fig.5.16. Soil textural class In front of Shopping Complex and Temple

Particle size (μm)	Weight (%)	Soil fraction	Fraction percentage
>1000	11.5	Sand	11.5%
>600	11.0	Silt	69%
>250	14.0		
>125	14.0		
>63	30.0		
>37	18.0	Clay	19%
<37	1		

Table 5.3. Sample no.1 In front of shopping complex and temple

The value of the various fractions signifies that the soil is silty loam. The top layer of the soil is silty loam while below 50cm the medium to coarse-grained sand is present making the site actually good for installing deep tube wells as well as rainwater harvesting

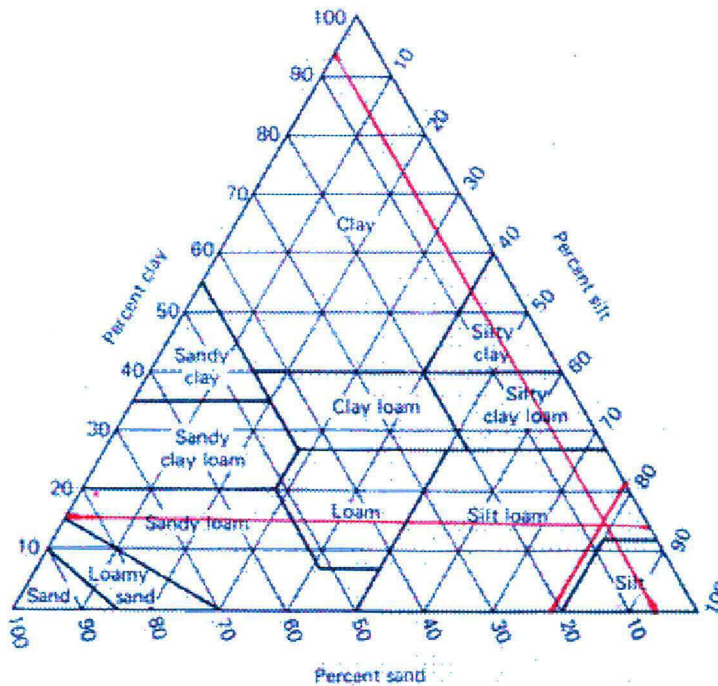


Fig.5.17. In front of officer’s mess

Particle size (μm)	Weight (%)	Soil fraction	Fraction percentage
>1000	6	Sand	6%
>600	11	Silt	78%
>250	16		
>125	14		
>63	37		
>37	14	Clay	16%
<37	2		

Table 5.4. Sample no.2 in front of officer mess

RESULT AND DISSCUSSION

As the soil here is siltier it makes the soil less useful for recharge but considering the magnetic and resistivity data as well as the vegetation anomaly it can be used as an alternate bore well.

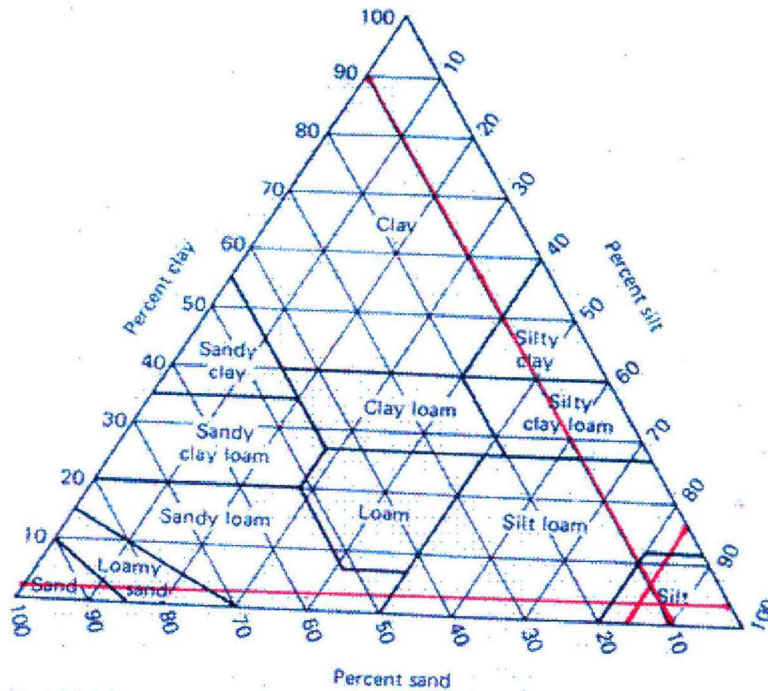


Fig.5.18. Soil textural class in front of mortuary, Personnel Lines

Particle size (m μ)	Weight (%)	Soil fraction	Fraction percentage
>1000	10	Sand	10%
>600	11.5	Silt	88.4%
>250	23.4		
>125	38.5		
>63	15		
>37	1.5	Clay	2.0%
<37	0.5		

Table 5.5. Sample no.3 in front of mortuary, Personnel Lines

Here the soil is even siltier making it less useful for ground water exploration as well as not suitable for recharge purpose.

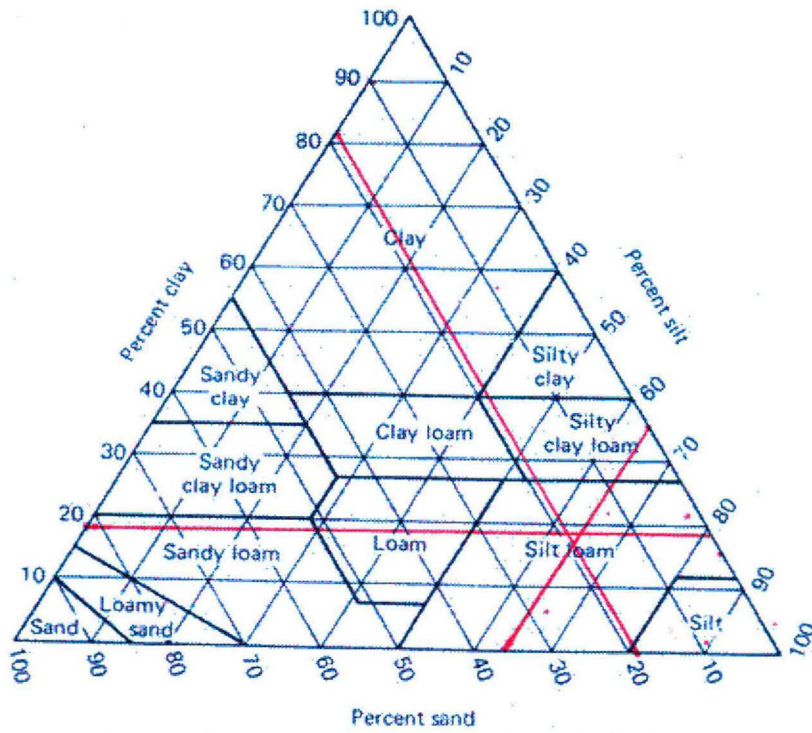


Fig.5.19. Soil textural class in front of Cafeteria

Particle size (m μ)	Weight (%)	Soil fraction	Fraction percentage
>1000	19	Sand	19%
>600	9	Silt	64%
>250	20		
>125	10		
>63	25		
>37	15	Clay	18%
<37	3		

Table 5.6. Sample no.4 in front of Cafeteria

As the silt portion is less it can serve as an alternative site for ground water exploration

5.5 RESISTIVITY SURVEY CARRIED OUT AT VARIOUS SITES IN R. R. HOSPITAL

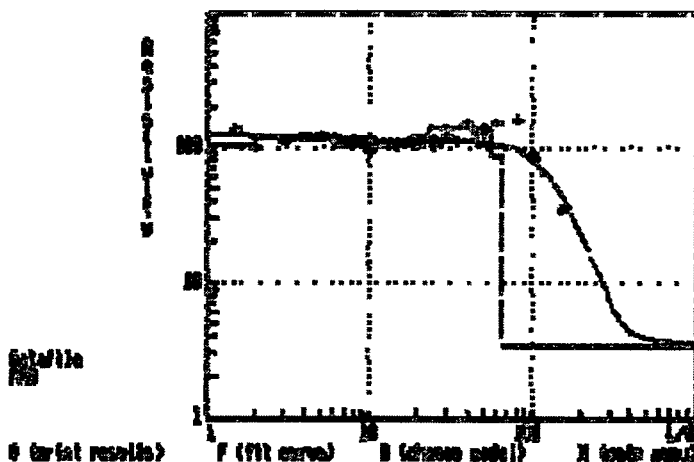


Fig.5.20. Vertical Electrical Sounding Plot of Parade Ground
 Geo Coordinates $28^{\circ}34'50.10''N$ $77^{\circ}09'26.90''E$

Standard (Gamma)	Obtained(Gamma)	Signal Strength
47,000	47,277	Very high
47,000	24,782	Very very high

Table 5.7. Magnetic Data of Parade Ground at Center in RR Hospital

5.5.1 Parade Ground:

- (a) The first layer resistivity shows hard and compact sandy soil but this soil is only a few centimetres. Down to 1m.bgl to 35m.bgl the soil condition is expected to be highly porous sandy materials are present which is highly suitable for groundwater exploration as well as artificial recharge. Down to 35m.bgl the clay rich strata forms impermeable zone. However this site is very promising for construction of shallow tube wells (Battery of tube wells) with 500m horizontal spacing.
- (b) Based on resistivity data it is clear that the premises of parade ground are promising for groundwater exploration. Several points were investigated by the instrument Proton Precision Magnetometer (PPM). The most promising site for groundwater exploration appears to be parade ground. (Research & Referral Hospital, New Delhi). The anomaly in the magnetic value is

RESULT AND DISSCUSSION

significant in terms of the range of reading. The magnetic anomaly ranging from 28,000 Gamma to 34,000 Gamma approximately with very high signal. It is expected that below the coarse grained sandy aquifer the quartzite are fractured. Since the values of magnetic anomaly detected 100m east of this point also shows similar values of magnetic as well as resistivity data, it can be confirmed that the surface water bearing fractures in quartzite (secondary porosity) exist in this area.

- (c) High spectral reflectance in remote sensing data when supported by low resistivity value is suggestive of high groundwater potential; however without low resistivity value high reflectance may show granitic pediments, quartzites without substantial porosity-permeability. Spectral reflectance was observed on pixel in this area on all the bands shows very high values which further confirms suitability of this area for groundwater exploration as well as rain water harvesting.
- (d) In this area drilling can be carried out by direct rotary (DR) cum down the hole hammering (DTH) rig down to 200m. It is expected that down to 35mbgl buried pediments mixed with weathered friable loose formations are in existence. Further there are possibilities of multilevel fractured quartzite.

Since this area is showing promising sub-surface aquifer just 1m below the surface, can also be considered as suitable for roof top rain water infiltration in the pit with specific size.

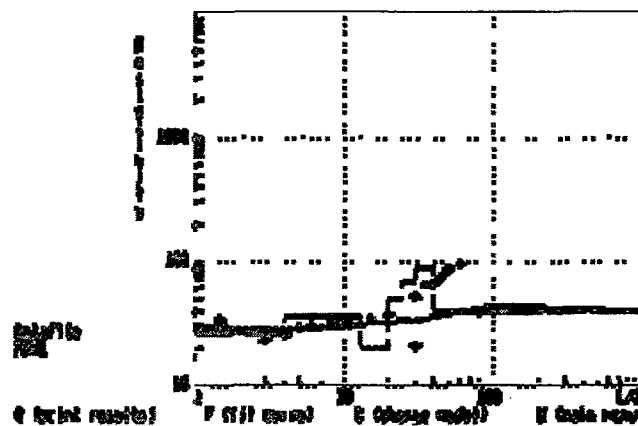


Fig.5.21. Vertical Electrical Sounding Plot of point in front of JRC and MRI

RESULT AND DISSCUSSION

Standard (Gamma)	Obtained(Gamma)	Signal Strength
47,000(Gamma)	28,832	Very very high
47,000(Gamma)	26,609	Very very high
46,000(Gamma)	37,693	High
48,000(Gamma)	29,080	Medium

Table 5.8. Magnetic Data in front of JRC and MRI at RR Hospital

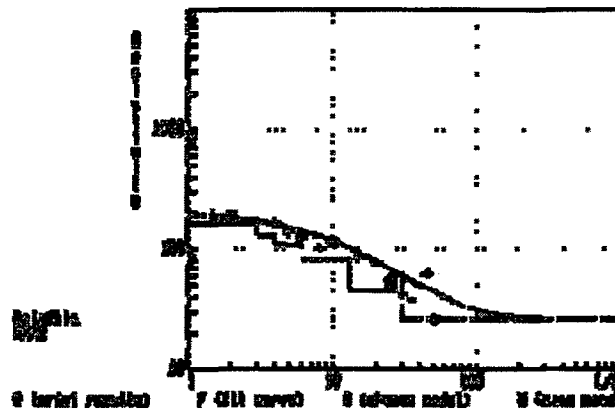


Fig.5.22. Vertical Electrical Sounding Plot at near Personnel lines

Geo Coordinates 28°34'45.63"N 77°09'23.10"E

Standard (Gamma)	Obtained (Gamma)	Signal Strength
47,000(Gamma)	46,951	Very high
47,000(Gamma)	47,447	Very high

Table 5.9. Magnetic Data at near personnel lines

5.5.2 Personnel Lines:

(a) In this area near Personnel Lines the resistivity values were found out to be decreasing continuously down to 20mbgl which denotes the possibility of subsurface clay below 10mbgl from ground level. However the resistivity values in the upper layer indicates a surficial aquifer. The discharge in this area cannot be expected to be very high.

RESULT AND DISSCUSSION

- (b) For rain water harvesting point of view also this area doesn't seems to be promising.
- (c) The magnetic value in this gives very high signal in 47,000 Gamma ranges which denotes that no promising fracture zones is existing in this area.
- (d) The spectral reflectance in Personnel Lines is low which denotes that compact clay mixed with fine sand exists in this area. All these information justifies that this area is neither promising for groundwater exploration nor for rain water harvesting.

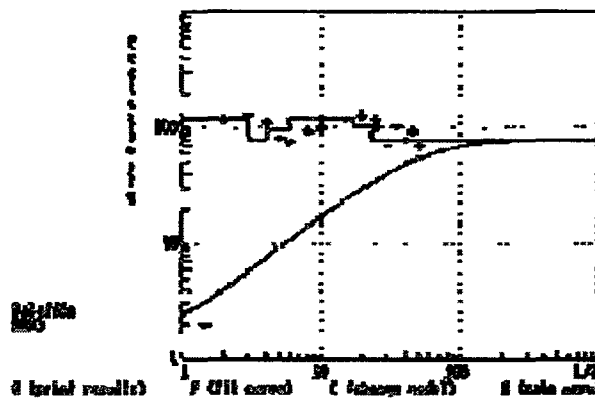


Fig.5.23. Vertical Electrical Sounding Plot at P-18 ground residence

Geo Coordinates $28^{\circ}34'49''N$ $77^{\circ}09'23.10''$

Standard (Gamma)	Obtained (Gamma)	Signal Strength
47,000	47,353	High
47,000	47,299	High
46,000	43,881	Very very high
47,000	32,184	Low

Table 5.10. Magnetic Data at P-18 ground residence

RESULT AND DISSCUSSION

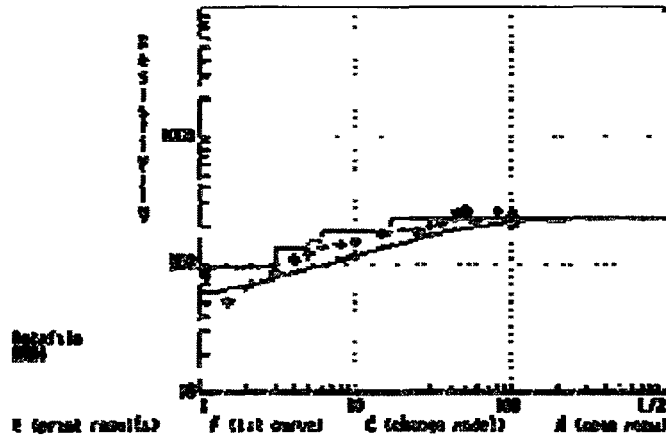


Fig.5.24. Vertical Electrical Sounding Plot behind P-18 and civil officers quarters

Geo Coordinates 28°34'45.44"N 77°09'32.75"

Standard (Gamma)	Obtained(Gamma)	Signal Strength
47,000	40,223	Medium

Table 5.11. Magnetic Data behind P-18 and civil officers quarters

- (a) As per resistivity survey points of view this area appears to be highly promising for drilling as well as rain water harvesting.
- (b) Magnetic value and spectral reflectance also suggest the suitability.
- (c) The drilling should be carried out by direct rotary cum DTH rig machine.

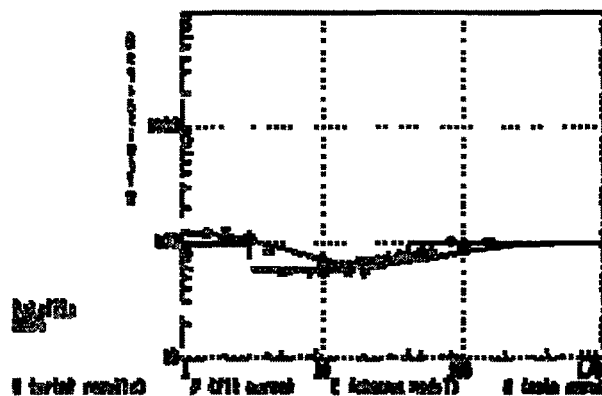


Fig.5.25. Vertical Electrical Sounding Plot in front of RR hospital Adjacent to parade ground

Geo Coordinates 28°34'54.46"N 77°09'30.81"E

RESULT AND DISSCUSSION

Standard (Gamma)	Obtained (Gamma)	Signal Strength
47,000	30,470	Very very high

Table 5.12. Magnetic Data in front of RR hospital Adjacent to parade ground

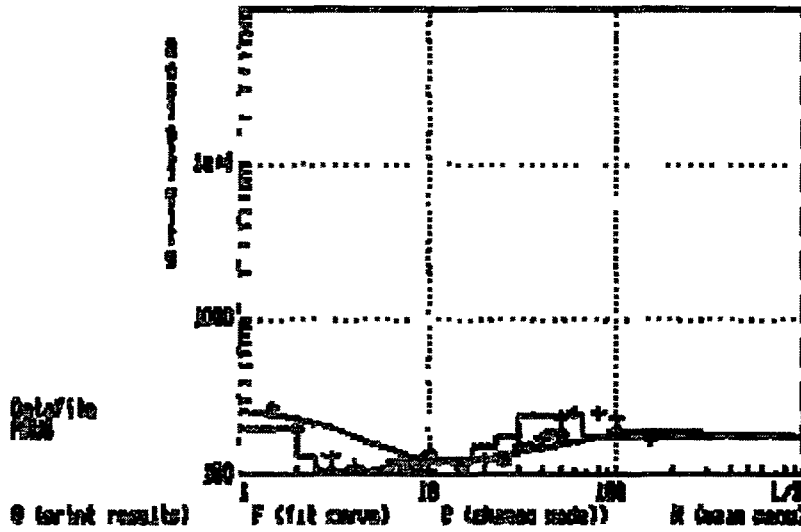


Fig.5.26. Vertical Electrical Sounding Plot of behind RR hospital
Geo Coordinates $28^{\circ}35'04.27''N$ $77^{\circ}09'26.73''E$

Standard (Gamma)	Obtained (Gamma)	Signal Strength
47,000(Gamma)	24,994	Very high
47,000(Gamma)	47,460	Medium
47,000(Gamma)	40,449	High

Table 5.13. Magnetic data of Plot of behind RR hospital

5.6 IMAGE PROCESSING OF SATELLITE IMAGE FOR JNU AREA

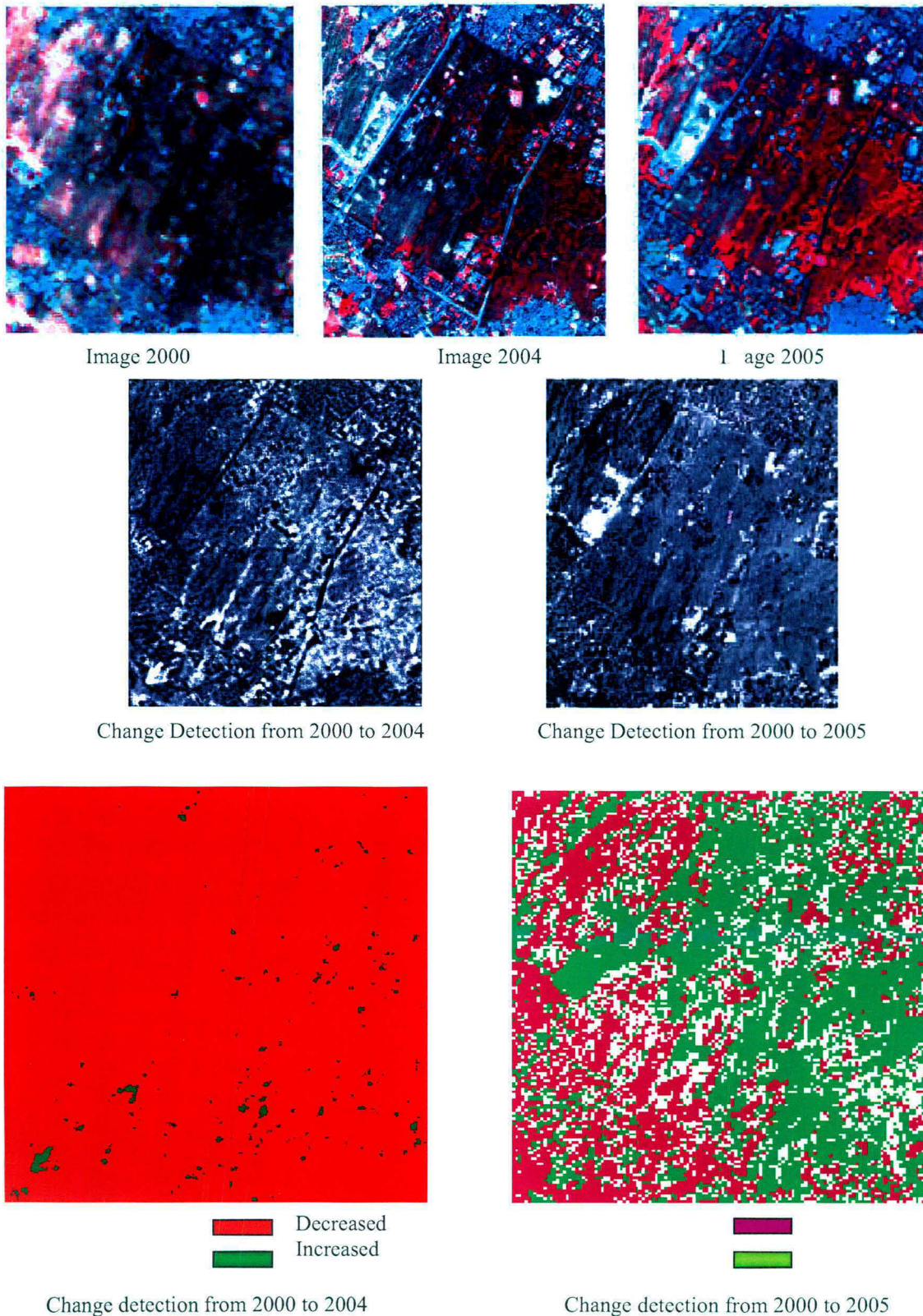


Fig.5.27. Image analysis to infer change detection in JNU between year 2000 & 2004, 2000 & 2005

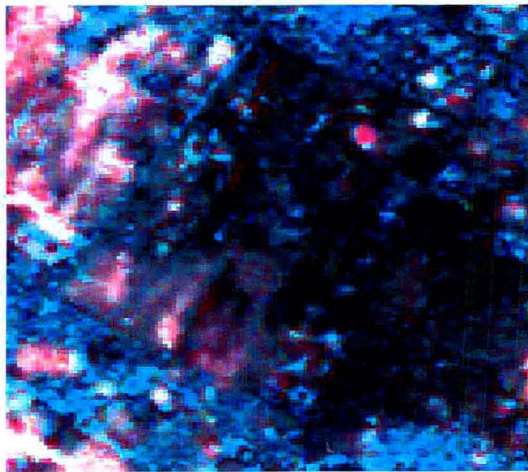


Image 2000

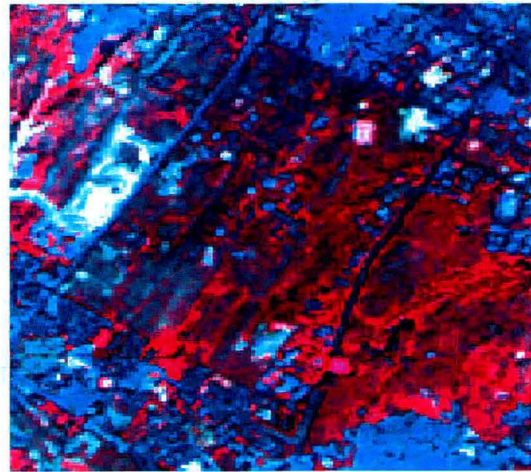
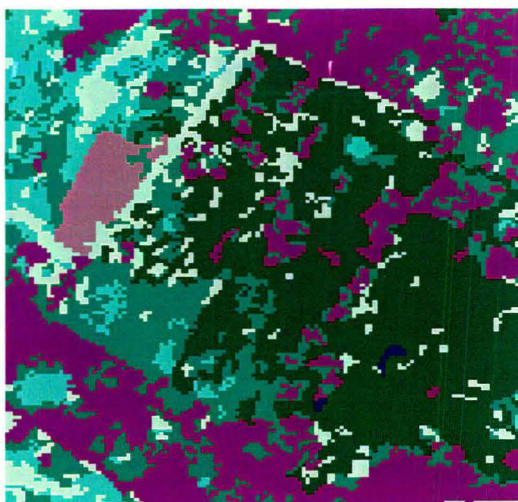
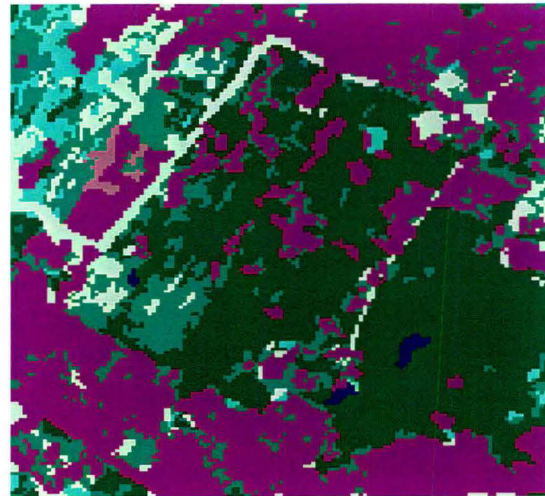


Image 2005



Hybrid Classification of Image 2000



Hybrid Classification of Image 2005

Row	Class Names	Color	Histogram
0	Unclassified		0
1	Builtup		4648
2	Industrial		0
3	Water		31
4	Barren Rock		438
5	Grass		1319
6	Low Forest		3998
7	Open		1611
8	Dense Forest		5687

Attributes of Classified Image of 2000

Row	Class Names	Color	Histogram
0	Unclassified		0
1	Builtup		7815
2	Industrial		0
3	Water		81
4	Barren Rock		97
5	Grass		604
6	Low Forest		3430
7	Open		1462
8	Dense Forest		7281

Attributes of Classified Image of 2005

Fig.5.28. Image classification of RR hospital to infer change in land use and land cover (2000 & 2005)

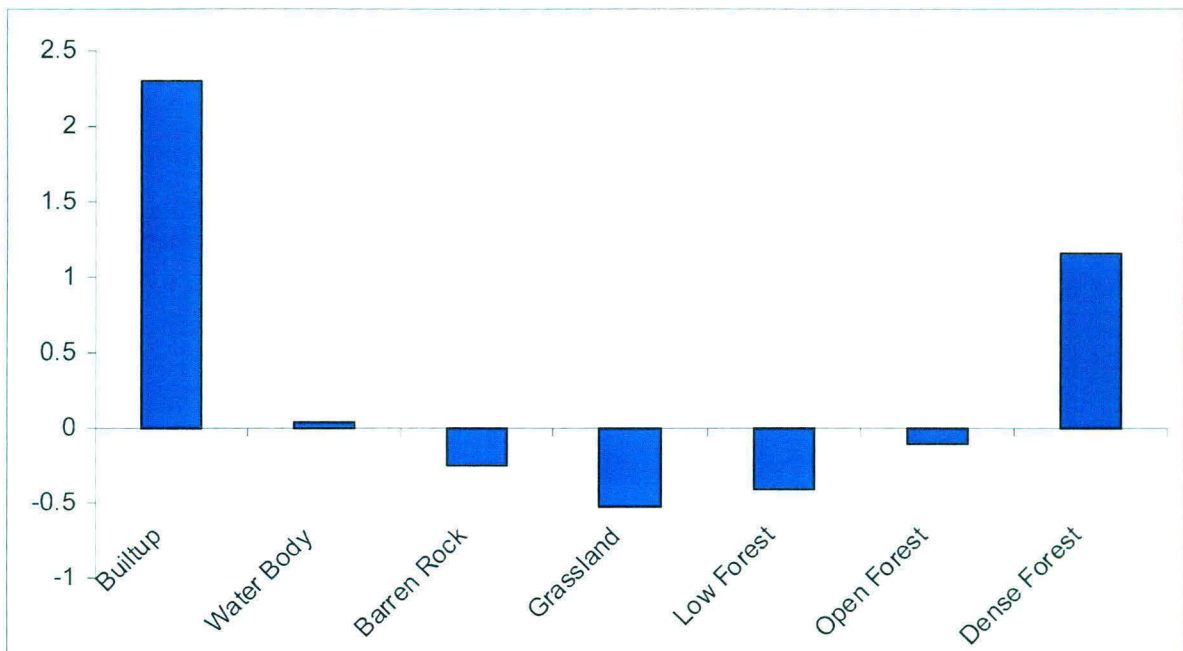
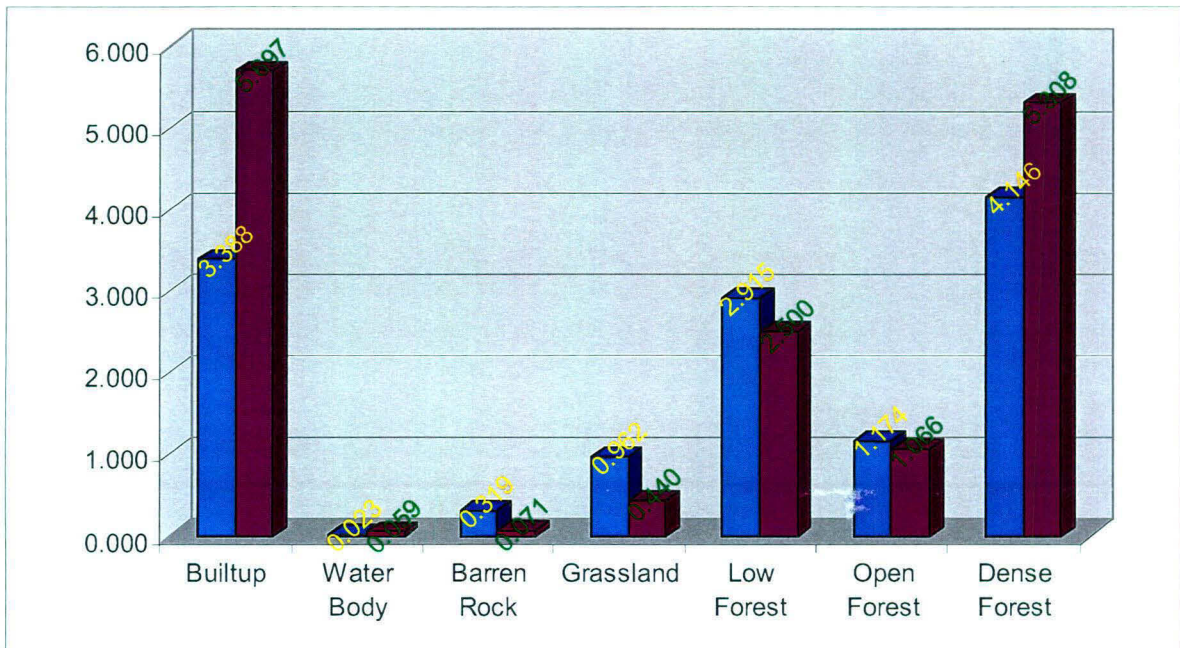


Fig.5.29.Change in various classes of land use and land cover in RR Hospital area from year 2000 & 2005

5.7 COMPARISON OF LULC OF YEAR 2000 AND 2005

A subset image of area of interest (JNU and its surrounding area) was taken into consideration for LULC analysis for the following classes-

- 6. Built up
- 7. Water body
- 8. Barren rock
- 9. Grassland
- 10. Low forest
- 11. Open/fallow land
- 12. Dense forest

A Landsat image of year 2000 was classified for the above mentioned classes using unsupervised classification technique. Similarly LISS III image of year 2005 was also classified using unsupervised (hybrid) classification technique. It was observed from the classification that the built-up, dense forest and water body area has increased with built-up accounting to 2.308sq.km and dense forest area increased by 1.162sq.km. A marginal increase in area of water bodies was also observed i.e. (0.036 sq.km). A decrease was observed in grassland area together with barren rocky surface, open forest/ sparse forest and low forest area. The decrease in the above mentioned area can be well attributed to good amount of increase in built-up

Class	2000 (Area in Sq.km)	2005 (Area in Sq.km)	% Change (Area in Sq.km)
Built-up	3.388	5.697	2.309
Water	0.023	0.059	0.036
Barren Rock	0.319	0.071	-0.249
Grass	0.962	0.440	-0.521
Low Forest	2.915	2.500	-0.414
Open	1.174	1.066	-0.109
Dense Forest	4.146	5.308	1.162

Table 5.14 Change in various classes of land use and land cover in sq.km in JNU area from year 2000 & 2005

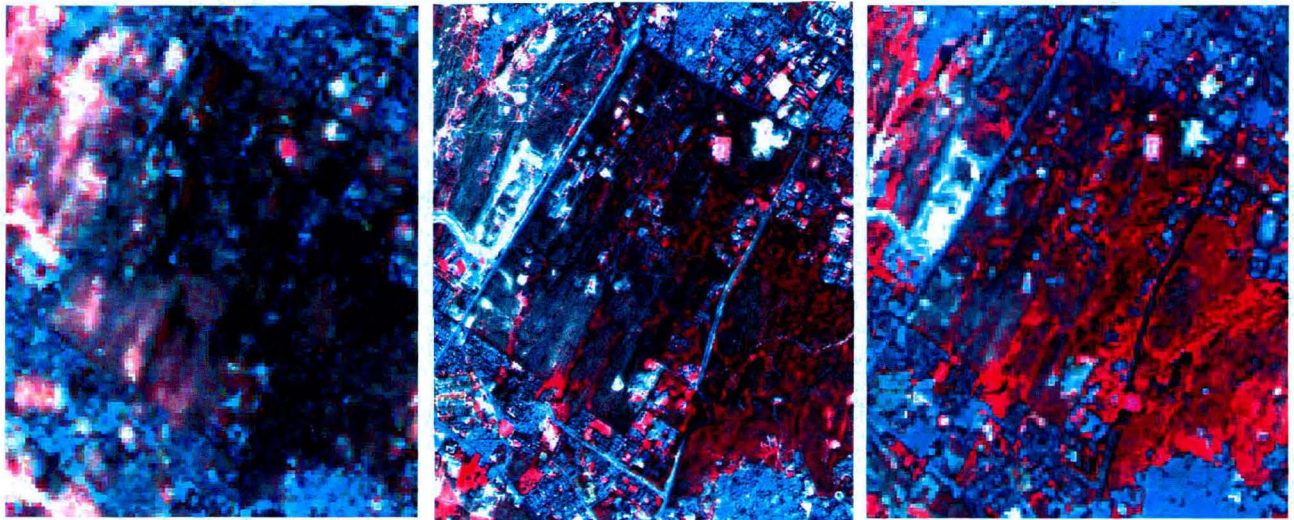
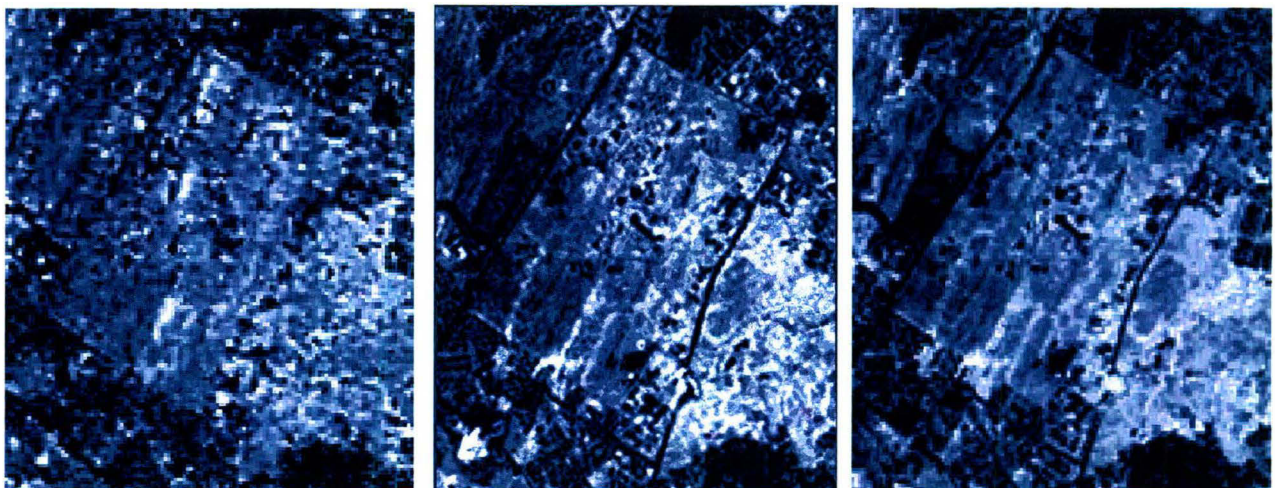


Image 2000

Image 2004

Image 2005



NDVI Image 2000

NDVI Image 2004

NDVI Image 2005

Fig.5.30. NDVI output for the respective images of years 2000, 2004, 2005

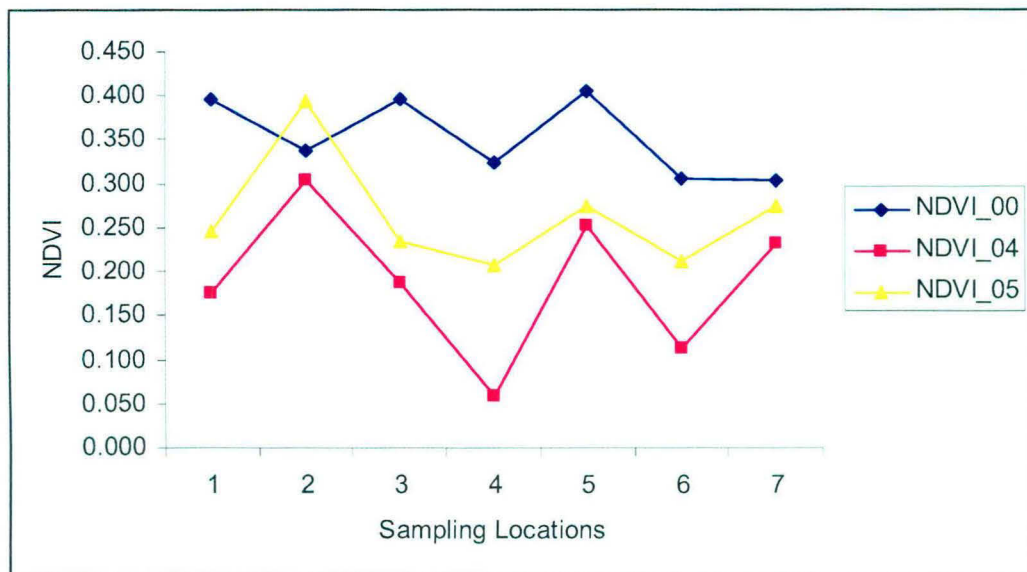
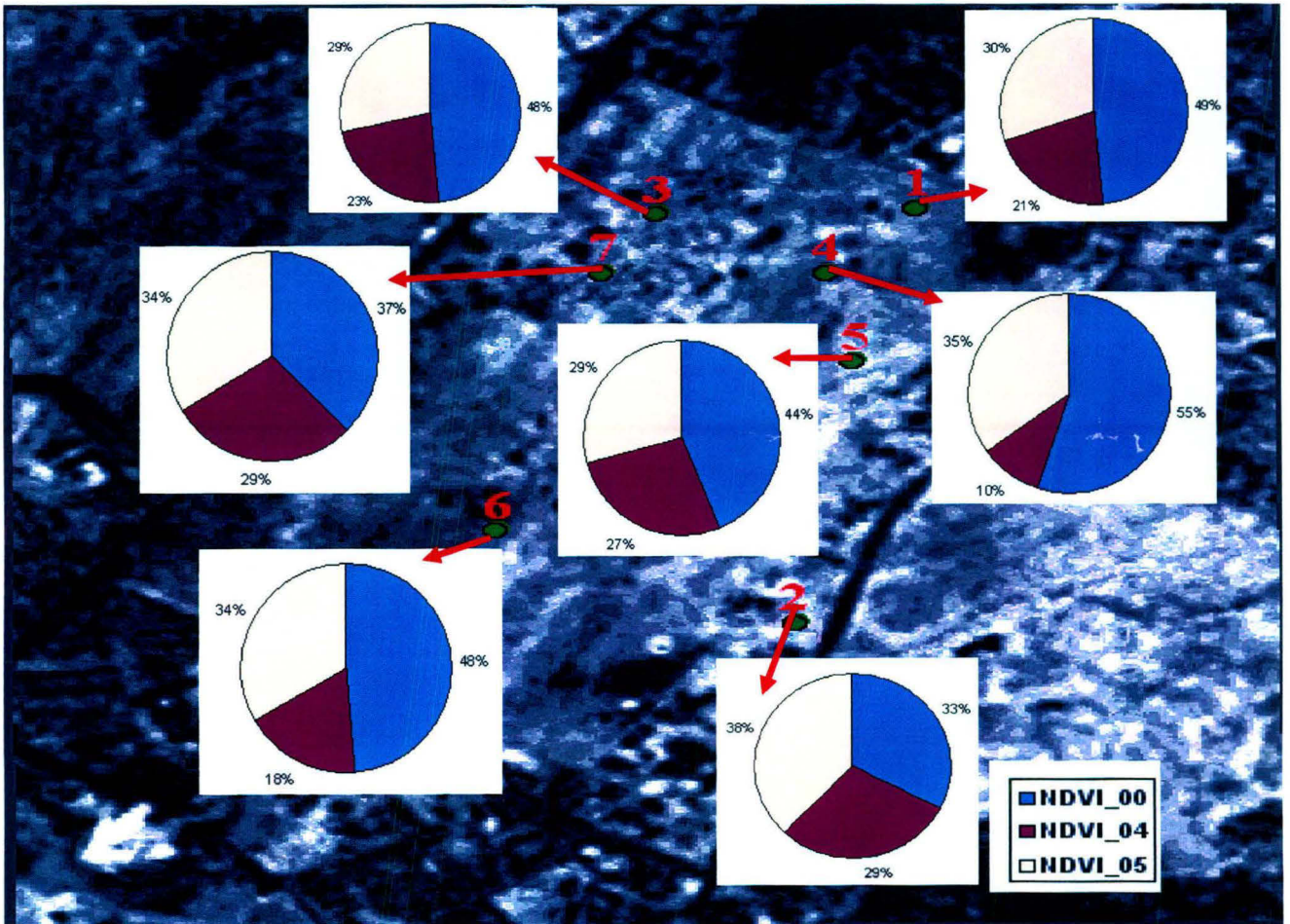


Fig 5.31 NDVI values at different sites in jnu in year 2000, 2004 and 2005

RESULT AND DISSCUSSION

The NDVI determines the ‘healthy’ vegetation. It takes advantage of the differences exhibited by the vegetation in its spectral behaviour. The pigment in plant leaves, chlorophyll, strongly absorbs visible light (from 0.4 to 0.7 μm) for use in photosynthesis. It is true especially for the ranges 0.4-0.5 μm and 0.6-0.7 μm more than the range 0.5-0.6 μm . The cell structure of the leaves, on the other hand strongly reflects near-infrared light (from 0.7 to 1.1 μm). The formula used to calculate NDVI is

$$\text{NDVI} = \frac{\text{IR} - \text{R}}{\text{IR} + \text{R}}$$

in which ‘IR’ means the reflectance value in near-infrared and ‘R’ means the reflectance value between 0.6 and 0.7 μm (red). The index is higher when the vegetation is in mature state because then difference between ‘IR’ and ‘R’ is higher. The NDVI calculated for water, for example, gives negatives values.

The plant/vegetation, which is healthy, absorbs more Red radiation as compared to the stressed vegetation. Thus when one computes the NDVI equation in real values (i.e. 8 % becomes 0.08 and so on), a number is obtained representing the health status of the plant involved $\frac{3}{4}$ for example, 0.72 for the healthy plant. An important fact of the obtained values is that for a given NDVI image the resulting NDVI pixel value always ranges from -1 to +1. Also it is important to note that the areas devoid of any vegetation give a negative value or a value close to zero. In simpler words a negative number or a number close to zero means no vegetation and a number close to +1 (0.8 - 0.7) represents Luxurious vegetation. Therefore, when an array of such NDVI numbers is computed and projected in the form of an image; a grey scale image is obtained where the grey scale intensity of each pixel is proportional to NDVI value it represents.

Drilling Locations	NDVI 00	NDVI 04	NDVI 05
1	0.395	0.175	0.246
2	0.338	0.304	0.393
3	0.395	0.186	0.234
4	0.325	0.059	0.207
5	0.406	0.252	0.274
6	0.306	0.113	0.212
7	0.303	0.232	0.274

Table 5.15 NDVI values at various drilling sites in year 2000, 2004, 2005

The NDVI map generated showed that the NDVI values were quite higher in year 2000 than in 2004 and 2005. The decrease in NDVI values can be attributed to cutting of plantations for new built-ups but what was more interesting to observe that the NDVI increased in the area from year 2004 to 2005.

The drilling site 1 showed that the NDVI value which was 0.395 in year 2000 decreased to mere 0.175 in year 2004 and then increased to 0.246 in year 2005. Similar trends were observed for drilling sites 3, 4, 5, 6 and 7. Only site 2 accounted for a good amount of increase in NDVI values even in comparison to year 2000 i.e. the NDVI increased from 0.338 in year 2000 to 0.393 in year 2005. The NDVI values were not very high but it was observed that the selected sites showed anomalous vegetation growth and thus these sites were selected for drilling as this suggested that the vegetation growth was not hampered as it regained in one year. In some places of the study area interconnected fractures show high NDVI value supporting groundwater exploration. Although in some depressions of ridge area the rainwater accumulates which supports growth of vegetation. These areas were not inferred suitable for groundwater exploration.

5.8 TIN & DIGITAL ELEVAATION MODEL OF JNU

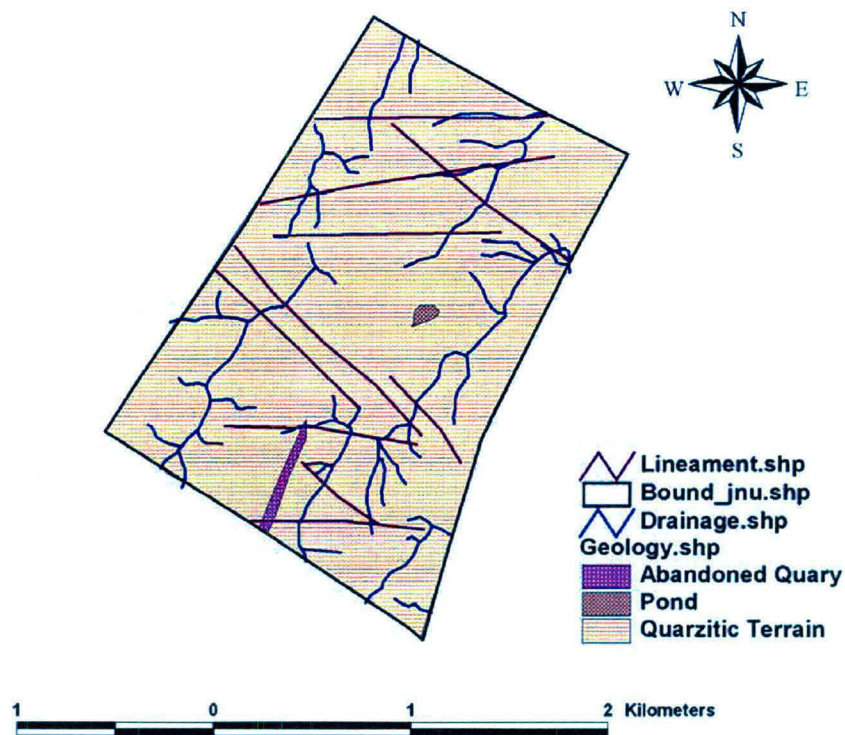


Fig 5.32 JNU map showing lineament and geology

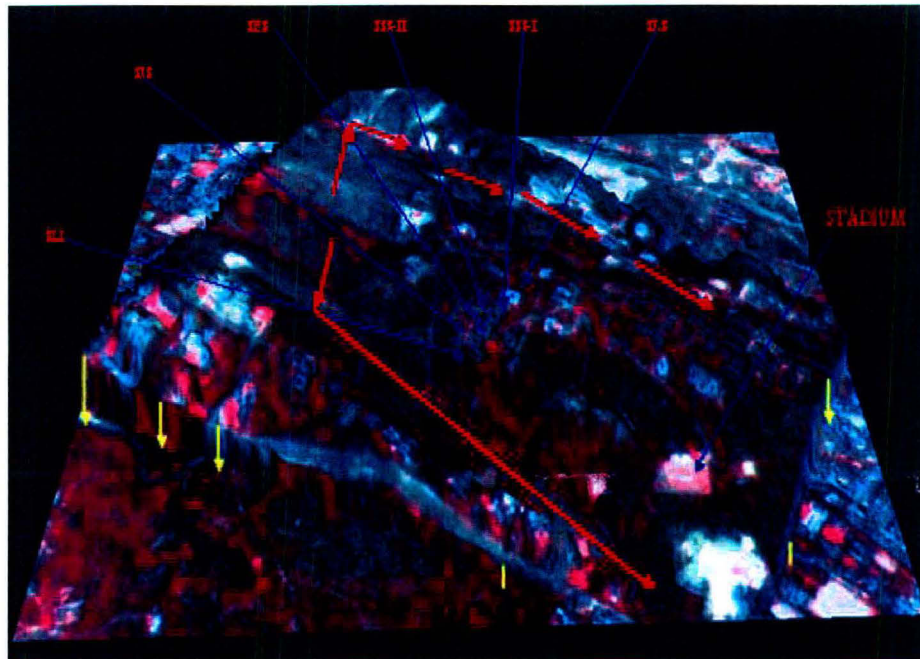


Fig 5.33 Digital Elevation Model of JNU

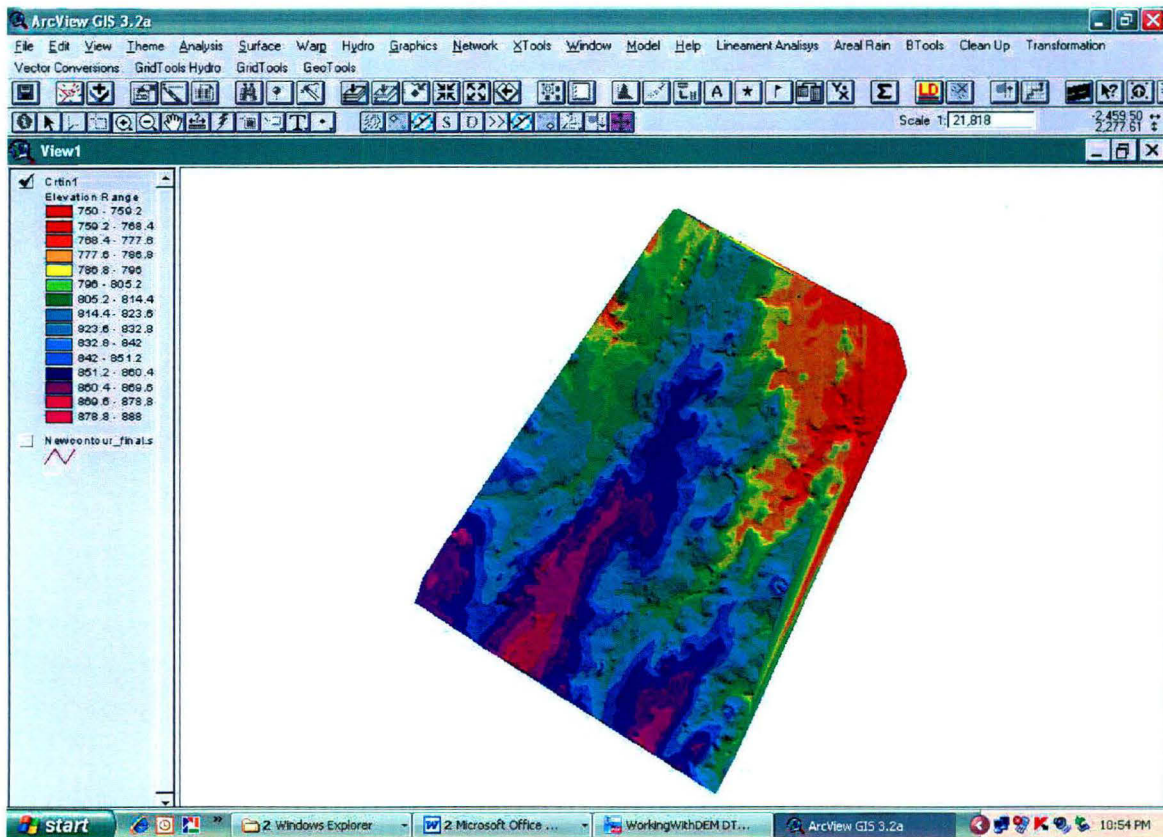


Fig 5.34 Triangular Irregular Network of JNU

RESULT AND DISSCUSSION

A TIN theme represents one or more surface information, usually at least a surface layer, where space is partitioned into a set of non-overlapping triangles. Attribute and geometry information is stored for the points, lines, and faces that comprise each triangle. This information is used for display, query, and analysis purposes. Each TIN theme has its own legend display in the view's Table of Contents. A TIN theme's legend specifies whether the triangle points, lines, or faces are drawn and what colours are used to draw them. A TIN theme merely points to the geographic data it represents; it does not contain the data itself. The triangle vertices are usually sample points collected from the surface. This model that uses the triangle edges allows that important morphologic feature such as discontinuities represented by linear slope features (peaks) and drainage (valleys) to be considered during the generation of triangular grid. This way, the terrain surface is modelled preserving its geomorphic features. The rectangular grids are generally used in qualitative applications for general surface visualization while the irregular grid model was used when the user needs more precision on quantitative analysis. Grids represent surfaces using a mesh of regularly spaced points. TIN represent surfaces using contiguous, non-overlapping, triangular facets. One can estimate a surface value anywhere in a triangulation by averaging nearby triangle node values, thus giving more weight and influence to those that are closer to the location being estimated.

Since TINs are variable resolution models, they can be more detailed in areas where the surface is complex and less detailed in areas where the surface is simple. The positional information of the source data was incorporated directly into the surface model so subsequent analysis will accurately reflect it. The TIN of JNU was prepared from the contour lines spaced at 2cm and it was used to study the slope, aspect, flow direction, flow accumulation, stream direction and watershed in JNU which is a part of NCR region.

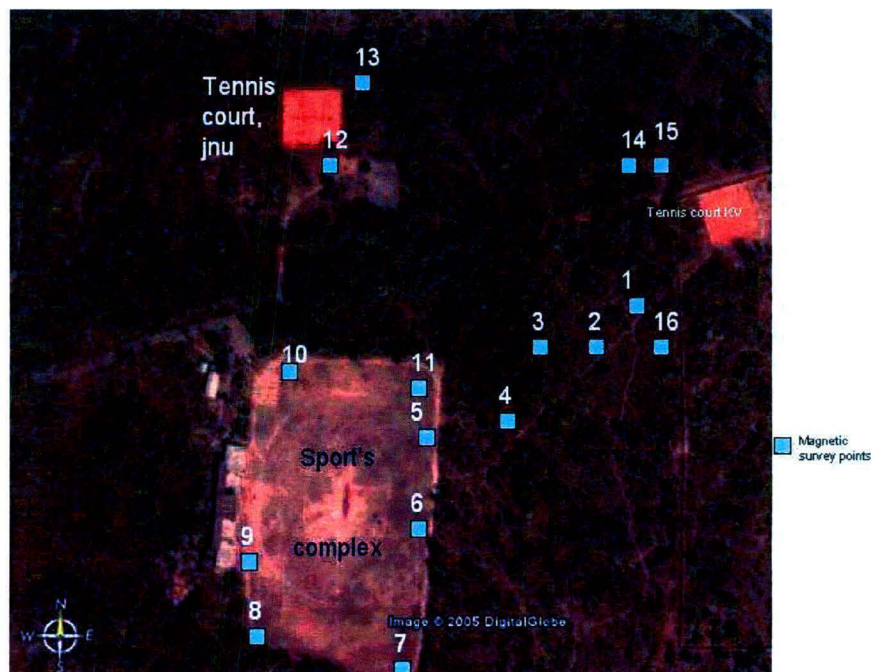


Fig 5.35 Magnetic survey points in JNU campus

5.9 GEO-MAGNETIC SURVEY

Magnetic survey was carried out in and around JNU Campus, which is situated on Aravali hill extension of Delhi-Haridwar ridge. Magnetic survey was carried out in 2005-2006, using the instrument Proton Precession Magnetometer Geomatrix G-816/826 A USA & IGIS.

Proton precession magnetometer utilizes the precession of spinning protons or nuclei of the hydrogen atom to measure the total magnetic intensity. The spinning of protons behaves as small, spinning magnetic dipoles. These magnets are temporarily aligned or polarized by application of uniform magnetic field generated by a current in a coil of wire. When the current is removed the spin of the protons causes them to process about the direction of the ambient or earths magnetic field. The precession proton then generate a small signal in the same coil used to polarize them, a signal whose frequency is precisely proportional to the total magnetic field intensity and independent of the orientation of the coil, i.e. sensor of the magnetometer.

JNU lineaments inferred by IRS-1A, SPOT and IRS-1C data shows a strong trend in NE-SW direction, which passes though JNU Sports Complex (stadium). Measurements were taken along this lineament, which is inferred as sudden decrease in magnetic values (average magnetic value of Delhi region is 47,000 gamma). Based on the spot magnetic values in and around JNU eleven profiles were done. Contour maps were made along the profile. Contour lines were drawn at every ten gammas interval; low magnetic values were noticed in lineaments on ferruginous quartzite (Mukherjee 1997).

Section of drilling points was based on the points inferred by magnetometer showing low magnetic values and interconnected lineaments.

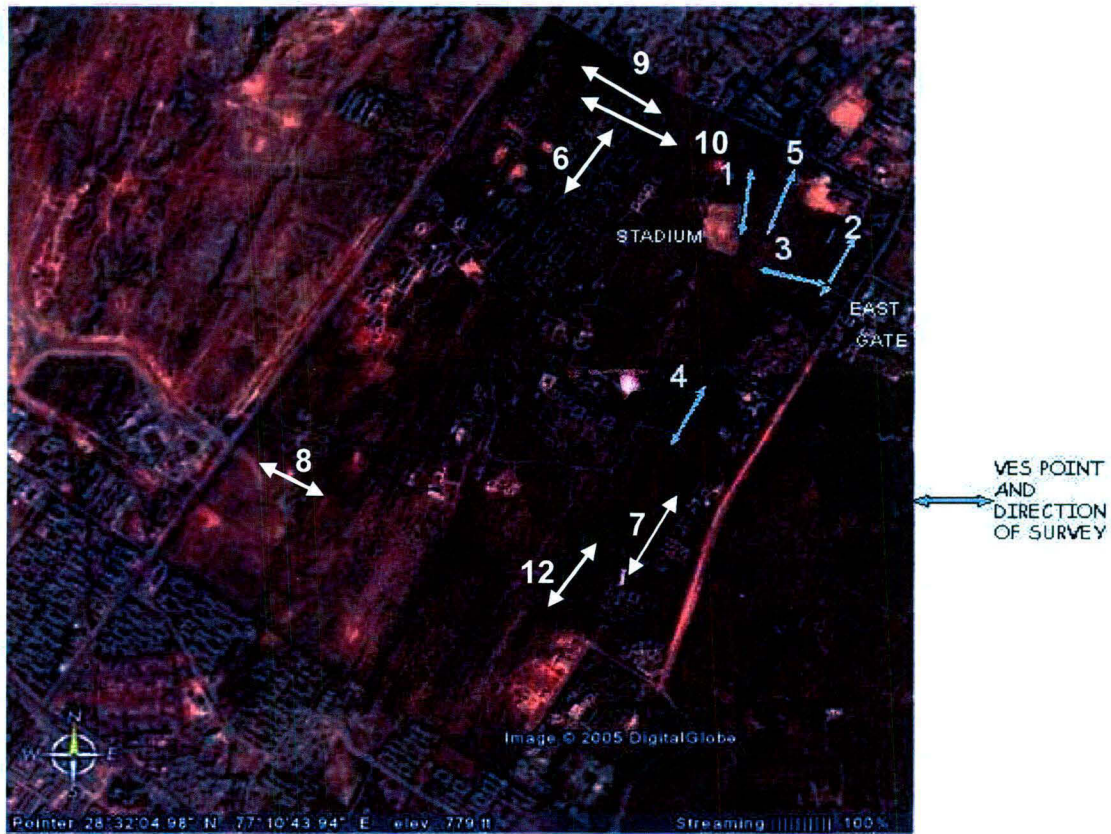


Fig 5.36 VES survey points of JNU

5.10 GEO-ELECTRICAL SURVEY IN JNU

Geo-electrical survey was carried out in and around JNU Campus, 2005-2006, using the instrument DC Resistivity Meter Model DDR-3.

Geological investigation based on electrical measurements help in understanding the sub-surface geological conditions so that the exploratory drilling can be restricted to only favourable areas. Vertical Electrical Sounding (VES) is a technique by which the apparent resistivity variation in vertical direction is studied. The field measurements for DC resistivity investigations involves sending a known current into the ground through the current electrodes and observing the resulting voltage across potential electrodes, to get the resistance values. The resistance values were obtained as direct readout on liquid crystal display. In VES the goal is to observe the variation of resistivity with depth. The schlumberger configuration is most commonly used for VES investigation. The midpoints of array are kept fixed while the distance between current electrodes is progressively increased. This

causes the current lines to penetrate to greater depths, depending on the vertical distribution of conductivity.

5.10.1 LAYOUT OF GEOELECTRICAL SURVEY

The location of VES points to study the nature of subsurface structure and its petrology which shown in the fence diagram. During VES the alignments here made in such way that it should encounter minimum lateral in-homogenities. Basically profiling and sounding technique were used in groundwater exploration. The interpretation of profiling data is more of a quantitative nature where the apparent resistivity for given electrode spacing of one area was compared with that of the adjoining area to evaluate the relative geological and hydrogeological condition, the interpretation of VES data on the other hand is more complicated and is essentially quantitative in nature. VES data was utilized to find the nature of the subsurface structures. The data was used to identify zones of low resistivity of weathered and fractured rock, which are generally favourable location for groundwater storage. Quantitative interpretation of VES data is corroboration with Borehole data suggests with precision the availability of groundwater in-depth.

On the basis of this survey and other initial details four sites were chosen for drilling.

1. The low electrical resistivity value ranging from 11ohm meter to 53ohm meter of the overburden indicates that these are predominantly Silty and Clayey. Hence, these locations were not suitable for drilling for high discharge(example near CRS Pumping Station).
2. If the electrical resistivity is ranging from 100ohm meter to 200ohm meter, it indicates the existence of fractured/weathered quartzite and resistivity value ranging from 300ohm-meter to 600ohm-meter indicates that they are less fractured quartzites. These formations appeared to be favourable for artificial recharge and drilling. Further, these sites are having good fracture zones if deeper investigations are carried out.
3. If at a depth of 70mbgl, the resistivity value is more than 1000ohm-meter and interpretation of plots shows more than 45° in XY 2D plot it is compact quartzite. Even a drop of a few ohmmeters downwards can have possibility of deep-seated fracture zones. In all the places electrode spacing was not possible to extend beyond 2000m either side of the Resistivity meter. In these locations magnetic anomaly confirms the deep seated fractures.

RESULT AND DISSCUSSION

Probable Lithology	Hydrogeology	Resistivity (ohm-meter)
Top Soil	Dry to Moist	15-170
Weathered/Fractured quartzite with mica schist	Saturated	100-200
Less fractured quartzite	Saturated	300-600
Compact quartzite	Dry to little moist	More than 1000

Table 5.16 Resistivity of different zones as per litholog

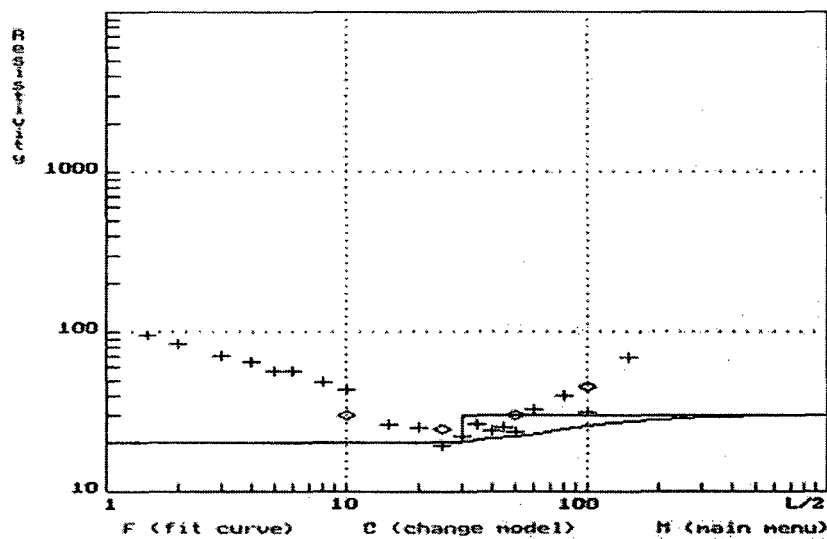


Fig 5.37 Vertical Electrical Sounding Plot in JNU at site 1

5.10.2 SITE 1 (JNU 1):

The surface resistivity data near Site 1 shows the resistivity value of 60ohmmeter at 3.33mbgl. Observed magnetic values are low in this area. The resistivity value of site 1 starts from 100ohmm which shows arenaceous buried pediment plain. The resistivity values decreases from 100 to 30ohmm down to 10m depth. From 10mbgl down to 50mbgl the resistivity value shows remarkable dip. Interpretation of this data suggests sufficient soil moisture which is indicative of shallow water zone. From 50mbgl to 120mbgl the resistivity value shows consistent rise (90ohmm). The interpretation of this data shows the angle of curve is less than 45 degree which is suggestive of saturated zone.

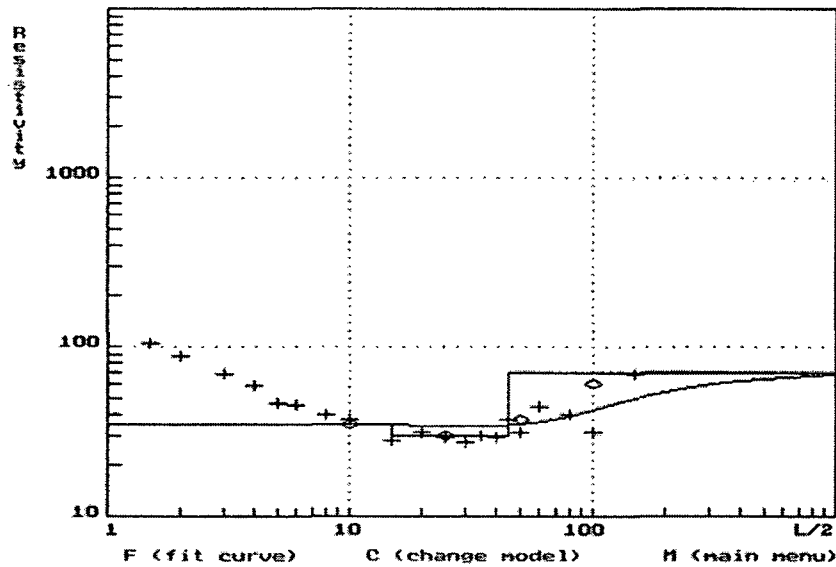


Fig 5.38 Vertical Electrical Sounding Plot in JNU at site 2

5.10.3 SITE 2 (JNU 2):

The soil resistivity on the Site No.2 shows more than $100\Omega\text{m}$ initially which is suggestive of arenaceous soil and low moisture content which is supported by low Normalized Difference Vegetation Index value (0.228873) and the litholog also. Further down to 6mbgl the resistivity value sharply decreases to $35\Omega\text{m}$ which is supported by silt and clay in the litholog record. Further 10mbgl the ferruginous intercalation overlying ferruginous quartzite shows the possibility of shallow aquifer material which is further supported by the resistivity value, which is ranging in between 25 to $40\Omega\text{m}$. Further down to 50meters the resistivity value remains low ranging between 40 to 60 ohmmeter which is further supported by the presence of weathered mica schist, quartz vein and ferruginous quartzite. Magnetic value in this site has been recorded very low (29,000 Gamma) which further suggests the possibility of interconnected fractures with good aquifer zones.

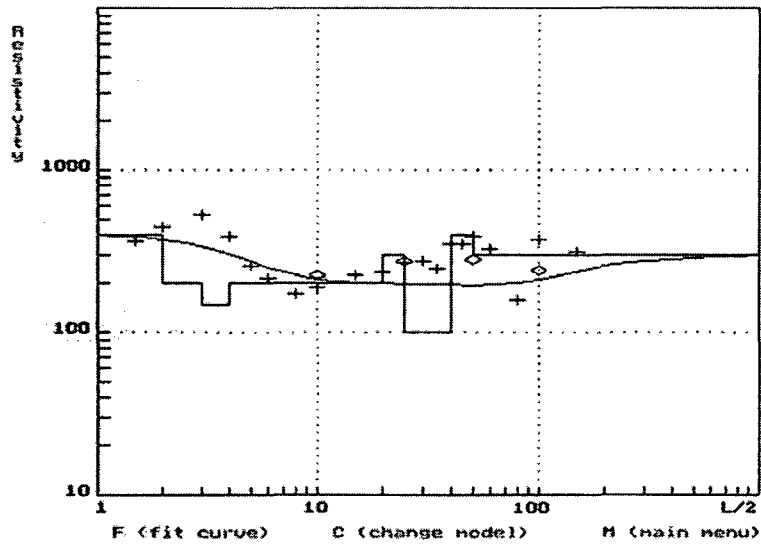


Fig 5.39 Vertical Electrical Sounding Plot in JNU at site3

5.10.4 SITE 3 (JNU3):

The resistivity data interpretation of Site 3 (JNU3) shows that initially top soil mixed with weathered rock shows very high resistivity of $400\Omega\text{m}$. 4mbgl the resistivity value shows further rise upto $600\Omega\text{m}$ which is suggestive of top layer of hard ferruginous quartzite from 10mbgl the resistivity value started decreasing and it was ranging in between 200 to $300\Omega\text{m}$ down to 20mbgl. It shows that fractured quartzite with potential groundwater zone possibility at a shallow depth. The resistivity values were found to be fluctuating in between $150\Omega\text{m}$ to $400\Omega\text{m}$ in between 12mbgl to 40mbgl which comprises groundwater bearing fracture zone. From 42mbgl to 45mbgl the resistivity value has shown a rising trend which is suggestive of mica-schist and quartzite intercalations. From 46mbgl to 80mbgl the resistivity data shows a sharp downfall it was ranging in between $300\Omega\text{m}$ to $150\Omega\text{m}$. This zone comprises of 2 sets of groundwater bearing fracture in quartz mica-schist and gneissose granite. Further down to 10mbgl the resistivity value shows a rise up to $300\Omega\text{m}$ which is suggestive of granite and quartzite with less fracture. From 100mbgl down to 150mbgl a sharp decrease in the resistivity value infers groundwater bearing fractured quartzite.

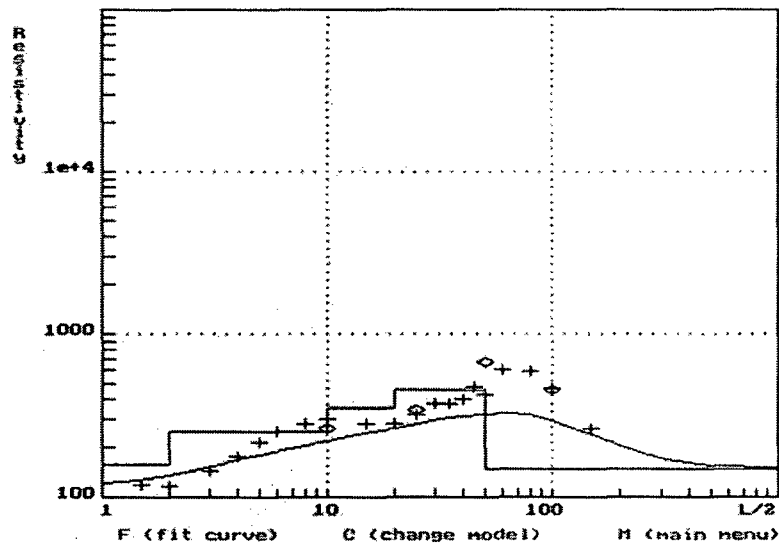


Fig 5.40 Vertical Electrical Sounding Plot in JNU at site 4

JNU SITE 4

Geo Coordinates 77.17078 E 28.54283 N (In Degree Decimal)

Standard (Gamma)	Obtained(Gamma)	Signal Strength
47,000(Gamma)	31,000	Very high
47,000(Gamma)	33,000	Medium
47,000(Gamma)	33,000	High

Table 5.17 Magnetic data of Site 4 (PSR JNU)

5.10.5 SITE 4 (JNU4):

Resistivity value at Site 4 shows compact overburden below the ferruginous quartzite. At a depth of 27mbgl ferruginous quartzite was found overlying on a quartzite and aplite veins. This is the beginning of potential groundwater bearing zone in this area. Further down to 50mbgl fractured quartzite with high discharge of groundwater encountered. The resistivity curve shows an initial rise due to presence of ferruginous quartzite. When the curve was matched with standard curve it was found that angle in between X-Y plot shows less than 45° which further suggest the possibility of groundwater bearing zone 27mbgl. The litholog also supports the interpreted resistivity curve. The litholog also supports the interpreted resistivity curve. The magnetic value shows very high anomaly from its standard value in Delhi area which is suggestive of multiple fractures below ground level. Beyond 100mbgl the presence of mice schist intercalated with thin quartzite veins further lowers the

resistivity value which suggests that wherever there is change in litho-facies it is a marker of potential fracture zone.

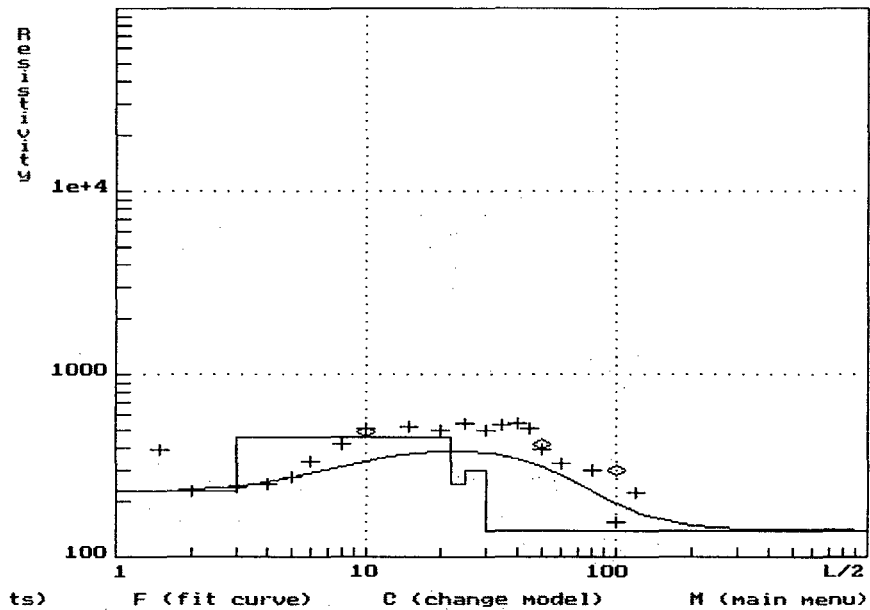


Fig 5.41 Vertical Electrical Sounding Plot in JNU at site 5

5.10.6 SITE 5 (JNU 5):

Geo Coordinates: 77.1563^o E 28.5381^o N

Resistivity survey carried out at Site 5 shows high top soil resistivity down to 2mbgl which falls abruptly from 120Ωm to 100Ωm at 2.5mbgl, which is suggestive of very shallow weathered quartzite with some moisture content. Resistivity value further rises up to 300Ωm from 5mbgl to 35mbgl which is suggestive of massive quartzite. From 35mbgl to 45mbgl the resistivity shows the presence of groundwater in the fractured metamorphics.

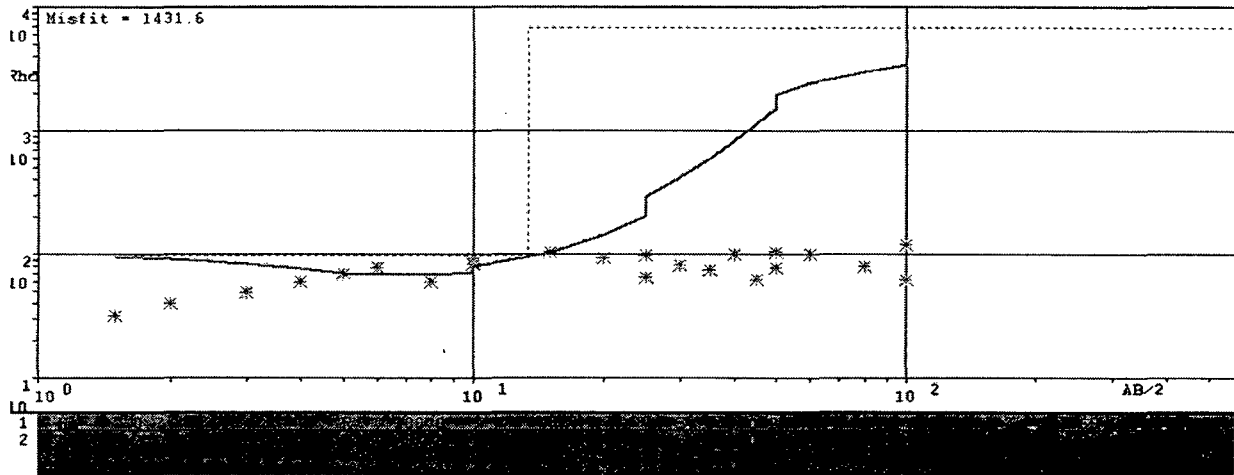


Fig 5.42 Vertical Electrical Sounding Plot in JNU at site 6

5.10.7 SITE 6 (JNU6):

Geo Coordinates 77.1619⁰ E 28.544⁰ N

Standard (Gamma)	Obtained(Gamma)	Signal Strength
47,000	29,500	Very high
47,000	28,000	Very very high

Table 5.18 Magnetic Data at Site 6

The resistivity from Site 6 shows that 4mbgl of soil is of sandy clay in nature which is overlying non-ferruginous quartzite down to 30mbgl. From 30mbgl the ferruginous quartzite starts which is the upper zone of very promising aquifer in multiple veins. Then below 52mbgl very fine fractures of groundwater bearing fractured quartzite increases the yield of groundwater which has been found to be extended down to 85mbgl. From 85mbgl to 115mbgl non-ferruginous quartzite shows intermittent aquifer. From 115mbgl to 150mbgl very high grade graphite schist with quartzite occurs. Quartzites/Aplites/Pegmatites are not considered good aquifers if there are no interconnected fracture system develops secondary porosity and permeability in these rocks. The graphite schist and quartzite contains good amount of groundwater but this zone was not tapped to avoid the graphite impurities in groundwater. At 150mbgl ferruginous quartzite shows very high discharge down to 180mbgl where

RESULT AND DISSCUSSION

the quartzite was found non ferroginous from 155mbgl to 190mbgl. The water quality analysed by ICPAES shows insignificant major and trace elements concentration.

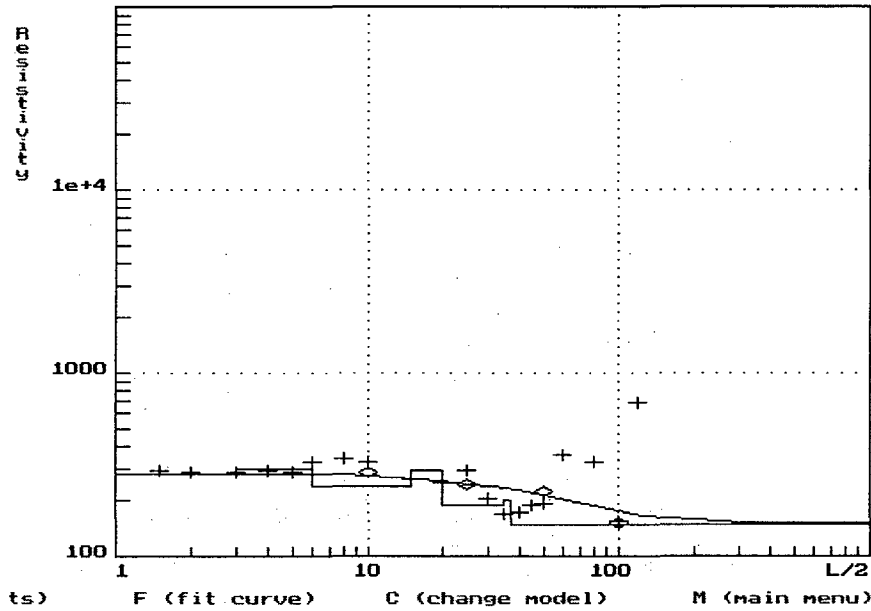


Fig 5.43 Vertical Electrical Sounding Plot in JNU at site7

5.10.8 SITE 7 (JNU 7):

Standard (Gamma)	Obtained (Gamma)	Signal Strength
47,000	32,340	Very high
47,000	34,441	High
48,000	31,718	Very High

Table 5.19 Magnetic Data at Site 7

The resistivity data interpretation of Site7 (JNU7) shows that these are uniform resistivity ranging in between 200Ωm to 180Ωm from surface down to 6mbgl, which is suggestive of sandy soil cover with some moisture content. From 6mbgl down to 8mbgl it shows slow rise in resistivity value which is suggestive of a compact soil above the aquifer. From 10mbgl down to 35mbgl the resistivity value was ranging in between 200 to 100Ωm which is suggestive of groundwater bearing weathered ferruginous quartzite. From 36mbgl to 50mbgl potential fracture zone was encountered with high discharge of groundwater which was inferred by the resistivity value ranging 120Ωm to 140Ωm. From 50mbgl the

RESULT AND DISSCUSSION

resistivity value shows an increase up to 300Ωm down to 60mbgl which is suggestive of compact schist rock. The compaction due to high grade metamorphism is further proved by the presence of garnet in the mica schist. From 60mbgl to 100mbgl the resistivity value was ranging in between 200Ωm to 80Ωm which is suggestive of very good multiple fractured aquifers with high discharge of groundwater. From 100mbgl the resistivity value shows increasing trend up to 110mbgl which is suggestive of less fractured rocks. Further down to 100mbgl to 150mbgl potential fracture was inferred by using magnetic anomaly studies.

The resistivity survey in Mahanadi area of JNU shows that there is a uniform resistivity of 140Ωm from ground level down to 10mbgl. Further, there is a distinct fall of resistivity value from 25mbgl to 50mbgl. This is highly fractured ferruginous quartzite with very high discharge of groundwater. The fractured quartzite continued down to 75mbgl beyond which is suggestive of confining quartzite and schistose rocks. Inferred fractured granite was confirmed during drilling at a depth 145mbgl. The layer resistivity when further analysed was found out to be ranging in between 50 to 200Ωm in the excellent groundwater bearing zone which is an excellent groundwater bearing zone which is an indication of presence of fresh groundwater with less TDS. The ICPAES data of groundwater further confirms this observation.

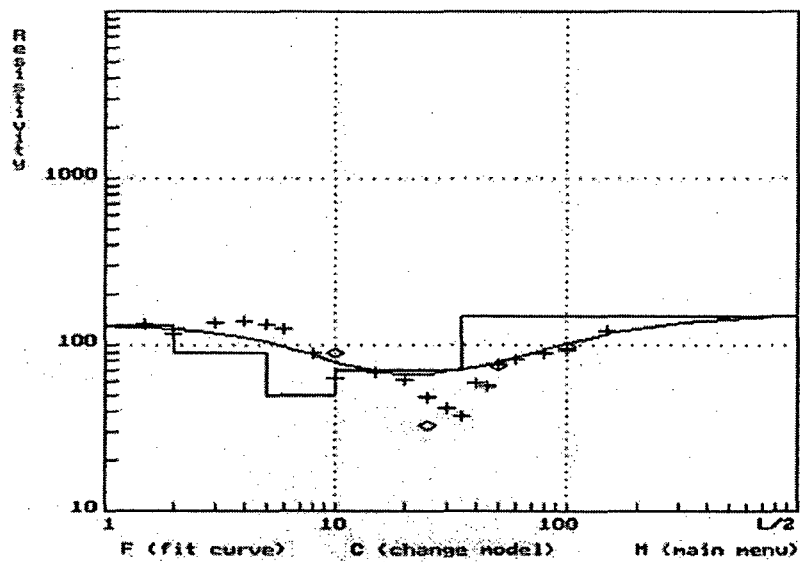


Fig 5.44 Vertical Electrical Sounding Plot in JNU at site 8

5.10.9 SITE 8 (JNU8):

Geo Coordinates 77°10'00.9" E 28°33'05.2" N

The resistivity at Site No 8 in JNU shows that top soil is hard compact clay down to 8mbgl. Further, steep downwards trend of resistivity value shows that from 8mbgl to 80mbgl there are clay, silt and sand are prominent. 80mbgl to 100mbgl a curve rises slowly which shows that below the sticky clay there are chances of hard rocks. The slow and uniform rising trend of the curve with 100mbgl is not suggestive of any interconnected fractures groundwater bearing formations. The drilling was not carried out on this site because there were chances of sticky clay inside which could not have supported DTH drilling and rig would have stuck off in this area.

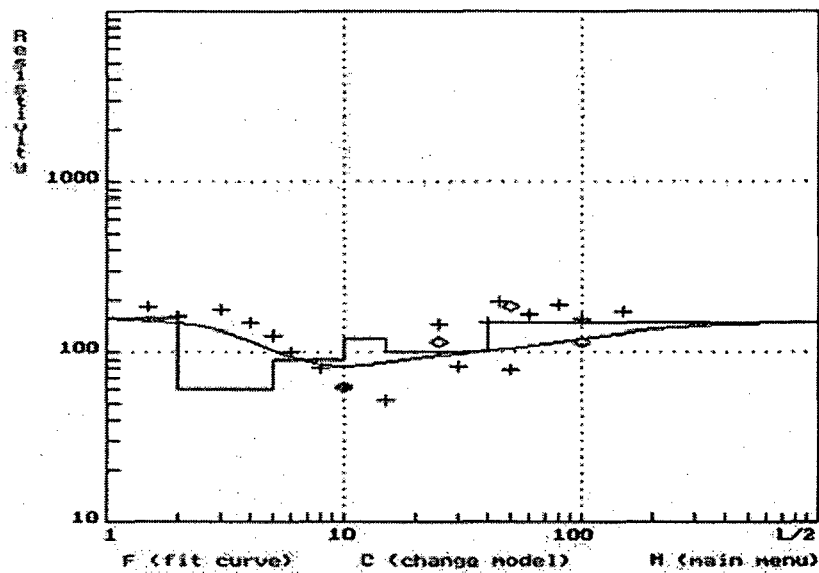


Fig 5.45 Vertical Electrical Sounding Plot in JNU at site 9

5.10.10 SITE 9 (JNU 9):

Geo Coordinates 77°10'02.0" E 28°33'02.2" N

The resistivity survey in JNU at Site 9 shows that top soil is hard compact clay down to 9mbgl. Further, steep downwards trend of resistivity value shows that from 9mbgl to 25mbgl there are clay, silt and sand are prominent. 75mbgl to 100mbgl a curve rises slowly which shows that below the sticky clay there are chances of hard rocks. The slow and uniform rising trend of the

RESULT AND DISSCUSSION

curve with 100mbgl is not suggestive of any interconnected fractures groundwater bearing formations. The drilling was not carried out on this site because there were chances of sticky clay inside which could not have supported DTH drilling and rig would have stuck off in this area and it was concluded to reject the drilling site.

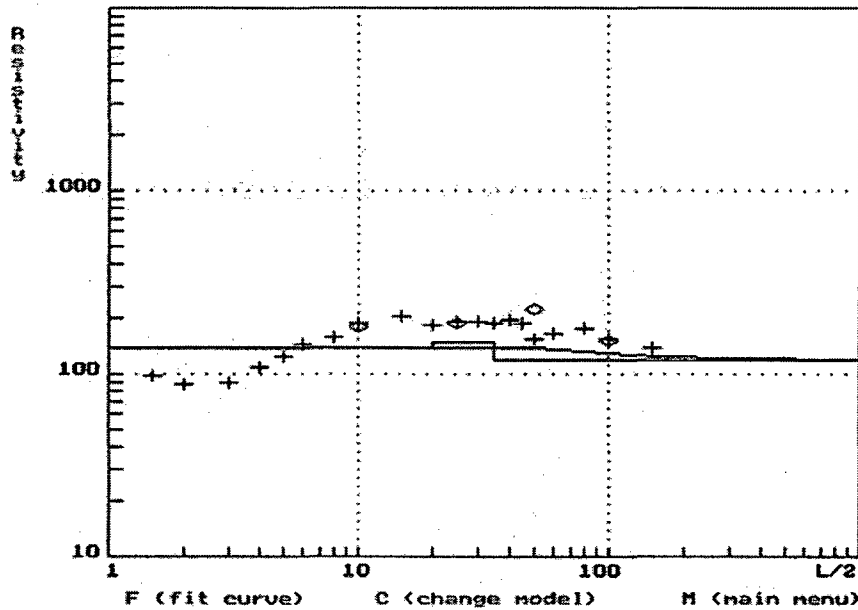


Fig 5.46 Vertical Electrical Sounding Plot in JNU at site 10

5.10.11 SITE 10 (JNU10):

The resistivity curve at site 10 in side the JNU shows that top soil resistivity is less than 100ohmm down to 6mbgl which rises up to 120ohmm up to 10mbgl. Below 10mbgl further it goes down to less than 100ohmm. The fluctuating resistivity suggests that there are possibilities of sub-surface boulders with saturated aquifer. The drilling was not carried out in this site because there were chances of collapse during drilling due to the presence of boulders of different sizes.

RESULT AND DISSCUSSION

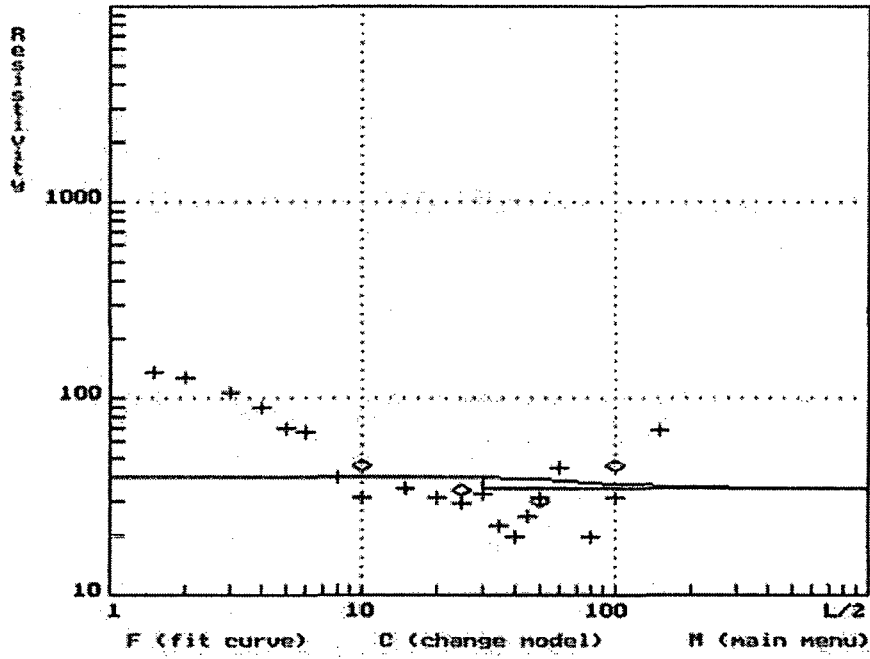


Fig 5.47 Vertical Electrical Sounding Plot in JNU at site 11

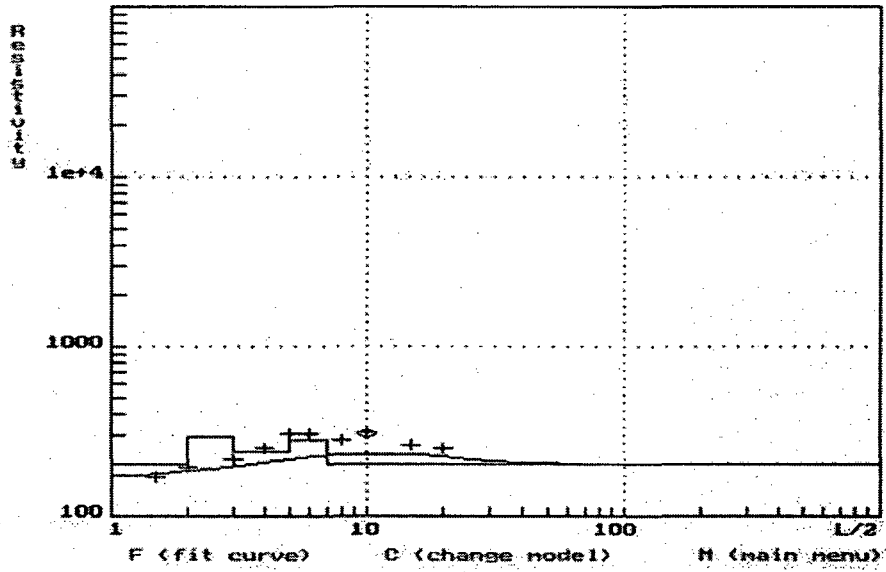


Fig 5.48 Vertical Electrical Sounding Plot in JNU at site 12

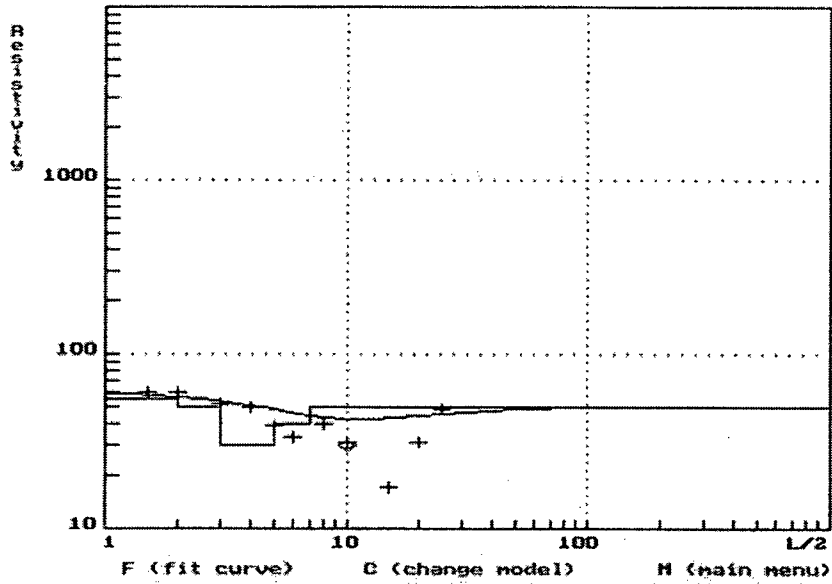


Fig 5.49 Vertical Electrical Sounding Plot in JNU at site 13

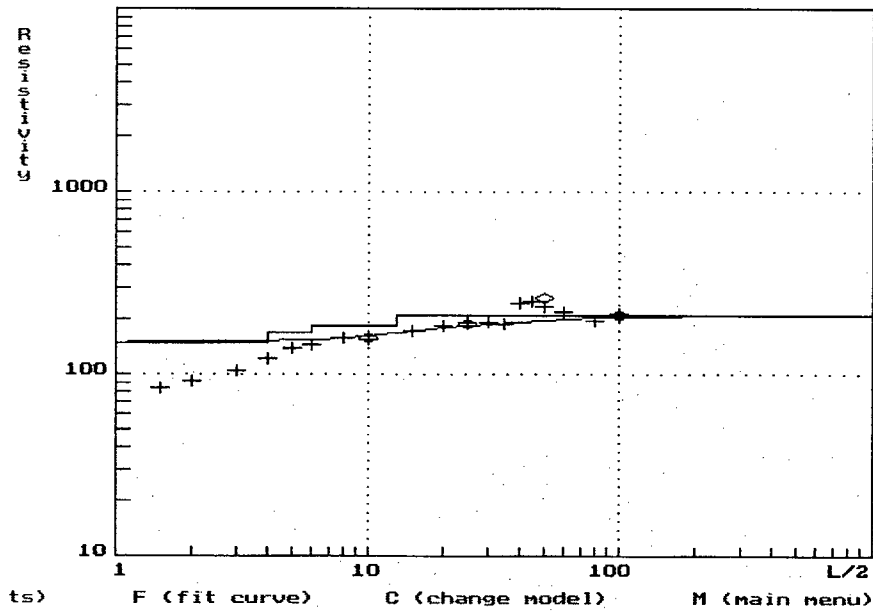


Fig 5.50 Vertical Electrical Sounding Plot in JNU at site Pashimabad

5.10.12 Paschimabad (Discarded Site):

The resistivity survey carried out at Paschimabad shows that top soil resistivity is less than 70Ωm is slowly rises up to 200Ωm. In this area the presence of inselbergs shows that there is no fractured

RESULT AND DISSCUSSION

quartzite present in this area. The formation resistivity is suggestive of very shallow buried pediment plain with in situ inselbergs. This area is not found suitable for groundwater exploration.

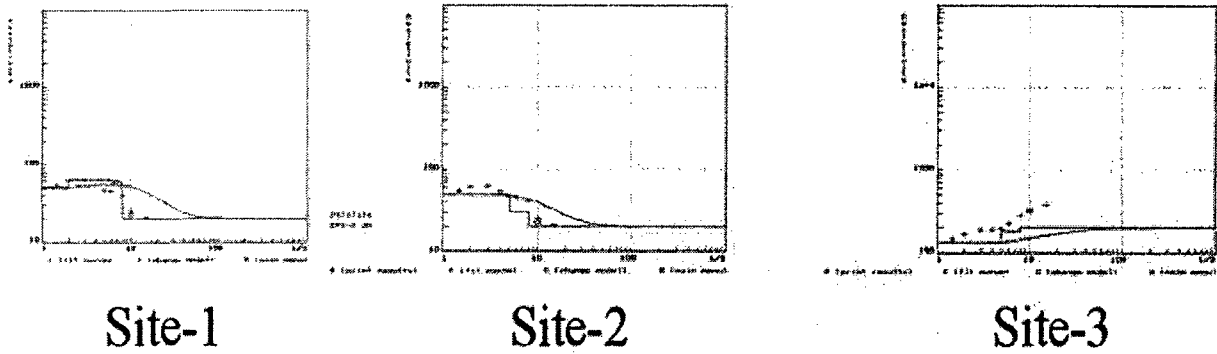


Fig 5.51 Vertical Electrical Sounding Plot in JNU at site 14

(Site-1 and Site-2 are scientifically considered best for construction of pit for Rooftop Rainwater Harvesting)

RESULT AND DISSCUSSION

Based on the resistivity and magnetic surveys carried out in the study area 7 sites were selected within JNU campus area for primary drilling. The diagram below gives an outline plan of their locations with respect to each other.

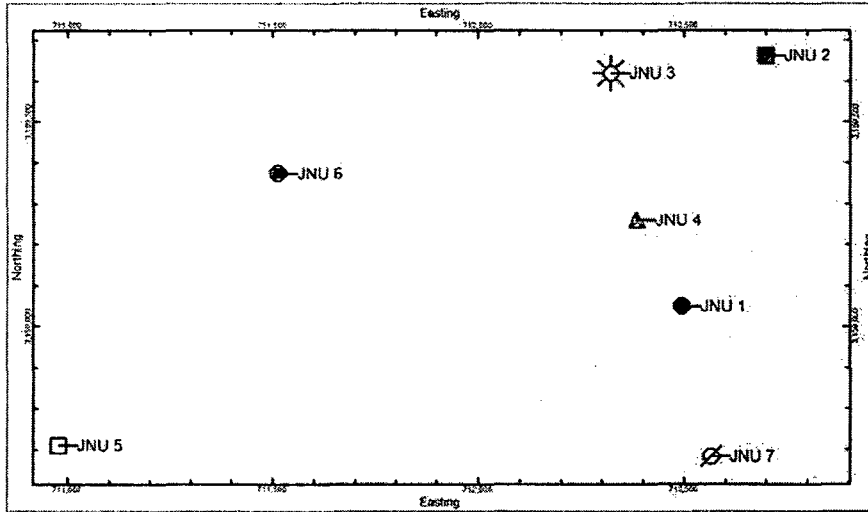


Fig 5.52 Location Plan for 7 sites selected for primary drilling

Bore	Longitude	Latitude	Easting	Northing	Elevation (in Metres)	Total Depth (in Metres)
JNU 1	77.17186	28.54092	712494.9	3159050	248	182.92
JNU 2	77.17406	28.54642	712698.5	3159663	236	182.92
JNU 3	77.17019	28.54608	712321.4	3159619	250	164.63
JNU 4	77.17078	28.54283	712385	3159260	253	160.06
JNU 5	77.1563	28.5381	710977.6	3158710	263	166.15
JNU 6	77.1619	28.544	711513.9	3159374	250	198.17
JNU 7	77.17251	28.5376	712565.1	3158683	256	146.34

Table 5.20 Details of different Drilling sites

RESULT AND DISSCUSSION

5.11 YIELD DESCRIPTION:

Tabulation of discharge of exploratory tubewells in a part of NCR (JNU area) is shown in table 5.21. Groundwater occurs in Delhi system of Rocks in confined aquifer at various levels in JNU area (24mbgl to 185mbgl). After drilling on scientifically selected suitable sites 100% success rate was achieved in this water starved, metamorphic terrain. Based on the litholog prepared by Remote Sensing Application Laboratory, SES, JNU slotted pipes were lowered down to scientifically corrected accurate depth zones. The compressor test was carried out. In this process a pipe of diameter inch with orifice diameter of 2.5inch was fitted in the discharge pipe. Head of the orifice was measured through a transparent rubber tube. Table 5.21 shows discharge of groundwater in Lt/hr from circular orifice.

	JNU 1	JNU2	JNU3	JNU4	JNU5	JNU6	JNU7
Head of water in tube above centre of orifice in (inches)	9	18	25	10	20	9	20
4 inch pipe with 2.5 inch opening in (Lt/hr)	20,475	28,938	34,125	21,840	30,576	20,475	30,576

Table 5.21 Tabulation of discharge in Lt/hr from circular-orifice

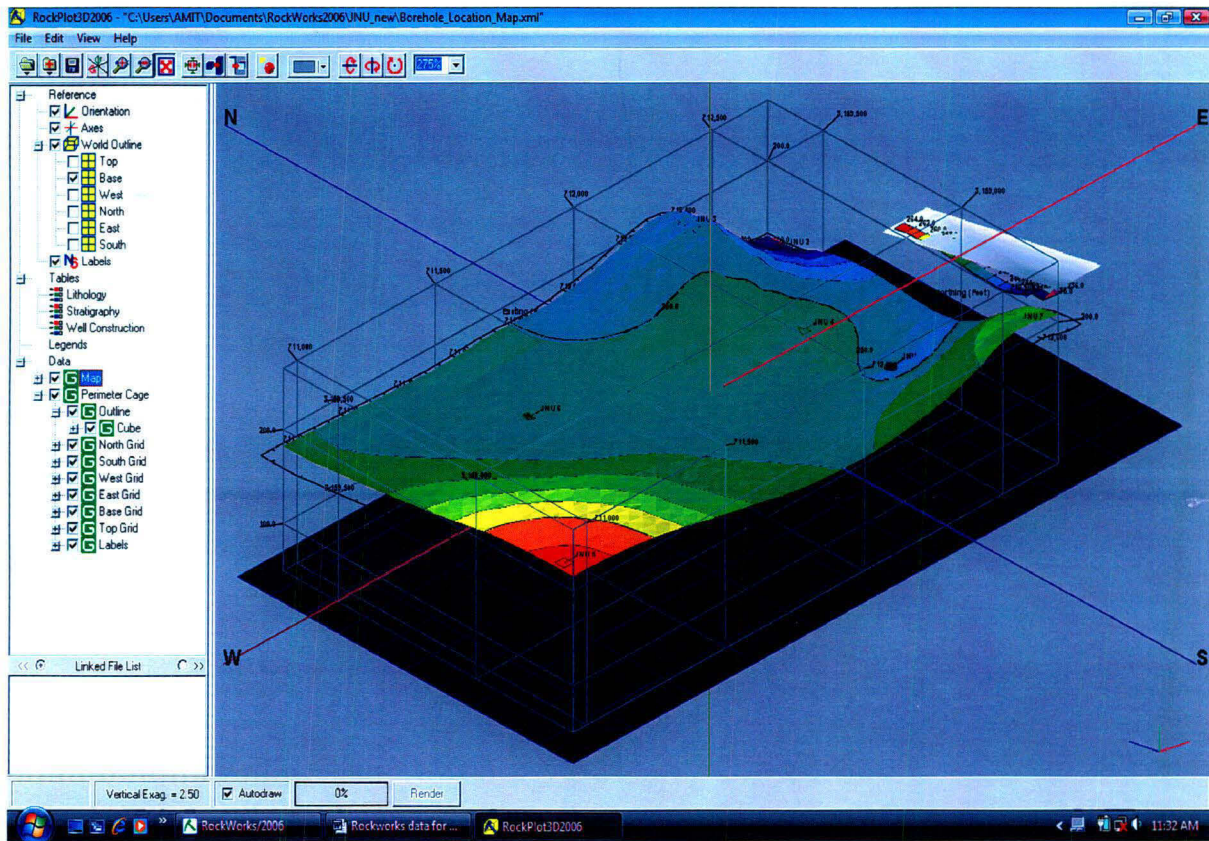


Fig 5.53. Three dimensional elevation contours of the sites within study area

Elevation contours of the sites within study area selected for drilling indicate that elevation naturally increases towards south-west region. Towards eastern and north-eastern parts of study area elevation decreases sharply.

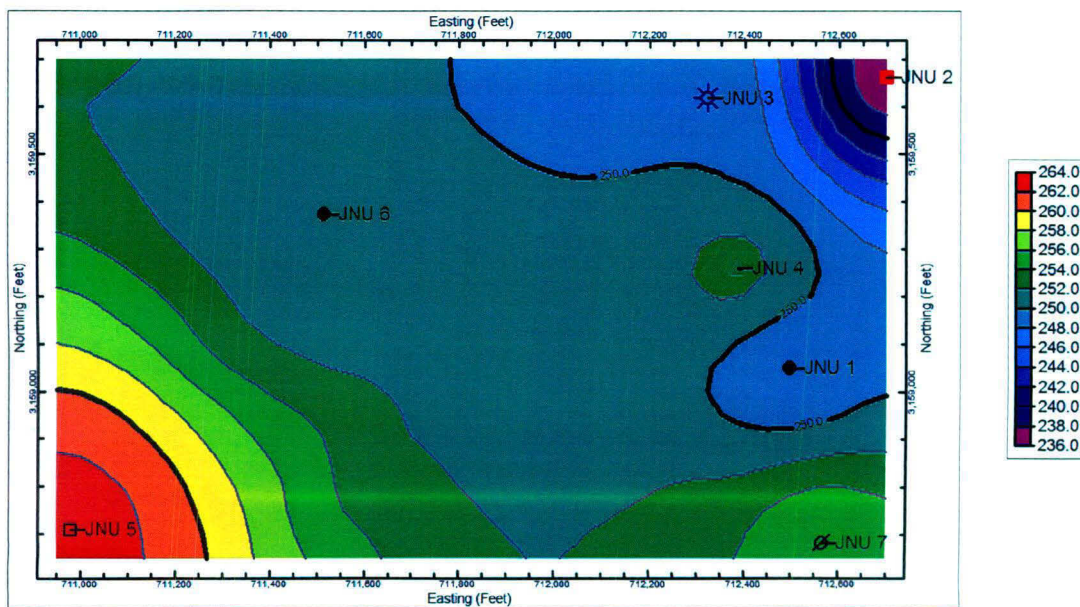


Fig 5.54 Elevation contours of the sites within study area

5.12 STRIPILOGS OF DRILLING SITES IN JNU

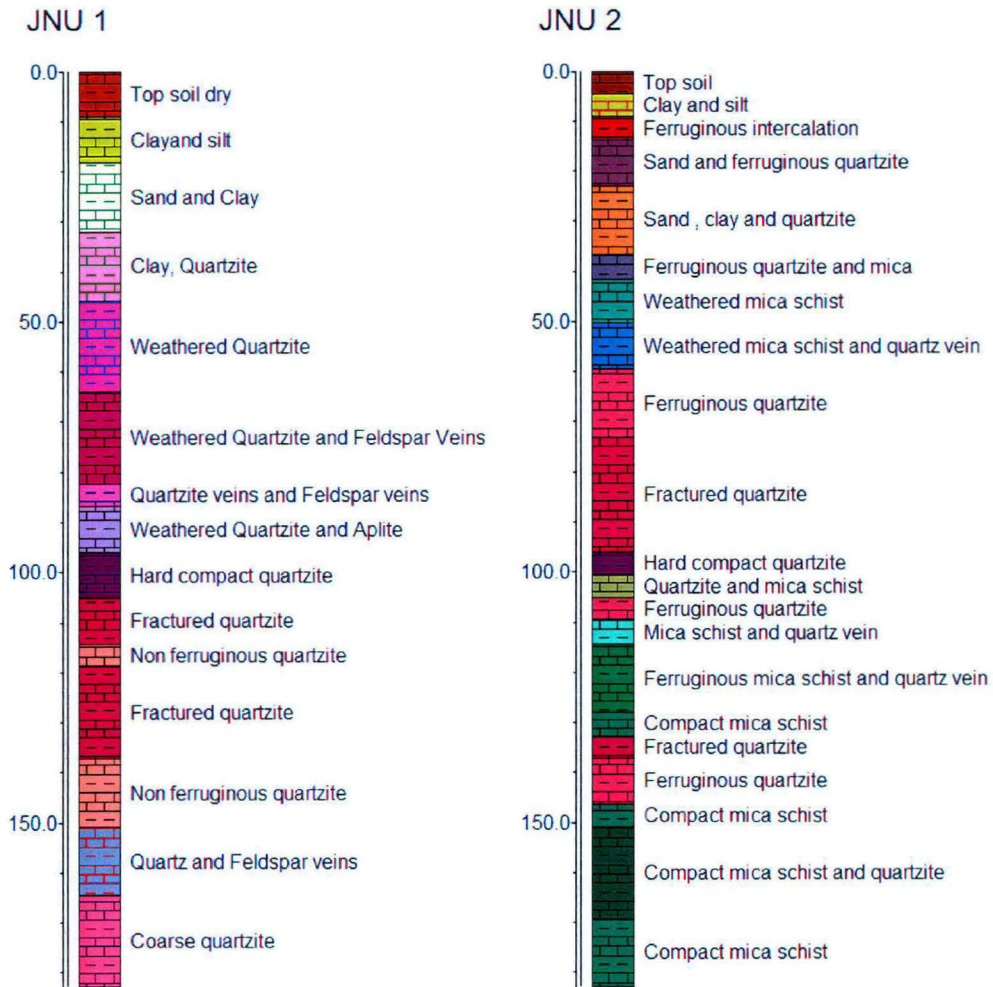


Fig 5.55 Striplogs of drilling sites, Site 1 (JNU1) and Site 2 (JNU2) (depth in metres)

RESULT AND DISSCUSSION

Bore	Depth1 (in metres)	Depth2 (in metres)	Lithology
JNU 1	0	9.14	Top soil dry
JNU 1	9.14	18.29	Clay and silt
JNU 1	18.29	32.01	Sand and Clay
JNU 1	32.01	45.73	Clay, Quartzite
JNU 1	45.73	64.02	Weathered Quartzite
JNU 1	64.02	82.31	Weathered Quartzite and Feldspar Veins
JNU 1	82.31	86.89	Quartzite veins and Feldspar veins
JNU 1	86.89	96.03	Weathered Quartzite and Aplite
JNU 1	96.03	105.18	Hard compact quartzite
JNU 1	105.18	114.32	Fractured quartzite
JNU 1	114.32	118.9	Non ferruginous quartzite
JNU 1	118.9	137.19	Fractured quartzite
JNU 1	137.19	150.91	Non ferruginous quartzite
JNU 1	150.91	164.63	Quartz and Feldspar veins
JNU 1	164.63	182.92	Coarse quartzite
JNU 2	0	4.57	Top soil
JNU 2	4.57	9.14	Clay and silt
JNU 2	9.14	13.71	Ferruginous intercalation
JNU 2	13.71	22.86	Sand and ferruginous quartzite
JNU 2	22.86	36.58	Sand , clay and quartzite
JNU 2	36.58	41.58	Ferruginous quartzite and mica
JNU 2	41.58	50.3	Weathered mica schist
JNU 2	50.3	59.45	Weathered mica schist and quartz vein
JNU 2	59.45	73.17	Ferruginous quartzite
JNU 2	73.17	96.03	Fractured quartzite
JNU 2	96.03	100.6	Hard compact quartzite
JNU 2	100.6	105.18	Quartzite and mica schist
JNU 2	105.18	109.75	Ferruginous quartzite
JNU 2	109.75	114.32	Mica schist and quartz vein
JNU 2	114.32	128.04	Ferruginous mica schist and quartz vein
JNU 2	128.04	132.62	Compact mica schist
JNU 2	132.62	137.19	Fractured quartzite
JNU 2	137.19	146.34	Ferruginous quartzite
JNU 2	146.34	150.91	Compact mica schist
JNU 2	150.91	169.2	Compact mica schist and quartzite
JNU 2	169.2	182.92	Compact mica schist

Table 5.22. The lithology of primary drilling Sites Site 1 (JNU1) and Site 2 (JNU2) within JNU

5.12.1 DESCRIPTION OF SITE1 (JNU 1)

Drilling at Site 1 (JNU 1) went up to 182.92metres depth. Upper layers are composed of sand and clay probably because the area around the site has seen developmental activity and soil from other areas spread over in thick layers to assist vegetation (particularly tree growth) as the area had thin soil cover. Below the soil cover several layers of weathered quartzite were observed followed by hard compact quartzite. This bore had non-ferruginous quartzite and deeper layers are full of fractures. Some veins of quartz and feldspar were also observed in lower layers. These interconnected fractures serve as good sites for storing groundwater in deep layers of confined aquifers like this one. The litholog prepared in this site shows clay and silt below top soil down to 10m depth. The peak of quartz (SiO_2) is dominating in X-Ray analysis of the bulk minerals of the sediments. A few peaks in X-Ray also showing calcium carbonate (CaCO_3) which confirms the litholog as well as resistivity values. Occurrence of groundwater in weathered quartzite has been found at a depth of 35mbgl although the seepages of groundwater have been recorded at 17.5mbgl. Amount of aquifer water increases down to 96mbgl which is composed of weathred quartzites, Feldspar and Aplite veins. The quartzites below 82mbgl show some peaks of haematite along with a few traces of Chromite, Fluorite and Bornite. The fracture width within quartzite are wide as manifested by resistivity survey are suggestive of very high transmissivity of the aquifer. Fractured pegmatites shows secondary porosity in which groundwater can percolate and flow. The high discharge of groundwater makes the presence of $\text{Cr}_2\text{O}_3^{2-}$ insignificant. The ICPAES data analysed (in the Geochemical Laboratory, of Geological Survey of India) shows that a concentration of trace elements geochemically insignificant. Further the ICPAES data shows that Al_2O_3 , Fe_2O_3 , MgO and CaO are decreasing from 68.59mbgl to 121.95mbgl. These finding shows the improving trend of deeper level groundwater quality.

5.12.2 DESCRIPTION OF SITE 2 (JNU 2)

Excellent aquifer has been encountered from 60mbgl down to 96mbgl. The litholog as well as compressor test in the field has further confirmed the high potential aquifer in this area. X-Ray and ICPAES a result shows that at a deeper level water quality remain excellent as in the upper level. At the depth 108.5mbgl the mineral peak shows mainly quartz with some accessories of calcium carbonate. Down to 146.34mbgl the fractured quartzite further shows another good layer of aquifer. Beyond ferruginous quartzite at depth of 146 to 150mbgl the compact mica schist shows some garnet crystals in thin section petrography. The presence of garnet in mica schist is suggestive of high grade metamorphism which is further supported by X-Ray and ICPAES investigations. The presence of

RESULT AND DISSCUSSION

Barium is decreasing from 4.57mbgl to 77.74mbgl which is suggestive of the selective chemical mobility of the ions during metamorphism leading to pegmatiation.

Groundwater quantity depends on structural and tectonic history of the rocks i.e. amount of secondary porosity and permeability in the form of jointing, fracturing, shearing and faulting within the rocks.

Drilling at Site 2 (JNU 2) went upto 182.92metres depth. Here also upper layers up to 9metres depth (approx.) were composed of silt and clay. This was followed by several layers of sand and ferruginous quartzite. Zone around 36-40metres depth marked the transition to mica schist dominant layers.

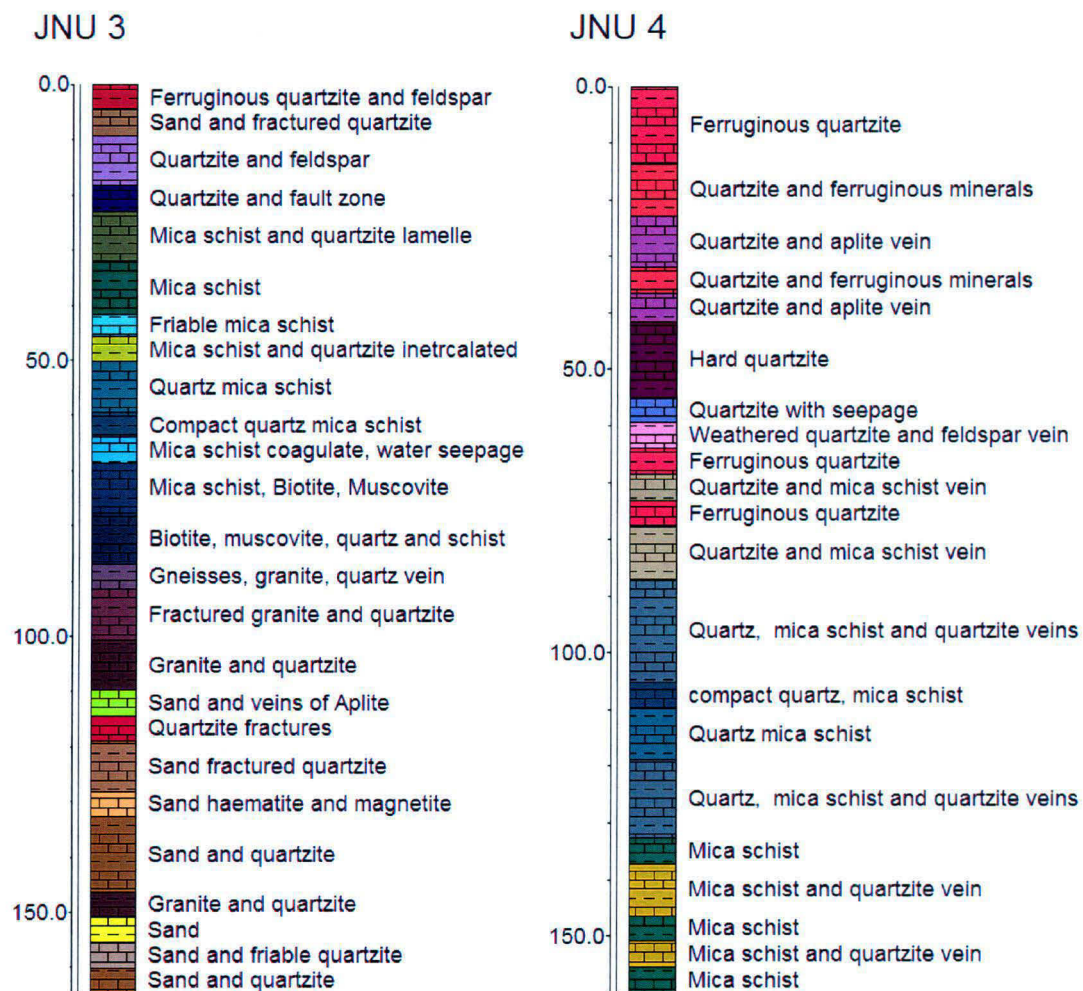


Fig 5.56 Striplogs of drilling sites, Site 3 (JNU3) and Site 4 (JNU4) (depth in metres)

RESULT AND DISSCUSSION

Bore	Depth1 (in metres)	Depth2 (in metres)	Lithology
JNU 3	0	4.57	Ferruginous quartzite and feldspar
JNU 3	4.57	9.14	Sand and fractured quartzite
JNU 3	9.14	18.29	Quartzite and feldspar
JNU 3	18.29	22.86	Quartzite and fault zone
JNU 3	22.86	32.01	Mica schist and quartzite lamelle
JNU 3	32.01	41.58	Mica schist
JNU 3	41.58	45.73	Friable mica schist
JNU 3	45.73	50.3	Mica schist and quartzite intercalated
JNU 3	50.3	59.54	Quartz mica schist
JNU 3	59.45	64.02	Compact quartz mica schist
JNU 3	64.02	68.59	Mica schist coagulate, water seepage
JNU 3	68.59	77.74	Mica schist, Biotite, Muscovite
JNU 3	77.74	86.89	Biotite, muscovite, quartz and schist
JNU 3	86.89	91.46	Gneisses, granite, quartz vein
JNU 3	91.46	100.6	Fractured granite and quartzite
JNU 3	100.6	109.75	Granite and quartzite
JNU 3	109.75	114.32	Sand and veins of Aplite
JNU 3	114.32	118.9	Quartzite fractures
JNU 3	118.9	128.04	Sand fractured quartzite
JNU 3	128.04	132.62	Sand haematite and magnetite
JNU 3	132.62	146.34	Sand and quartzite
JNU 3	146.34	150.91	Granite and quartzite
JNU 3	150.91	155.48	Sand
JNU 3	155.48	160.06	Sand and friable quartzite
JNU 3	160.06	164.63	Sand and quartzite
JNU 4	0	13.71	Ferruginous quartzite
JNU 4	13.71	22.86	Quartzite and ferruginous minerals
JNU 4	22.86	32.01	Quartzite and aplite vein
JNU 4	32.01	36.58	Quartzite and ferruginous minerals
JNU 4	36.58	41.58	Quartzite and aplite vein
JNU 4	41.58	54.87	Hard quartzite
JNU 4	54.87	59.45	Quartzite with seepage
JNU 4	59.45	64.02	Weathered quartzite and feldspar vein
JNU 4	64.02	68.59	Ferruginous quartzite
JNU 4	68.59	73.17	Quartzite and mica schist vein
JNU 4	73.17	77.74	Ferruginous quartzite
JNU 4	77.74	86.89	Quartzite and mica schist vein
JNU 4	86.89	105.18	Quartz, mica schist and quartzite veins
JNU 4	105.18	109.75	compact quartz, mica schist
JNU 4	109.75	118.9	Quartz mica schist
JNU 4	118.9	132.62	Quartz, mica schist and quartzite veins
JNU 4	132.62	137.19	Mica schist
JNU 4	137.19	146.34	Mica schist and quartzite vein
JNU 4	146.34	150.91	Mica schist
JNU 4	150.91	155.48	Mica schist and quartzite vein
JNU 4	155.48	160.06	Mica schist

Table 5.23. The lithology of primary drilling Sites Site 3 (JNU3) and Site 4 (JNU4) within JNU

5.12.3 DESCRIPTION OF SITE 3 (JNU 3)

The top soil resistivity in site No.3 shows a higher resistance due to presence of coarse grained weathered ferruginous quartzite at 4m depth the fracture quartzite with seepages of groundwater has been found out from 10 to 15mbgl interconnected fractures and a fault line was traced. This is supported by the litholog as well as consistent lowering of the resistivity value which is ranging from 50Ωm to 200Ωm from 10mbgl to 25m.bgl. From 30mbgl intercalations of mica schist and quartzite started down to 60m.bgl. The schist and quartzite interface from 35 to 85mbgl shows 10 numbers of groundwater bearing formations. From 85mbgl to 88mbgl biotite, muscovite, quartz, schist was found to highly crushed. This is suggestive of fault zone below this formation. Further from 90mbgl downwards fractured granite and quartzite with intermittent veins of aplite has been found. From 88mbglto 165mbgl the groundwater discharge was very high. It was measured by orifice method and found out to be 30,000 to 35,000Lt/hr. Very low magnetic anomaly further proves the occurrence of interconnected fracture zone in this granite-pegmatite-quartzite-schistose complex which after drilling was found to be water bearing. The crushed rock borehole samples and groundwater was analysed by ICPAES and through X-Ray diffraction method. It was found out that the water quality at Site 3 is excellent for drinking purpose.

5.12.4 DESCRIPTION OF SITE 4 (JNU 4)

The drilling was varied out at site 4 which is at highest elevation point in NCR showing very thin veneer of soil development due to in situ weathering at ferruginous quartzite lying beneath the soil. From 1mbgl to 25mbgl ferruginous quartzite occurs without any prominent groundwater zone from 26mbgl to 38mbgl. Alterations of quartzite and aplite veins has been recorded to be promising aquifer/ groundwater zones in this area with less amount of groundwater discharge. Quartzites/Aplites/Pegmatites are not considered good aquifers if there are no interconnected fracture system develops secondary porosity and permeability in these rocks. From 42mbgl down to 55mbgl hard compact quartzite forms the confining zone of subsurface aquifer. At 56mbgl fractured quartzite occurs with very high discharge of groundwater. This groundwater is under confined condition and the piezometric head reached approximately up to 12mbgl. This is an excellent example of recharging dried up surficial aquifer and through confined zone exploration. From 56mbgl down to 70mbgl groundwater discharge was very high in ensuring inter-connected fracture system. From 70mbgl down to 88mbgl mica schist occurs. From 88mbgl to 148mbgl alteration of groundwater bearing quartzite vein and mica schist has been encountered. From 148mbgl down to 154mbgl a very promising zone of groundwater has increased the cumulative yield of site 4 (JNU4). The piezometric head of

RESULT AND DISCUSSION

groundwater in this tube well has come near the surface. Submersible pump has been lowered in this tube well which is supplying excellent quality of groundwater being used for water in the whole adjacent area.

5.12.5 DESCRIPTION OF SITE 5 (JNU 5)

Drilling at Site 5 (JNU 5) it was found out that ferruginous quartzite forms the upper layer of the groundwater bearing horizon with intermittent pegmatite veins down to 70mbgl. Further from 70mbgl to 125mbgl the ferruginous quartzite shows few fractures with groundwater but 125mbgl very promising pegmatite zone shows multiple fractures with very high discharge of groundwater. The ferruginous quartzite intruded by pegmatite shows further rise in groundwater bearing fractured zones. Below 150mbgl clear fractured quartzite shows excellent discharge of groundwater. The water quality tested by ICPAES shows that there are negligible to nil amount of any major or trace elements. However presence of Ba, Sr and B further proves that groundwater is coming from fractured pegmatite and quartzite.

5.12.6 DESCRIPTION OF SITE 6 (JNU 6)

The resistivity from site 6 (JNU 6) shows that 4mbgl of soil are of sandy clay in nature which is overlying non-ferruginous quartzite down to 30mbgl. From 30mbgl the ferruginous quartzite starts which is the upper zone of very promising aquifer in multiple veins. Below 52mbgl water bearing fracture cumulates the yield of groundwater which has been found to be extended down to 85mbgl. From 85mbgl to 115mbgl non ferruginous quartzite shows intermittent aquifer. From 115mbgl to 150mbgl very high grade graphite schist with quartzite occurs. The graphite schist and quartzite contains good amount of groundwater but this zone was not tapped to avoid the graphite impurities in groundwater. At 150mbgl ferruginous quartzite shows very high discharge down to 180mbgl where the quartzite was found non-ferruginous from 155mbgl to 190mbgl.

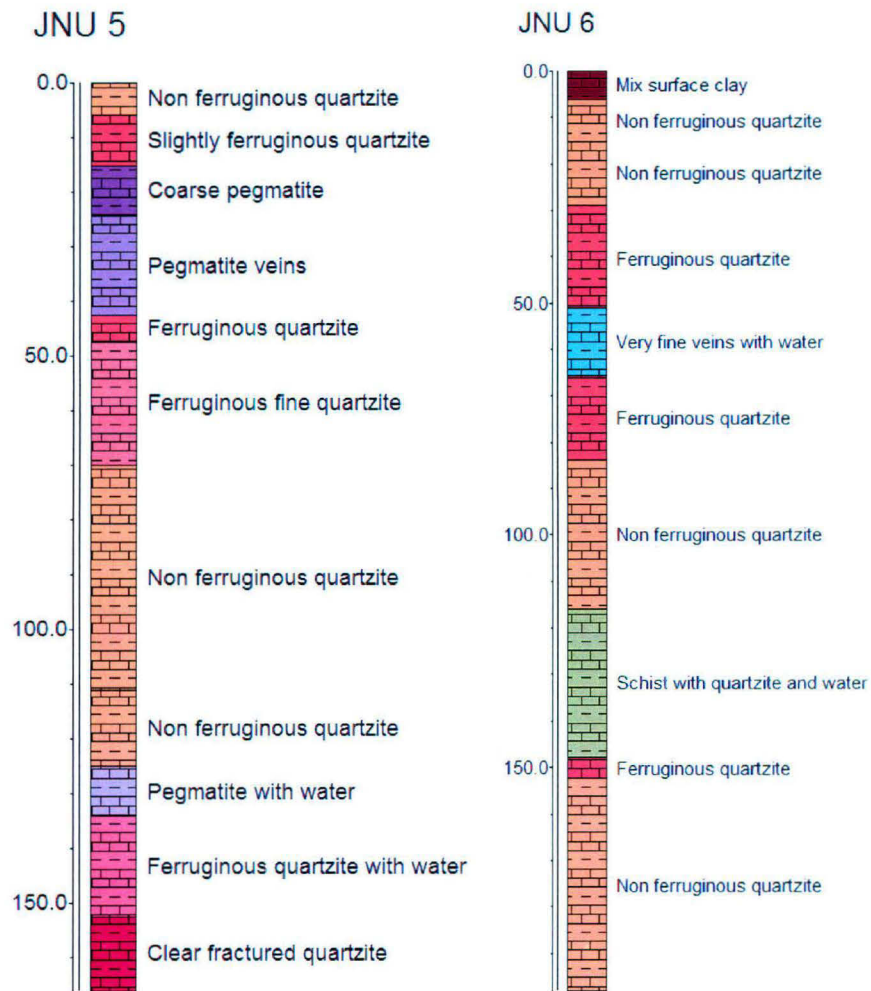


Fig 5.57 Striplogs of drilling sites, Site 5 (JNU5) and Site 6 (JNU6) (depth in metres)

RESULT AND DISSCUSSION

Bore	Depth1 (in metres)	Depth2 (in metres)	Lithology
JNU 5	0	6.09	Non ferruginous quartzite
JNU 5	6.09	15.24	Slightly ferruginous quartzite
JNU 5	15.24	24.39	Coarse pegmatite
JNU 5	24.39	42.68	Pegmatite veins
JNU 5	42.68	47.25	Ferruginous quartzite
JNU 5	47.25	70.12	Ferruginous fine quartzite
JNU 5	70.12	111.28	Non ferruginous quartzite
JNU 5	111.28	125	Non ferruginous quartzite
JNU 5	125	134.14	Pegmatite with water
JNU 5	134.14	152.43	Ferruginous quartzite with water
JNU 5	152.43	166.15	Clear fractured quartzite
JNU 6	0	6.09	Mix surface clay
JNU 6	6.09	15.24	Non ferruginous quartzite
JNU 6	15.24	28.96	Non ferruginous quartzite
JNU 6	28.96	51.82	Ferruginous quartzite
JNU 6	51.28	65.54	Very fine veins with water
JNU 6	65.54	83.84	Ferruginous quartzite
JNU 6	83.84	115.85	Non ferruginous quartzite
JNU 6	115.85	147.86	Schist with quartzite and water
JNU 6	147.86	152.43	Ferruginous quartzite
JNU 6	152.43	198.17	Non ferruginous quartzite

Table 5.24. The lithology of primary drilling Sites Site 5 (JNU5) and Site 6 (JNU6) within JNU

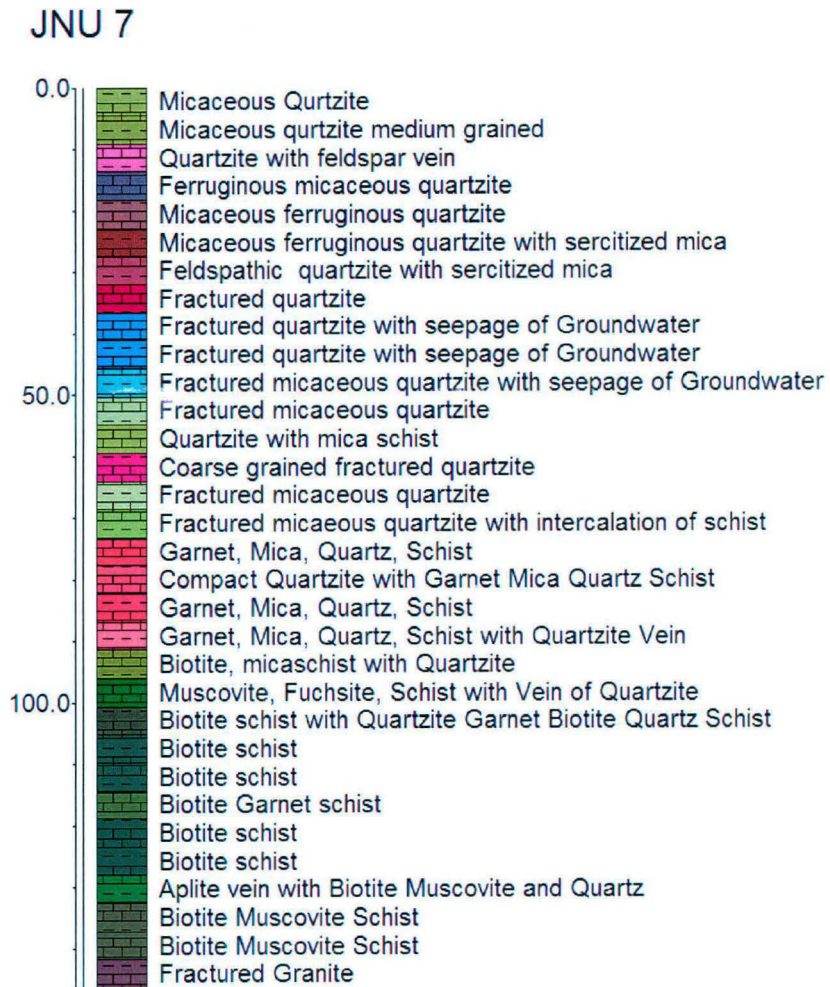


Fig 5.58 Striplogs of drilling Site 7 (JNU7) (depth in metres)

RESULT AND DISSCUSSION

Bore	Depth 1 (in metres)	Depth 2 (in metres)	Lithology
JNU 7	0	4.57	Micaceous Quartzite
JNU 7	4.57	9.14	Micaceous quartzite medium grained
JNU 7	9.14	13.71	Quartzite with feldspar vein
JNU 7	13.71	18.29	Ferruginous micaceous quartzite
JNU 7	18.29	22.86	Micaceous ferruginous quartzite
JNU 7	22.86	27.43	Micaceous ferruginous quartzite with sercitized mica
JNU 7	27.43	32.01	Feldspathic quartzite with sercitized mica
JNU 7	32.01	36.58	Fractured quartzite
JNU 7	36.58	41.15	Fractured quartzite with seepage of Groundwater
JNU 7	41.15	45.73	Fractured quartzite with seepage of Groundwater
JNU 7	45.73	50.3	Fractured micaceous quartzite with seepage of Groundwater
JNU 7	50.3	54.87	Fractured micaceous quartzite
JNU 7	54.87	59.45	Quartzite with mica schist
JNU 7	59.45	64.02	Coarse grained fractured quartzite
JNU 7	64.02	68.59	Fractured micaceous quartzite
JNU 7	68.59	73.17	Fractured micaceous quartzite with intercalation of schist
JNU 7	73.17	77.74	Garnet, Mica, Quartz, Schist
JNU 7	77.74	82.31	Compact Quartzite with Garnet Mica Quartz Schist
JNU 7	82.31	86.89	Garnet, Mica, Quartz, Schist
JNU 7	86.89	91.46	Garnet, Mica, Quartz, Schist with Quartzite Vein
JNU 7	91.46	96.03	Biotite, mica schist with Quartzite
JNU 7	96.03	100.6	Muscovite, Fuchsite, Schist with Vein of Quartzite
JNU 7	100.6	105.18	Biotite schist with Quartzite Garnet Biotite Quartz Schist
JNU 7	105.18	109.75	Biotite schist
JNU 7	109.75	114.32	Biotite schist
JNU 7	114.32	118.9	Biotite Garnet schist
JNU 7	118.9	123.47	Biotite schist
JNU 7	123.47	128.04	Biotite schist
JNU 7	128.04	132.62	Aplite vein with Biotite Muscovite and Quartz
JNU 7	132.62	137.19	Biotite Muscovite Schist
JNU 7	137.19	141.76	Biotite Muscovite Schist
JNU 7	141.76	146.34	Fractured Granite

Table 5.25. The lithology of primary drilling Sites Site 5 (JNU5) and Site 6 (JNU6) within JNU

5.12.7 DESCRIPTION OF SITE 7 (JNU 7)

The resistivity survey in site 7 (JNU 7) shows that there is a uniform resistivity of 140Ωm from ground level down to 10mbgl. Further, there is a distinct fall of resistivity value from 25mbgl to 50mbgl. This is highly fractured ferruginous quartzite with very high discharge of groundwater. The fractured quartzite continued

RESULT AND DISSCUSSION

down to 75mbgl beyond which is suggestive of confining quartzite and schistose rocks. Inferred fractured granite was confirmed during drilling at a depth 145mbgl. The resistivity when further analysed was found out to be ranging in between 50 to 200 Ω m in the excellent groundwater bearing zone which is indication of presence of fresh groundwater with low TDS (1-1000mg/l). The ICPAES data of groundwater further confirms these observations.

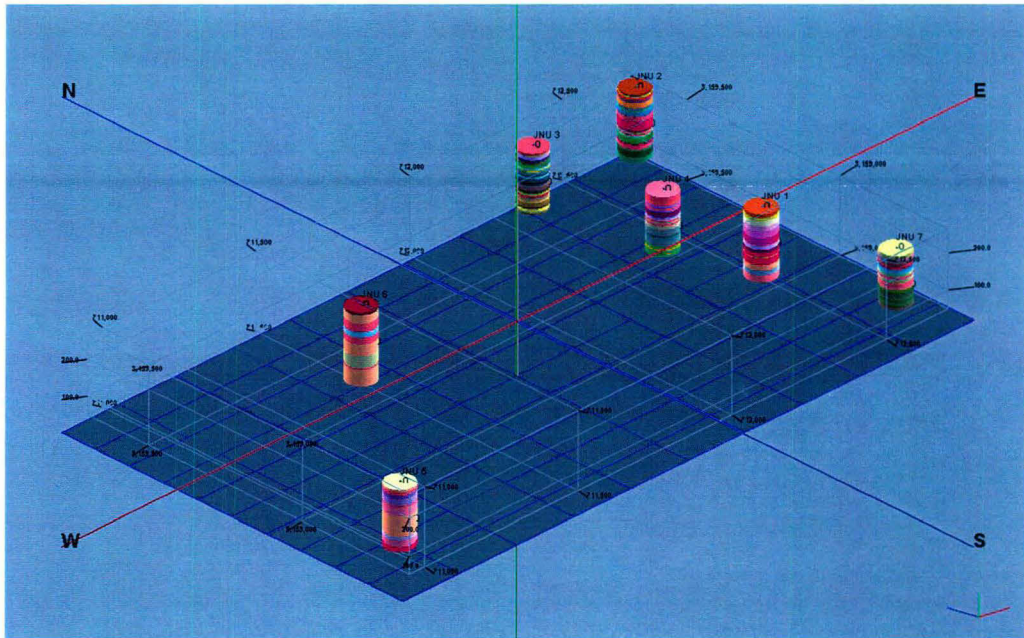


Fig 5.59 Three Dimensional Lithologs generated for Drilling Sites (View 1)

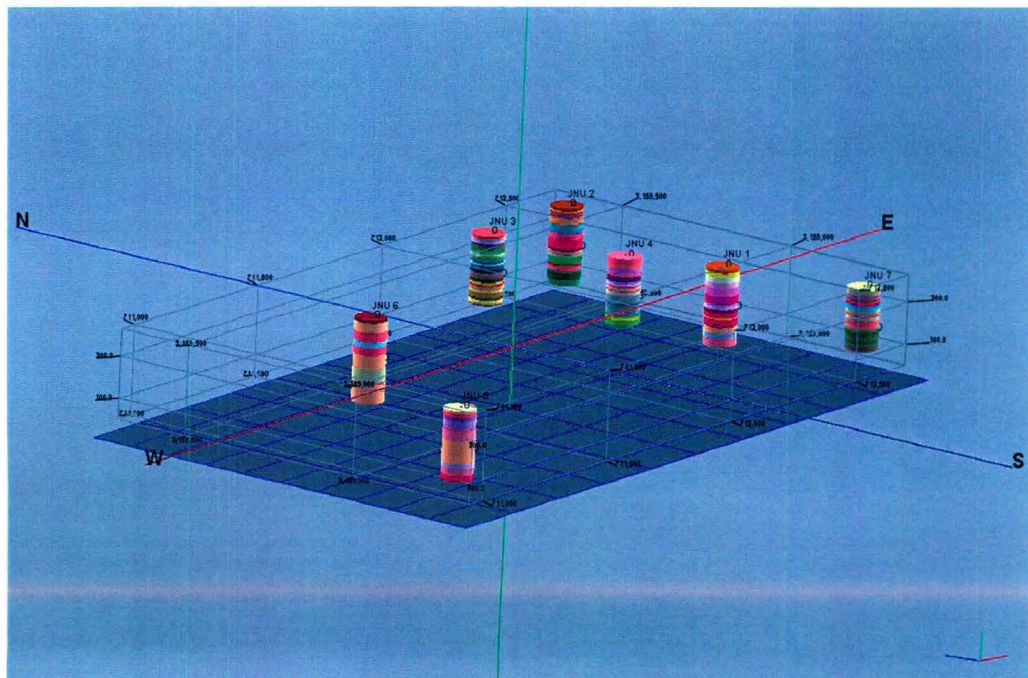


Fig 5.60 Three Dimensional Lithologs generated for Drilling Sites (View 2)

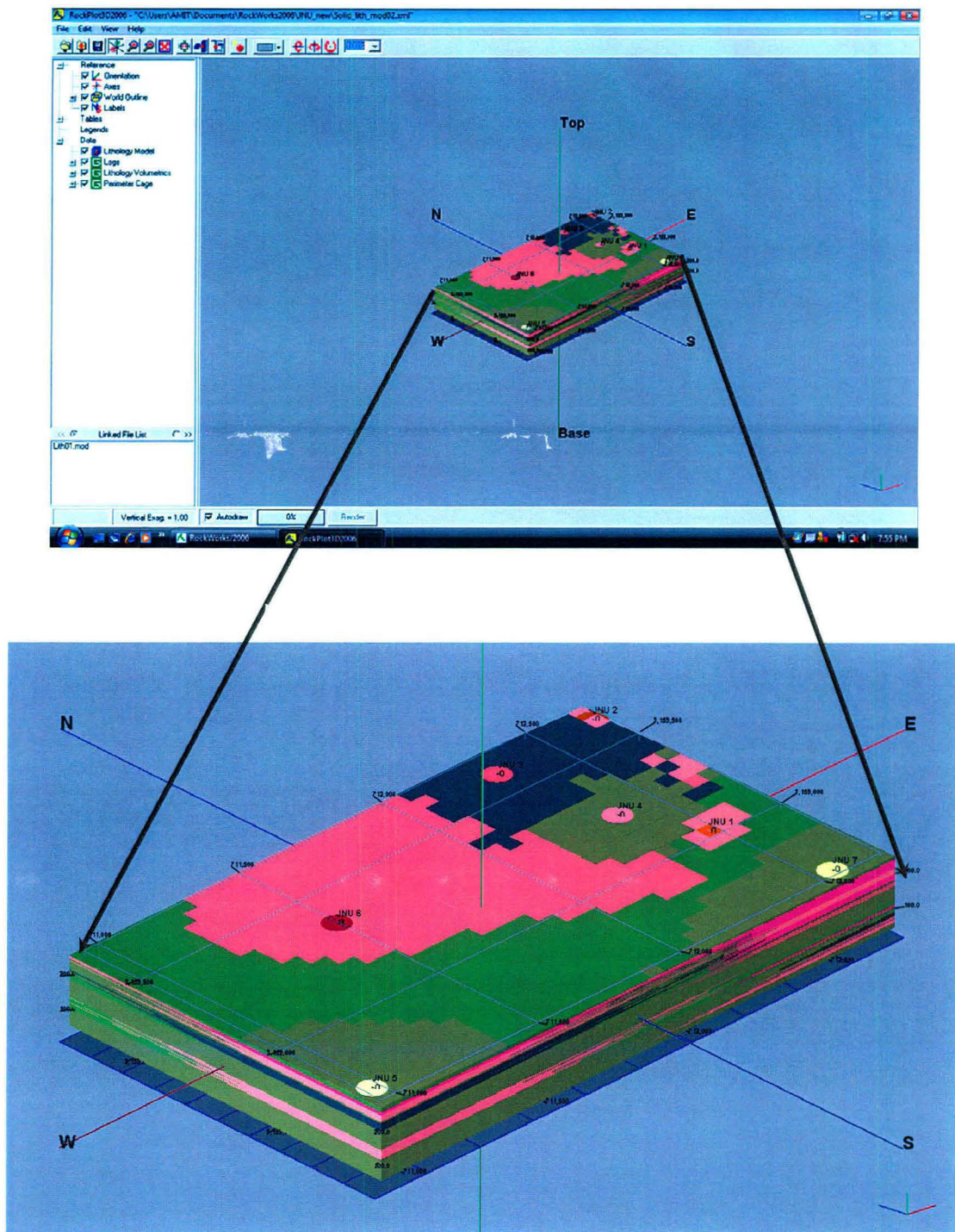


Fig 5.61 Lithology Solid Model (generated using data from drilling sites)

- Sub-surface lithological information was used to generate a lithology solid model for drilling sites predicting the possible sub-surface lithological connections and extrapolating the information to the whole region apart from primary drilling sites. The software (Rockworks) determines the lithology types along each borehole in the project, and assigns certain values to those nodes along the wells. It then uses the “lithoblending” method to assign lithology to nodes lying between wells. Finally, it will reset those nodes above the ground surface to a value of 0.
- Slicing the lithology solid model across different faces generated panels between drilling sites creating a three dimensional fence diagram.

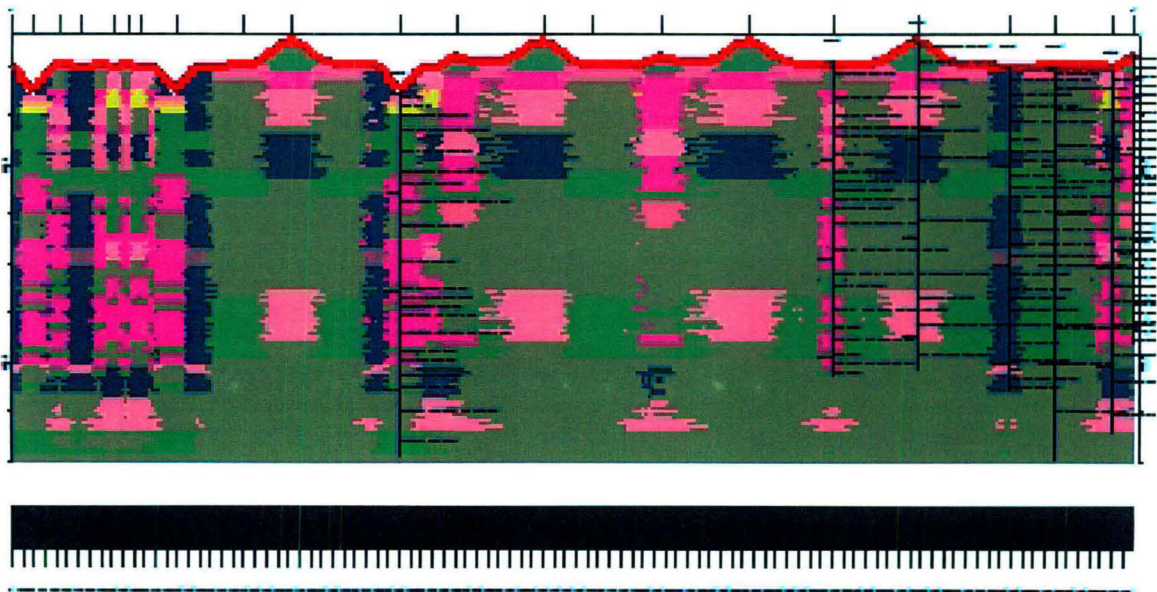


Fig 5.62 A sliced panel from Lithology Solid Model across all 7 drilling sites

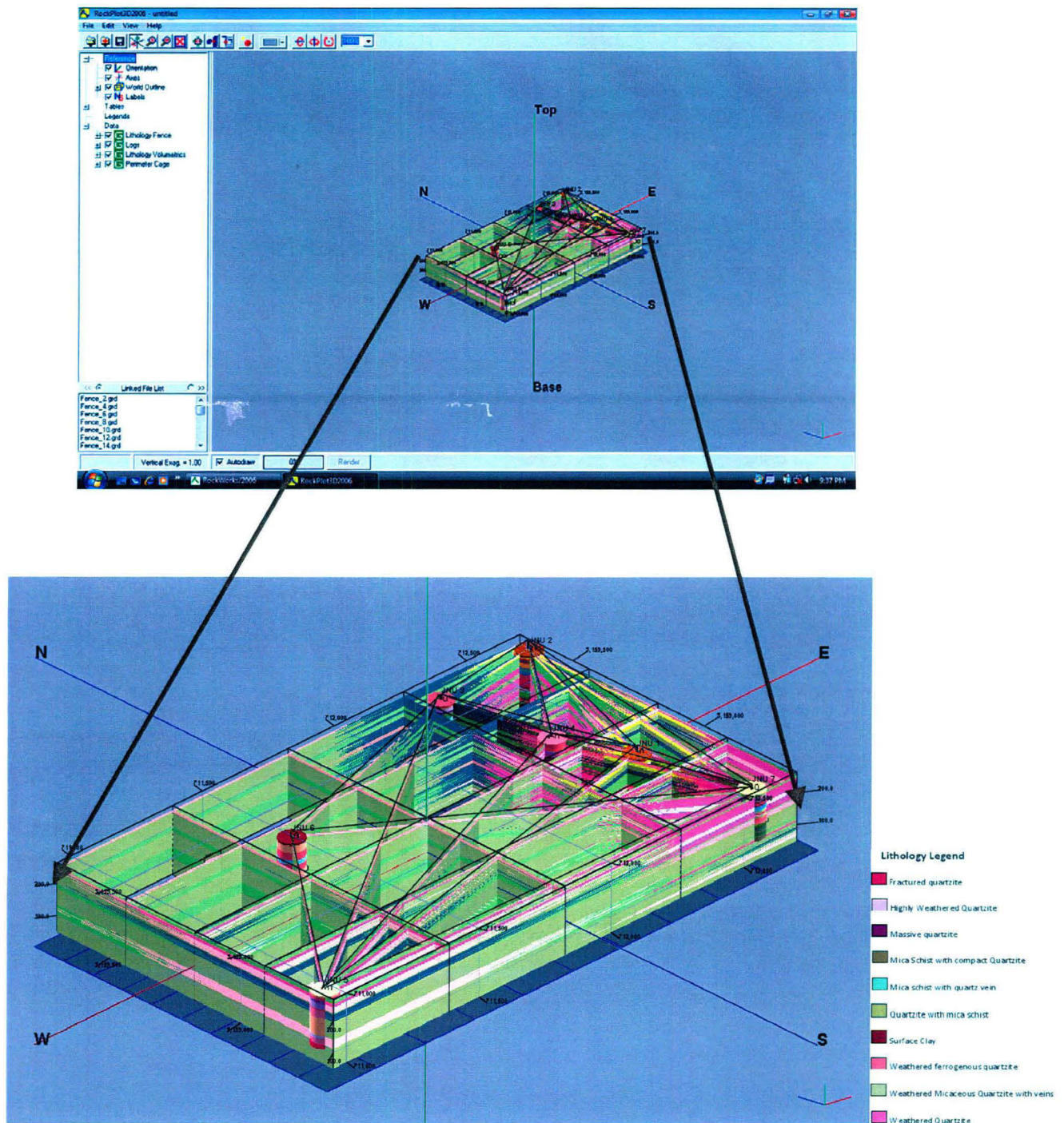


Fig 5.63 Three Dimensional Fence Diagram

Three dimensional fence diagrams generated for the part of study area covered by 7 drilling locations shows that top layers in most parts are predominantly composed of Weathered/Fractured Ferruginous Quartzite. On the other hand the lower layers throughout this part of study area are mostly composed of Mica Schist and Compact Quartzite.

RESULT AND DISSCUSSION

Bore	Depth 1 (in metres)	Depth2 (in metres)
JNU 1	123	128
JNU 1	164	169
JNU 2	86	90
JNU 2	123	128
JNU 2	150	160
JNU 3	45	50
JNU 3	50	160
JNU 4	86.95	100.28
JNU 4	124.7	151
JNU 5	42	59.54
JNU 5	72.39	114.6
JNU 5	120.44	150.91
JNU 6	44.6	50.69
JNU 6	86.97	112.28
JNU 6	124.7	151
JNU 7	32.1	54.87
JNU 7	64.02	73.17
JNU 7	100.6	128.04
JNU 7	137.19	146.34

Table 5.26 Water levels observed at 7 primary drilling locations in JNU

	JNU 1	JNU2	JNU3	JNU4	JNU5	JNU6	JNU7
Head of water in tube above centre of orifice in (inches)							
	9	18	25	10	20	9	20
4 inch pipe with 2.5 inch opening in (Lt/hr)							
	20,475	28,938	34,125	21,840	30,576	20,475	30,576

Table 5.27 Individual Cumulative Water yields of 7 bore wells

5.13 GRIDDING METHODS

The program Rockworks reads the depth intervals for the selected water level data and internally translates depths to elevations based on the boreholes' surface and downhole surveys.

There are various gridding methods available in Rockworks – Closest Point, Cumulative, Directional Weighting, Distance to Point, Inverse-Distance, Kriging, Multiple Linear Regression, Sample Density, Trend Surface Polynomial, Trend Surface Residuals, Triangulation (grid-based) and Hybrid. Since the dataset is not very huge 3 gridding methods (Inverse-Distance, Kriging and Triangulation) were chosen but only two were finalized for application due to their simplicity.

5.13.1 INVERSE-DISTANCE: A common method using a weighted average approach to compute node values.

Triangulation (grid-based): It uses a network of triangles to determine grid node values. Both gridding methods produced quite similar results but finally the output from Inverse-Distance Method was chosen because it produces smooth and continuous grid and will not exaggerate its extrapolations beyond the given data points (range of grid values will be smaller than the data point range: The highest grid value will be less than the maximum data point, and the lowest grid value will be greater than the minimum data point). Inverse-Distance is one of the more common gridding methods. With this method, the value assigned to a grid node is a weighted average of either all of the data points or a number of directionally distributed neighbours. The value of each of the data points is weighted according to the inverse of its distance from the grid node, taken to a user-selected power. The greater the value of the exponent specified, the more localized the gridding since distant points will have less influence on the value assigned to each grid node.

Weighting Exponent: This value determines how "local" or "global" the gridding process will be in assigning node values, the value of each data point is weighted according to the inverse of its distance (d) from the grid node, taken to the n^{th} power, as shown in following diagram.

Sector-Based Searching: tells the program that instead of simply finding the nearest neighbours for the Inverse-Distance gridding, regardless of where they lie, it should look for points in each x -degree sector around the node. This kind of directional search can improve the interpolation of grid values that lie between data point clusters. It can also increase processing time.

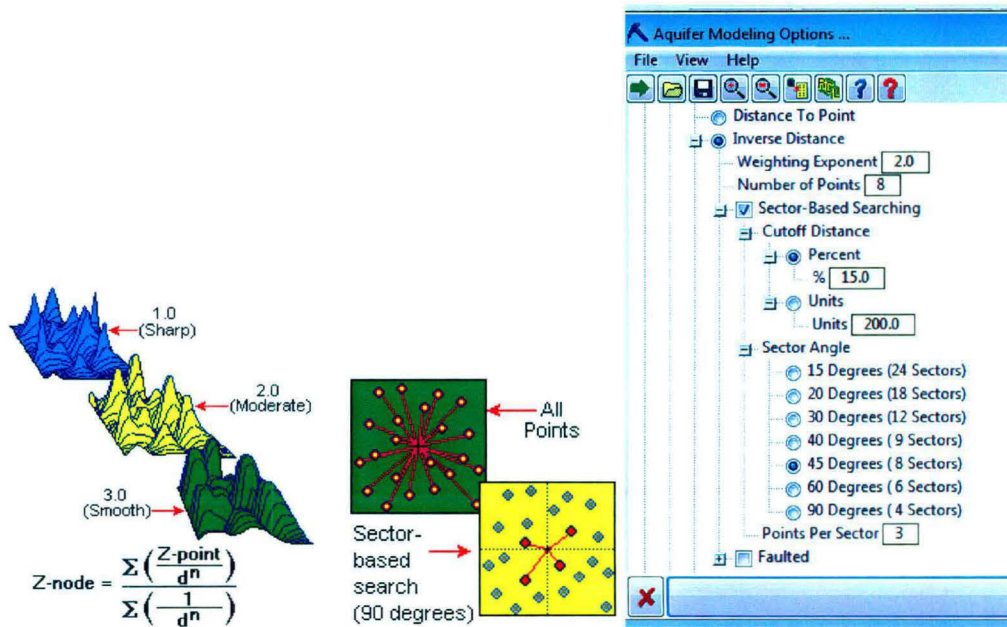


Fig 5.64 The Weighting Exponent was chosen as 2.0 and Sector Angle as 45⁰(8 Sectors) with 3 points per sector.

More refined gridding was not required simply because the area of the region covered by 7 drilling sites is not much and shows very less variability in terms of slope, strike and aspect which was again reconfirmed from the statistical report of the generated grid. Refining the grid parameters even more would have resulted in unnecessary increase in processing time and varied outputs. Thus was created a grid model of the layer's upper elevations or thickness using the selected gridding method, and from this model created a 2-dimensional map with the selected layers and 3-dimensional model. The maps illustrate the surface elevations (Superface) of the aquifer or the aquifer's thickness (Isopach).

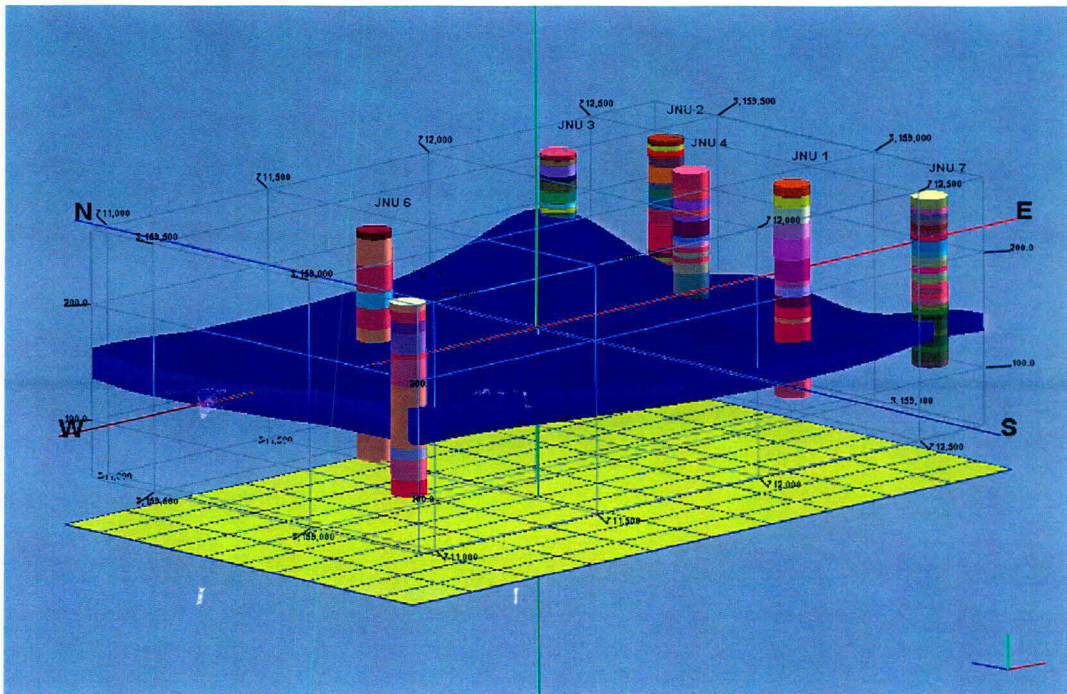


Fig 5.65 Aquifer Model generated for seven primary drilling sites (View 1)

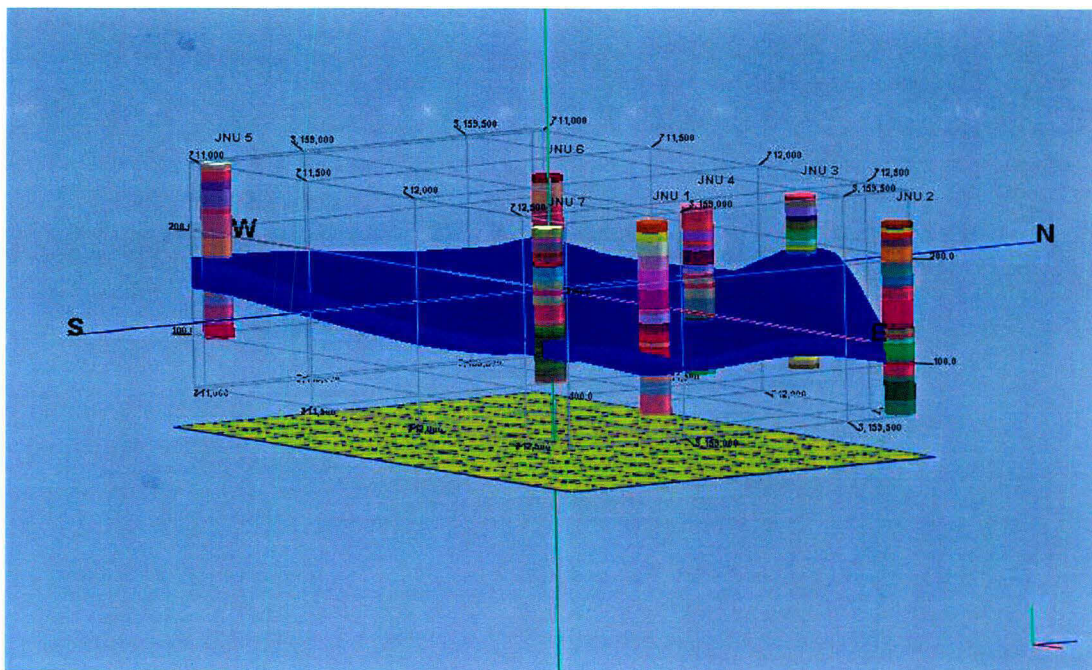


Fig 5.66 Aquifer Model generated for seven primary drilling sites (View 2)

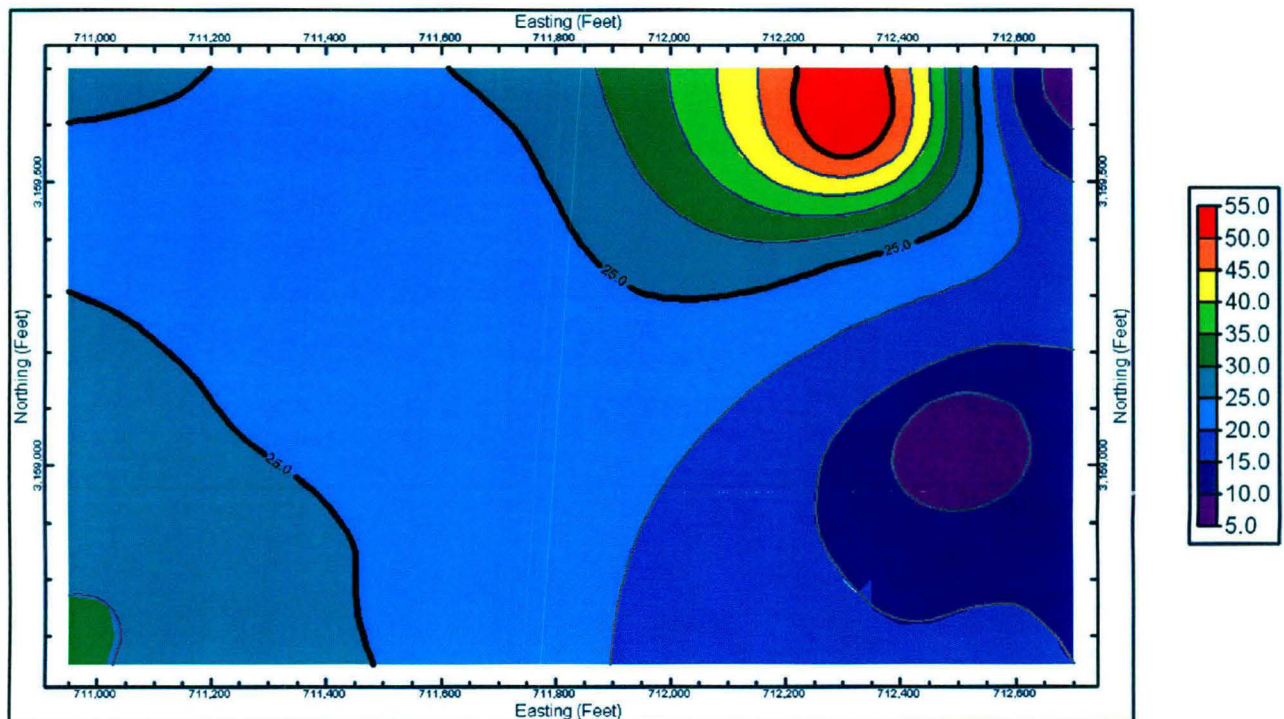


Fig 5.67 Aquifer Thickness (Isopach) for JNU - (in metres)

Aquifer Thickness was modelled for the area covered by seven primary drilling locations in JNU based on the water level data from each of the borewells, total depth and elevation contours. As per the results thickest layers of water are found towards north-eastern part of the sampled area. South-western part of the sampled area also shows moderate aquifer thickness but for this part the accuracy of predicting aquifers with ample water is lesser due to lesser number of primary drilling sites. But for the South-eastern and Eastern parts it was found that aquifer thickness decreases to 5-10 metres.

Aquifer thickness alone can't be a criteria for groundwater exploration or management. It should be considered coupled with the topography as per the elevation contours (or rather flow direction of rainwater) as well as the aquifer depth model and the geology of the terrain. As water follows the natural depressions over the terrain the chances of water getting accumulated in these areas increases. If such pockets are having high primary porosity or interconnected fractures (particularly in hard rock terrain such as JNU) then chances of finding water increases. Confined aquifers in such cases may show lesser aquifer thickness. These conditions can be studied remotely using satellite data but that has to be again reconfirmed through ground-based geophysical surveys (resistivity and magnetic).

Even in this case the changes in aquifer thickness towards north-eastern and south-western parts coincides to a larger extent with the changes in elevation contours (rapid decrease in elevation).

5.14 SPATIAL DISTRIBUTION OF WATER QUALITY PARAMETERS:

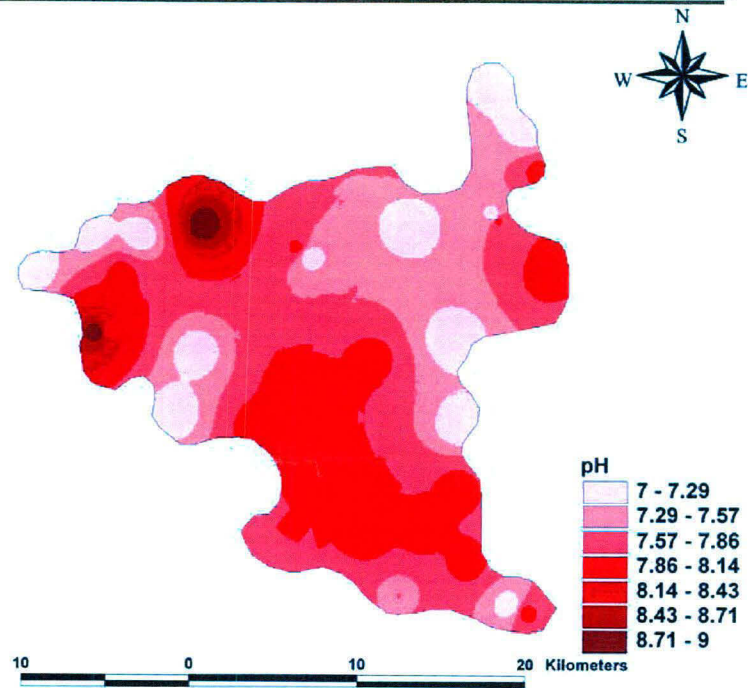


Fig.5.68 Spatial distribution of pH in the study area

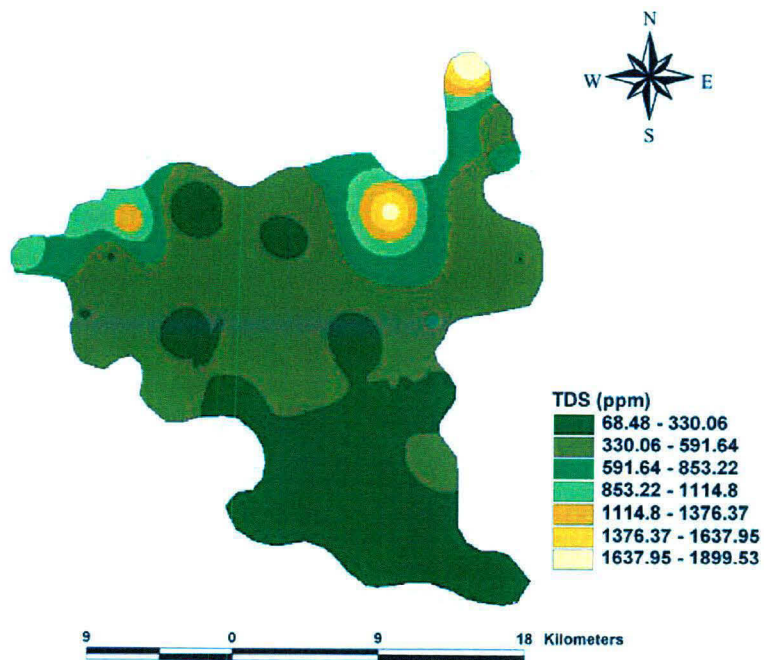


Fig.5.69 Spatial distribution of TDS in the study area

5.14.1 pH

The pH of the groundwater varied between 7.30 to 8.65 while mean pH was 7.77. The highest pH was observed at Kharkhari Nahar which was 8.73. The maximum value is slightly higher than the desirable limit of 8.5. In general the groundwater of the study area is alkaline in nature. The standards for pH values as per WHO and Bureau of Indian standards ranges from 6.5 to 8.2 thus most of the samples were found to be within permissible limits.

5.14.2 Total dissolved solids

Total dissolved solids in the area comes out to be average 565.53mg/l and minimum comes out to be the 68mg/l at Tilangpur Kota DW and maximum at 1899mg/l at Indirapuri market which exceeds the permissible limit of the BIS.

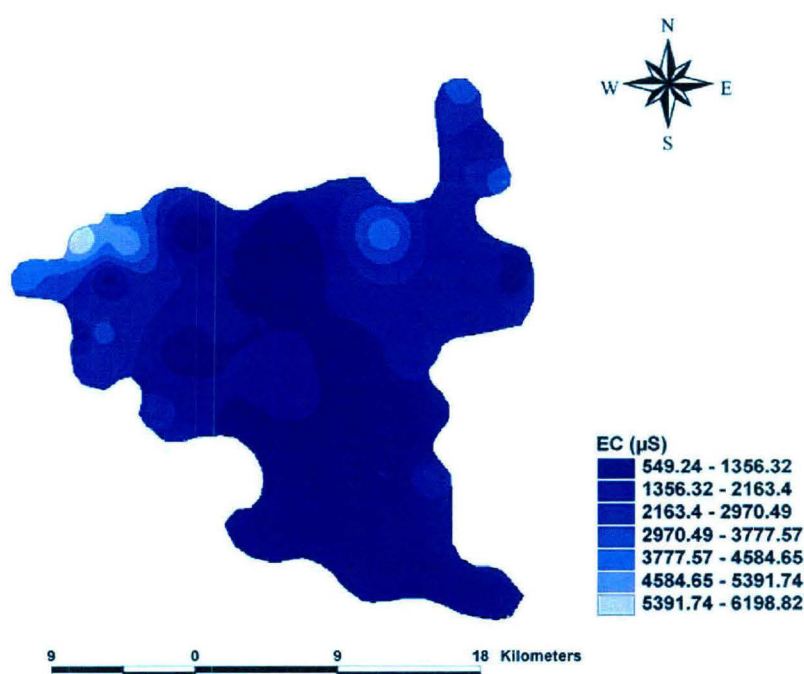


Fig 5.70 Spatial distribution of TDS in the Study Area

5.14.3 Electrical Conductivity

Electrical conductivity (EC) ranged between 549µS/cm (Ayanagar) to 6199µS/cm (Indirapuri market). The mean value was 2014.08µS/cm. The recommended value for EC by WHO are 250µS/cm and it was observed that all the samples had higher EC values. All groundwater contains natural dissolved minerals derived from rocks and soils. The high electrical conductivity at Kharkhari Nahar is mainly used for the agricultural practices. Their high EC values suggest high mineralization. This could be supplemented by the fact that the source for groundwater for all these locations could arise from the same aquifer. The ease with which electrical current passes through water is proportional to the salt

concentration in the water, therefore, the higher the EC, the greater the salt concentration. Electrical Conductivity is an indirect measure of soil salinity. All groundwater contains natural dissolved minerals derived from the soils and rocks. The total amount of dissolved solids in groundwater can be estimated by measuring the electrical conductivity of the water, and this is often used as a rough indication of natural groundwater quality. The higher this measurement, the more brackish or salty the water will taste. EC determines the amount of salts present in water. If the total quantity of salts in the irrigation water is high enough then the availability of water to the crops is decreased and crop yield are affected. Based upon the total dissolved salt (mg/L), the waters are classified as:

- Fresh < 500
- Marginal 500-1500
- Brackish 1500-5000
- Saline >5000
- Brine 35000
- Bitter >350000

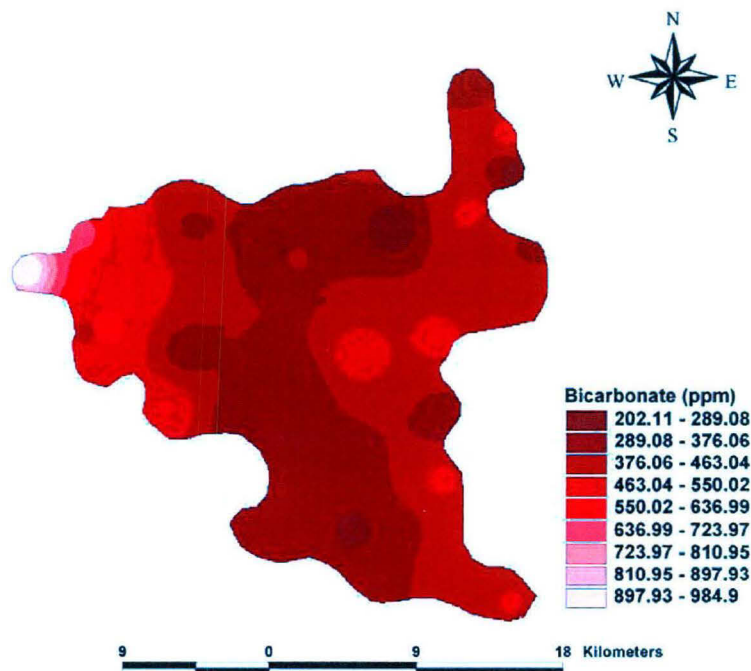


Fig.5.71 Spatial distribution of Bicarbonate in the Study Area

5.14.4 Bicarbonate

Bicarbonate concentration varies from 215mg/l at Indirapuri market to 985mg/l at Kair with average at 430.91mg/l. Dissolution of carbonates and reaction of silicates with carbonic acid accounts for the

addition of HCO_3 to the groundwater. In almost all natural waters the alkalinity is produced by dissolved carbon dioxide species. The principal source of carbon dioxide species that produce alkalinity in surface or groundwater is the CO_2 gas fraction of the atmosphere, or the atmospheric gases present in the soil or in unsaturated zone lying between the surface of land and the water table. High levels of HCO_3 in the groundwater are due to carbonate concentrations in the Delhi lithology. However, seasonal and lithological variations in major ions, such as HCO_3 , are significant, indicating that more than a single mechanism, such as carbonate or silicate equilibria, regulates composition of Delhi groundwater. Alkalinity of water is the measure of its capacity for neutralization. Bicarbonate represents the major sources of alkalinity. Bicarbonate is slightly higher in the post-monsoon period indicating the contribution from carbonate weathering process. There was a slight variation in seasonal and spatial distribution and are very significant at certain locations, HCO_3^- was high due to contribution from carbonate lithology.

5.14.5 Chloride

Hard rock has the poor hydraulic conductivity may be responsible for high chloride concentration in water due to blockage of the lineament opening by clay deposition. The anthropogenic source of the chloride includes fertilizer, road salt, human and animal waste and industrial waste. The concentration of chloride ranged from 25ppm at Sanjayvan check dam to 1640 ppm at Jharoda Kalan. The average value is 421ppm. At maximum places the chloride concentration is within the permissible limit of the Indian standards 1991. At some places a higher value was observed such as Dhirpur Pz (1119ppm), ISBT (Kashmiri Gate) (1056ppm), Dichaon Kalan (1320ppm). The high concentration of chloride is due to high mineralization. An increase in chloride concentration at groundwater indicates that chloride may be diluted at surface due to the recharge to older alluvium and /or chloride may up where in groundwater from bedrock below the alluvium. The average value of chloride is higher in the study area, which is perhaps due to the rising water table in the post-monsoon periods which dissolves more salts from the soils (Ramesam 1982; Ballukraya and Ravi 1999). The chloride concentrations were found higher in the area covered with sand dunes, especially the western and northern parts of the study area. High chloride weathering of ridge material also contributed to the salinity problem in the area. In the sand dunes, rainwater may react with the evaporate deposits to enhance the topsoil with Cl, HCO_3 and Na (Subramanian and Saxena 1983). Besides these, anthropogenic sources such as domestic waste-water and industrial discharge also have an impact on groundwater quality. The large lateral variations of chloride concentration indicate recharge and discharge zones of lateral flow regime. Local recharge to the unconfined aquifer is more dominant than recharge from lateral flow (Datta and

Tyagi 1996). The chloride ion is also considered to be conservative in groundwater of the Delhi Area (Datta et al. 1996). Groundwater is under-saturated with respect to NaCl. Therefore, physical processes such as mixing with another aquifer of different Cl concentration and change in evaporation rate during recharge either spatially or temporally may cause the changes in the chloride content of groundwater.

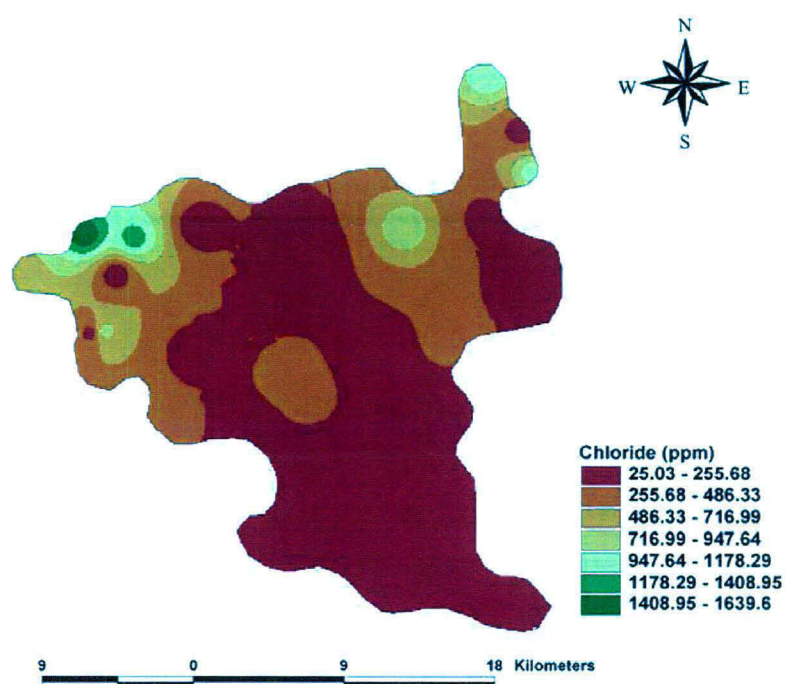


Fig 5.72 Spatial distribution of Chloride in the Study Area

Probable effect at high chloride concentration may be injurious to some people suffering from diseases of heart or kidneys. Taste, indigestion, corrosion and palatability are affected. Chloride distribution in groundwater around Delhi indicates that, irrespective of lithology, there are pockets of high chloride zones in the groundwater of Delhi.

5.14.6 Fluoride

The concentration of fluoride varied between the 0.2ppm at Rajokri to 4.92ppm India Gate. Average fluoride concentration 0.967ppm. In most part of the study area it is in permissible limit 1.5mg/l. The sources for the fluoride consist of fluorite, which occurs in pegmatitic terrain of Precambrian age. Due to similar ionic charge and size ratio substitution of fluoride for hydroxide ions at mineral surfaces is an obvious possibility. Probable health impacts of high fluoride concentration reduces dental caries, very high concentration may causes crippling and skeletal fluorosis. High fluoride concentration in some parts of the study area may be due to the presence of micaceous content in the alluvial plains.

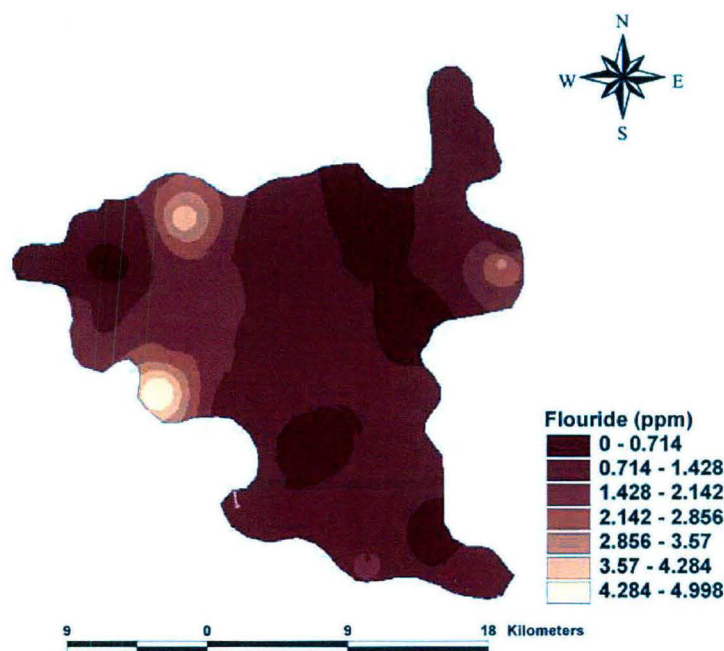


Fig 5.73 Spatial distribution of Fluoride in the Study Area

High fluoride concentration in some parts of the study area may be due to the presence of micaceous content in the alluvial plains.

5.14.7 Nitrate

In the study area nitrate values are in the range of 0.5ppm at Indirapuri market to 138ppm at Chattarpur and an average 35.25ppm. Most of the part of the study area has nitrate within the desirable limit of Indian Standards and WHO standards 50ppm. The excess of nitrate may be attributed to drainage from nearby pipeline leakage in sewer lines. The excess of amount of nitrogen fertilizer used on agricultural land may also result in increase in nitrate in groundwater. The common sources of nitrate in water are the leachates from the landfill sites, local agricultural fields, domestic sewage etc. However, because of laminar flow condition and due to difference in specific gravity and viscosity between nitrate slugs and the natural freshwater, some diffusion is bound to occur. But no such natural sources are reported to exist in the area for NO_3 (Handa 1988). Even then, the average value of NO_3 is close to the permissible limit for drinking water, which is an alarming situation and shows the anthropogenic impact on the groundwater quality. In order to investigate fertilizer input as a probable common source of potassium and nitrate to the groundwater as was thought in the earlier studies (Datta et al. 1997), a cross plot between NO_3 and K was examined, instead of relying on their weak correlation coefficient. It was observed that an excess nitrate above a median value is normally associated with a low potassium content (<20ppm). This indicates a different source for the nitrate and

not a common source as it was thought earlier. The excess of nitrate present in groundwater is a serious health hazard causing infant methaemoglobinemia (bluebaby syndrome), gastric cancer.

And adversely effects central nervous system and cardiovascular system. Dissolved nitrogen in form of NO_3 is the most common contaminant of groundwater. High levels of nitrate accelerate the eutrophication of surface waters. Nitrates consumed over a very long period of time by human being may result in the formation of nitroso or nitro-amino compounds, which may be carcinogenic. The major natural and anthropogenic sources of nitrates are:

- Atmospheric precipitation
- Land fills
- Industrial waste
- Sewage and animal waste
- Agricultural sources

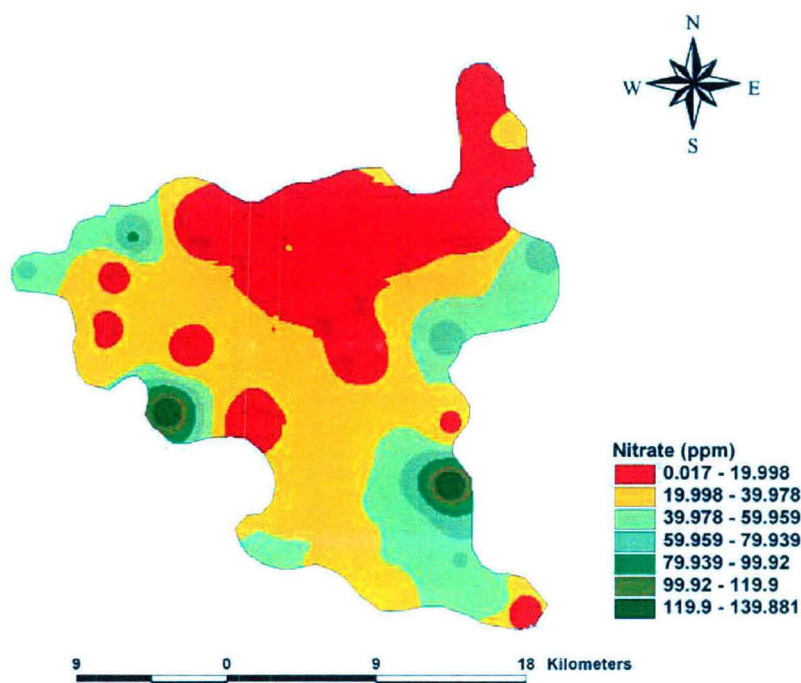


Fig 5.74 Spatial distribution of Nitrate in the Study Area

The nitrate pollution in the study area is attributed mainly due to

1. Percolation of waste water from unlined surface drains carrying sewage
2. Land fills and street drainage
3. Insanity conditions, waste water stagnation at Jhuggi Jhopri clusters and unauthorised human settlement

4. Agricultural sources

The huge amount of garbage, solid waste and sewage sludge are being generated in the area due to rapid urbanization, population increase and intensification and expansion of urban activities.

5.14.8 Sulphate

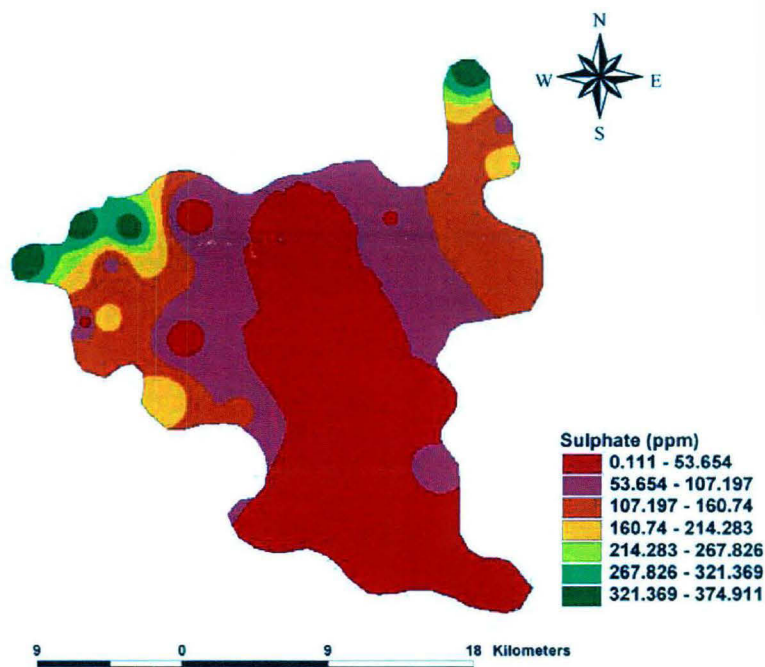


Fig 5.75 Spatial distribution of Nitrate in the Study Area

Sulphate concentration ranges from 0.11ppm at Palam road to maximum 375ppm at Jharoda Kalan. The average concentration of sulphate in the study area is 91.50ppm. Most of the area is under permissible limit 940ppm of Indian Standards. Low concentration of sulphate due to leaching out along with iron in cation exchange and the sulphate may be lost by reduction as water over through aquifers. The variation indicates the constituents of leaching and dissolved solids from sand dunes/alluvium. Its high concentration in groundwater causes gastrointestinal irritation.

5.14.9 Silica

The concentration of silica varies from 12mg/l at Indirapuri market to 37 m/l at IGNOU. The average value of silica is 24.96 mg/l in the study area. Silica occurs as silicic acid (H_4SiO_4) in natural water at $pH < 9$. The average value of dissolved silica is found to be higher than the prescribed value for groundwater, i.e. 17 mg/l (Davis 1986), which is due to the silicate weathering in the study area.

Dolomite is the stable assemblage; surface waters in the Delhi region also fall in the same field (Subramanian, 1979). In Delhi, dolomitic concretions are common in the aquifers comprising of alluvium. These are precipitated from supersaturated groundwater at aquifer interfaces. Since the groundwater samples are supersaturated with respect to dolomite, no lithological or seasonal controls are obvious. Minerals such as kaolinite, illite and chlorite are common in aquifer rocks (Subramanian, 1979). Though the water composition also falls in the gibbsite field, it is rarely present due to the high silica levels (34ppm) in the groundwater. The concentration of silica in groundwater samples did show some seasonal fluctuations. The existence of alkaline environment enhances the solubility of silica and it reveals secondary impact of silicate weathering.

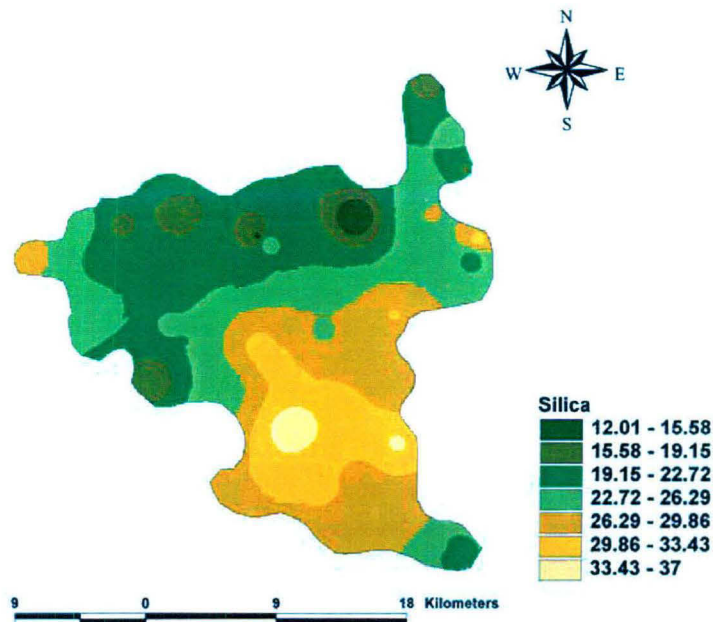


Fig 5.76 Spatial distribution of Silica in the Study Area

5.14.10 Sodium

The sodium concentration is in the range at 45ppm at Ayanagar to 856ppm with average at 232.15ppm in the study area. In some places the concentration of sodium exceeds the WHO standards (200ppm).

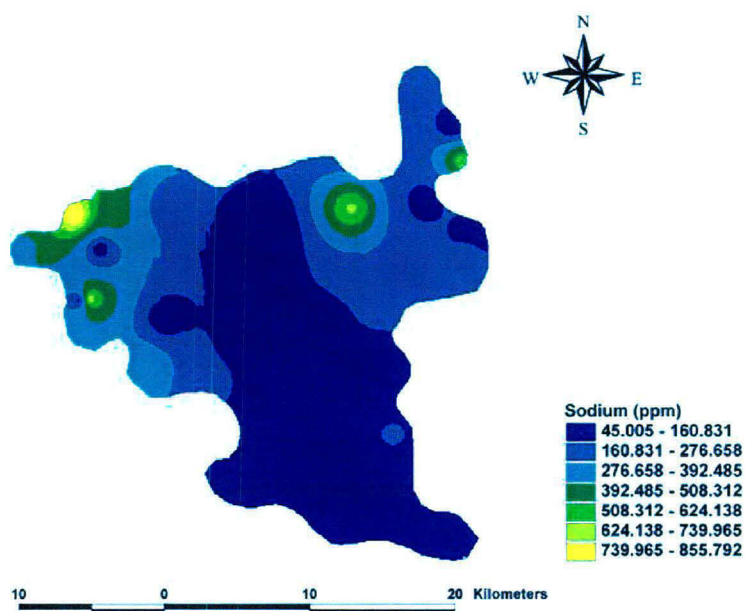


Fig 5.77 Spatial distribution of Sodium in the Study Area

Groundwater contains some sodium because most rocks and soil contains sodium compounds from which sodium is easily dissolved. The most common source of increased concentration of sodium in groundwater is the feldspars and other mafic minerals have undergone chemical alteration to form clay minerals.



Albite

Kaolinite

-Erosion at salt deposits and sodium bearing rock minerals.

-Irrigation and precipitation induced leaching through soils high in sodium.

-Infiltration of leachate from landfills or industrial sites.

The high concentration of sodium may be due to Base Exchange phenomenon.

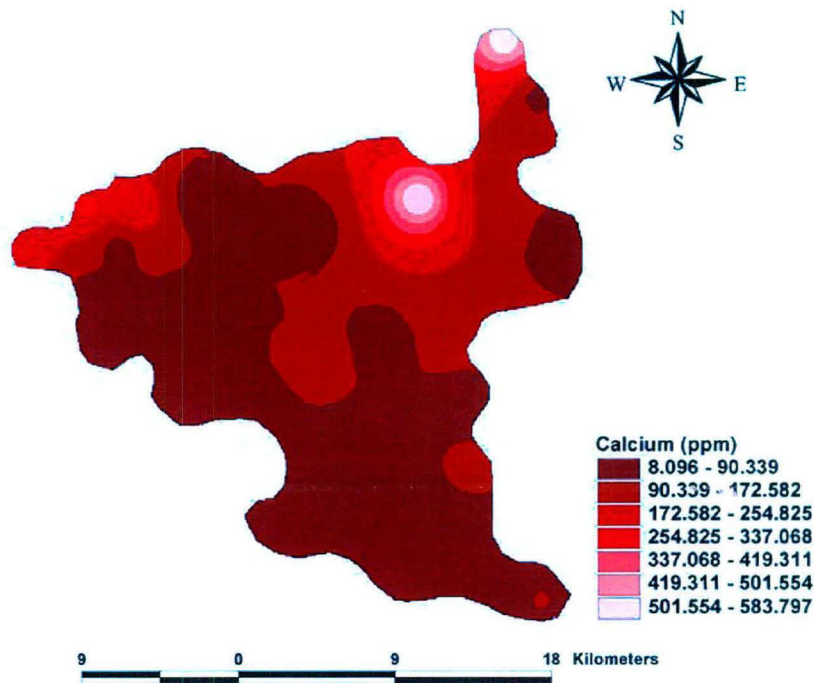


Fig 5.78 Spatial distribution of Calcium in the Study Area

5.14.11 Calcium

The calcium concentration varies from 8.12 ppm at Tilangpur Kotla to 584 ppm at Indirapuri market with an average of 115.06 ppm. In most part of the study area i.e. southwest Delhi, Gurgaon, South Delhi, West Delhi and part of North Delhi, the concentration of calcium is within the permissible limit of Indian Standards 75 ppm and WHO standards 75 ppm. High concentration of calcium causes encrustation in water supply system. While insufficiency causes a severe type of rickets, excess leads to concentration in the body organs such as kidney in the form of stones in bladder and cause irritation in urinary passage. It is essential for nervous and muscular system, cardiac function and in coagulation of blood.

5.14.12 Potassium

The concentration of potassium varied from 1ppm at Hauz Khas and SanjayVan to 400ppm at Kair. The average value of potassium is 27.59ppm. The potassium plays vital role in plant metabolism and its deficiency causes low protein , higher amino acids concentration and also disturbs carbohydrate metabolism .The main source of potassium in groundwater include:

- rainwater
- weathering of potash silicate minerals
- use of potash fertilizers
- use of surface water for irrigation

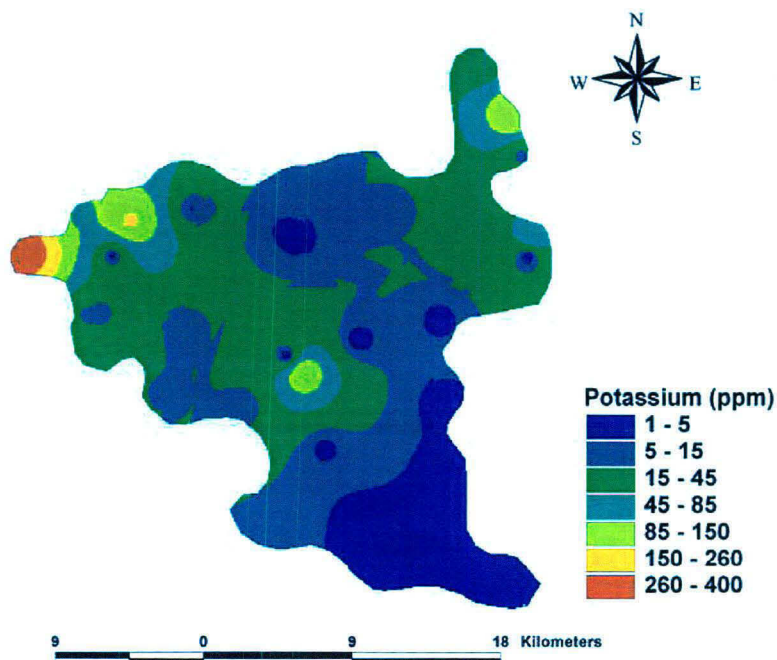


Fig 5.79 Spatial distribution of Potassium in the Study Area

Potassium is abundant in granitic/schistose/ gneissose country rocks.

Potassium is extensively used in fertilizers, dye industries and in chemical industries in form of hydroxide, iodide, cyanide, sulphate and chromates. The Bureau of Indian Standards (BSI) has not included potassium in drinking water standards. However the European Economic Community (1980) prescribed guideline level of potassium at 10ppm in drinking water.

5.14.13 Magnesium

The concentration of magnesium varied from 12ppm at Tilangpur Kotla to 276ppm at Indirapuri market. The average value of magnesium is 66.45ppm. Concentration of magnesium in the study area falls within the permissible limit.

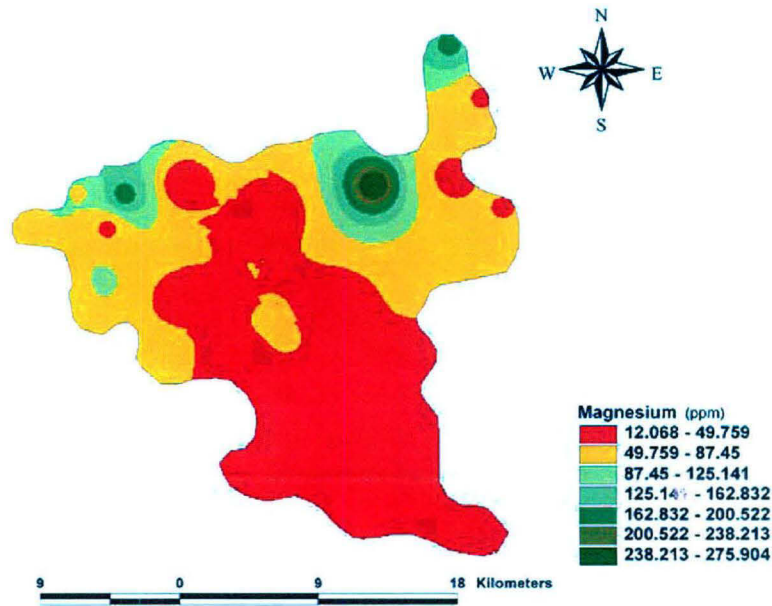


Fig 5.80 Spatial distribution of Magnesium in the Study Area

5.14.14 Sodium Absorption Ratio

The SAR varies from 1 at Ayanagar to 18 at Dhausa. The average value of SAR is 4.55. The total dissolved solids content measured in terms of specific electrical conductance gives the salinity hazard of irrigation water. Besides the salinity hazard excessive sodium concentration in water renders it unsuitable for soils containing exchangeable Ca^{2+} and Mg^{2+} ions. The sodium hazard in irrigated water is expressed by determining the sodium absorption ratio (SAR) by the relation

$$\text{SAR} = \text{Na} / \sqrt{(\text{Ca} + \text{Mg}/2)}$$

The SAR determines if the soil is going to experience infiltration problems due to an excess of sodium in relation to calcium and magnesium. High SAR waters can cause severe permeability problems. Meeting the crop water requirement under these conditions may become extremely difficult. For SAR values greater than 6 to 9, the irrigation water is expected to cause permeability problem on the shrinking swelling types of soil. Permeability refers to the ease with which water enters and percolates down through the soil and is usually measured and reported as infiltration rate. An infiltration rate of 3 mm/hour is considered low while a rate above 12 mm/hour is relatively high. At a given SAR, infiltration rate increases with increasing salinity of water.

Based on EC, SAR and RSC groundwater are grouped for irrigation as follows:

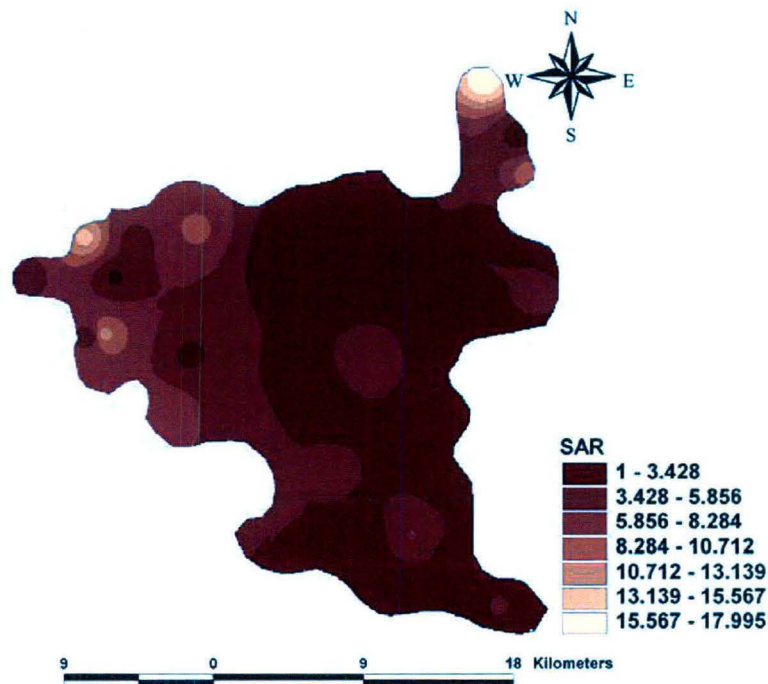


Fig 5.81 Spatial distribution of SAR in the Study Area

If the percentage of Na^+ to Ca^{2+} Mg^{2+} , Na^+ is considerably high in irrigated waters, soil containing exchangeable calcium and magnesium takes up sodium and in exchange for calcium and magnesium causing deflocculation and impairment of filth and permeability of soils.

Water Quality	EC_{iw} (dS/m)	SAR_{iw}	RSC (meq L-1)
A. Good	<2	<10	<2.5
B. Saline			
-Marginally saline	2-4	<10	<2.5
-Saline	>4	<10	<2.5
-High SAR saline	>4	>10	<2.5
C. Alkali waters			
-Marginally alkali	<4	<10	2.5-4.0
-Alkali	<4	<10	>4.0
-Highly alkali	Variable	>10	>4.0

Table 5.28 A few part of study area in north and south west falls in very high salinity category.

5.15 STATISTICAL ANALYSIS

The multivariate and regionalized character of geochemical variables makes them an interesting candidate for numerical analysis using both geostatistics (Matheron, 1970; Journel and Huijbregts, 1978) and data analysis methods (Benzecri, 1973; Davis, 1987) in order to identify geochemical anomalies.

Correlation coefficients measure of the strength of association between two continuous variables. Of interest is whether one variable generally increases as the second increases, whether it decreases as the second increases, or whether their patterns of variation are totally unrelated. Correlation measures observed co-variation. It does not provide evidence for causal relationship between the two variables. One may cause the other, as precipitation causes runoff. They may also be correlated because both share the same cause, such as two solutes measured at a variety of times or a variety of locations. (Both are caused by variations in the source of the water). Evidence for causation must come from outside the statistical analysis from the knowledge of the processes involved. Measures of correlation (here designated in general as ρ) have the characteristic of being dimensionless and scaled to lie in the range $-1 \leq \rho \leq 1$. When there is no correlation between two variables, $\rho = 0$. When one variable increases as the second increases, ρ is positive. When they vary in opposite directions, ρ is negative. The significance of the correlation is evaluated using a hypothesis test:

$$H_0: \rho = 0 \text{ versus } H_1: \rho \neq 0.$$

When one variable is a measure of time or location, correlation becomes a test for temporal or spatial trend.

5.15.1 PRINCIPAL COMPONENT ANALYSIS

This is the most widely used method of multivariate data analysis owing to the simplicity of its algebra and its straightforward interpretation. A linear transformation is defined which transforms a set of correlated variables into uncorrelated factors. These orthogonal factors can be shown to extract successively a maximal part of the local variance of the variables. The basic problem solved by principal component analysis is to transform a set of correlated variables into uncorrelated quantities, which could be interpreted in an ideal, multi-Gaussian, context as independent factors underlying the phenomenon (Wackernagel, 1995).

Principal component analysis seems an appropriate method for establishing element associations. When this technique is applied to a geochemical data set, it is possible to obtain several components,

as linear functions of the original chemical elements, which identify subsets of correlated variables. Some of these components can be used for studying a specific group of variables, giving conclusions about an association of elements, which is geochemically more significant than the study of individual variables. In this way, we can use one of the principal components for identifying geochemical anomalies by means of a geostatistical approach. Experimental and theoretical variograms of the selected component are computed. Then, by applying factorial kriging analysis, it is possible to identify geochemical anomalies of this component, which are representative of a related group of elements. In this sense, the results become more important than isolated anomalies of individual elements.

5.15.2 CORRELATION ANALYSIS

The water samples collected from the study area were analyzed for fourteen water quality parameters. The different variables obtained through analysis were subjected to correlation analysis and a correlation matrix was obtained as shown in table 5.29. A correlation analysis is a bivariate method applied to describe the degree of relation between two hydrochemical parameters. The result of the correlation analysis is considered in the subsequent interpretation. A high correlation coefficient (near 1 or 1) means a good relationship between two variables and its value around zero means no relationship between them at a significant level of $p < 0.05$. More precisely, it can be said that parameters showing $r > 0.7$ are considered to be strongly correlated whereas r between 0.5 and 0.7 shows moderate correlation. The correlation coefficient of 0.7 and above was considered strongly correlated while the correlation coefficient values from 0.5 to 0.7 were considered moderately correlated. It can be observed from the table that a strong correlation exists between electrical conductivity (EC) and total hardness (TH), EC-chloride (Cl⁻), EC-sulphate (SO₄²⁻), EC-magnesium (Mg) and EC-sodium (Na). Similarly a strong correlation existed between TH-Cl⁻, TH-calcium (Ca), TH-Mg, Cl⁻-SO₄²⁻, Cl⁻-Ca, Cl⁻-Mg, Cl⁻-Na, Ca-Mg whereas a moderate correlation was observed between bicarbonate (HCO₃⁻)-SO₄²⁻, HCO₃⁻-K (potassium), SO₄²⁻-Ca, SO₄²⁻-Mg, SO₄²⁻-Na, SO₄²⁻-K, Ca-Na, Mg-Na, The soils of Delhi and the alluvium have significant amounts of illite, which may fix K from water. Hence groundwater in Delhi at Vasant Kunj, Badarpur, Dwarka and Inderpuri has very low K⁺ values (Subramanian and Saxena 1983). Sodium ion shows higher concentrations because it behaves like a conservative element as it is not used up in biological process, and also as a non-conservative element as it gets fixed in clay mineral formation by ion exchange (Subramanian and Saxena 1983). Ca²⁺ and Mg²⁺ show good correlation among themselves and also with Na, indicating a same source. In this study, the relationship between various elements has been studied using Spearman

RESULT AND DISSCUSSION

rank coefficient which is based on the ranking of the data and not their absolute values. The resultant matrix shows up the negative correlation of pH with most of the variables.

	pH	EC	TH	HCO ₃	Cl	SO ₄	NO ₃	F	PO ₄	Ca	Mg	Na	K	SiO ₂
pH	1.000													
EC	-0.386	1.000												
TH	-0.452	0.795	1.000											
HCO ₃	-0.297	0.376	0.106	1.000										
Cl	-0.341	0.970	0.827	0.224	1.000									
SO ₄	-0.381	0.820	0.678	0.499	0.810	1.000								
NO ₃	-0.170	0.152	0.000	0.311	0.047	0.220	1.000							
F	0.170	-0.093	-0.222	0.074	-0.119	0.073	0.255	1.000						
PO ₄	-0.191	-0.038	0.003	0.159	-0.065	0.047	-0.149	-0.035	1.000					
Ca	-0.448	0.682	0.959	0.004	0.719	0.519	-0.099	-0.290	0.016	1.000				
Mg	-0.360	0.750	0.918	0.020	0.739	0.537	0.015	-0.142	-0.042	0.861	1.000			
Na	-0.234	0.912	0.604	0.329	0.867	0.671	0.092	0.025	-0.063	0.525	0.636	1.000		
K	-0.280	0.449	0.323	0.627	0.345	0.549	0.188	-0.072	-0.013	0.232	0.232	0.220	1.000	
SiO ₂	0.127	-0.332	-0.402	0.115	-0.337	-0.269	0.220	-0.369	0.039	-0.377	-0.503	-0.368	0.108	1.000

Table 5.29 Correlation matrix of water quality parameters

RESULT AND DISSCUSSION

	Band 1	Band 2	Band 3	NDVI	Ph	EC	TH	HCO ₃	Cl	SO ₄	NO ₃	F	PO ₄	Ca	Mg	Na	K	SiO ₂
Band 1	1.000	-0.353	-0.245	0.491	-0.001	0.236	0.103	0.088	0.236	0.205	0.219	0.242	-0.272	-0.045	0.175	0.126	0.188	-0.203
Band 2	-0.353	1.000	0.951	-0.899	0.011	0.284	0.258	0.148	0.315	0.361	-0.227	-0.049	-0.003	0.246	0.176	0.311	0.119	-0.112
Band 3	-0.245	0.951	1.000	-0.732	-0.003	0.358	0.312	0.187	0.380	0.491	-0.232	0.029	0.008	0.258	0.241	0.348	0.212	-0.259
NDVI	0.491	-0.899	-0.732	1.000	-0.061	-0.098	-0.105	-0.061	-0.123	-0.081	0.191	0.130	0.017	-0.151	-0.046	-0.174	0.013	-0.100
pH	-0.001	0.011	-0.003	-0.061	1.000	-0.386	-0.452	-0.297	-0.341	-0.381	-0.170	0.170	-0.191	-0.448	-0.360	-0.234	-0.280	0.127
EC	0.236	0.284	0.358	-0.098	-0.386	1.000	0.795	0.376	0.970	0.820	0.152	-0.093	-0.038	0.682	0.750	0.912	0.449	-0.332
TH	0.103	0.258	0.312	-0.105	-0.452	0.795	1.000	0.106	0.827	0.678	0.000	-0.222	0.003	0.959	0.918	0.604	0.323	-0.402
HCO ₃	0.088	0.148	0.187	-0.061	-0.297	0.376	0.106	1.000	0.224	0.499	0.311	0.074	0.159	0.004	0.020	0.329	0.627	0.115
Cl	0.236	0.315	0.380	-0.123	-0.341	0.970	0.827	0.224	1.000	0.810	0.047	-0.119	-0.065	0.719	0.739	0.867	0.345	-0.337
SO ₄	0.205	0.361	0.491	-0.081	-0.381	0.820	0.678	0.499	0.810	1.000	0.220	0.073	0.047	0.519	0.537	0.671	0.549	-0.269
NO ₃	0.219	-0.227	-0.232	0.191	-0.170	0.152	0.000	0.311	0.047	0.220	1.000	0.255	-0.149	-0.099	0.015	0.092	0.188	0.220
F	0.242	-0.049	0.029	0.130	0.170	-0.093	-0.222	0.074	-0.119	0.073	0.255	1.000	-0.035	-0.290	-0.142	0.025	-0.072	-0.369
PO ₄	-0.272	-0.003	0.008	0.017	-0.191	-0.038	0.003	0.159	-0.065	0.047	-0.149	-0.035	1.000	0.016	-0.042	-0.063	-0.013	0.039
Ca	-0.045	0.246	0.258	-0.151	-0.448	0.682	0.959	0.004	0.719	0.519	-0.099	-0.290	0.016	1.000	0.861	0.525	0.232	-0.377
Mg	0.175	0.176	0.241	-0.046	-0.360	0.750	0.918	0.020	0.739	0.537	0.015	-0.142	-0.042	0.861	1.000	0.636	0.232	-0.503
Na	0.126	0.311	0.348	-0.174	-0.234	0.912	0.604	0.329	0.867	0.671	0.092	0.025	-0.063	0.525	0.636	1.000	0.220	-0.368
K	0.188	0.119	0.212	0.013	-0.280	0.449	0.323	0.627	0.345	0.549	0.188	-0.072	-0.013	0.232	0.232	0.220	1.000	0.108
SiO ₂	-0.203	-0.112	-0.259	-0.100	0.127	-0.332	-0.402	0.115	-0.337	-0.269	0.220	-0.369	0.039	-0.377	-0.503	-0.368	0.108	1.000

Table 5.30 Correlation matrix of water quality parameters together with spectral reflectance of various bands of satellite image and NDVI values

RESULT AND DISSCUSSION

In the present study, the factor analysis was used as an alternative tool for corroboration of the concept obtained from molar concentrations. Factor analyses serve for basic, independent dimensions of variables. With the help of linear combinations, an originally large number of variables are reduced to a few factors. These factors can be interpreted in terms of new variables. Factor analysis aims to explain observed relation between numerous variables in term of simpler relations. It is also a way of classifying manifestation of variables (Cattel 1965). Factor analysis is used here as a numerical method of discovering variables that are more important than others for representing parameter variation and identifying hydrochemical processes. The factor model used is expressed as:

$$X_j = \sum_{r=1}^p a_{jr} f_r \varepsilon_j$$

where f_r are the r^{th} common factors, p is the specified number of factors, ' ε_j ' is the random variation unique to the original variable X_j , a_{jr} is the loading of the j^{th} variate on the r^{th} factor. It corresponds to the loading or weights on principal components.

The principal component approach starts by extracting Eigenvalues and Eigenvectors of the correlation matrix and then discarding the less important of these (Davis 1986). Eigenvectors are then transformed to the factors of the data set. The number of variables retained in the factors or communalities is obtained by squaring the elements in the factor matrix and summing the total within each variable. The magnitude of communalities is dependent upon the number of factors retained. This type of analysis is called R-mode factor analysis. Varimax rotation was then adopted. The results of the factor analysis are summarized in Table 5.32.

RESULT AND DISSCUSSION

Component	Initial Eigen values			Extraction Sums of Squared Loadings			Rotation Sums of Squared Loadings		
	Total	% of Variance	Cumulative %	Total	% of Variance	Cumulative %	Total	% of Variance	Cumulative %
Pixel 1	6.59	36.61	36.61	6.59	36.61	36.61	5.918	32.878	32.878
Pixel 2	2.905	16.141	52.752	2.905	16.141	52.752	3.094	17.19	50.068
Pixel 3	2.055	11.416	64.168	2.055	11.416	64.168	2.466	13.698	63.766
NDVI	1.686	9.369	73.537	1.686	9.369	73.537	1.601	8.893	72.659
pH	1.189	6.604	80.141	1.189	6.604	80.141	1.347	7.482	80.141
EC	0.862	4.787	84.928						
TH	0.74	4.111	89.039						
HCO ₃	0.526	2.92	91.959						
Cl	0.459	2.547	94.506						
SO ₄	0.327	1.818	96.325						
NO ₃	0.266	1.479	97.804						
F	0.2	1.114	98.917						
PO ₄	0.099	0.552	99.469						
Ca	0.057	0.318	99.787						
Mg	0.033	0.183	99.97						
Na	0.003	0.018	99.988						
K	0.002	0.01	99.998						
SiO ₂	0	0.002	100						

Table 5.31 Extraction Method: Principal Component Analysis.

RESULT AND DISSCUSSION

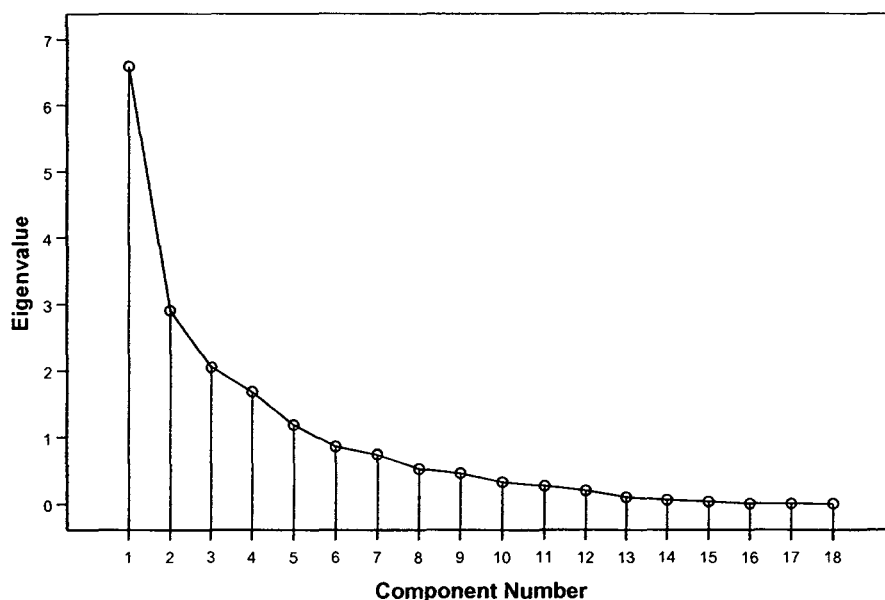


Fig 5.82. Scree Plot

Principal component analysis was performed using varimax rotation method with Kaiser normalization. When Principal component analysis was performed on water quality parameters including NDVI and various bands of satellite image it was found that five factors were sufficient to explain 80% of the data. Factor 1 explained 32.87% of the data and higher positive loading was observed for Electrical conductivity, total hardness, chloride, sulphate, calcium, magnesium, sodium and higher negative loading was observed for pH and silica. Factor 2 explained about 17.19% of data and higher positive loading was observed for spectral reflectance of band 1 and band 2 while higher negative loading was observed for band 3 and NDVI. Factor 3 explained 13.69% of the data and showed higher positive loading for bicarbonate, sulphate, nitrate and potassium. Factor 4 and factor 5 explained 8.89% and 7.48% of total data respectively with factor 4 showing higher positive loading for fluoride and negative loading for silica while factor 5 showed higher positive loading for spectral reflectance of band 1 and pH while negative loading for phosphate.

The concentration of Mn for all sampling seasons is higher in the eastern part of the study area which may be attributed to anthropogenic activities such as waste discharge from industrial units. The lower concentration of Ni and Cu in surface water as compared to

RESULT AND DISSCUSSION

groundwater favors the point that there could be a decrease in trace element concentration in the river (Durum and Haffty, 1963). The Cu concentration in groundwater is higher in the western part of study area, but it is well within the WHO standards for drinking water. The groundwater samples show relatively higher concentration of Zn especially in the southern and western parts, which may be attributed to agricultural field runoff.

Parameters	Factor 1	Factor 2	Factor 3	Factor 4	Factor 5
Pixel 1	0.206	-0.502	0.231	0.356	0.422
Pixel 2	0.194	0.964	0.042	0.028	0.016
Pixel 3	0.269	0.894	0.086	0.174	-0.004
NDVI	-0.019	-0.919	0.038	0.168	-0.033
pH	-0.453	0.163	-0.281	0.168	0.476
EC	0.877	0.122	0.368	0.072	0.067
TH	0.954	0.066	0.030	-0.099	-0.072
HCO ₃	0.071	0.127	0.851	0.069	-0.217
Cl	0.899	0.149	0.234	0.053	0.108
SO ₄	0.681	0.211	0.543	0.199	-0.048
NO ₃	-0.034	-0.295	0.599	0.064	0.214
F	-0.196	-0.039	0.120	0.879	0.055
PO ₄	-0.059	0.018	0.028	0.047	-0.885
Ca	0.901	0.080	-0.115	-0.198	-0.132
Mg	0.926	-0.009	-0.070	0.012	0.002
Na	0.747	0.206	0.255	0.199	0.108
K	0.269	0.053	0.735	-0.128	-0.033
SiO ₂	-0.510	-0.009	0.340	-0.671	0.086

Table 5.32 Extraction Method: Principal Component Analysis. Rotation Method: Varimax with Kaiser Normalization.

RESULT AND DISSCUSSION

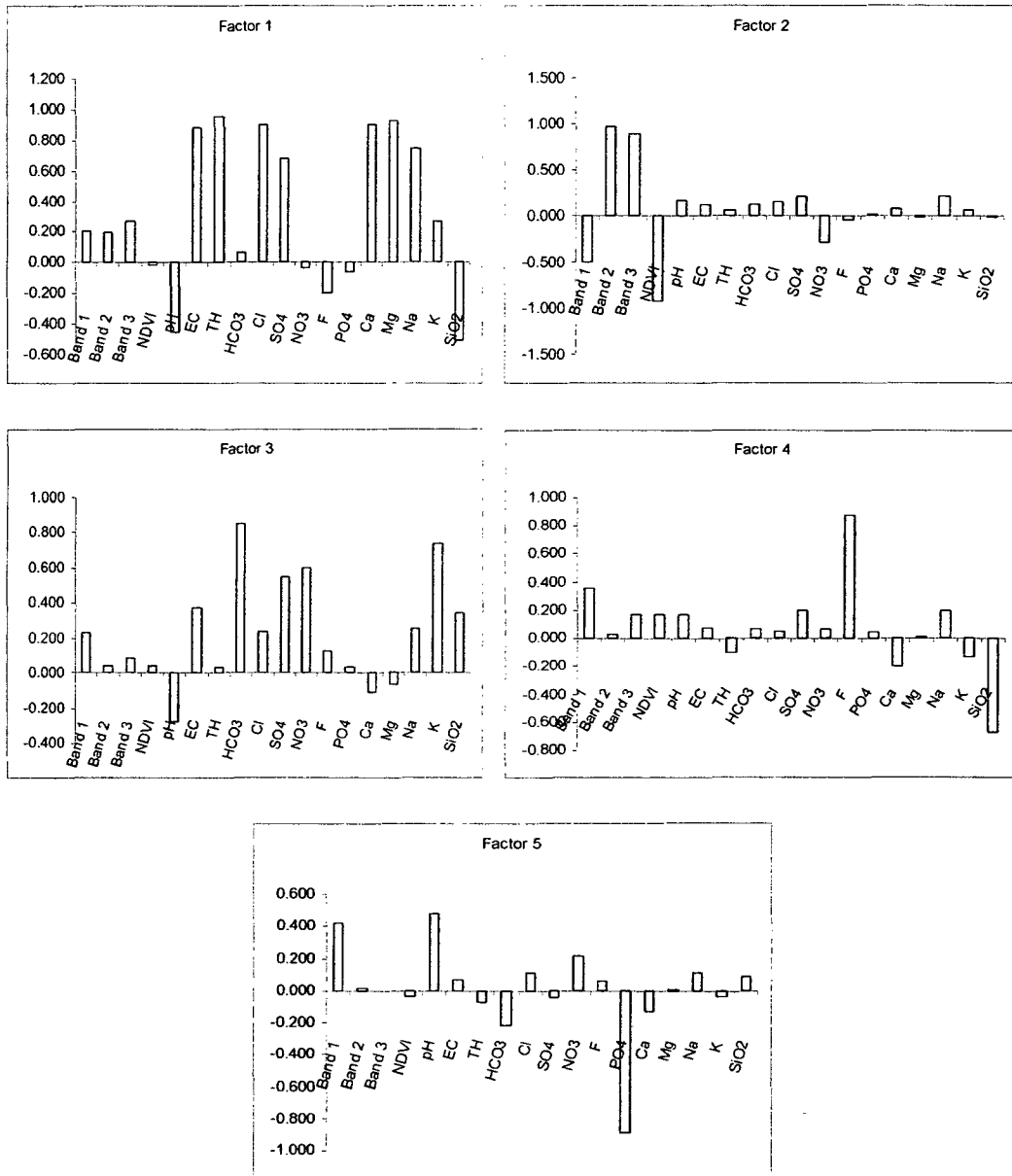


Fig 5.83 PCA Analysis: Factor loading (Component Loading for various PCA factors)

RESULT AND DISSCUSSION

	Band 1	Band 2	Band 3	NDVI	ME %	CaO %	MgO %	K2O %	TiO2 %	P2O5 (ppm)	Li	B
Site1	88	40	85	0.36048	2.1	0.6	0.2	1.3	0.04	232	138	34
Site2	94	65	101	0.22887	2.8	1.3	0.4	1.1	0.04	226	125	40
Site3	77	48	88	0.32328	2.5	0.9	0.3	1.3	0.04	236	144	36
Site4	77	42	82	0.32328	2.4	1.1	0.4	0.9	0.04	222	103	38
Site5	91	43	86	0.3333	2.7	1.3	0.7	0.7	0.04	222	101	45
Site6	81	43	86	0.31184	1.9	0.5	0.4	1	0.04	234	112	47
Site7	89	61	101	0.24604	2.4	1.1	0.4	0.9	0.04	220	110	43

	V	Zn	Sr	Nb	Ag	Sn	Sb	Ba	Ce	W	Pb	Bi	Zr
Site1	2	10	21	8	0.9	0	4	106	82	2	18	7	2
Site2	2	27	52	9	0.2	0	9	104	66	6	14	1	3
Site3	3	13	39	9	0.4	0	9	103	81	8	13	4	2
Site4	2	13	51	8	0.9	0	3	103	70	5	14	9	2
Site5	1	17	63	8	0.5	8	9	106	59	5	14	8	3
Site6	1	9	42	8	0.4	3	6	105	79	4	11	6	2
Site7	2	12	51	7	0.7	12	9	104	67	7	16	9	2

Table 5.34 Various ICP-AES parameter and NDVI, spectral reflectance at different sites in JNU

Summary and Conclusion

SUMMARY AND CONCLUSION

Chapter- VI

National Capital Region is a part of Precambrian Aravalli formation with little water availability. During pre-Mughal period the water conservation and extraction was restricted to the troughs of quartzite and pegmatites in hard rock areas. Although the study area is a grey zone according to Central Ground Water Board (CGWB). That is to say, CGWB does not recommend groundwater exploration in grey zones because of uncertainty of availability of groundwater.

The land use of National Capital Region in general and Delhi in particular has undergone under drastic change. Change in land use, population growth and seismic instability (Mukherjee.S. 2001, Mukherjee et.al. 2003) have all contributed in changing the hydrgeomorphology of NCR.

Besides water resources, the growing awareness about the mountain ranges and the alarm of environmental degradation has forced the administration of NCR to arrest the deteriorating environment. The present work might be helpful in mitigating looming ecological crisis. As has been said earlier that this work aims at hard rocks, colluvial and alluvial aggregates for exploration, exploitation and management of water resources. It required a geo-scientific database of water resources for generation of development plans for optimal use of potential resources. Although it is difficult to make all information relating to subsurface water available at one place, nevertheless the present thesis attempts to give a clear evaluation of a part of National Capital Region. To achieve above a systematic approach of understanding the terrain characteristic at a regional level and then going for detailed mapping by using geological, geophysical, drilling and analysis of drill cuttings and groundwater samples have been adopted. Remote sensing and GIS is used here which has emerged as the most optimal means for monitoring and management of water resources on global, regional and local scale. Being at higher elevation of NCR region with such condition i.e. fault zones, groundwater bearing fracture system and buried pediment plains, major part of the study area has become ideal recharge zone for better groundwater conditions. At higher elevations drainage system which follows the

SUMMARY AND CONCLUSION

structural lineament and fault zone limit the capacity to hold and retain surface runoff of the rainwater.

An approach was made by drilling in Delhi system of rocks at seven locations in a part of JNU and four locations in Research and Referral Hospital.

Information from the drilled litholog was correlated with resistivity, magnetic and attributes of NDVI from satellite data. Analysis of drilled logs and groundwater samples from different zones were done to correlate these data with remote sensing geological and geophysical information. These data along with ancillary information were analysed in Arc/GIS software for attribute data creation, derivation of secondary maps of groundwater prospects and quality zonation.

For the present investigation satellite data IRS 1C, IRS 1D (LISS III), Resourcesat and Landsat were used. For geo-referencing Survey of India toposheets and NATMO maps has been used. The data collected from different sources have been used as groundtruth information for the preparation of various thematic maps. Detailed ground truthing has been carried out in some selected points of study area. These ground truthing includes resistivity and magnetic surveys and drilling by Down the Hole Hammering (DTH) rig. This process involved following steps:

- 1) Interpretation of data available (Geophysical, Geological, Geochemical, Soil texture and Drilling) for locating suitable groundwater exploration points.
- 2) Interpretation of IRS, Resourcesat, SPOT, and Landsat data for demarcation of groundwater zone including its quality.
- 3) To identify the structural control of the area through Digital Elevation Model generated Shuttle Radar Terrain Mission (SRTM).
- 4) Interpretation of lineament and fracture system in the NCR region. (fig. 3.3, page 31)
- 5) Collection of samples for detailed geochemical and petrological analysis.
- 6) Confirmation of recently identified groundwater zone based on distinct vegetation anomaly and lineament fabrics depicted on satellite images.
- 7) Identification of possible groundwater zones based on drilling data.
- 8) Identification of groundwater quality based on NDVI attributes. In quartzites the presence of interconnected fractures develops higher moisture conditions which

SUMMARY AND CONCLUSION

support the growth of vegetation. The NDVI attributes are suggestive of groundwater qualities in these areas (Mukherjee, 2008).

Remote Sensing and GIS: - Remote Sensing has been found to be very useful in the study. These tools and techniques were useful for water resource management in following ways.

- 1) Homogenization of the data: - This enabled to bring all the old and new data on common platform and on uniform scale. This uniformity of scale is the prime need for any analysis on one common platform. In this process entire data have been organized in the common projection system, scale and on common GIS format.
- 2) Updating of information with the use of remote sensing technology, field verification and laboratory analysis. The information have been updated and correlated with each other.

Field Observation: - The interconnected fracture in Delhi quartzite has been found to have potential for groundwater exploration. Within Delhi quartzite the ferruginous variety was found to be more fracture prone together with intrusion of Pegmatites, Aplite and Quartz vein. Schistose rocks exhibit multiple fracture system.

It has been observed that from Delhi quartzite to River Yamuna there are three prominent watershed boundaries in existence. The buried pediment plains and alluvial plain boundary is demarcated by a very thick layer of fine grained sediments. Hydrogeomorphologically this boundary is not suitable for groundwater exploration.

Elemental composition (rock analysis) of the selected rock samples were analysed by ICPAES. The rock sample represents potential fracture zones encountered during groundwater exploration. The analytical data reveals the following features.

- In all the drilling sites silica content increases with depth which is suggestive of good to excellent groundwater quality at depth.
- Concentration of Al_2O_3 decreases with depth which is also suggestive of excellent groundwater quality.
- Concentration of Zr (245ppm) is found higher in upper zone (75m-80m) which reduces to bare (<20ppm) at greater depth (133m-140m) this suggests that the upper part of pegmatite might have undergone friction during faulting.(Mukherjee, 2001).

SUMMARY AND CONCLUSION

The conclusions inferred from the research work is more than eloquent i.e. it was found that wherever the lineament density were high there were also resistivity and magnetic anomaly with lower values. At all those places groundwater is available in large quantity. Higher NDVI is suggestive of higher moisture zones.

High fluoride concentration in India Gate of the study area may be due to the presence of micaceous content in the alluvial plains. The nitrate pollution in the study area is attributed mainly due to percolation of waste water from unlined surface drains carrying sewage, land fills, street drainage & agricultural sources. The concentration of silica in groundwater samples did show some seasonal fluctuations. The existence of alkaline environment enhances the solubility of silica and it reveals secondary impact of silicate weathering. In some places the concentration of sodium exceeds the WHO standards (200ppm). The most common source of increased concentration of sodium in groundwater is the feldspars and other mafic minerals have undergone chemical alteration to form clay minerals. The high concentration of sodium may be due to Base Exchange phenomenon & infiltration of leachate from landfills or industrial sites. The Cu concentration in groundwater is higher in the western part of study area, but it is well within the WHO standards for drinking water. The groundwater samples show relatively higher concentration of Zn especially in the southern and western parts, which may be attributed to agricultural field runoff. The SAR values indicate that some parts in N-E and N-W parts the water is marginally to highly saline.

The correlation as well as PCA analysis yielded that Sodium ion shows higher concentrations because it behaves like a conservative element as it is not used up in biological process, and also as a non-conservative element as it gets fixed in clay mineral formation by ion exchange. Ca^{2+} and Mg^{2+} show good correlation among themselves and also with Na, indicating same source. In this study, the relationship between various elements has been studied using Spearman rank coefficient which is based on the ranking of the data and not their absolute values. The resultant matrix shows up the negative correlation of pH with most of the variables.

Principal component analysis was performed on water quality parameters including NDVI and various bands of satellite image it was found that five factors were sufficient to explain 80% of the data.

SUMMARY AND CONCLUSION

The concentration of Mn for all sampling seasons is higher in the eastern part of the study area which may be attributed to anthropogenic activities such as waste discharge from industrial units.

Grade of metamorphism will affect the primary porosity adversely by recrystallization of the rock which will seal the existing open spaces amongst the grains. Since all the aquifers are situated at great depth, they are beyond anthropogenic perturbations. On the other hand alluvial aquifers are more prone to anthropogenic pollution as they are shallow and therefore not potable. Further, it was found that wherever there has been change in the landuse the natural recharge potential too has declined. Digital Elevation Model (DEM) could tell us about the course of water run-off and it will help in recharging the aquifer. Besides recharge from rainwater aquifers in the study area has been recharged by the drilled tube well under confined condition. In view of total area of study in JNU which is approximately 5sqkm the number of tube wells were restricted to seven based on the delineation of micro-watershed. As per the National Water Policy there should not be more than one tube well in one micro-watershed. The research work carried out in this thesis recommends that there should not be further drilling in JNU area for sustainable performance of the aquifers. Although the discharge of the tube wells are ranging between 24,475Lt/hr to 34,125Lt/hr with less than 10mts draw down in 72hrs of pumping but it is recommended that the groundwater can be pumped from the tub wells for 8Hrs then it should be allowed to recover for 5hrs. In this area most of the drilling site fractures are interconnected with high transmissivity, it has been observed that 80% recovery of draw down takes place within 1hr, if surrounding tube wells are also stopped. Remaining 20% recovery takes 4hr due to elastic nature of the aquifer. Hence it will be safer if the tube wells are not pumped together with more than 8hrs. If the above recommendations are not followed and tube wells are operated continuously then it may result in permanent decline of groundwater level.

Similar work has been done from Remote Sensing Laboratory, SES, JNU in Humanyun Tomb, IGNOU and Research and Referral Hospital areas. The result and effect is arrest of lowering down of the water level in the areas mentioned above further supports the lateral recharge hypothesis in confined aquifers.

References

REFERENCES

- Abu-Jaber NS, El Aloosy AS, Jawad Ali A (1997) Determination of aquifer susceptibility to pollution using statistical analysis. *Environ Geol* 31(1–2):92–106.
- Agarwal,C.S(1988) Hydrogeological Investigation in Bundelkhand Region using Remote Sensing Techniques, Unpublished M.Sc. Civil Engg Dissertation. University of Roorkee, Roorkee.
- Ahmad T., Khanna P. P., Chakrapani G. J. and Balakrishnan S. (1998) Geochemical characteristics of water and sediments of the Indus river, Trans-Himalaya, India: constraints on weathering and erosion. *Journal of Asian Earth Sciences*. Vol. 16, Nos. 2-3, pp. 333-346.
- APHA, 20th Edition, 1998.
- Almeddeij J. and Al-Ruwaih F. 'Periodic behavior of groundwater level fluctuations in residential areas', *Journal of Hydrology*, 328, 677-684.(Year)
- Al-Rousan, N., Cheng, P. Petrie, G., Toutin, T., Valadan Zoej, M., (1997): Automated DEM extraction and orthoimage generation from SPOT level 1B imagery. - *Photogr. Eng. Rem. Sens.* 63: 965-974.
- Arafin, M.S. and Lee, C.Y., (1985) 'A resistivity survey for ground water in perils using Offset Wenner Technique', *Karat Water Resources, Proceedings of the Ankara Antalya Symposium*, July 1985.
- Aronoff,S. (1989). *Geographic Information System: a management perspective*.WDL publication, Ottawa, Canada.
- Azeem. A(2000) Environmental Impact Analysis of Vijaywada Thermal Power Station With respect to Landuse Pattern of the Area of Vijaywada Using Remote Sensing and GIS Techniques, Unpublished PhD Thesis , JNU, N.Delhi.
- Ashley RP, Lloyd JW (1978) An example of the use of factor analysis and cluster analysis in ground water chemistry interpretation. *J Hydrol* 39:355–364
- Banks, D., Rohr- Trop, E., and Skarphagen, H., (1993), 'Groundwater resources in hard rock; Experiences from the Hvaler study, Southeastern Norway, *Memoirs of the XXIV th Congress of Iah,*' *Hydrogeology of Hard Rocks*, Oslo, 39-51.

- Banks, D., Solbjorg, M.L., and Rohr- Trop, E., (1992), 'Permeability of fracture zones in Precambrian granite, quarter.' *Journal of Engineering Geology*, 25, 377-388.
- Bening. J. and Bayor J., (2007) An improved means of groundwater exploration using a combination of geophysical methods and groundwater modeling; *Geophysical Research Abstract*, Vol.9, 00191, 2007.
- Benzecri, J.P., 1973. *L'Analyse des Donnees. Tome 1: La Taxonomie: Tome 2: L' Analyse des Correspondences.* Dunod, Paris, pp 619.
- Bhuiyan, C., 2006, Ph.D Thesis (Unpublished). Modelling of Groundwater recharge potentiality, Impacts of Aravali region, India- A GIS approach.
- Bouraoui F., Vachaud G., Li l. Z. X., Treut Le and Chen T.,1999, Evaluation of the impact of climate changes on water storage and groundwater recharge at the watershed scale; *Climate Dynamics* 15: 153-161.
- Brockelbank, D.C. & Tam, A.P., (1991): Stereo elevation determination techniques for SPOT imagery.- *Photogr. Eng. Rem. Sens.* 57: 1065- 1073
- Brown, N.N., (1994), 'Integrating structural geology with remote sensing in Hydrogeological resource evaluation and exploration,' In: *Proceedings of the 10th*
- Burley, T.M. (1961) Land use or land utilization. *Professional Geographer.* 13 (6); 18-20.
- Burrough, P. A., (1986), *Principles of Geographic Information System for Land Resources Development* (New York: Oxford University Press).
- Cartwright and Mccomas (1968). Geophysical surveys in the vicinity of sanitarylandfills in North-eastern Illinois, *Groundwater*, v.6, no.5, pp.23-30.
- Ceron JC, Jimenez-Espinosa R, Pulido-Bosch A (2000) Numerical analysis of hydrogeochemical data: a case study. *Appl Geochem* 15:1053–1067
- Chaitanya S. Agarwal and Garg,P.K (2000) *Textbook on Remote Sensing in Natural Resource Monitoring and Management.*
- Chatterjee R., Gupta B. K., Mohiddin S. K., Singh P. N., Shekhar S., and Purohit, R. (2009) Dynamic groundwater resources of National Capital Territory, Delhi: assessment, development and management options *Environmental Earth Sciences* DOI 10.1007/s12665-009-0064-y
- Chi, k. and lee, b. (1994) Extracting potential groundwater areas using remotely sensed data and geographic information system techniques .In *Proc. Regional seminar on integrated*

- applications of remote sensing and Geographic Information Systems for Land and water resource management, Bangalore, India 16-19 November 64-69.
- Chopra R. and Sharma P.K. (1993) 'Landform analysis and ground water potential in the Bist Doab area, Punjab, India', *International Journal of Remote Sensing*, Vol.14, No. 17, 3221-3229.
- Compaigne Generale de Geophysique, Master curve for electrical soundings, 2nd rev. ed., European Association Exploration Geophysicists, The Hague, Netherlands, 49 pp.1963.
- Connors-Sasowski, K., Petersen, G.W., Evans, B.M., (1992): Accuracy of SPOT digital elevation model and derivatives: Utility for Alaska's North Slope. - *Photogr. E Rem. Sens.* 58: 815-824.
- Cooke, R. U. and Doornkamp, J. C. (1974) *Geomorphology in environmental management*. Clarendon Press, Oxford, 412p.
- Central Ground Water Board (CGWB, 1999), *Status of Groundwater Quality And Pollution Aspects in NCT-Delhi*
- Central Ground Water Board (CGWB, 2005-06). *Annual Report on NCT*.
- Dahan O., Shani Y., Enzel Y., Yechieli Y. and Yakirevich A. 'Direct measurement of floodwater infiltration into shallow alluvial aquifers', *Journal of Hydrology*, no. of pages 14, model 6+.
- Davis, J.C., 1987. *Statistics and Data Analysis*. 2nd ed. Wiley, New York, pp 550.
- Degnan R. J., Moore B. R. and Mack J. T. (2001) 'Geophysical Investigations of Well Fields to Characterize Fractured- Bedrock Aquifers in Southern New Hampshire', *Water – Resources Investigaton Report 01-4183*, U.S. Department of the Interior, U.S. Geological Survey.
- Donker, N. H. W., (1992), Automatic extraction of catchment hydrologic properties from digital elevation data. *ITC Journal*, Issue No. 3, 257–265.
- Drury S. A., (1998), 'Images of the earth a guide to remote sensing', Second Edition, Oxford Science Publications.
- Drury, S. A. (1986) Remote sensing of geological structures in temperate agricultural terrain. *Geol. Mag.* 123 (2): 113-121.
- Duprat, A., (1991) *Geophysics applied to water exploration*, CGG technical series, Paris.

- Dymond, J. mapping using digital terrain models. ITC Journal, Issue No. 2, 129– 138.R,
and Harmsworth, G. R., (1994), towards automated land resource
- Dmond, J. R., Derose, R. C., and Harmsworth, G. R., (1995), Automated mapping of land
components from digital elevation data. Earth Surface Processes and Landforms, 20,
131–137.
- Ebraheem,A.M., M.W.Hamburger, E.R Bayless and N-C Krothe, (1990), Application of earth
resistivity methods to groundwater contamination at the wheat land reclamation site,
south-western Indiana: Groundwater v. 28, no. 3,p. 361-368.
- Ellyett, C.D., and Pratt, D. A., (1975), 'A review of the potential applications of remote sensing
techniques to hydrogeological studies in Australia.' Australian Water Resource Council
technical paper 13.
- Engman,E.T and Gurney, R.J(1991) Remote Sensing in Hydrology, Chapman and Hall, New
York.
- ERDAS, (1999), ERDAS Field Guide, 5th edn (Atlanta, USA: ERDAS Inc.).
- Farr, T., Kobrick, M.,(2001).The shuttle radar topography mission. Eos, Transactions of the
American Geophysical Union 81, 583 585.
- Fetter CW (1994) Applied hydrogeology, 3rd edn. Prentice Hall, New York
- Feyen L., and Gorelick M.S. (2004) 'Reliable Groundwater Management in hydroecologically
sensitive areas', Water resources Research, Vol.40, W07408, doi: 10.1029/2003
WR003003
- Faruqi.N.I, Biswas A.K and Bino.M.J (2001) Water management in Islam, United Nations
University Press New York
- Flügel, W.A., (1996): Hydrological Response Units (HRU's) as modeling entities for
hydrological river basin simulation and their methodological potential for
modelling complex environmental process systems. - Results from the Sieg
catchment., Die Erde , 1996, 127: 43-62.
- Gadgil S., Vinayachandran P. N. and Francis P. A. 'Droughts of the Indian summer monsoon:
Role of clouds over the Indian Ocean', Current Science, Vol. 85, No. 12, 1713-1719.
Year not specified

- Giardino C., Brando V. E., Dekker A. G., Strombeck N. and Candiani G (2007) 'Assessment of water quality in Lake Garda (Italy) using Hyperion', *Remote Sensing of Environment*, 109, 183-195.
- Gils H. V, Huizing, H.; Kannegieter, A. Zee, D.V.D. (1991) The evolution of the ITC system of rural land use and land cover classification (LUCC). *ITC journal* 1991-3. 163-167.
- Goetz, A.F.H. Rowan L.C. (1981) *Geological Remote Sensing Science*. 211:781-791.
- Gowd S. S. (2005) 'Assessment of groundwater quality for drinking and irrigation purposes: a case study of Peddavanka watershed, Anantapur district, Andhra Pradesh, India'. *Environmental Geology*, DOI 10.1007/s00254-005-0009-z.
- Grande JA, Gonzalez A, Beltran R, Sanchez-Rodas D (1996) Application of factor analysis to the study of contamination in the aquifer system of Ayamonte-Huelva (Spain). *Ground Water* 34(1):155–163
- Greenbaum D., (1987), 'Lineament studies in Masvingo Province,' Zimbabwe, British Geological Survey Report WC/87/7.
- Greenbaum, D. (1992). Structural influence on the occurrence of groundwater in SE Zimbabwe. In hydrology of crystalline Basement Aquifers in Africa, Wright, E.P. and Burgess, W.G. (Eds) Geological Society Special Publication no.66; 7- 85
- Griffith, D.H. & R.F. King, (1965). *Applied Geophysics for engineers and geologists*, Pergamon, Oxford, 223 pp.
- Güler C, Thyne GD, McCray JE, Turner AK (2002) Evaluation of graphical and multivariate statistical methods for classification of water chemistry data. *Hydrogeology J* 11:607–608.
- Gupta, R.P., (1991), 'Remote Sensing Geology,' Springer Verlag, Heidelberg.
- Haitjema, H.M., and Mitchell-Bruker, S., (2005), Are water tables a subdued replica of the topography. *Ground Water*, 43(6), 781-786.
- Hastings, D.A., Dunbar, P.K., (1998). Development and assessment of the global land one-km base elevation digital elevation model (GLOBE). *ISPRS Archives* 32 (4), 218–221. *International journal of Applied Earth Observation and Geoinformation*, 8, 289-302.
- Heath, R.C., (1983), *Basic Ground-Water Hydrology*, USGS Water-Supply Paper 2220.
- Helmschrot, J., (2000): Application of remote sensing data for distributed hydrological model parameterisation of large scale afforested areas in the North East Cape Province, South

- Africa). Proc. 28th Int. Symp. On Remote Sensing Of Environment, Cape Town, 27-31 March, 2000.
- Heron, A.M. (1917) Geology of north-eastern Rajputana and adjacent districts. Mem. Geol. Surv. India, 45, 25
- Hydrogeologic 'Evaluation' Phase III and IV water monitoring system and water quality report: RUST, Environment and Infrastructure Incorporation, Minnesota unpublished.
- Jaiswal R.K., Mukherjee S., Krishnamurthy J. and Saxena R. (2003) 'Role of remote sensing and GIS techniques for generation of groundwater prospect zones towards rural development –an approach', International Journal of Remote Sensing, Vol. 24, No. 5, 993-1008.
- Janardhana Raju N. (2007) 'Hydrogeochemical parameter for assessment of ground water quality in the upper Gunjanaeru river basin, Cuddapah district, Andhra Pradesh, South India', Journal of Environmental Geology, 52:1067-1074.
- Janardhana Raju N. and Reddy T. V. K. (1998) 'Fracture pattern and electrical resistivity studies for groundwater exploration', Journal of environmental Geology, 34 (2/3), 175-182.
- Jayakumar R. (1997) 'A study on depth persistence of lineaments in Hard rock Terrain and its application to Groundwater Exploration. Geocarto International, Vol. 12, No. 3, September 1997.
- Jenson, S.K. and Domingue, J.O., (1988), 'Extracting topographic structure from digital elevation data for geographic information system analysis', Photogrammetric Engineering and Remote Sensing, 54, pp. 1593–1600.
- Jenson, S.K. and Domingue, J.O., (1988), Extracting topographic structure from digital elevation data for geographic information system analysis. Photogrammetric Engineering and Remote Sensing, 54, pp. 1593–1600
- Journel, A.G. and Huijbregts, Ch.J., 1978. Mining Geostatistics. Academic Press, New York, pp 599.
- Karpuzcu, M. & S_enes, S. Design of Monitoring Systems for Water Quality by Principal Component Analysis and a Case Study". Proceedings of the International Symposium on Environmental Management. Environment '87. Vol.1, 673-690. Istanbul 1987.
- Kehew AE (2001) Applied chemical hydrogeology. Prentice Hall, Upper Saddle River, NJ.

- Kelly, W.E., (1976), Geoelectric sounding for delineating groundwater contamination: Groundwater, V-14, no.1, p. 6-10.
- Kumar G.M., Agarwal A.K and Bali R, (2008) Delineation of Potential sites for water harvesting structures, J. Ind. Soc. Rem. Sens 36 : 323- 334(Springer).
- Kumar Pramod (2003). Ph.D Thesis Microzonation of Environmentally stressed areas, due to Air and Water pollution in Delhi, using Remote sensing and GIS techniques (Unpublished).
- Kripalani R.H. and Kulkarni A. (1996) 'Assesing the impacts of El Nino and Non- El Nino-related droughts over India', Drought Network News.
- Krishnamurthy J., Kumar Venkatesa N., Jayaraman V. and Manivel M. (1996) 'An approach to demarcate ground water potential zones through remote sensing and a geographical information system', International Journal of Remote Sensing, Vol.17, No. 10, 1867-1884.
- Krishnamurthy J., Manavalan P., and Saivasan V. (1992) ' Application of digital enhancement techniques for groundwater exploration in a hard-rock terrain', International Journal of Remote Sensing, Vol. 13, No. 15, 2925-2942.
- Krishnamurthy J., Mani A., Jayaraman V. and Manivel M.(2000) 'Groundwater resource development in hard rock terrain- an approach using remote sensing and GIS techniques', Journal of applied geology, volume 2, Issue ¾, 204-215.
- Krishnamurthy, J. and Srinivasan, G. (1995) Role of Geological and geomorphological factors in groundwater exploration: a study using IRS LISS data. Int. J. Remote Sensing. 16 (14): 2595-2618.
- Krishnamurthy, J. and Srinivasan, G. (1995) Role of Geological and geomorphological factors in groundwater exploration: a study using IRS LISS data. Int. J. Remote Sensing. 16 (14): 2595-2618.
- Krishnamurthy, J., Manavalan, P., and Saivasan, V. (1992) Application of digital enhancement technique for groundwater exploration in hard rock terrain. Intl. J. of Remote Sensing. 13 (15): 2925-2942.
- Kushwaha, S.P.S. (1985) Environmental monitoring and cyclone impact assessment on Sriharikota Island, India. Project report, N.R.S.A. Hyderabad.
- Larsson, I. (1972) 'Ground water in granite rocks and tectonic models.' Nordic Hydrology, 3, 111-129.

- Lawrence FW, Upchurch SB (1983) Identification of recharge areas using factor analysis. *Ground Water* 20:680–687.
- Luong, P.T. and Cuong, T.D. (1992) The application of remote sensing and geoexpert system for soil evaluation in soil erosion hazard mapping. *Asian Pacific Remote Sensing Journal*. 4 (2): 93-100.
- Macaz, O., W.E. Kelly and I. Landa (1987), Surface geoelectrics for groundwater pollution and protection studies: *Journal of Hydrology*, V. 93, no. 3, p. 277-294.
- Mahloch, J.L. *Multivariate Techniques for Water Quality Analysis*", *J. Environ. Eng. Div. Amer. Soc. Civil Eng.*, 100, No. EE5, 1119-1132, 1974.
- Mark, D. M., (1984), Automated detection of drainage network from digital elevation models. *Cartographica*, 21, 168–178.
- Mark, D., Dozier, J., and Frew, J., (1984), Automated basin delineation from digital elevation data. *Geo-Processing*, 2, 299–311.
- Matheron, G., 1970. *La Theorie des Variables Regionalisees et ses Applications*. CGMM, ENSMP, Fontainebleau, Fasc. No. pp 5,212.
- Mc Dermid, G.J. and Franklin, S.E. (1994) Spectral, spatial and geomorphometric variables for the remote sensing of slope processes. *Remote Sensing Environment*. 49; 57-71.
- Mc Kean, J., Buechel, S. and Gaydos, I. (1991) Remote sensing and landslide hazard assessment. *Photogramm. Eng. Remote Sensing*. 57 (9): 1158-1193.
- McKee D., Cunningham A. and Dudek A. 'Optical water type discrimination and tuning remote sensing band-ratio algorithms; Application to retrieval of chlorophyll and K_d (490) in the Irish and Celtic Seas', *Estuarine Coastal and Shelf Science*, 73, 827-834.
- Meijerink, A. M. J., De Brouwer, A. M., Mannaerts, C. M., and Valenzuela, C., (1994), Introduction to the use of Geographic Information Systems for practical hydrology. ITC–UNESCO Publication No. 23, The Netherlands.
- Meng SX, Maynard JB (2001) Use of statistical analysis to formulate conceptual models of geochemical behavior: water chemical data from the Botucatu aquifer in Sao Paulo state, Brazil. *J Hydrol* 250:78–97
- Merkel, R.H. (1972). The use of resistivity technique to delineate acid mine drainage in groundwater: *Groundwater*, V.10. no. 5 and p. 38-42.

- Meyer, W and Welch,R.I(1975) Chapter 19, In Manual of Remote Sensing Vol.II, 1st edition ASPRS Publication, Virginia, USA.
- Mitchell, B. (1979) Geography and resource Analysis. Longman, London.
- Monti Guarnieri, A., Prati, C., (1996). SAR focusing and interferometry. IEEE Transactions on Geoscience and Remote Sensing 34 (4), 1029–1038.
- Moore, I. D., Grayson, R. B., and Ladson, A. R., (1991), Digital terrain modelling: a review of hydrological, geomorphological and biological applications. In Terrain Analysis and Distributed Modelling in Hydrology, edited by K. J. Beven and I. D. Moore (Chichester, UK: John Wiley and Sons), pp. 7–34.
- Mukherjee S., Sashtri S., Gupta M., Pant M.K., Singh C.K., Singh S.K., Srivastava P.K., Sharma K.K (2007) 'Integrated water resource management using remote sensing and geophysical techniques: Aravali quartzite, Delhi, India', Journal of Environmental Hydrology, volume 15,paper 10.
- Mukherjee, S. (1996) Targetting saline aquifer by remote sensing and geophysical methods in a part of Hamirpur- Kanpur, India. Hydrology Jour. 19 (1): 53-64.
- Mukherjee,S.,(2008) Role of Satellite Sensors in Groundwater Exploration. Sensors Journal 2008, 8 pp 2006-2017.
- Mukherjee, S., (2004). Text Book of Environmental remote Sensing. Published by Macmillan India Limited, New Delhi.
- Mukherjee, S., and Sarin, V. (1990), Targeting Potential groundwater sites in parts of Jhanshi district, Utter Pradesh by using satellite remote sensing techniques. Proc AIS on GWIMGT December 11- 12. CGWB report. Pp T 1-11, 23-31.
- Mukherjee, S., (1998). Eco conservation of a part of J.N.U. campus by GIS analysis. Proc CGWB seminar on artificial recharge of groundwater. Dec 15-16, 1998, New Delhi. 103-119.
- Mukherjee, S., (1999). Remote sensing Applications in Applied Geosciences. Published by Manak Publications. New Delhi.
- Mukherjee, S., (2007). New Trends in Groundwater Research. ISBN: 1-906083-03-7, COOPERJAL LTD London, UK.

- Mukherjee.S., (2001). Quantitative and qualitative improvement in groundwater by artificial recharge: A case study in Jawaharlal Nehru University, New Delhi, India FACT & IRCSA Vienna Margraf Verlag ISBN 3-8236-1354-5.
- Mukherjee.S, Jaiswal R.K and Krishnamurthy.J (2005); Regional study for mapping the natural resource prospect. Geocarto International Journal Vol 20 No3 pp 1-11.
- Mukherjee.A, Kumar A and Kortvellessey.L.(2005); Assessment of groundwater quality in South 24 Parganas, West Bengal Cost, India; Journal of Environ.Hydrol.(USA), Paper 15 Vol.13 p1-8.
- Mukherjee.S., (2001). Seismogenic potentiality of Delhi using remote sensing , Soil geochemistry and geophysical data , Indian Geological Congress Vol.2No.1 pp 289-297.
- Mukherjee.S., (2006). Integrated water resources management in Aravalli Quartzite of Delhi, India by remote sensing and geophysical techniques, Proc. International Workshop on Impacts of Reforestation of degraded land on Landscape Hydrology in Asian Region, Roorkee, Indian 6-10 March 2006.
- Mukherjee.S, Yadav.S, and Das A.K(2003). Microwave and visible spectral measurement variations to infer groundwater recharge potentiality. Proc.Symp.on Advances in Microwave Remote sensing Applications. Jan.21-23, 2003 IIT Bombay, India.
- Mukherjee.S., (1998). Groundwater pollution- An Environmental hazard, Proc. National Seminar on “Advancement in Groundwater Hydrology and Management of Irrigated Lands “ February 25, 1988, SVRCET-SURAT, pp-176-177.
- Mukherjee S., Pant.M and Shashtri.S (2004): Groundwater contamination by organic compounds. Geophysical research Abstract, Vol.00599, 2004, European Geosciences Union Proc.2004.
- Mukherjee, S (1989). Geology and geochemistry of Pegmatites and associated rocks in a part of Jorasewar and Sapahitola area district Hazaribagh Bihar with reference to application of remote sensing technique in exploration of natural resources. Unpublished PhD Thesis, B.H.U. Varanasi.
- Mukherjee, S., (1998). Change in Groundwater environment with land-use pattern in a part of south Delhi: A remote sensing approach. Jour. Asia- Pacific Remote sensing and GIS journal Vol.9, No.2. pp 9-14.

- Murthy K.S. R. (2000) 'Ground water potential in semi arid region of Andhra Pradesh – a geographical information system approach', *International Journal of Remote Sensing*, Vol. 21, No.9, 1867-1884.
- Nagarajan R. and Suresh M. (2002) 'Performance assessment of water resource project using remote sensing and a Geographical Information System – a case study' ,*International Journal of Remote Sensing*, 23;20, 4475 – 4484.
- Ochsenkühn KM, Kontoyannakos J, Ochsenkühn-Petroulu M (1997). A new approach to a hydrochemical studies of groundwater flow. *J Hydrol* 194:64–75.
- Onorati, G., Poscolieri, M., Salvi, S., and Cirillo, T., (1985), 'Statistical comparison between streams and lineaments orientation in a test area of northern Mozambique,' In: *Proceedings of International Conference on Advanced Technology for monitoring and processing Global Environmental Data*, Remote Sensing Society and GERMA, 10-12 September, 233-243.
- Prasad R.K., Mondal N.C., Banerjee Pallavi, Nandkumar M.V. and Singh V.S.(2007) 'Deciphering potential groundwater zones in hard rock through the application of GIS',*Environmental Geology* DOI 10.1007/s00254-007-0992-3.
- Piper AM (1994) A graphic procedure in chemical interpretation of water analysis. *Am Geophysics Union Trans* 25; 914-923.
- Rabus, B., Eineder, M., Roth, A., Bamler, R., (2003). The shuttle radar topography mission — a new class of digital elevation models acquires by spaceborne radar. *ISPRS Journal of Photogrammetry and Remote Sensing* 57, 241–262.
- Rathore, C.S. and Wright, R. (1992) Monitoring mining operations in apart of India's Jharia coalfield using Thematic Mapper data. *Asian – Pacific Remote Sensing Jour.* 5 (1): 37-47.
- Reeder SW, Hitchon B, Levinson AA (1972) Hydrogeochemistry of the surface waters of the Mackenzie River drainage basin, Canada-I. Factors controlling inorganic composition. *Geochim Cosmochim Acta* 36:825–865.
- Rekha V.B., Vijith H. and Thomas A.P. 'Integrated remote sensing and GIS for groundwater potentiality mapping in Koduvan Ar sub-watershed of Meenachil River Basin, Kottayam District, Kerala, India.' Year and journal not specified

- Riazanoff, S., Cerville, B., and Chorowicz, J., (1988), Ridge and valley line extraction from digital terrain models. *International Journal of Remote Sensing*, 9, 1175–1183.
- Rijks Water Stat (1969), standard graphs for resistivity prospecting, European association of Exploration Geophysics. The Hague pp 4.
- Rowan L.C. (1975) Application of satellites to geological exploration. *American Scientists*. 63 (4), 393-403.
- Roy, A.B. (1998) Stratigraphic and tectonic framework of the Aravalli mountain range. In A. B. Roy (Ed.) *Precambrian of the Aravalli mountain, Rajasthan, India*. *Memoir of Geol. Soc. India*. 48; 49-54.
- Ruiz F, Gomis V, Blasco P (1990) Application of factor analysis to the study of a coastal aquifer. *J Hydrol* 119:169–177.
- Sabins, F.F.Jr. (1997) *Remote sensing: principles and interpretation* (third edition) W.H. Freeman and Company, New York. 495pp.
- Sahai B., Sood R.K., and Sharma S.C. (1985) 'Groundwater exploration in the Saurashtra peninsula', *International Journal of Remote Sensing*, Vol.6, Nos. 3 and 4, 433-441.
- Sahai, B., Bhattacharya A and Hedge, V.S. (1991). IRS-1A. Application for groundwater targeting, *Current Science* 61(3&4): 172-179.
- Sander. P., (2007) Lineaments in ground water exploration; a review of application and limitations. *Hydrogeology Journal* (2007) 15: 71-74.
- Saraf A.K. and Choudhary P.R. (1998) 'Integrated remote sensing and GIS for groundwater exploration and identification of artificial recharge sites', *International Journal of Remote Sensing*, Vol.19, No.10, 1825-1841.
- Saraf, A. K., (1999), Landuse modeling in GIS for Bankura District. Department of Science and Technology, New Delhi, Sponsored Project Report. Department of Earth Sciences, University of Roorkee (unpublished).
- Saraf, A. K., and Choudhury, P. R., (1997), Integrated application of remote sensing and GIS for groundwater exploration in hard rock terrain. *Proceedings of International Symposium on Emerging Trends in Hydrology*, 25–27 September 1997, Department of Hydrology, University of Roorkee, Roorkee, pp. 435–442
- Saraf, A. K., Srivastava, A., Roy, B., Pradhan, B. S., and Choudhury, P. R., (1999), Landuse modelling in Geographic Information System for Dwarkeshwar watershed, Bankura

- District. Proceedings of the National Symposium on Remote Sensing Applications for Natural Resources: Retrospective and Perspective, 19– 21 January 1999, Indian Space Research Organisation, Bangalore, pp. 99–100.
- Satyanarayan Rao, R., (1983), 'Application of integrated deformation model to ground water targeting in Peninsular gneissic complex through remote sensing studies,' In: Proceedings of the National Symposium on Remote Sensing in Development and Management of Water Resources, Hyderabad, India.
- Schetagne, R. The Use of Multivariate Methods in the Interpretation of Water Quality Monitoring Data of a Large Northern Reservoir". Proceedings of the Workshop Held at the Canada Center for Inland Waters, October 7-10, 1985. Edited by A.H. El-Shararawir. E. Kwi Atkowski. Statistical Aspects of Water Quality Monitoring, 31-43, 1985.
- Seasoran, A., (1985) 'Potential of remote sensing use in karstic area. Antalya region of South Turkey,' In; Proceedings of the Ankara Symposium "Karst Water Resources", July 1985 IAHS Publication 161, 271-277.
- Shahid S. and Nath S.K.(2007) 'GIS integration of remote sensing and electrical sounding data for hydrogeological exploration', Journal of Spatial Hydrology ,Vol.2, No.1, 1-12.
- Shahid S., Nath S.K. and Roy J. (2000) 'Groundwater potential modeling in soft rock area using a GIS', International Journal of Remote Sensing, Vol.21, No. 9, 1919-1924.
- Sharma S.K. and Anjanyulu, D. (1993) Application of remote sensing and GIS on water resource management. Intl. J. of Remote Sensing. 14(3) : 209-220.
- Singh, C.K. (2007). Integrated water resource management in a part of Punjab by using satellite data. M.Phil. Dissertation. (Unpublished). , JNU, N.Delhi
- Singh P.K (1999) Natural Resource Management for Sustainable Development of Delhi Using Remote Sensing and GIS Techniques , Unpublished PhD Thesis , JNU, N.Delhi.
- Singh K. Amresh and Prakash R. S. (2004) 'Integration of thematic maps through GIS for identification of groundwater potential zones', Map India 2004 Proceeding.
- Singh, R.P., Mishra, D.R., Sahoo, A.K., and Dey, S.,(2005a), 'Spatial and temporal variability of soil moisture over India using IRS P4 MSMR data', International Journal Of Remote Sensing (in press).
- Singhal, B.B.S., and Gupta, R.P., (2001), Applied Hydrogeology of Fractured Rocks, Kluwer Academic Publishers, Dordrecht, The Netherlands.

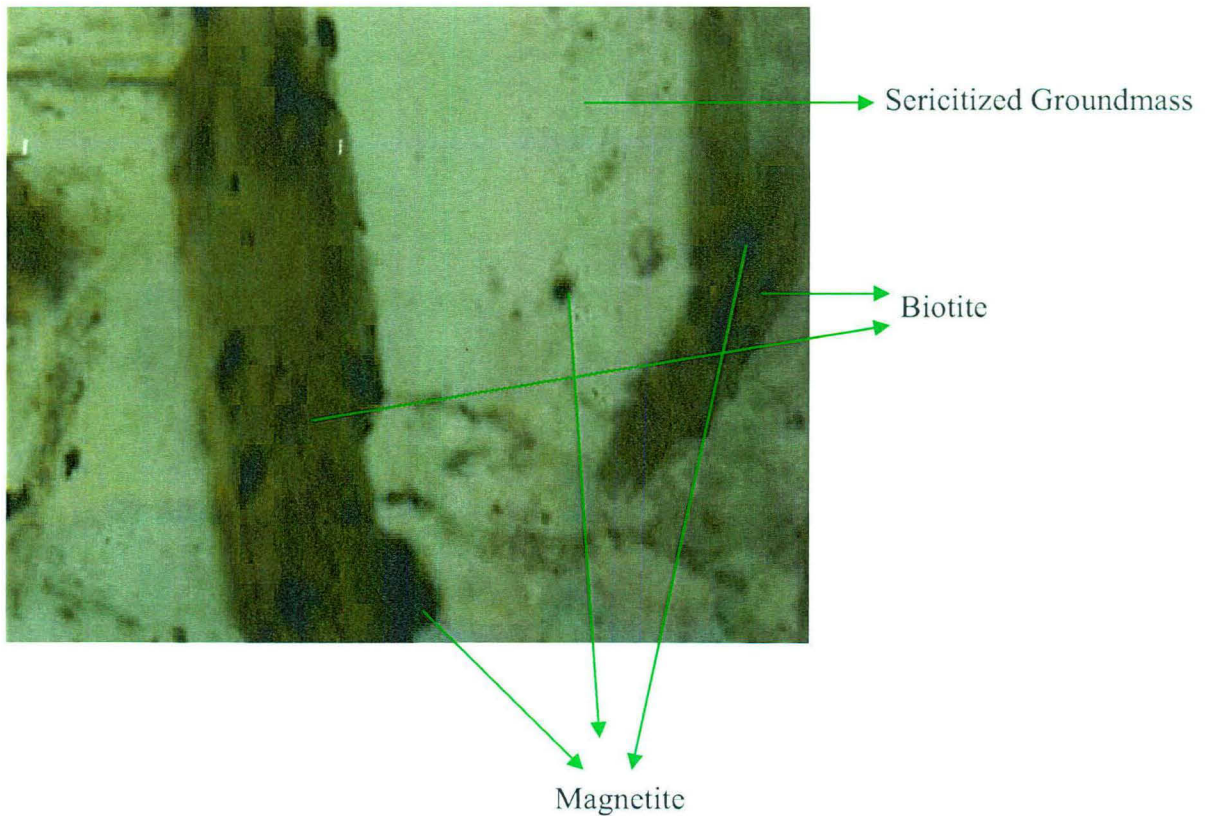
- Snader, P., (1996), 'Remote sensing and GIS for groundwater assessment in hard rock areas: Application to water well siting in Ghana and Botswana,' Geologiska Institutionen, Publ. A 80. Goteborg.
- Srinivas Rao. Y. and Jugran.D.K., (2003) 'Delineation of groundwater potential zones and zones of groundwater quality suitable for domestic purposes using remote sensing and GIS'. Hydrological Sciences Journal; 48(5), October 2003.
- Stollar, R.L. and P. Roux, (1975), Earth resistivity surveys – a method for defining groundwater contamination: Groundwater, V.13, no.2, p.145-150.
- Strahler, A.N., (1952), Dynamic basis geomorphology. Geological Society of America Bulletin, 63, pp. 923–938.
- Subba Rao N. (2002) 'Geochemistry of groundwater in parts of Guntur district, Andhra Pradesh, India', Environmental Geology, 41:5 52-562.
- Sujatha D. and Reddy B. R. (2003) 'Quality characterization of groundwater in the south-eastern part of the Ranga Reddy district, Andhra Pradesh, India.' Environmental Geology, 44:579-586.
- Suk H, Lee KK (1999) Characterization of a ground water hydrochemical system through multivariate analysis: clustering into ground water zones. Ground Water 37(3):358–366
- Syed Munaf A, Hussain M, Abderrahman W (2005) Using multivariate factor analysis to assess surface\logged water quality and source of contamination at a large irrigation project at Al-Fadhli, Eastern Province, Saudi Arabia. Bull Eng Geol Environ 64:319-Systat Statistical Software", Version 5.0. Systat Inc.Copyright 1990.
- Tarboton, D.G., Bras, R.L. and Rodriguez-Iturbe, I.,(1991), On the extraction of channel networks from digital elevation data. Hydrological Processes, 5, pp. 81–100.
- Trivedi & Goyal, 1984 Chemical and Biological Method for water Pollution Studies.
- Trvaglia C., and Dainelli N.(2003) 'Groundwater search by remote sensing: A methodological approach', Environmental and Natural resources working Paper no. 13, FAO,Rome,41 pp., 16 figures, 1 table
- Turner, B.L. (1985), Linking the natural and social sciences: the landuse/landcover change. Care Project of IGBP News letter No. 22. U.S. Geological Survey, (1999). GTOPO30 — Global 30 Arc Second Elevation Data.

- Vidal M, Melgar J, Lopez A, Santoalla MC (2000) Spatial and temporal hydrochemical changes in groundwater under the contaminating effects of fertilizer and wastewater. *J Environ Manage* 60:215–225
- Vieux, B.E., (2001), *Distributed Hydrologic Modeling Using GIS*, Kluwer Academic Publishers, The Netherlands.
- Vink, A.P.A. (1975), *Landuse and advancing agriculture*. Springer, Berlin/ Heidelberg.
- Voutilainen A., Pyhalahti T., Kallio K. Y., Puliainen j., Haario H. and Kaipio J. P.(2006) 'A filtering approach for estimating lake water quality from remote sensing data.' *International journal of Applied Earth Observation and Geoinformation*, 9, 50-64.
- Wackernagel, H. (1995) *Multivariate Geostatistics: An Introduction with Applications*. Springer-Verlag, Berlin, Germany
- Wang, F., Wang, J. and Wan, Y., (2000), 'A test research to probe water resources over arid areas with Radarsat remote sensing technology', *Remote sensing for Land and Resources*, 4, 14-18.
- Warner, D.L., (1969). Preliminary field studies using earth resistivity measurements for delineating zones of contaminated groundwater: *Groundwater*, V. 7, no.1. , p. 9-16.
- Weibel, R., and Heller, M., (1991), Digital terrain modelling In *Geographical Information Systems: Principles and Applications*, edited by D. J. Maguire, M. F. Goodchild and D. W. Rhind (London: Longman), pp. 269–297
- Worrall, L. (1990) GIS: prospects and challenges. In: *Geographic Information Systems: Developments and Applications*. Ed. Less Worall, Belhaven Press, London, 1-12.
- Yadav G.S. and Singh S.K. (2007): Integrated resistivity survey for delineation of fractures for groundwater exploration in hard rock areas. *Applied Geophysics* 62 (2007): 301-312.
- Zanini L, Novakowski KS, Lapcevic P, Bickerton GS, Voralek J, Talbot C (2000) Ground water flow in a fractured carbonate aquifer inferred from combined hydrogeological and geochemical methods. *Ground Water* 38(3):350–360

APPENDIX – I

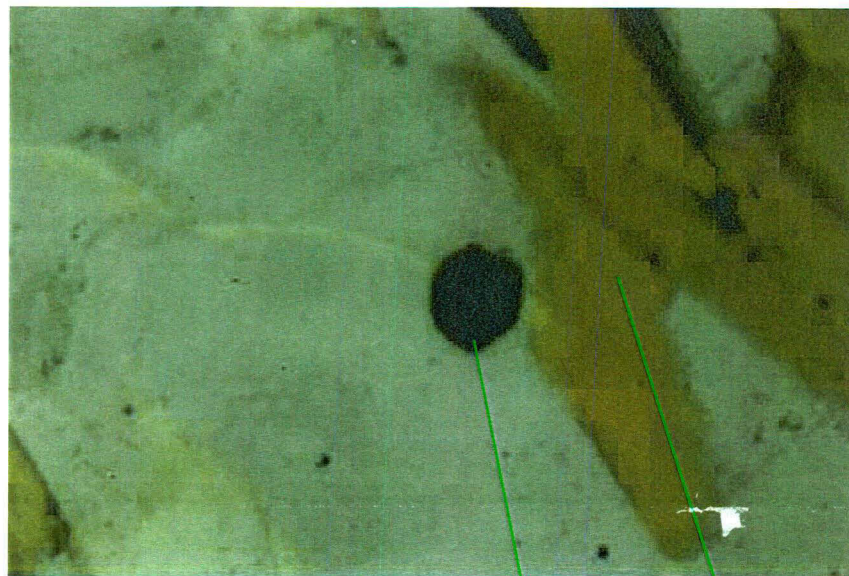
PHOTOMICROGRAPHS

Crystal of biotite mica embedded within sericitised groundmass. A few opaque magnetite crystals were found embedded within the groundmass as well as muscovite. The mineral assemblage within the rock shows that there are 25% Biotite mica with approximately 65% quartz crystals are present. 10% accessory minerals were found which consists of magnetite, zircon and potash feldspar. The mineral assemblage and paragenesis are suggestive of the geological history of high grade metamorphism. The crystal of biotite and quartz are showing fractures with secondary filling by opaque minerals



Slide 1- IMG0003_1.JPG

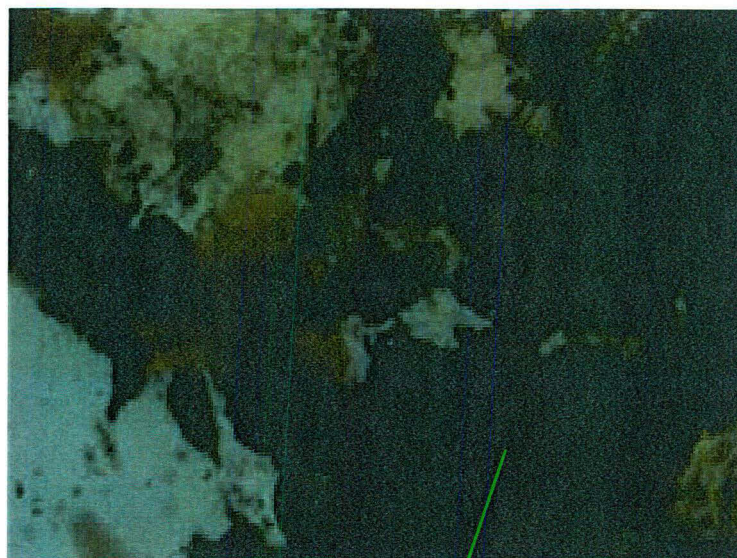
The slide shows garnet crystal under cross Nicol shows dark colour. The anomalous garnet crystals are characteristics of contact metamorphic zones.



Garnet

Biotite

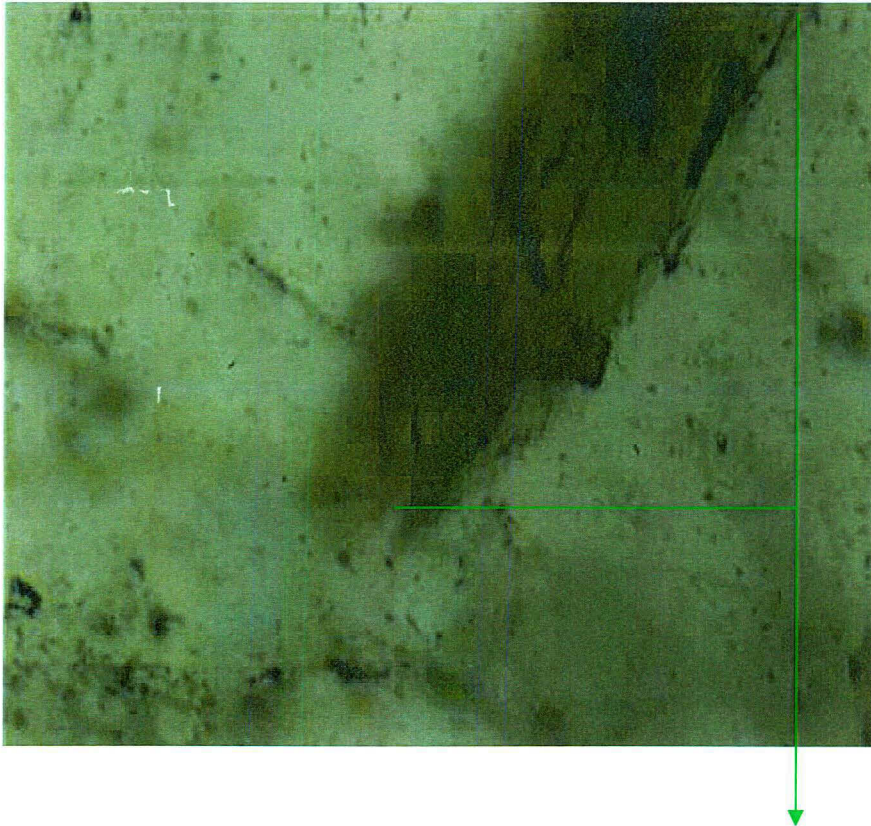
Slide 1- 0004_1.JPG



Haematite Crystal (Crushed)

IMG 0003.JPG

Highly crushed biotite crystal and fracture filling shows that the rock at 273ft depth was structurally disturbed. Hazy green coloured tinge surrounding biotite and magnetite crystals are proofs of serpentinization of mafic (Fe-Mg rich) minerals. The serpentinization further proves hydrolysis of the minerals due to the presence of the groundwater in the fractured zones.



Serpentinization - is process due to Hydrolysis

IMG0003_1.JPG

Brown and pleochroic from pale brown crystal of allanite crystal adjacent to a feldspar crystal is suggestive of an overgrowth on epidote crystal allanite is altered to amorphous substance in other places by the breakdown of the space lattice in this granite pegmatite contact.

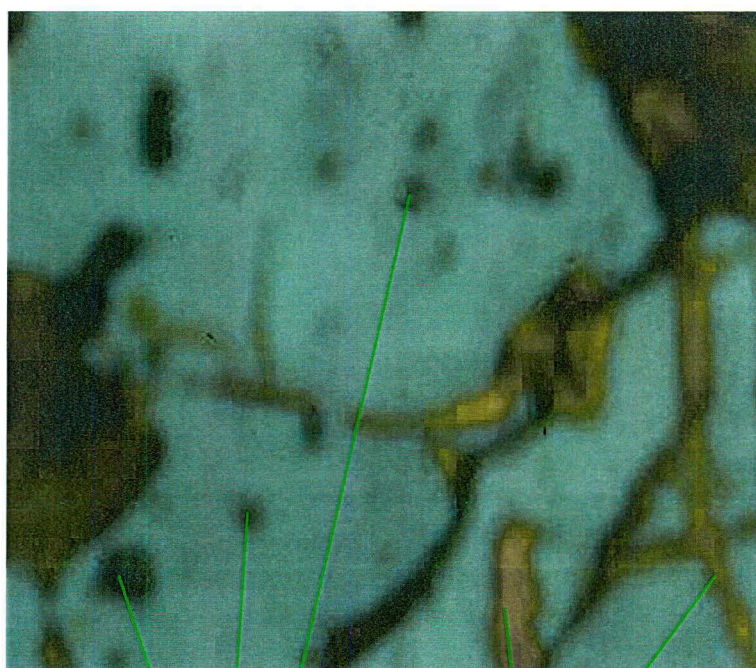


Feldspar Crystal

Allanite Crystal

Slide 4- 0001_1.JPG

Reddish brown to olive green haloes in biotite is caused by alpha particle bombardment from small zircon crystals containing radioactive impurities. When the stage of the microscope was rotated near the extinction position peculiar crinkly appearance is noticed in biotite. All the above features are suggestive of highly crushed granite pegmatite fractured zone developed in contact metamorphic zones.

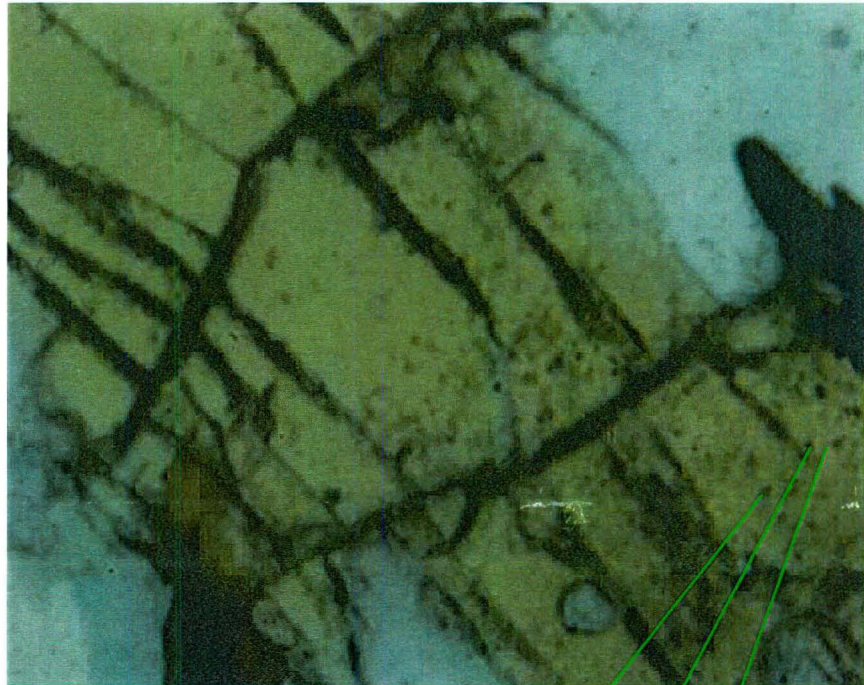


Zircon Crystal

Crushed Biotite Crystal

Slide 2- 0002_1JPG:

A section of single tourmaline crystal in matrix of quartz, mica and feldspar. It shows strong absorption normal to the plane of the polarizer. The colour is yellowish brown the mineral identified is Mg (Magnesium) tourmaline. The variety is commonly known as **Dravite**. The crystals are highly distorted as shown by the curved-cleavage the extinction is practically parallel to the cleavage traces. It occurs in stage which shows the metamorphism of granite pegmatite. Within dravite crystal a few fluid intrusion with secondary mineralization is suggestive of recrystallization due to high grade metamorphism.



Fluid Intrusion in Dravite
(Tourmaline) Crystal

Slide 2- 0003_2.JPG

Sericitization of Dravite mica shows the evidence of crushed zone in pegmatite mica schist boundary.

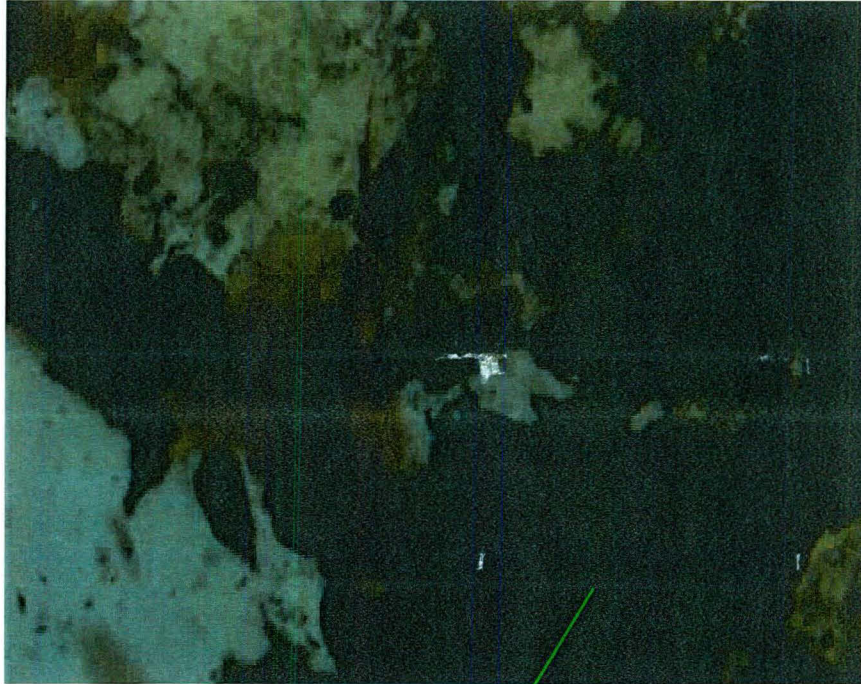


Sericitization

Biotite Crystal

Slide-2 0004_1.JPG

High concentration of crushed mafic minerals in crushed zone of biotite- schist-pegmatite fracture zone.



Haematite Crystal (Crushed)

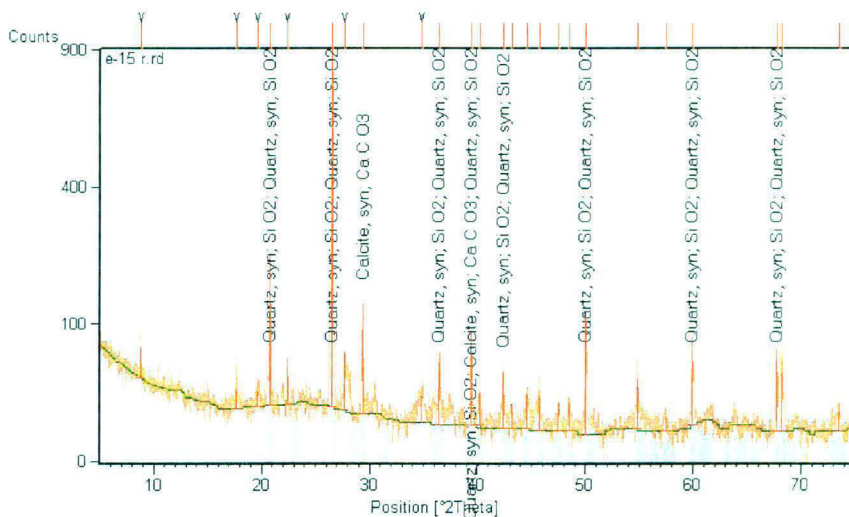
Slide5-0006.JPG

Dumortierite crystal occurs within the quartzite vein. Dumortierite occurs in quartzite adjacent to granite pegmatite and schist. It typically occurs in high temperature Aluminium rich regional metamorphic rocks those resulting from contact metamorphism and also in Boron rich pegmatite. Dumortierite is a fibrous variable coloured Aluminium borosilicate mineral $\text{Al}_{6,5-7} \text{BO}_3 (\text{SiO}_4)_3 (\text{OH})_3$.

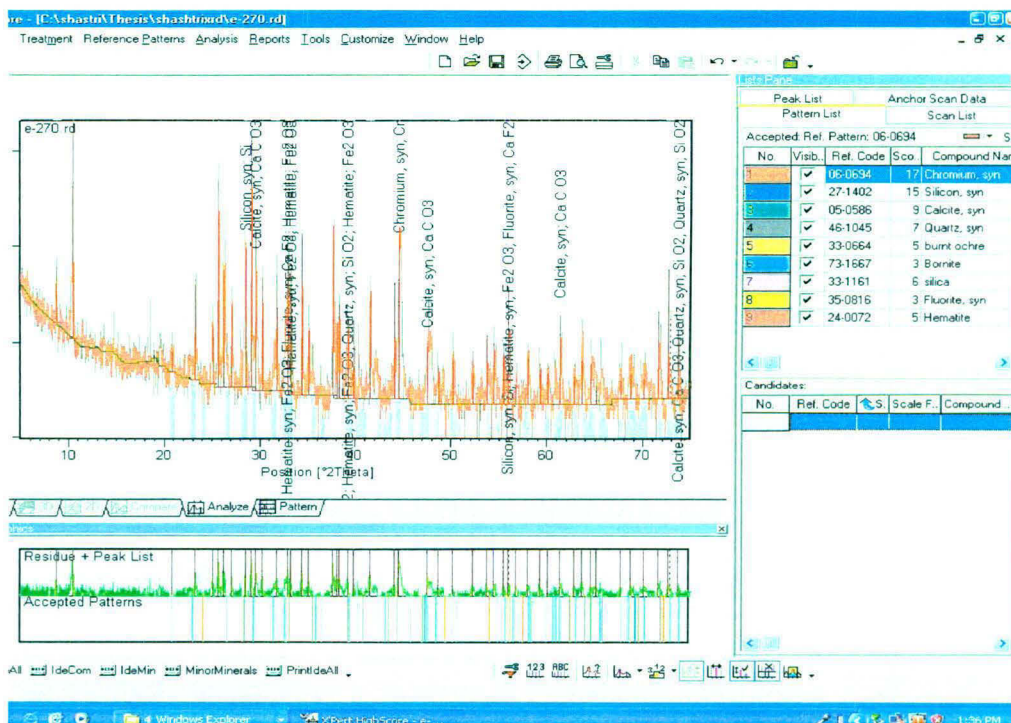
APPENDIX - II

XRD DATA ANALYSIS

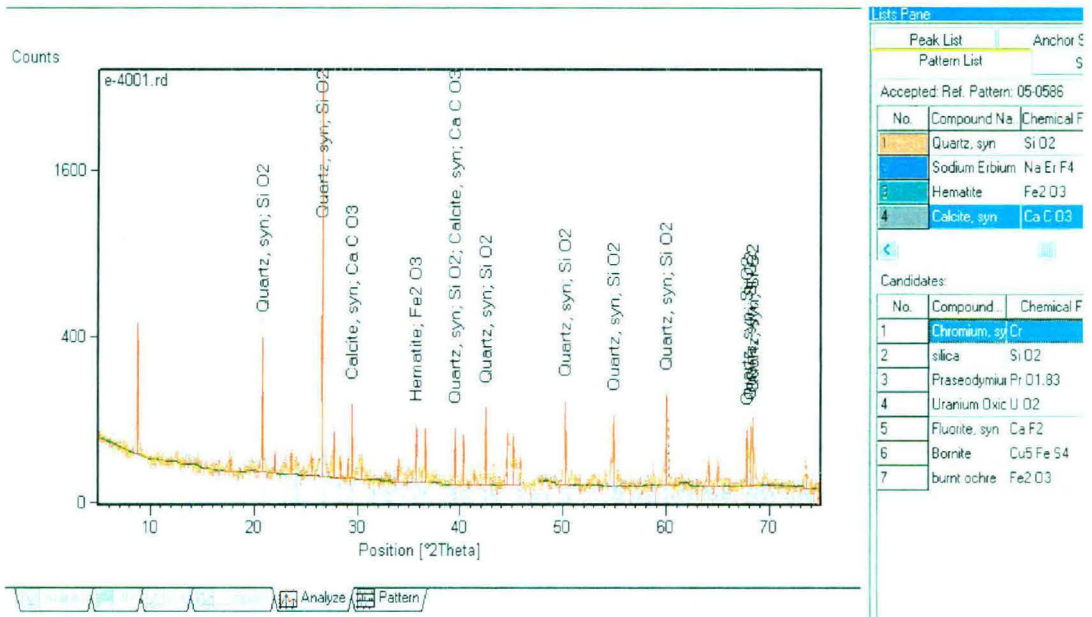
XRD Data for Bore 1 (JNU 1)



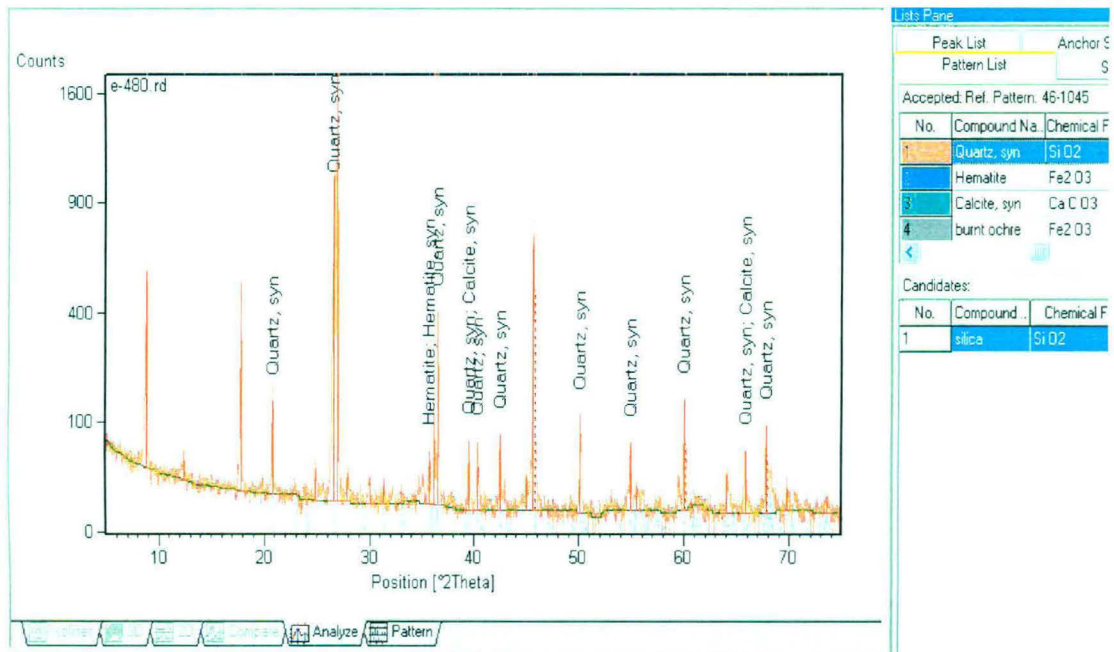
Mineral composition at the Depth of 3.28m bgl



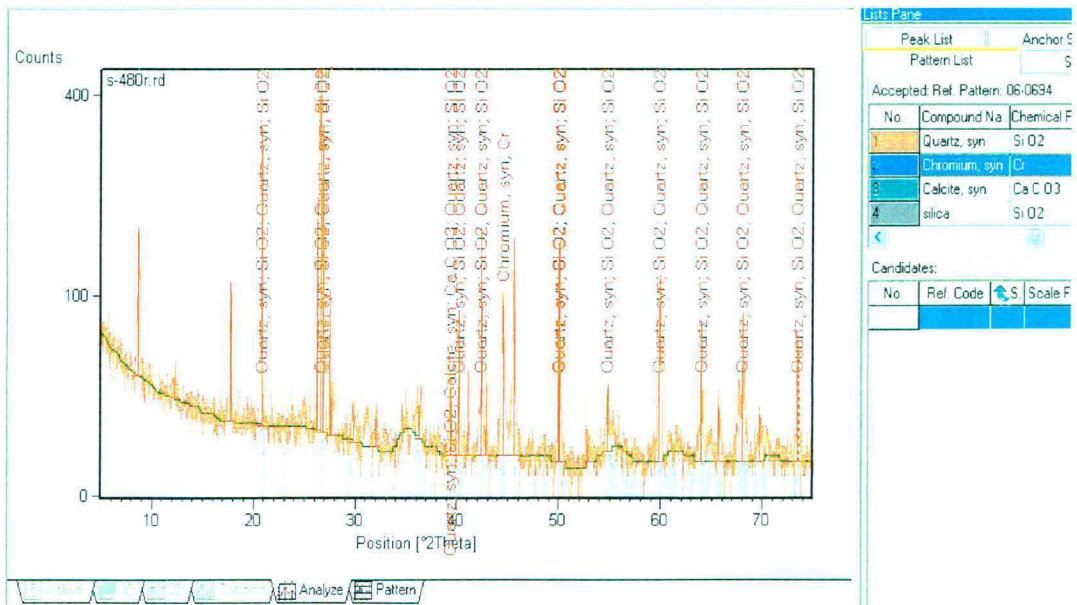
Mineral Composition at the Depth of 82.31m bgl



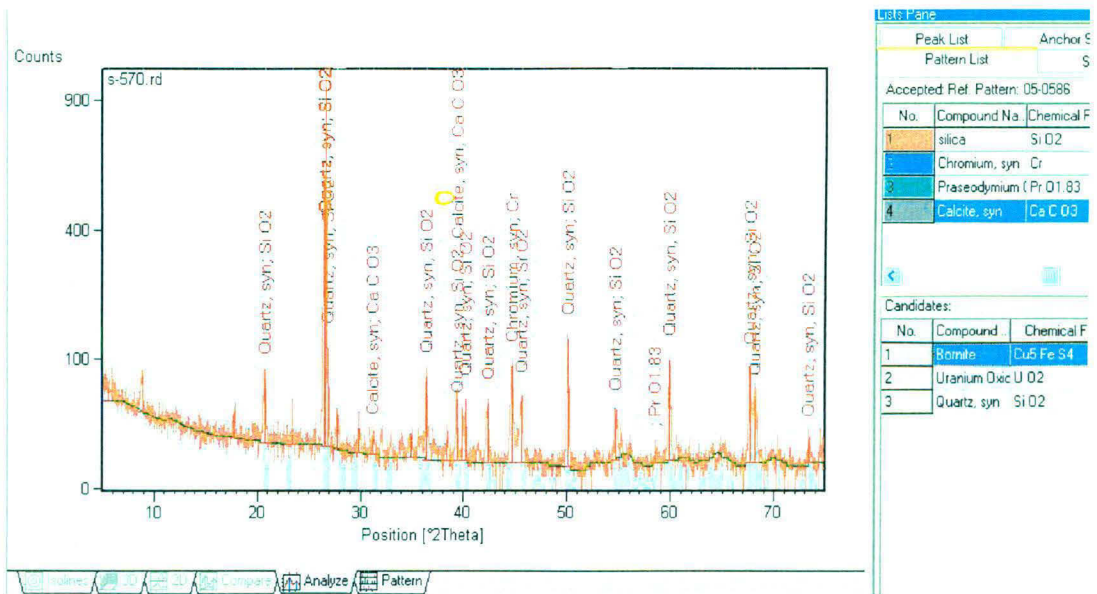
Mineral Composition at the Depth of 121.95m bgl



Minerals Composition at the Depth of 146.34m bgl

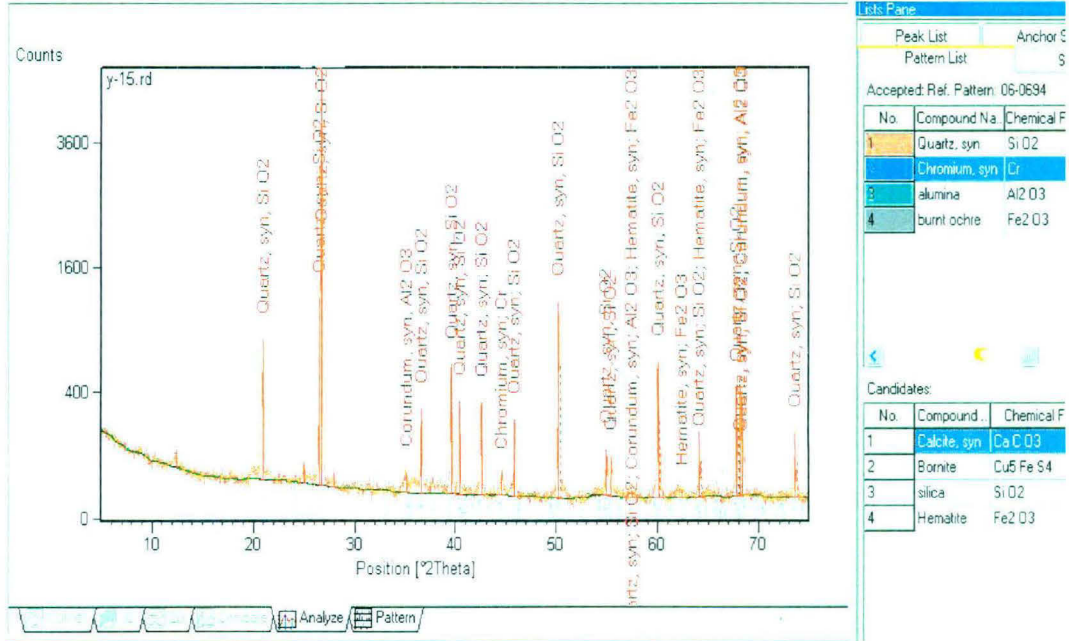


Mineral Composition at the Depth of 146.34m bgl

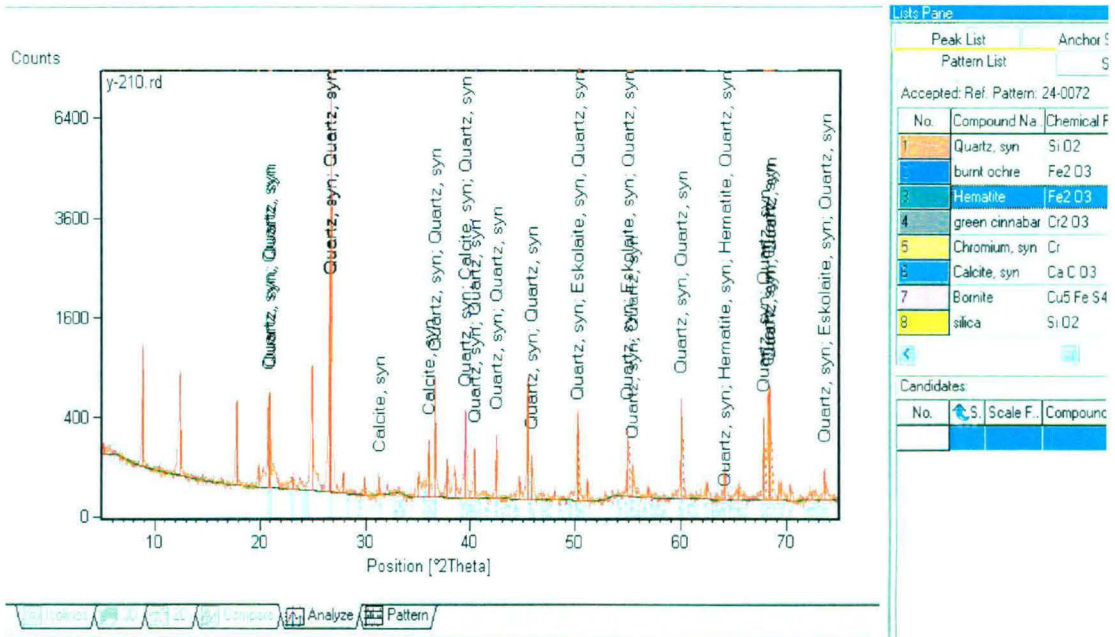


Mineral Composition at the Depth of 173.78m bgl

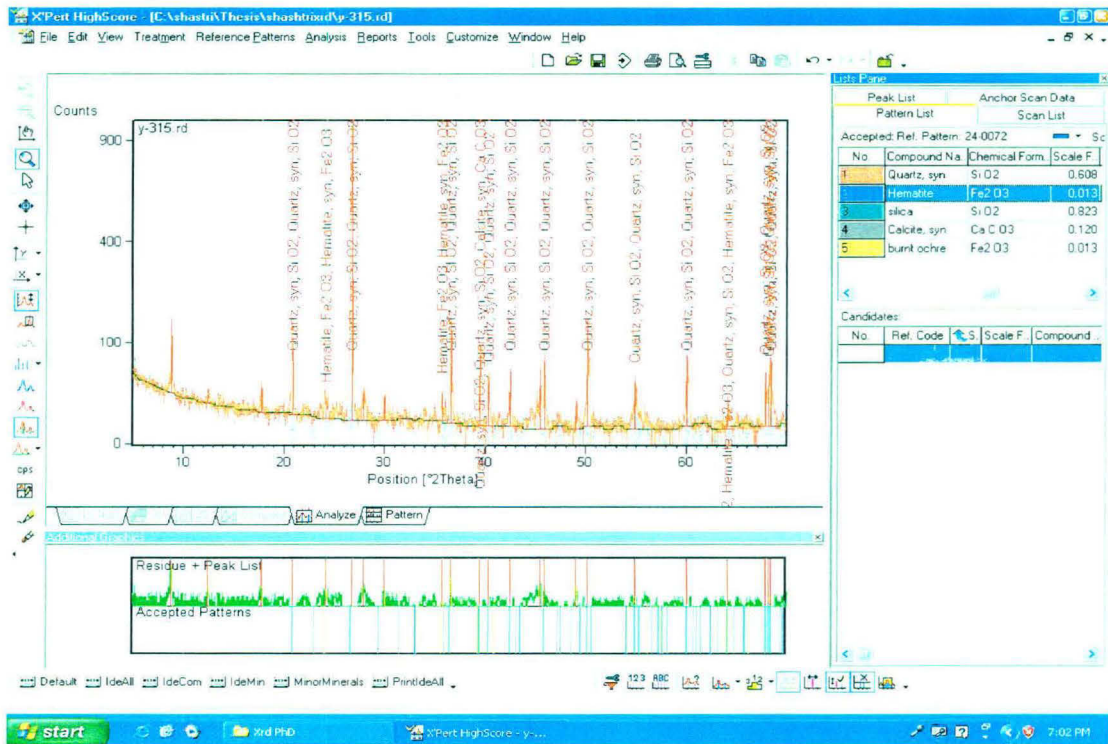
XRD Data for Bore 3 (JNU 3)



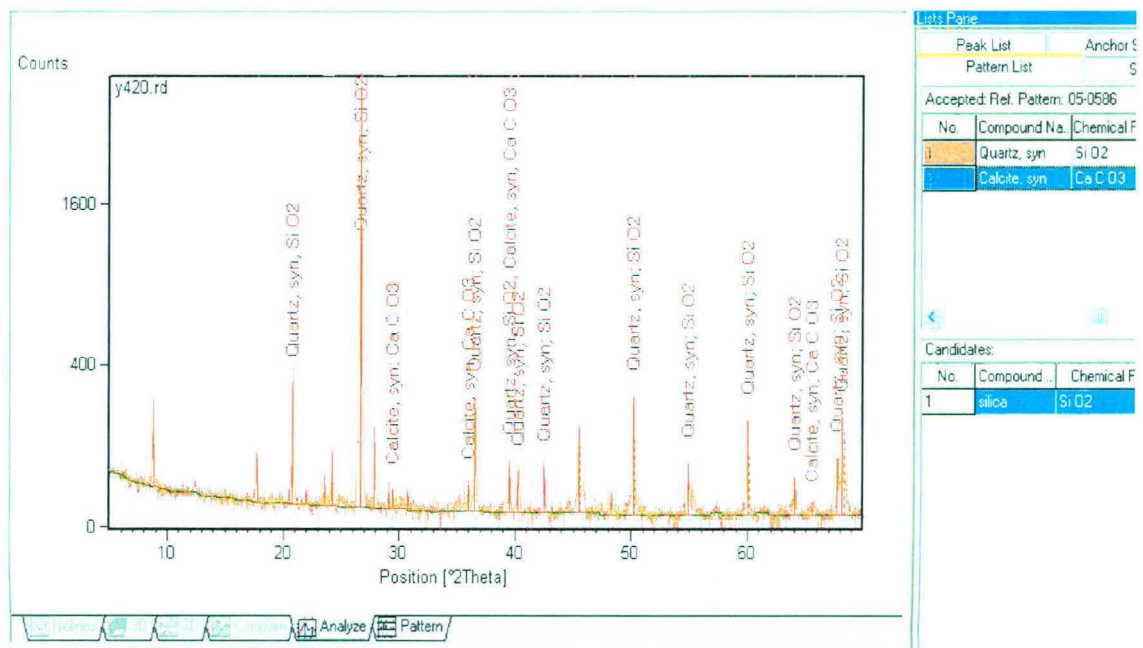
Mineral Composition at the Depth of 3.28m bgl



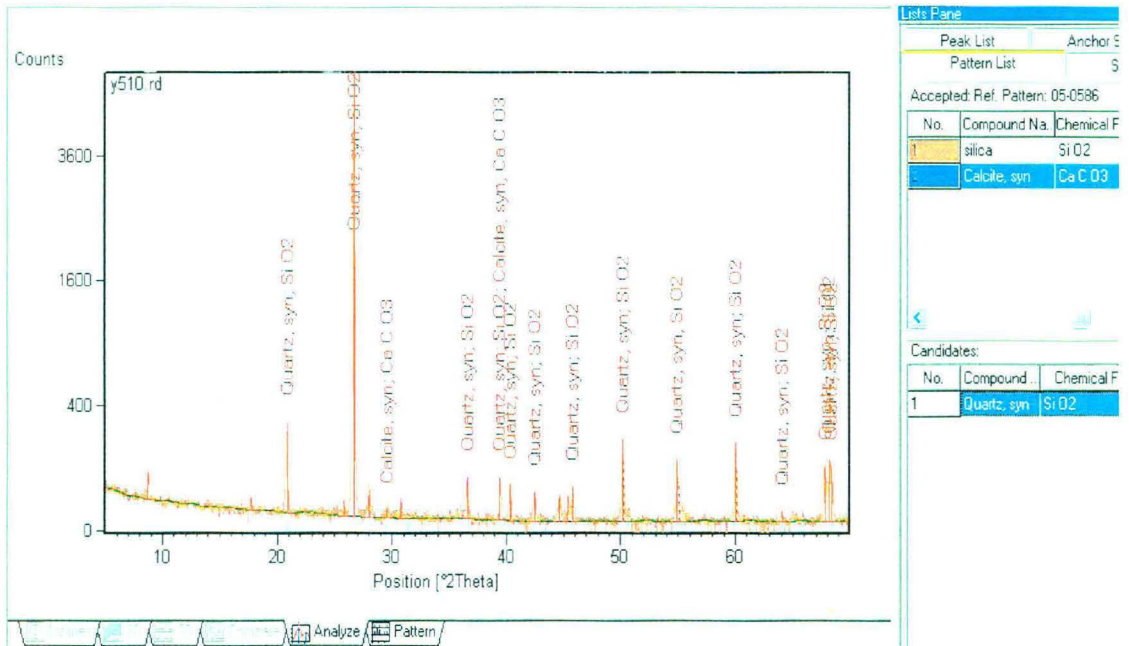
Mineral Composition at the Depth of 64.02m bgl



Mineral Composition at the Depth of 96.03m bgl

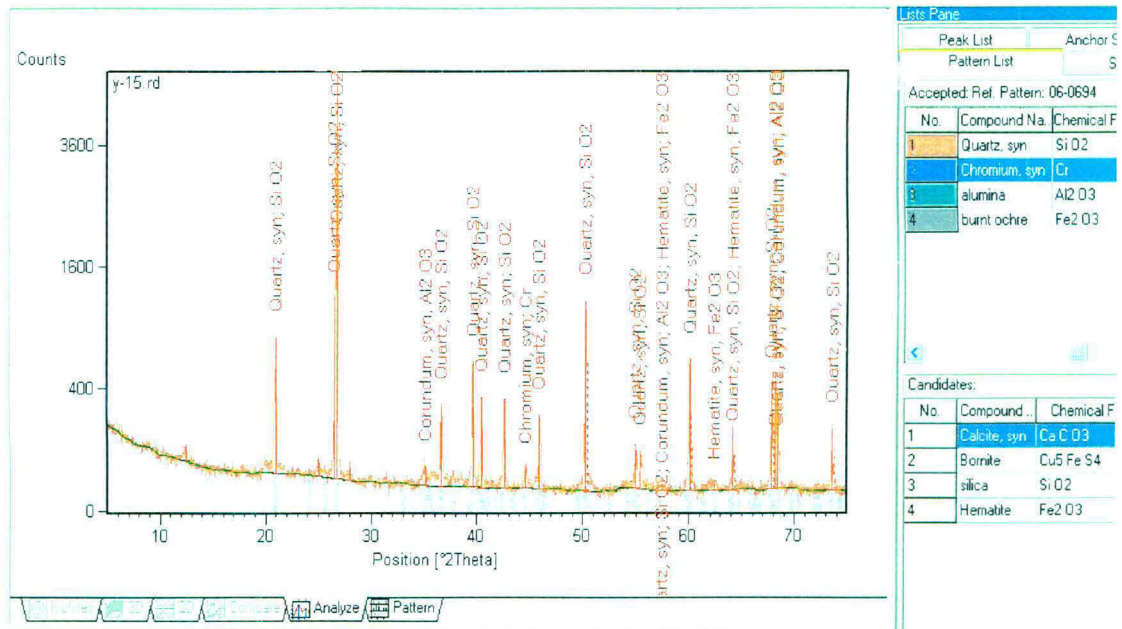


Mineral Composition at the Depth of 128.04m bgl

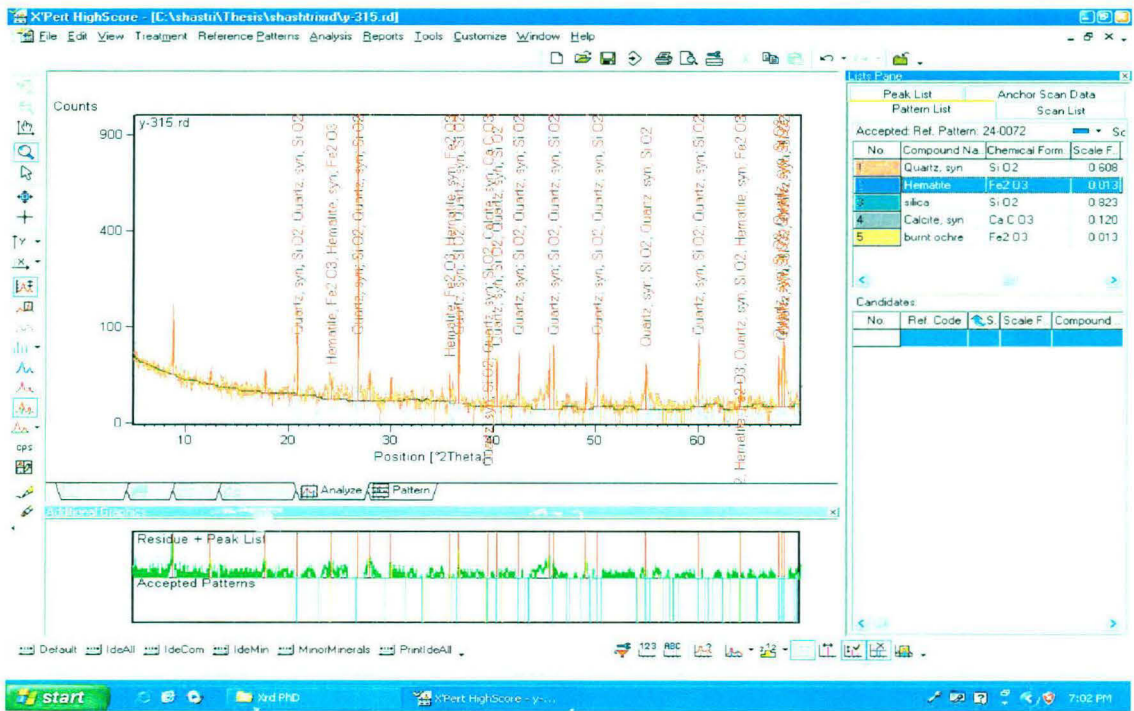


Mineral Composition at the Depth of 155.48m bgl

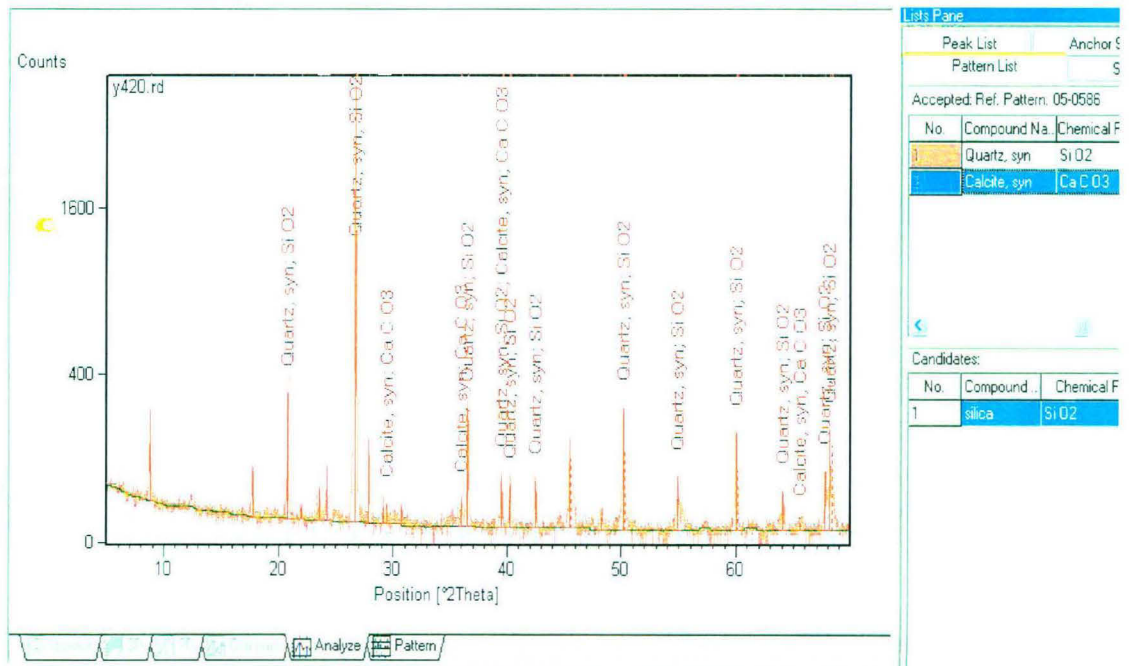
XRD Data for Bore 4 (JNU 4)



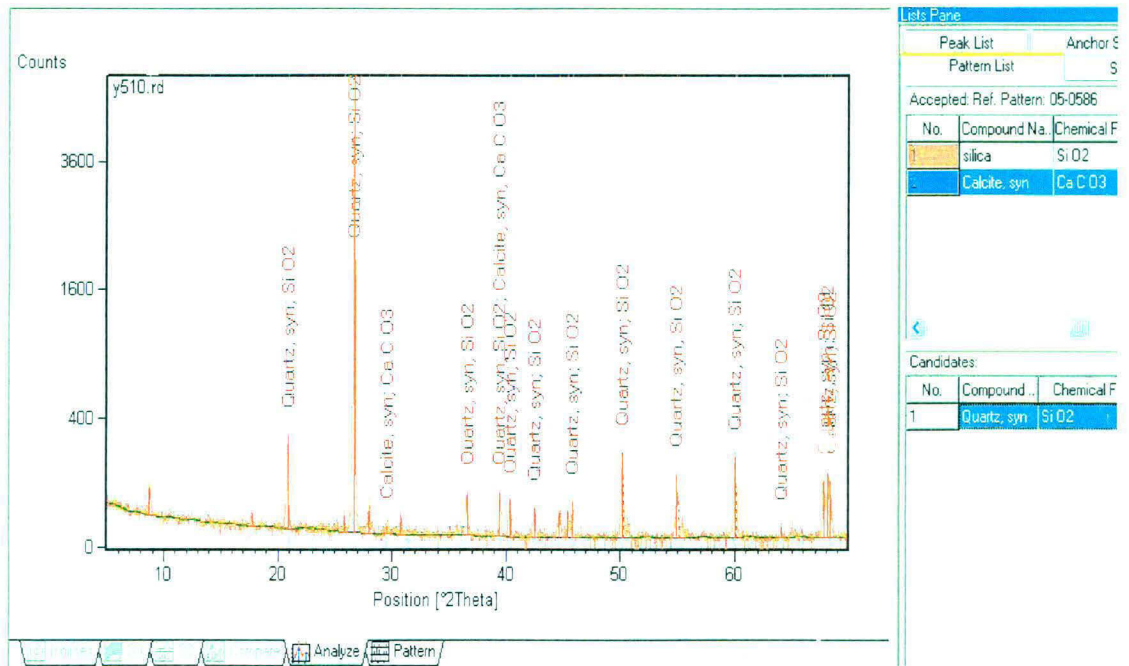
Mineral Composition at the Depth of 4.57m bgl



Mineral Composition at the Depth of 90.03m bgl



Mineral Composition at the Depth of 128.04m bgl



Mineral Composition at the Depth of 155.48m bgl

APPENDIX – III

ICPAES ANALYSIS

ICPAES data of site1 at various depths

Element	Site1		
	E-225(Ft)	E-270(Ft)	E-400(Ft)
Major Element (%)	85.8	86.3	90.8
SiO ₂ (%)	43.6	43.8	66.1
Al ₂ O ₃ (%)	13.9	13.8	11.8
Fe ₂ O ₃ (%)	9	9.7	5.1
CaO (%)	11.2	9.8	1.9
MgO (%)	6.8	7.3	1.2
K ₂ O (%)	0.7	1.2	3.5
MnO (%)	0.08	0.07	0.11
TiO ₂ (%)	0.52	0.61	0.5
P ₂ O ₅	495ppm	426ppm	425ppm
Li	<10ppm	<10ppm	<10ppm
Be	2ppm	2ppm	2ppm
B	40ppm	43ppm	102ppm
V	251ppm	272ppm	51ppm
Cr	410ppm	397ppm	42ppm
Co	49ppm	54ppm	9ppm
Ni	131ppm	120ppm	43ppm
Cu	37ppm	24ppm	32ppm
Zn	30ppm	33ppm	18ppm
As	<20ppm	<20ppm	<20ppm
Sr	52ppm	42ppm	37ppm
Y	<20ppm	<20ppm	<20ppm
Nb	26ppm	27ppm	25ppm
Mo	<5ppm	<5ppm	<5ppm
Ag	<1.0ppm	<1.0ppm	<1.0ppm
Cd	6ppm	7ppm	<2ppm
Sn	<20ppm	<20ppm	<20ppm
Sb	<10ppm	<10ppm	<10ppm
Ba	264ppm	124ppm	400ppm
La	<20ppm	<20ppm	27ppm
Ce	<10ppm	<10ppm	102ppm
W	<10ppm	11ppm	12ppm
Pb	37ppm	35ppm	20ppm
Bi	31ppm	31ppm	18ppm
Zr	301ppm	144ppm	119ppm

ICPAES data of the site2 at various depths

Element	S-15(Ft)	S-210(Ft)	S-255(Ft)
Major Element (%)	90	95.8	96.6
SiO ₂ (%)	61.4	78.1	84.7
Al ₂ O ₃ (%)	12.9	9.4	6.1
Fe ₂ O ₃ (%)	3.9	5.7	3.7
CaO(%)	8.8	<1.0	<1.0
MgO (%)	1.9	1	<1.0
K ₂ O (%)	<.5	<.5	<.5
MnO (%)	0.07	0.05	0.04
TiO ₂ (%)	0.59	0.6	0.47
P ₂ O ₅	855ppm	<100ppm	<100ppm
Li	<10ppm	<10ppm	<10ppm
Be	3ppm	<2ppm	<2ppm
B	69ppm	62ppm	72ppm
V	75ppm	82ppm	48ppm
Cr	52ppm	37ppm	14ppm
Co	<5ppm	8ppm	<5ppm
Ni	29ppm	25ppm	14ppm
Cu	22ppm	42ppm	26ppm
Zn	19ppm	21ppm	20ppm
As	<20ppm	<20ppm	<20ppm
Sr	18ppm	42ppm	38ppm
Y	<20ppm	<20ppm	<20ppm
Nb	23ppm	<20ppm	<20ppm
Mo	<5ppm	<5ppm	<5ppm
Ag	<1.0ppm	<1.0ppm	<1.0ppm
Cd	<2ppm	<2ppm	<2ppm
Sn	<20ppm	<20ppm	<20ppm
Sb	<10ppm	<10ppm	<10ppm
Ba	384ppm	233ppm	163ppm
La	21ppm	<20ppm	<20ppm
Ce	<10ppm	37ppm	18ppm
W	<10ppm	<10ppm	<10ppm
Pb	<10ppm	<10ppm	<10ppm
Bi	<10ppm	<10ppm	<10ppm
Zr	151ppm	120ppm	177ppm

Water Quality ICPAES data at the Site 2

Element	Concentration
Major Element (%)	2.8
SiO ₂ (%)	0
Al ₂ O ₃ (%)	0
Fe ₂ O ₃ (%)	0
CaO (%)	1.3
MgO (%)	0.4
K ₂ O (%)	1.1
MnO (%)	0
TiO ₂ (%)	0.04
P ₂ O ₅	226ppm
Li	125ppm
Be	0ppm
B	40ppm
V	2ppm
Cr	0ppm
Co	0ppm
Ni	0ppm
Cu	0ppm
Zn	27ppm
As	0ppm
Sr	52ppm
Y	0ppm
Nb	9ppm
Mo	0ppm
Ag	0.2ppm
Cd	0ppm
Sn	0ppm
Sb	9ppm
Ba	104ppm
La	0ppm
Ce	66ppm
W	6ppm
Pb	14ppm
Bi	1ppm
Zr	3ppm

ICPAES data of the site3 at various depths

Element	Site 3		
	Y-210(Ft)	Y-315(Ft)	Y-420(Ft)
Major Element (%)	95.3	94.9	92.5
SiO ₂ (%)	69.8	78.3	80.3
Al ₂ O ₃ (%)	18.1	7.4	5.1
Fe ₂ O ₃ (%)	5.1	6.1	3.5
CaO (%)	<1.0	1	1.8
MgO (%)	<1.0	<1.0	<1.0
K ₂ O (%)	<.5	0.6	0.5
MnO (%)	0.02	0.06	0.05
TiO ₂ (%)	1.18	0.5	0.58
P ₂ O ₅	<100ppm	318ppm	232ppm
Li	<10ppm	<10ppm	<10ppm
Be	<2ppm	<2ppm	<2ppm
B	223ppm	105ppm	88ppm
V	155ppm	53ppm	46ppm
Cr	99ppm	14ppm	<10ppm
Co	<5ppm	9ppm	<5ppm
Ni	<10ppm	22ppm	11ppm
Cu	60ppm	59ppm	24ppm
Zn	25ppm	27ppm	24ppm
As	<20ppm	<20ppm	<20ppm
Sr	45ppm	37ppm	30ppm
Y	<20ppm	<20ppm	<20ppm
Nb	25ppm	<20ppm	20ppm
Mo	<5ppm	<5ppm	<5ppm
Ag	<1.0ppm	<1.0ppm	<1.0ppm
Cd	<2ppm	<2ppm	<2ppm
Sn	<20ppm	<20ppm	<20ppm
Sb	<10ppm	<10ppm	<10ppm
Ba	103ppm	119ppm	115ppm
La	23ppm	<20ppm	<20ppm
Ce	62ppm	43ppm	41ppm
W	<10ppm	<10ppm	<10ppm
Pb	<10ppm	<10ppm	<10ppm
Bi	<10ppm	<10ppm	<10ppm
Zr	245ppm	21ppm	<20ppm

Water Quality at Site 3	
Element	Concentration
Major Element (%)	2.5
SiO ₂ (%)	0
Al ₂ O ₃ (%)	0
Fe ₂ O ₃ (%)	0
CaO (%)	0.9
MgO (%)	0.3
K ₂ O (%)	1.3
MnO (%)	0
TiO ₂ (%)	0.04
P ₂ O ₅	236ppm
Li	144ppm
Be	0ppm
B	36ppm
V	3ppm
Cr	0ppm
Co	0ppm
Ni	0ppm
Cu	0ppm
Zn	13ppm
As	0ppm
Sr	39ppm
Y	0ppm
Nb	9ppm
Mo	0ppm
Ag	.4ppm
Cd	0ppm
Sn	0ppm
Sb	9ppm
Ba	103ppm
La	0ppm
Ce	81ppm
W	8ppm
Pb	13ppm
Bi	4ppm
Zr	2ppm

Water Quality ICPAES data at the Site 3

Water Quality at Site 4	
Element	Concentration
Major Element (%)	2.4
SiO ₂ (%)	0
Al ₂ O ₃ (%)	0
Fe ₂ O ₃ (%)	0
CaO (%)	1.1
MgO (%)	0.4
K ₂ O (%)	0.9
MnO (%)	0
TiO ₂ (%)	0.04
P ₂ O ₅	222ppm
Li	103ppm
Be	0ppm
B	38ppm
V	2ppm
Cr	0ppm
Co	0ppm
Ni	0ppm
Cu	0ppm
Zn	13ppm
As	0ppm
Sr	51ppm
Y	0ppm
Nb	8ppm
Mo	0ppm
Ag	0.9ppm
Cd	0ppm
Sn	0ppm
Sb	3ppm
Ba	103ppm
La	0ppm
Ce	70ppm
W	5ppm
Pb	14ppm
Bi	9ppm
Zr	2ppm

Water Quality ICPAES data at the Site 4

Water Quality at Site 5	
Element	Concentration
Major Element (%)	2.7
SiO ₂ (%)	0
Al ₂ O ₃ (%)	0
Fe ₂ O ₃ (%)	0
CaO (%)	1.3
MgO (%)	0.7
K ₂ O (%)	0.7
MnO (%)	0
TiO ₂ (%)	0.04
P ₂ O ₅	222ppm
Li	101ppm
Be	0ppm
B	45ppm
V	1ppm
Cr	0ppm
Co	0ppm
Ni	0ppm
Cu	0ppm
Zn	17ppm
As	0ppm
Sr	63ppm
Y	0ppm
Nb	8ppm
Mo	0ppm
Ag	0.5ppm
Cd	0ppm
Sn	8ppm
Sb	9ppm
Ba	106ppm
La	0ppm
Ce	59ppm
W	5ppm
Pb	14ppm
Bi	8ppm
Zr	3ppm

Water Quality ICPAES data at the Site 5

Water quality at site 6	
Element	Concentration
Major Element (%)	1.9
SiO ₂ (%)	0
Al ₂ O ₃ (%)	0
Fe ₂ O ₃ (%)	0
CaO (%)	0.5
MgO (%)	0.4
K ₂ O (%)	1
MnO (%)	0
TiO ₂ (%)	0.04
P ₂ O ₅	234ppm
Li	112ppm
Be	0ppm
B	47ppm
V	1ppm
Cr	0ppm
Co	0ppm
Ni	0ppm
Cu	0ppm
Zn	9ppm
As	0ppm
Sr	42ppm
Y	0ppm
Nb	8ppm
Mo	0ppm
Ag	0.4ppm
Cd	0ppm
Sn	3ppm
Sb	6ppm
Ba	105ppm
La	0ppm
Ce	79ppm
W	4ppm
Pb	11ppm
Bi	6ppm
Zr	2ppm

Water Quality ICPAES data at the Site 6

Water Quality at Site 7	
Element	Concentration
Major Element (%)	2.4
SiO ₂ (%)	0
Al ₂ O ₃ (%)	0
Fe ₂ O ₃ (%)	0
CaO (%)	1.1
MgO (%)	0.4
K ₂ O (%)	0.9
MnO (%)	0
TiO ₂ (%)	0.04
P ₂ O ₅	220ppm
Li	110ppm
Be	0ppm
B	43ppm
V	2ppm
Cr	0ppm
Co	0ppm
Ni	0ppm
Cu	0ppm
Zn	12ppm
As	0ppm
Sr	51ppm
Y	0ppm
Nb	7ppm
Mo	0ppm
Ag	0.7ppm
Cd	0ppm
Sn	12ppm
Sb	9ppm
Ba	104ppm
La	0ppm
Ce	67ppm
W	7ppm
Pb	16ppm
Bi	9ppm
Zr	2ppm

Water Quality ICPAES data at the Site 7

Field Photographs



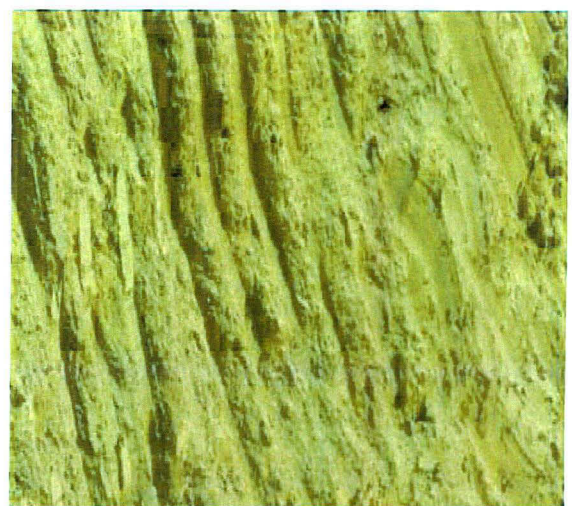
Fractured ferrogenous quartzite showing weathering and brittleness In JNU



Weathered quartzite showing fracture zones in JNU



Buried pediment plain (BPP) in Vasant Kunj showing deposited rock debris



Zoomed view of buried pediment plain (BPP, medium) in Vasant Kunj



Site 3 (JNU 3) groundwater exploration point showing 34,125 liters per hour discharge. The depth of drilling was 164.63 meters with five prominent fracture zones



Site 2 (JNU 2) groundwater exploration showing 28,938 liters per hour discharge. The depth of drilling was 182.92 meters with four prominent fracture zones



Seepage from the fractured quartzite in RR Hospital Area



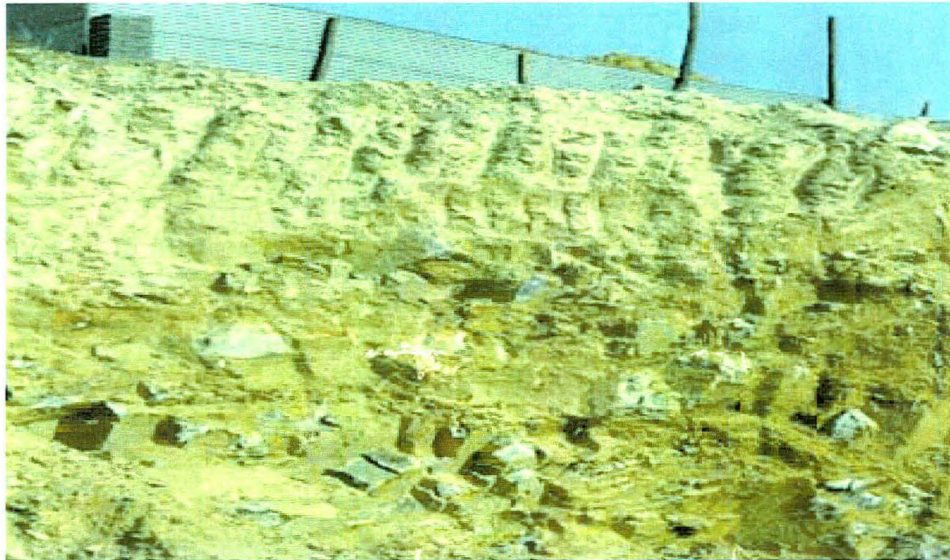
Two sets of fracture in ferrogenous quartzite along a microfault in RR Hospital



Zoomed view of fault in quartzite in RR Hospital Area



Water body in RR Hospital Area



Variable buried pediment plain showing 5-20 meters of deposition over ferrogenous quartzite layer in Vasant Kunj